

G. Stupakov

**Lecture notes on Classical Mechanics
and Electromagnetism in Accelerator
Physics**

The US Particle Accelerator School
June 13-24, 2011
Melville, New York

2011

Contents

1 Preliminaries	7
1.1 Introductory remarks	7
1.2 Maxwell's equations	7
1.3 SI versus Gaussian system of units	8
1.4 Wave equations	9
1.5 Vector and scalar potentials	9
1.6 Relativistic equations...	9
1.7 Energy balance and the Poynting theorem	10
1.8 Photons	10
1.9 Recommended references	11
2 Linear and Nonlinear Oscillators	13
2.1 Linear Oscillator	13
2.2 Resonance	15
2.3 Random kicks	16
2.4 Parametric resonance	17
2.5 Adiabatic variation of parameters	18
2.6 Nonlinear oscillator	19
2.7 Nonlinear resonance	23
3 Lagrangian and Hamiltonian equations of motion	25
3.1 Lagrangian	25
3.2 Lagrangian of a relativistic particle...	28
3.3 From Lagrangian to Hamiltonian	29
3.4 Hamiltonian of a charged particle in an electromagnetic field	31
3.5 Poisson brackets	32
4 Canonical transformations	33
4.1 Canonical transformations	33
4.2 Poisson brackets and canonical transformations	35
4.3 Generating functions	36
4.4 Four types of generating functions	38
4.5 Examples of canonical transformations	39

5	Liouville's theorem. Action-angle variables.	41
5.1	Hamiltonian flow	41
5.2	Action-angle variables in 1D	43
5.3	Liouville's theorem	45
6	Coordinate system and Hamiltonian in an accelerator	47
6.1	Coordinate system	47
6.2	Hamiltonian in curvilinear coordinate system	50
6.3	Using s as a time variable	51
6.4	Small amplitude approximation	53
6.5	Time dependent Hamiltonian	54
7	Equations of motion in accelerator	57
7.1	Vector potential for different types of magnets	57
7.2	Taylor expansion of the Hamiltonian	60
7.3	Hill's equation, betatron function and betatron phase	61
8	Action-angle variables for circular machines	65
8.1	Action-angle variables and the Floquet transformation	65
8.2	Phase space motion at a given location	69
9	Field errors and nonlinear resonances	71
9.1	Closed orbit distortion	71
9.2	Effect of energy deviation	73
9.3	Quadrupole errors	74
9.4	The third-order resonance	76
10	Resonance overlapping and dynamic aperture	83
10.1	Standard model and resonance overlapping	83
10.2	Dynamic aperture in accelerators	86
11	The kinetic equation	89
11.1	The distribution function in phase space and kinetic equation	89
11.2	Integration of the Vlasov equation along trajectories	92
11.3	Steady state solutions of the kinetic equation	93
11.4	Phase mixing and decoherence	94
12	Radiation damping effects	97
12.1	Radiation damping in equations of motion	97
12.2	Synchrotron damping of betatron oscillations	98
12.3	Vlasov equation and Robinson's theorem	101
13	Primer in Special Relativity	103
13.1	Lorentz transformation and matrices	103
13.2	Lorentz contraction and time dilation	105
13.3	Doppler effect	106
13.4	Lorentz transformation of fields	107

13.5 Lorentz transformation and photons	108
14 Selected electrostatic and magnetostatic problems	109
14.1 Electric field of a 3D Gaussian distribution	109
14.2 Electric field of a continuous beam in a pipe	111
14.3 Magnetic field of a beam in a conducting pipe	113
14.4 Electric field of a charged metallic ellipsoid	113
14.5 Electric field near metallic edges and protrusions	114
15 Self field of a relativistic beam	117
15.1 Relativistic field	117
15.2 Interaction of Moving Charges in Free Space	119
15.3 Field of a long-thin	120
16 Effect of environment on electromagnetic field of a beam	125
16.1 Beam Moving in a Perfectly Conducting Pipe	125
16.2 Beam field inside a perfectly conducting cylindrical pipe	127
16.3 Skin effect and the Leontovich boundary condition	127
16.4 Round pipe with resistive walls	129
16.5 Point charge and Gaussian bunch passing through an iris	133
17 Plane electromagnetic waves and Gaussian beams	137
17.1 Plane electromagnetic waves	137
17.2 Gaussian beams	139
18 Radiation and retarded potentials	143
18.1 Radiation field	143
18.2 Retarded time and position	145
18.3 Liénard-Wiechert potentials	146
18.4 Retarded potentials for an ensemble of particles	147
19 Scattering of electromagnetic waves	149
19.1 Thomson scattering	149
19.2 Radiation reaction force	153
19.3 Light pressure	154
19.4 Inverse Compton scattering	155
20 Synchrotron radiation	157
20.1 Synchrotron radiation pulses in the plane of the orbit	157
20.2 Fourier transformation	159
20.3 Synchrotron radiation for $\psi \neq 0$	161
20.4 Integral characteristic	163
20.5 Quantum fluctuations	165

21 Undulator radiation	169
21.1 Undulators and wigglers	169
21.2 Undulator radiation for $K \ll 1$	170
21.3 Effects of finite length of the undulator	172
21.4 Wiggler radiation for $K \gtrsim 1$	174
22 Transition and diffraction radiation	177
22.1 Transition radiation	177
22.2 Diffraction radiation	180
23 Formation length of radiation and coherent effects	183
23.1 Longitudinal formation length	183
23.2 Transverse coherence length	185
23.3 Coherent radiation	186
23.4 Effect of the transverse size of the beam	188
24 Synchrotron radiation reaction force	191
24.1 Radiation reaction force for a relativistic charge	191
24.2 Radiation reaction field in a bunch of particles	195
25 Waveguides and RF cavities	197
25.1 TM modes in cylindrical waveguides	197
25.2 TE modes in cylindrical waveguides	198
25.3 RF modes in cylindrical resonator	199
25.4 Electromagnetic field pressure	202
25.5 Slater's formula	203
25.6 Excitation of a cavity mode by a beam	205
26 Laser acceleration in vacuum. Inverse FEL acceleration	207
26.1 The Lawson-Woodward theorem	207
26.2 Laser acceleration in space with material boundaries	209
26.3 Inverse FEL acceleration	210

Lecture 1

Preliminaries

1.1 Introductory remarks

- This is the course where we study several subjects from classical mechanics and electrodynamics which I consider as essential to accelerator physics. This is not an accelerator physics course.

Of course, the choice of these subjects is somewhat subjective.

- I assume knowledge of basics of classical mechanics, electrodynamics, and the special theory of relativity.
- The course is designed to be self-contained. We will go over every important derivation in detail. You should be able to follow these derivations in the class.

• 1.2 Maxwell's equations

Classical electrodynamics in vacuum is governed by the Maxwell equations. In the SI system of units, the equations are

$$\begin{aligned}\nabla \cdot \mathbf{D} &= \rho \\ \nabla \cdot \mathbf{B} &= 0 \\ \nabla \times \mathbf{E} &= -\frac{\partial \mathbf{B}}{\partial t} \\ \nabla \times \mathbf{H} &= \mathbf{j} + \frac{\partial \mathbf{D}}{\partial t}\end{aligned}\tag{1.1}$$

where ρ is the charge density, \mathbf{j} is the current density, with $\mathbf{D} = \epsilon_0 \mathbf{E}$, $\mathbf{H} = \mathbf{B}/\mu_0$. \mathbf{B} is called the magnetic induction, and \mathbf{H} is called the magnetic field.

In the Gaussian system of units Maxwell's equations are

$$\begin{aligned}
 \nabla \cdot \mathbf{E} &= 4\pi\rho \\
 \nabla \cdot \mathbf{B} &= 0 \\
 \nabla \times \mathbf{E} &= -\frac{1}{c} \frac{\partial \mathbf{B}}{\partial t} \\
 \nabla \times \mathbf{B} &= \frac{4\pi}{c} \mathbf{j} + \frac{1}{c} \frac{\partial \mathbf{E}}{\partial t}.
 \end{aligned} \tag{1.2}$$

The equations are linear: the sum of two solutions, $\mathbf{E}_1, \mathbf{B}_1$ and $\mathbf{E}_2, \mathbf{B}_2$, is also a solution corresponding to the sum of densities $\rho_1 + \rho_2, \mathbf{j}_1 + \mathbf{j}_2$.

For a point charge moving along a trajectory $\mathbf{r} = \mathbf{r}_0(t)$,

$$\rho(\mathbf{r}, t) = q\delta(\mathbf{r} - \mathbf{r}_0(t)), \quad \mathbf{j}(\mathbf{r}, t) = q\mathbf{v}(t)\delta(\mathbf{r} - \mathbf{r}_0(t)), \tag{1.3}$$

with $\mathbf{v}(t) = d\mathbf{r}_0(t)/dt$.

Proper boundary conditions should be specified in each particular case. On a surface of a good conducting metal the boundary condition requires that the tangential component of the electric field is equal to zero, $\mathbf{E}_t|_S = 0$.

1.3 SI versus Gaussian system of units

We will use the SI system of units throughout this course.

To convert an equation written in SI variables to the corresponding equation in Gaussian variables, replace according to the following table (from [1]):

Table 1.1: Conversion table

Quantity	SI	Gaussian
Velocity of light	$(\mu_0\epsilon_0)^{-1/2}$	c
Electric field, potential	\mathbf{E}, ϕ	$\frac{\mathbf{E}}{\sqrt{4\pi\epsilon_0}}, \frac{\phi}{\sqrt{4\pi\epsilon_0}}$
Charge density, current	q, ρ, \mathbf{j}	$q\sqrt{4\pi\epsilon_0}, \rho\sqrt{4\pi\epsilon_0}, \mathbf{j}\sqrt{4\pi\epsilon_0}$
Magnetic induction	\mathbf{B}	$\mathbf{B}\sqrt{\frac{\mu_0}{4\pi}}$

We will use the quantity Z_0 that is often called the *vacuum impedance*

$$Z_0 = \sqrt{\frac{\mu_0}{\epsilon_0}} \approx 377 \text{ Ohm}. \tag{1.4}$$

In CGS units $Z_0 = 4\pi/c$.

See a more detailed discussion about conversion in the Appendix of Jackson's book.

1.4 Wave equations

In free space with no charges and currents field components satisfy the wave equation

$$\frac{1}{c^2} \frac{\partial^2 f}{\partial t^2} - \frac{\partial^2 f}{\partial x^2} - \frac{\partial^2 f}{\partial y^2} - \frac{\partial^2 f}{\partial z^2} = 0. \quad (1.5)$$

A particular solution of this equation is a sinusoidal wave characterized by frequency ω and wave number \mathbf{k} and propagating in the direction of unit vector \mathbf{n} :

$$f = A \sin(\omega t - \mathbf{k}\mathbf{n} \cdot \mathbf{r}), \quad (1.6)$$

where A is a constant and $\omega = ck$.

1.5 Vector and scalar potentials

It is often convenient to express the fields in terms of the *vector potential* \mathbf{A} and the *scalar potential* ϕ :

$$\begin{aligned} \mathbf{E} &= -\nabla\phi - \frac{\partial\mathbf{A}}{\partial t} \\ \mathbf{B} &= \nabla \times \mathbf{A} \end{aligned} \quad (1.7)$$

Substituting these equations into Maxwell's equations, we find that the second and the third equations are satisfied identically. We only need to take care of the first and the fourth equations.

1.6 Relativistic equations of motion in electromagnetic field

For a point charge q moving with velocity \mathbf{v} we have

$$\frac{d\mathbf{p}}{dt} = q\mathbf{E} + q\mathbf{v} \times \mathbf{B}. \quad (1.8)$$

On the right-hand side of this equation we have the *Lorentz force*.

A beam of charged particles can often be considered as a charge fluid characterized by the charge density $\rho(\mathbf{r}, t)$ the current density $\mathbf{j}(\mathbf{r}, t)$. The Lorentz force acting on a unit volume of such a fluid is

$$\mathbf{f} = \rho\mathbf{E} + \mathbf{j} \times \mathbf{B}. \quad (1.9)$$

1.7 Energy balance and the Poynting theorem

The electromagnetic field has an energy and momentum associated with it. The energy density of the field (energy per unit volume) is

$$u = \frac{1}{2}(\mathbf{E} \cdot \mathbf{D} + \mathbf{H} \cdot \mathbf{B}) = \frac{\epsilon_0}{2}(E^2 + c^2 B^2). \quad (1.10)$$

The Poynting vector

$$\mathbf{S} = \mathbf{E} \times \mathbf{H} \quad (1.11)$$

gives the energy flow (energy per unit area per unit time) in the electromagnetic field.

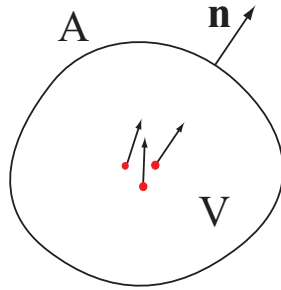


Figure 1.1: Charges moving inside volume V .

Consider charges that move inside a volume V enclosed by a surface A , see Fig. 1.1. The Poynting theorem states

$$\frac{\partial}{\partial t} \int_V u dV = - \int_V \mathbf{j} \cdot \mathbf{E} dV - \int_A \mathbf{n} \cdot \mathbf{S} dA, \quad (1.12)$$

where \mathbf{n} is the unit vector normal to the surface and directed outward. The left hand side of this equation is the rate of change of the electromagnetic energy due to the interaction with moving charges. The first term on the right hand side is the work done by the electric field on the moving charges. The second term describes the electromagnetic energy flow from the volume through the enclosing surface.

1.8 Photons

The quantum view on the radiation is that the electromagnetic field is represented by photons. Each photon carries the energy $\hbar\omega$ and the momentum $\hbar\mathbf{k}$, where the vector \mathbf{k} is the wavenumber which points to the direction of propagation of the radiation, $\hbar = 1.05 \cdot 10^{-34}$ J·sec is the Planck constant divided by 2π , and $k = \omega/c$.

1.9 Recommended references

Books [1–4] include most of the subjects covered in this course. Ref. [4] is available online at:

<http://mitpress.mit.edu/SICM/>

Lecture 2

Linear and Nonlinear Oscillators

A simple model of a linear oscillator lies in the foundation of many physical phenomena in accelerator dynamics. A typical trajectory of a particle in an accelerator can be represented as an oscillation around a so called reference orbit.

We will start with recalling the main properties of the linear oscillator. We will then consider what a small nonlinearity adds to these properties.

2.1 Linear Oscillator

A differential equation for a linear oscillator without damping has a form

$$\frac{d^2x}{dt^2} + \omega_0^2 x = 0, \quad (2.1)$$

where $x(t)$ is the oscillating quantity, t is time and ω_0 is the oscillator frequency. For a mass on a spring shown in Fig. 2.1, $\omega_0^2 = k/m$, where k is the spring constant. General solution of Eq. (2.1) is characterized by the amplitude A and



Figure 2.1: A mass attached to a spring.

the phase ϕ

$$x(t) = A \cos(\omega_0 t + \phi). \quad (2.2)$$

Damping due to a friction force which is proportional to the velocity introduces a term with the first derivative into the differential equation

$$\frac{d^2x}{dt^2} + \gamma \frac{dx}{dt} + \omega_0^2 x = 0, \quad (2.3)$$

where γ is the damping constant (it has the dimension of frequency). When damping is not too strong¹, a general solution to this equation is

$$x(t) = Ae^{-\gamma_1 t} \cos(\omega_1 t + \phi), \quad (2.4)$$

with

$$\begin{aligned} \omega_1 &= \omega_0 \sqrt{1 - \frac{\gamma^2}{4\omega_0^2}}, \\ \gamma_1 &= \frac{1}{2}\gamma. \end{aligned} \quad (2.5)$$

If $\gamma \ll \omega_0$, the frequency ω_1 is close to ω_0 , $\omega_1 \approx \omega_0$. Damping effect is often quantified by a so called *quality factor* Q defined as $Q = \omega_0/2\gamma$; weak damping is characterized $Q \gg 1$.

As an example, consider particle's oscillations in the Low Energy Ring in PEP-II at SLAC. In the transverse direction, the particle executes the betatron oscillations with the frequency about 40 times larger than the revolution frequency of 136 kHz. This makes $\omega_\beta \sim 2\pi \times 5.4$ MHz. The damping time γ_1^{-1} due to the synchrotron radiation is about 60 ms, which means that $\gamma = 2/(60\text{ms}) \approx 30$ Hz. We see that the ratio $\gamma/\omega_\beta \sim 10^{-6}$ is extremely small for these oscillations, and the damping can be neglected in first approximation.

If the oscillator is driven by an external force $f(t)$ then we have

$$\frac{d^2x}{dt^2} + \gamma \frac{dx}{dt} + \omega_0^2 x = f(t), \quad (2.6)$$

($f(t)$ is properly normalized here). From the ODE theory we know how to write a general solution to the above equation. We will write down here the result for the case $\gamma = 0$:

$$x(t) = x_0 \cos \omega_0 t + \frac{\dot{x}_0}{\omega_0} \sin \omega_0 t + \frac{1}{\omega_0} \int_0^t \sin \omega_0(t-t') f(t') dt', \quad (2.7)$$

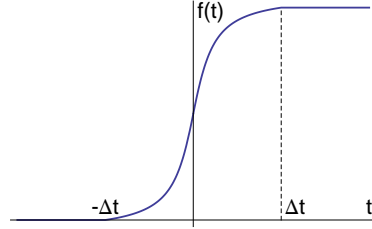
where x_0 and \dot{x}_0 are initial, at $t = 0$, coordinate and velocity of the oscillator.

Problem 2.1. Prove that Eq. (2.7) gives a solution to Eq. (2.6) with $\gamma = 0$. Verify that the initial conditions are satisfied. Generalize the solution Eq. (2.7) for the case when $\gamma \neq 0$.

Problem 2.2 . The function $f(t)$ is shown in Fig. 2.2: it is equal to zero for $t < -\Delta t$, and is constant for $t > \Delta t$ with a smooth transition in between. Describe the behavior of the linear oscillator driven by this force in the limits $\Delta t \ll \omega_0^{-1}$ and $\Delta t \gg \omega_0^{-1}$.

Problem 2.3. Prove that Eq. (2.1) conserves the quantity $x^2(t) + \dot{x}(t)^2/\omega_0^2$.

¹Eqs. (2.4) and (2.5) are valid for $\gamma < 2\omega_0$. In the opposite limit $x(t)$ exponentially decays in time.

Figure 2.2: Function $f(t)$.

2.2 Resonance

Let's assume that an oscillator is driven by a sinusoidal force, $f(t) = f_0 \cos \omega t$. A convenient way to study this problem is to use complex number. Instead of considering a real function $x(t)$ we will consider a complex function $\xi(t)$ such that $x(t) = \text{Re} \xi(t)$. The equation for ξ is

$$\frac{d^2 \xi}{dt^2} + \gamma \frac{d\xi}{dt} + \omega_0^2 \xi = f_0 e^{-i\omega t}. \quad (2.8)$$

Let us seek a solution in the form $\xi(t) = \xi_0 e^{-i\omega t}$ where ξ_0 is a complex number, $\xi_0 = |\xi_0| e^{i\phi}$. This means that the real variable x is $x(t) = \text{Re} \xi(t) = \text{Re} (|\xi_0| e^{-i\omega t + i\phi}) = |\xi_0| \cos(\omega t - \phi)$. We have

$$(-\omega^2 - i\omega\gamma + \omega_0^2)\xi_0 = f_0, \quad (2.9)$$

and

$$\xi_0 = \frac{f_0}{\omega_0^2 - \omega^2 - i\omega\gamma}. \quad (2.10)$$

For the amplitude squared of the oscillations we find

$$|\xi_0|^2 = \frac{f_0^2}{(\omega_0^2 - \omega^2)^2 + \omega^2 \gamma^2}. \quad (2.11)$$

The plot of the amplitude versus frequency ω is shown in Fig 2.3 for several values of the parameter γ . When the damping factor γ is small we have an effect of *resonance*: the amplitude of the oscillations increases when the driving frequency approaches the resonant frequency ω_0 . The *width* $\Delta\omega_{\text{res}}$ of the resonance is defined as a characteristic width of the resonant curve. It is easy to show that an estimate for $\Delta\omega_{\text{res}}$ is: $\Delta\omega_{\text{res}} \sim \gamma$. It makes sense to talk about the resonance only when $\gamma \ll \omega_0$.

Problem 2.4. Assume $\gamma = 0$. Show that if $\omega \gg \omega_0$ then one can neglect the term $\omega_0^2 \xi$ in the equation. In other words, the oscillator responds to the

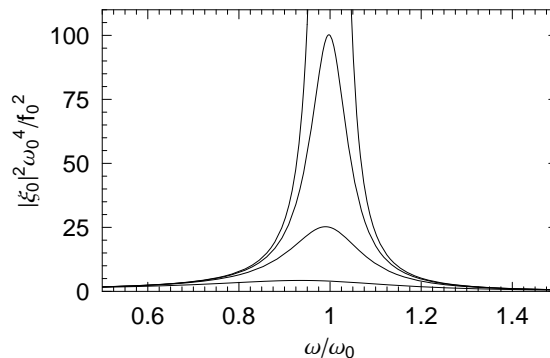


Figure 2.3: Resonant curves for $\gamma = 0.5, 0.2, 0.1, 0$.

driving force as a free particle. This fact explains why the dielectric response of many media to x-rays can be computed neglecting the binding of electrons to nuclei.

2.3 Random kicks

What happens if an oscillator is kicked at random times? Let us assume that the external force is given by the following expression,

$$f(t) = \sum_i a_i \delta(t - t_i), \quad (2.12)$$

where t_i are random moments of time, and the kick amplitudes a_i take random values. To deal with this problem we will use Eq. (2.7) (assuming for simplicity that $\gamma = 0$). We then have

$$\begin{aligned} x(t) &= \frac{1}{\omega_0} \int_0^t \sin \omega_0(t - t') f(t') dt' \\ &= \sum_i \frac{a_i}{\omega_0} \sin \omega_0(t - t_i), \end{aligned} \quad (2.13)$$

where we also assumed that at time $t = 0$ the oscillator was at rest. The result is a random function whose particular values are determined by the specific sequence of a_i and t_i . We would like to find some statistical characteristics of this random motion. An important quantity is the sum $x(t)^2 + \dot{x}^2(t)/\omega_0^2$ —for free oscillations it is equal to the square of the amplitude. So we want to find

the statistical average of this quantity:

$$\begin{aligned}
\langle x(t)^2 + \frac{\dot{x}^2(t)}{\omega_0^2} \rangle &= \\
&= \langle \omega_0^{-2} \sum_{i,j} a_i a_j (\sin \omega_0(t - t_i) \sin \omega_0(t - t_j) + \cos \omega_0(t - t_i) \cos \omega_0(t - t_j)) \rangle \\
&= \langle \omega_0^{-2} \sum_{i,j} a_i a_j \cos \omega_0(t_i - t_j) \rangle.
\end{aligned} \tag{2.14}$$

Because t_i and t_j are not correlated if $i \neq j$, the phase of the cosine function is random, and the terms with $i \neq j$ vanish after averaging. Only the terms with $i = j$ survive the averaging. The result is

$$\langle x(t)^2 + \frac{\dot{x}^2(t)}{\omega_0^2} \rangle = \frac{\langle a^2 \rangle}{\omega_0^2} \frac{t}{\Delta t}, \tag{2.15}$$

where Δt is an average time between the kicks. We see that the square of the amplitude grows linearly with time. This is a characteristic of a *diffusion* process.

2.4 Parametric resonance

Let us consider what happens if we vary parameters of our linear oscillator periodically with time. Since we have only one parameter, this means that $\omega_0(t)$ is a periodic function,

$$\frac{d^2 x}{dt^2} + \omega_0^2(t)x = 0. \tag{2.16}$$

Moreover, let us assume that

$$\omega_0^2(t) = \Omega^2(1 - h \cos \nu t) \tag{2.17}$$

(the resulting equation is called the Mathieu equation). Naively, one might think that if h is small, the solution will be close to that of a linear oscillator with constant parameters. This is not always the case, as numerical solutions show. It turns out that even if h is small, oscillations become unstable if the ratio of the frequencies Ω/ν is close to $n/2$, where n is an integer. In other words, for $\nu \approx 2\Omega$, Ω , $\Omega/2$, $\Omega/3 \dots$ the oscillator is unstable.

The exact pattern of stable and unstable regions in the plane Ω , h is rather complicated. It is shown in Fig. 2.4. Note that those regions become exponentially narrow if $h \lesssim 1$ and ν/Ω is small. For a small ν we have an oscillator whose parameters are varied *adiabatically* slow.

Again, consider as an example parameters of the high energy ring of the PEP-II accelerator at SLAC. As was pointed out earlier, the betatron frequency of transverse oscillations in the machine is 135 kHz. This frequency however

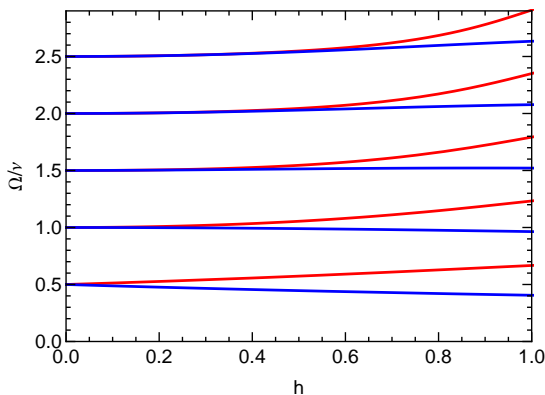


Figure 2.4: Unstable regions for Eq. (2.16) are bounded by red curves from above and blue curves from below.

depends on the particle energy, and the RF cavities in the ring modulate the energy causing its oscillations around an equilibrium value with the so called synchrotron frequency of about 7 kHz. In principle, such a modulation might lead to a parametric instability of the betatron oscillations, however, due to the small ratio of the frequencies, $7/135 \approx 0.05$, the system is in the adiabatic regime, and in the first approximation, the effect is extremely small (and in reality is suppressed by small damping of oscillations).

2.5 Adiabatic variation of parameters

We will now consider an example of a slow variation of the parameters of the oscillator. Let us assume that the frequency ω_0 varies in time from a value ω_1 to ω_2 over a time interval τ . A slow variation means that

$$\omega_0^{-2} \left| \frac{d\omega_0}{dt} \right| \ll 1, \quad (2.18)$$

which also means that the relative change of the frequency ω_0 over time ω_0^{-1} is small. This is the *adiabatic* regime.

How does the amplitude of the oscillations varies in time? Let us seek solution of Eq. (2.16) in the following (complex) form

$$\xi(t) = A(t) \exp \left(-i \int_0^t \omega_0(t') dt' + \phi_0 \right), \quad (2.19)$$

where $A(t)$ is the slowly varying amplitude of the oscillations and ϕ is the initial

phase. Substituting this formula into Eq. (2.16) yields

$$\frac{d^2 A}{dt^2} - 2i\omega_0 \frac{dA}{dt} - i \frac{d\omega_0}{dt} A = 0. \quad (2.20)$$

We expect that the amplitude A is a slow function of time, and neglect $d^2 A/dt^2$ in this equation, which gives

$$2\omega_0 \frac{dA}{dt} + \frac{d\omega_0}{dt} A = 0. \quad (2.21)$$

This equation can also be written as

$$\frac{d}{dt} \ln(A^2 \omega_0) = 0, \quad (2.22)$$

from which it follows that in the adiabatic regime $A(t)^2 \omega_0(t) = \text{const}$. We found an *adiabatic invariant* for our oscillator.

Fig. 2.5 shows the result of numerical integration of Eq. (2.16) in an adiabatic regime.

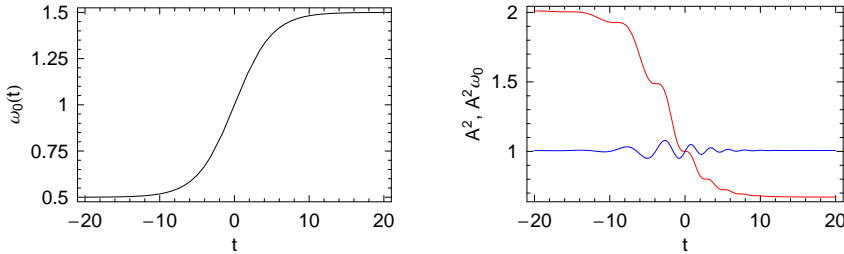


Figure 2.5: The left plot shows the function $\omega_0(t)$. The red curve on the right plot shows the quantity $x(t)^2 + \dot{x}^2(t)/\omega_0^2$ (which is close to the amplitude squared A^2) and the blue curve shows the product of this quantity with $\omega_0(t)$. We see that the product is approximately conserved, and hence is an adiabatic invariant.

2.6 Nonlinear oscillator

The linear oscillator is usually obtained as a first approximation in the expansion near the equilibrium position of a stable system. Higher order terms would lead to nonlinear terms in the equation

$$\frac{d^2 x}{dt^2} = -\omega_0^2 x + \alpha x^2 + \beta x^3 + \dots, \quad (2.23)$$

where the coefficients α, β , are small. What is the effect of these terms? The most important consequence of nonlinear terms is that they introduce a dependence of frequency of oscillations on amplitude.

Instead of studying Eq. (2.23) we will analyze first the *pendulum equation*

$$\ddot{\theta} + \omega_0^2 \sin \theta = 0, \quad (2.24)$$

where $\omega_0^2 = g/l$, l being the length of the pendulum. Note that for small amplitudes, $\theta \ll 1$, we have

$$\sin \theta \approx \theta - \frac{1}{6}\theta^3, \quad (2.25)$$

and we recover Eq. (2.23) with $\alpha = 0$ and $\beta = \omega_0^2/6$. The linear approximation for the pendulum equation is obtained if we neglect the cubic term in this expansion.

Of course, the pendulum can be solved exactly if we use the energy conservation. Multiplying Eq. (2.24) by $\dot{\theta}$ gives

$$\frac{1}{2} \frac{d}{dt} \dot{\theta}^2 - \omega_0^2 \frac{d}{dt} \cos \theta = 0, \quad (2.26)$$

from which it follows that the quantity

$$E = \frac{1}{2\omega_0^2} \dot{\theta}^2 - \cos \theta = \text{const} \quad (2.27)$$

is conserved. We call E the energy of the system; each orbit is characterized by its own energy. For a given energy E we have

$$\dot{\theta} = \pm \omega_0 \sqrt{2(E + \cos \theta)}. \quad (2.28)$$

This equation allows us to graph the *phase portrait* of the system where we plot trajectories on the plane $(\theta, \dot{\theta}/\omega_0)$, see Fig. 2.6. There are *stable points*, *unstable points* and the *separatrix* on this plot. Oscillations correspond to values of E such that $-1 < E < 1$ with rotation occurring at $E > 1$. The separatrix has $E = 1$.

Problem 2.5. Draw the phase portrait of a linear oscillator with and without damping.

Let us find now how the period of the pendulum T (and hence the frequency $\omega = 2\pi/T$) depends on the amplitude. We can integrate Eq. (2.28)

$$\omega_0 \int_{t_1}^{t_2} dt = \int_{\theta_1}^{\theta_2} \frac{d\theta}{\sqrt{2(E + \cos \theta)}}. \quad (2.29)$$

For a given energy E , inside the separatrix, the pendulum swings between $-\theta_0$ and θ_0 , where θ_0 is defined by the relation $\cos \theta_0 = -E$, hence

$$\omega_0(t_2 - t_1) = \frac{1}{\sqrt{2}} \int_{\theta_1}^{\theta_2} \frac{d\theta}{\sqrt{(\cos \theta - \cos \theta_0)}}. \quad (2.30)$$

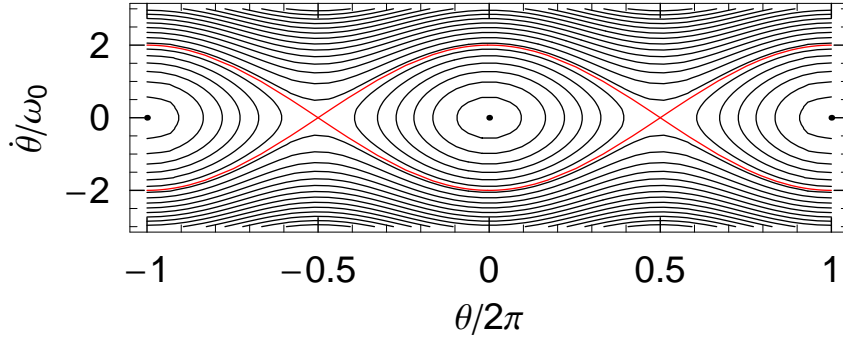


Figure 2.6: Phase space for the pendulum with the red curve showing the separatrix.

To find a half a period of the oscillations we need to integrate from $-\theta_0$ to θ_0 :

$$\frac{1}{2}T\omega_0 = \frac{1}{\sqrt{2}} \int_{-\theta_0}^{\theta_0} \frac{d\theta}{\sqrt{(\cos \theta - \cos \theta_0)}}. \quad (2.31)$$

The result can be expressed in terms of the elliptic function K of the first kind

$$\frac{T}{T_0} = \frac{2}{\pi} K \left(\sin^2 \left(\frac{\theta_0}{2} \right) \right), \quad (2.32)$$

where $T_0 = 2\pi/\omega_0$ is the period in the linear approximation. The plot of this function is shown in Fig. 2.7.

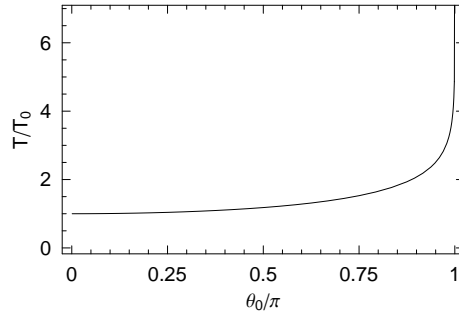


Figure 2.7: Period T as a function of the amplitude angle θ_0 in the range $0 < \theta_0 < \pi$.

For small values of the argument, the Taylor expansion of the elliptic function is: $(2/\pi)K(x) \approx 1 + x/4$. This means that for small amplitudes the frequency

of oscillations is given by

$$\omega \approx \omega_0 \left(1 - \frac{\theta_0^2}{16} \right), \quad (2.33)$$

it decreases with the amplitude.

Problem 2.6. Derive Eq. (2.33) directly from Eq. (2.31).

Near the separatrix, the period of oscillations becomes very large. The separatrix corresponds to $\theta_0 = \pi$, and we can use the approximation $(2/\pi)K(1-x) \approx -(\ln x)/\pi$ valid for $x \ll 1$, to find an approximate formula for T near the separatrix. We obtain

$$\frac{T}{T_0} \approx \frac{1}{\pi} \ln \frac{1}{1-E}. \quad (2.34)$$

As we see, the period diverges logarithmically as E approaches its value at the separatrix.

Problem 2.7. Fig. 2.8 shows a numerically computed function $\dot{\theta}(t)$ for a pendulum with $\omega_0 = 1$. Try to figure out what is the energy E for this trajectory and explain qualitatively the shape of the curve.

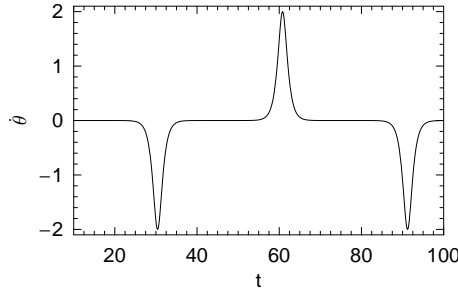


Figure 2.8: Dependence of $\dot{\theta}$ versus time for a pendulum trajectory.

In the general case of Eq. (2.23) the approximate solution will be

$$x(t) = A(t) \cos[\omega(A)t + \phi], \quad (2.35)$$

where the frequency ω now becomes a function of the amplitude

$$\omega(A) \approx \omega_0 + aA^2. \quad (2.36)$$

In this equation we have to assume that the correction to the frequency is small, $\omega_0 \gg aA^2$. One can show that [5]

$$a = -\frac{3\beta}{8\omega_0} - \frac{5\alpha^2}{12\omega_0^3}. \quad (2.37)$$

Problem 2.8. Verify that Eq. (2.37) gives the result (2.33) for the pendulum.

2.7 Nonlinear resonance

We saw in Section 2.2 that for a linear oscillator a resonant frequency can drive the amplitude to very large values, if the damping is small. The situation changes for a nonlinear oscillator. In this case, when the amplitude grows, the frequency of the oscillator changes and the oscillator detunes itself from the resonance.

Let us first make a rough estimate of the maximum amplitude of a nonlinear resonance. Take Eq. (2.11), set $\gamma = 0$ (no damping), replace ω_0 by $\omega_0 + aA^2$ and then set $\omega = \omega_0$ (the frequency of the driving force is equal to that of the *linear* oscillator). Using the smallness of aA^2 we find

$$A^2 \approx \frac{f_0^2}{(2a\omega_0 A^2)^2}. \quad (2.38)$$

This should be considered as an equation for A , from which we find

$$A \approx \left(\frac{f_0}{2a\omega_0} \right)^{1/3}. \quad (2.39)$$

We see that due to nonlinearity, even at exact resonance, the amplitude of the oscillations is finite: it is proportional to $a^{-1/3}$.

Lecture 3

Lagrangian and Hamiltonian equations of motion

The most general description of motion for a physical system is provided in terms of the Lagrange and the Hamilton functions. In this lecture we introduce the Lagrange equations of motion and discuss the transition from the Lagrange to the Hamilton equations. We write down the Lagrangian and Hamiltonian for a charged particle and introduce the Poisson brackets.

3.1 Lagrangian

How does one write equations of motion for a complicated mechanical system, like the spherical pendulum shown in Fig. 3.1? The Lagrangian formalism allows for easy formulation of such equations.

The first step in Lagrangian formulation consists of choosing *generalized coordinates* of the system, q_1, q_2, \dots, q_n , which uniquely define the state of the system. The number n is the number of degrees of freedom of our system. Each mechanical system possesses a Lagrangian function (or *Lagrangian* in short), which depends on the coordinates q_1, q_2, \dots, q_n , velocities $\dot{q}_1, \dot{q}_2, \dots, \dot{q}_n$ (with $\dot{q}_i = dq_i/dt$), and time t : $L(q_i, \dot{q}_i, t)$ [for brevity, we will write $L(q_i, \dot{q}_i, t)$ instead of $L(q_1, q_2, \dots, q_n, \dot{q}_1, \dot{q}_2, \dots, \dot{q}_n, t)$].

The Lagrangian has the following property: the integral

$$S = \int_{t_1}^{t_2} L(q_i, \dot{q}_i, t) dt \quad (3.1)$$

(which is called the *action*) reaches an extremum along the true trajectory of the system when varied with fixed end points, see Fig. 3.2. This property can be used directly to find trajectories of a system by numerically minimizing the

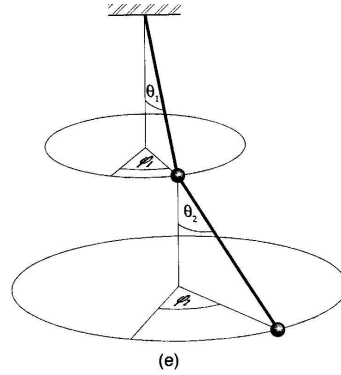


Figure 3.1: A spherical pendulum.

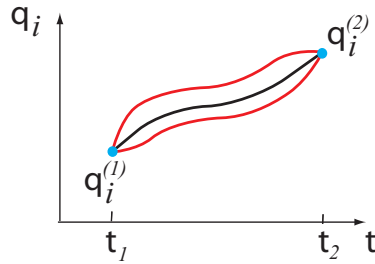


Figure 3.2: The Lagrangian reaches an extremum along the physical trajectory of the system.

action S . It is however not very practical, in part because the varied trajectory is specified by its initial, $q(t_1)$, and final, $q(t_2)$, positions. In applications we would prefer to specify a trajectory by its initial position and velocity instead.

For mechanical systems, the Lagrangian is equal to the difference between the kinetic energy and the potential energy of the system. For example, for the pendulum with the equation of motion given by Eq. (2.24), with the angle θ chosen as a generalized coordinate q , the Lagrangian is

$$L(\theta, \dot{\theta}) = \frac{m}{2} l^2 \dot{\theta}^2 + mgl \cos \theta. \quad (3.2)$$

As was mentioned above, knowing the Lagrangian is enough to be able to find trajectories of the pendulum by direct minimization of the action.

The most convenient approach to the problem of obtaining equations of motion for a given Lagrangian is based on the variational calculus. By direct

minimization of the action integral, requiring

$$\delta \int_{t_1}^{t_2} L(q_i, \dot{q}_i, t) dt = 0, \quad (3.3)$$

one can get equations of motion in the following form:

$$\frac{\partial L}{\partial q_i} - \frac{d}{dt} \frac{\partial L}{\partial \dot{q}_i} = 0, \quad i = 1, \dots, n. \quad (3.4)$$

These are ordinary differential equations which are much easier to solve than trying to directly minimize S .

Let us prove (3.4). Assume that $q_i(t)$ is a true orbit and $q(t_1)$ and $q(t_2)$ are fixed. Let $\delta q_i(t)$ be a deviation from this orbit; it has a property $\delta q_i(t_1) = \delta q_i(t_2) = 0$. Compute the variation of the action:

$$\begin{aligned} \delta \int_{t_1}^{t_2} L(q_i, \dot{q}_i, t) dt &= \\ &= \int_{t_1}^{t_2} L(q_i + \delta q_i, \dot{q}_i + \delta \dot{q}_i, t) dt - \int_{t_1}^{t_2} L(q_i, \dot{q}_i, t) dt \\ &= \int_{t_1}^{t_2} \left(\frac{\partial L}{\partial q_i} \delta q_i + \frac{\partial L}{\partial \dot{q}_i} \delta \dot{q}_i \right) dt \\ &= \int_{t_1}^{t_2} \left(\frac{\partial L}{\partial q_i} - \frac{d}{dt} \frac{\partial L}{\partial \dot{q}_i} \right) \delta q_i dt, \end{aligned} \quad (3.5)$$

where summation over repeated index i is assumed. Since $q_i(t)$ is a true orbit, the action reaches an extremum on it, and the variation of the action should be of second order, $\propto \delta q_i^2$. This means that the linear variation that we found above vanishes for arbitrary δq_i , hence Eq. (3.4) must be satisfied.

Problem 3.1. For a linear oscillator, the Lagrangian is

$$L = \frac{m}{2} \dot{x}^2 - \frac{m\omega^2}{2} x^2.$$

Find equations of motion.

The Lagrangian for a given system is not unique. There exist many Lagrangians for the same physical system that lead to identical equations of motion.

There are several advantages of using Lagrangian as a basic point for formulation of equations of motion: a) easy to choose convenient generalized coordinates, b) it is closely connected to the variational principles, and c) it relates symmetries of the Lagrangian to conservation laws for the system. One disadvantage is that the Lagrangian approach sometimes obscures the nature of the forces acting on the system.

A simple example of the relation between the symmetry of the Lagrangian and the conservation laws is given by the case when L does not depend on q_i . As follows from Eqs. (3.4), in this case the quantity $\partial L / \partial \dot{q}_i$ is conserved.

Problem 3.2. Consider a pendulum of length l and mass m , supported by a pivot that is driven in the vertical direction by a given function of time $y_s(t)$. Obtain the Lagrangian and derive equations of motion for the pendulum (Ref. [4], page 49).

Problem 3.3. Analyze particle's motion in a rotating frame using the Lagrangian approach (Ref. [2], pages 74-76).

3.2 Lagrangian of a relativistic particle in an electromagnetic field

This is the Lagrangian of a relativistic charged particle moving in electromagnetic field represented by the vector potential \mathbf{A} and the scalar potential ϕ :

$$\begin{aligned} L(\mathbf{r}, \mathbf{v}, t) &= -mc^2\sqrt{1 - v^2/c^2} + e\mathbf{v} \cdot \mathbf{A}(\mathbf{r}, t) - e\phi(\mathbf{r}, t) \\ &= -\gamma mc^2 + e\mathbf{v} \cdot \mathbf{A}(\mathbf{r}, t) - e\phi(\mathbf{r}, t), \end{aligned} \quad (3.6)$$

where $\gamma = (1 - \beta^2)^{-1/2}$ and $\beta = v/c$. In Cartesian coordinate system, $\mathbf{r} = (x, y, z)$, and the Lagrangian is given as a function $L(x, y, z, \dot{x}, \dot{y}, \dot{z}, t)$, where, of course, $\dot{x} = v_x$, $\dot{y} = v_y$, $\dot{z} = v_z$.

Problem 3.4. Derive equations of motion (1.8) from the Lagrangian (3.6).

As an example of using the Lagrangian formalism, let us study particle's motion in a uniform magnetic field using the above Lagrangian.

The field is directed along the z -axis:

$$\mathbf{B} = (0, 0, B_0). \quad (3.7)$$

It is easy to check that the vector potential can be chosen as

$$\mathbf{A} = (-B_0 y, 0, 0), \quad (3.8)$$

so that $\mathbf{B} = \nabla \times \mathbf{A}$. This gives for the Lagrangian

$$L = -mc^2\sqrt{1 - v^2/c^2} - eB_0 v_x y. \quad (3.9)$$

Let's first consider the direction of motion along the field. For the z -direction we have

$$\frac{d}{dt} \frac{\partial L}{\partial v_z} = 0 \quad \implies \quad \dot{v}_z = 0 \quad \implies \quad v_z = \text{const}. \quad (3.10)$$

We will now prove that motion in the constant magnetic field conserves the particle energy, $\gamma = \text{const}$. Since $v_z = \text{const}$, we need to prove that $v_x^2 + v_y^2 = \text{const}$. For the equation of motion in the x direction $\partial L/\partial x - d/dt(\partial L/\partial v_x) = 0$ we use the following formulae: $\partial L/\partial x = 0$ and $\partial L/\partial v_x = mc^2\gamma v_x/c^2 - eB_0 y$ which give

$$\frac{\partial L}{\partial x} - \frac{d}{dt} \frac{\partial L}{\partial v_x} = -m \frac{d\gamma v_x}{dt} + eB_0 v_y = 0. \quad (3.11)$$

The Lagrange equation in the y -direction gives

$$\frac{\partial L}{\partial y} - \frac{d}{dt} \frac{\partial L}{\partial v_y} = -m \frac{d\gamma v_y}{dt} - eB_0 v_x = 0. \quad (3.12)$$

Multiplying (3.11) by v_x and multiplying (3.12) by v_y and adding them gives

$$v_y \frac{d\gamma v_y}{dt} + v_x \frac{d\gamma v_x}{dt} = 0, \quad (3.13)$$

from which it follows that $\dot{\gamma} = 0$ (Why?). With $\dot{\gamma} = 0$ the equation (3.11) reads

$$\dot{v}_x = \omega_H v_y, \quad (3.14)$$

where the *cyclotron* frequency ω_H is

$$\omega_H = \frac{eB_0}{\gamma m}. \quad (3.15)$$

Eq. (3.12) reads

$$\dot{v}_y = -\omega_H v_x. \quad (3.16)$$

Combining Eqs. (3.14) and (3.16) yields $\ddot{v}_x + \omega_H^2 v_x = 0$, with the solution $v_x = v_0 \cos(\omega_H t + \phi_0)$. From Eq. (3.14) we then obtain $v_y = -v_0 \sin(\omega_H t + \phi_0)$. Integrating velocities, we find coordinates:

$$x = \frac{v_0}{\omega_H} \sin(\omega_H t + \phi_0) + x_0, \quad y = \frac{v_0}{\omega_H} \cos(\omega_H t + \phi_0) + y_0. \quad (3.17)$$

This is a circular orbit with the radius (*Larmor radius*)

$$R = \frac{v_0}{\omega_H} = \frac{p}{eB_0}. \quad (3.18)$$

Problem 3.5. Write the same Lagrangian in the cylindrical coordinate system with z directed along the magnetic field. Derive the equations of motion.

Problem 3.6. Do the same for the coordinate system (x', s, z) shown in Fig. 3.3.

Problem 3.7. The same magnetic field (3.7) can be represented by a different vector potential $\mathbf{A} = \frac{1}{2}(-B_0 y, B_0 x, 0)$. Show that the equations of motion are the same as for the vector potential (3.8).

3.3 From Lagrangian to Hamiltonian

Another way to describe a system motion is to use the Hamiltonian approach. It has some advantages over the Lagrangian one.

A transition from the Lagrangian to the Hamiltonian is made in three steps. First, we define the *generalized momenta* p_i :

$$p_i(q_k, \dot{q}_k, t) = \frac{\partial L(q_k, \dot{q}_k, t)}{\partial \dot{q}_i}, \quad i = 1, \dots, n. \quad (3.19)$$

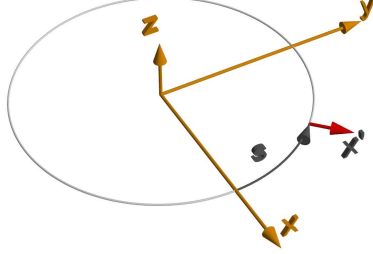


Figure 3.3: The coordinate system x', s, z . The circle radius is equal to the Larmor radius R . The coordinate x' is defined as a difference between the polar radius r and the circle radius R .

Second, from the n equations $p_i = p_i(q_k, \dot{q}_k, t)$, $i = 1, \dots, n$ we express all the variables \dot{q}_i in terms of $q_1, q_2, \dots, q_n, p_1, p_2, \dots, p_n$ and t

$$\dot{q}_i = \dot{q}_i(p_k, q_k, t), \quad i = 1, \dots, n. \quad (3.20)$$

Third, we construct a *Hamiltonian function* H as

$$H = \sum_{i=1}^n p_i \dot{q}_i - L(q_k, \dot{q}_k, t), \quad (3.21)$$

and express all \dot{q}_i on the right hand side through q_i, p_i and t using Eqs. (3.20) so that we get the Hamiltonian as a function of variables q_i, p_i and t : $H(q_1, q_2, \dots, q_n, p_1, p_2, \dots, p_n, t)$.

We claim that, with the Hamiltonian, the equations of motion of our system become:

$$\dot{p}_i = -\frac{\partial H}{\partial q_i}, \quad \dot{q}_i = \frac{\partial H}{\partial p_i}. \quad (3.22)$$

The variables p_i and q_i are called the *canonically conjugate* variables. Let us prove (3.22):

$$\begin{aligned} -\left(\frac{\partial H}{\partial q_i}\right)_p &= -\frac{\partial}{\partial q_i} \left(\sum_{k=1}^n p_k \dot{q}_k - L \right) = \sum_{k=1}^n \left(-p_k \frac{\partial \dot{q}_k}{\partial q_i} + \frac{\partial L}{\partial \dot{q}_k} \frac{\partial \dot{q}_k}{\partial q_i} \right) + \frac{\partial L}{\partial q_i} \\ &= \frac{\partial L}{\partial q_i} = \frac{d}{dt} \frac{\partial L}{\partial \dot{q}_i} = \frac{dp_i}{dt} \end{aligned} \quad (3.23)$$

$$\left(\frac{\partial H}{\partial p_i}\right)_q = \frac{\partial}{\partial p_i} \left(\sum_k p_k \dot{q}_k - L \right) = \dot{q}_i + \sum_k \left(p_k \frac{\partial \dot{q}_k}{\partial p_i} - \frac{\partial L}{\partial \dot{q}_k} \frac{\partial \dot{q}_k}{\partial p_i} \right) = \dot{q}_i \quad (3.24)$$

3.4 Hamiltonian of a charged particle in an electromagnetic field

We start from the Lagrangian (3.6)

$$L(\mathbf{r}, \mathbf{v}, t) = -mc^2 \sqrt{1 - v^2/c^2} + e\mathbf{v} \cdot \mathbf{A}(\mathbf{r}, t) - e\phi(\mathbf{r}, t).$$

First, we need to find the canonical conjugate momentum which we denote by $\boldsymbol{\pi}$ combining into vector notation three cartesian coordinates (π_x, π_y, π_z) :

$$\begin{aligned} \boldsymbol{\pi} &= \frac{\partial L}{\partial \mathbf{v}} \\ &= -mc^2 \frac{\partial \sqrt{1 - v^2/c^2}}{\partial \mathbf{v}} + e\mathbf{A} \\ &= m \frac{\mathbf{v}}{\sqrt{1 - v^2/c^2}} + e\mathbf{A} \\ &= m\gamma\mathbf{v} + e\mathbf{A}. \end{aligned} \tag{3.25}$$

Note that the conjugate momentum $\boldsymbol{\pi}$ differs from the kinetic particle's momentum $m\gamma\mathbf{v}$. Before proceeding, note also that as follows from the previous equation, $\gamma\boldsymbol{\beta} = (\boldsymbol{\pi} - e\mathbf{A})/mc$, and hence

$$\gamma^2\boldsymbol{\beta}^2 = \frac{(\boldsymbol{\pi} - e\mathbf{A})^2}{m^2c^2}. \tag{3.26}$$

Now let us derive the Hamiltonian

$$\begin{aligned} H &= \mathbf{v} \cdot \boldsymbol{\pi} - L \\ &= \mathbf{v} \cdot \boldsymbol{\pi} + mc^2 \sqrt{1 - v^2/c^2} - e\mathbf{v} \cdot \mathbf{A} + e\phi \\ &= m\gamma v^2 + \frac{mc^2}{\gamma} + e\phi \\ &= m\gamma c^2 \left(\beta^2 + \frac{1}{\gamma^2} \right) + e\phi \\ &= m\gamma c^2 + e\phi. \end{aligned} \tag{3.27}$$

Remarkably, the Hamiltonian is the sum of the particle's energy $m\gamma c^2$ and the potential energy associated with the electrostatic potential ϕ . The vector potential \mathbf{A} does not show up in this expression. This, however, is misleading—the vector potential is hidden in Eq. (3.27). To see that, remember, the we need to express H in terms of the conjugate coordinates \mathbf{r} and momenta $\boldsymbol{\pi}$. Using Eq. (3.26) we obtain:

$$\gamma^2 = 1 + \gamma^2\boldsymbol{\beta}^2 = 1 + \frac{(\boldsymbol{\pi} - e\mathbf{A})^2}{m^2c^2}, \tag{3.28}$$

which gives for the Hamiltonian

$$H(\mathbf{r}, \boldsymbol{\pi}, t) = \sqrt{(mc^2)^2 + c^2(\boldsymbol{\pi} - e\mathbf{A}(\mathbf{r}, t))^2} + e\phi(\mathbf{r}, t), \tag{3.29}$$

where now we explicitly indicated all the variables involved in the Hamiltonian.

Problem 3.8. Find conjugate momenta in cylindrical coordinates of a charged particle moving in electromagnetic field.

3.5 Poisson brackets

Let $f(q_i, p_i, t)$ be a function of coordinate, momenta and time. Assume that coordinates and momenta evolve according to the Hamilton equations, and $q_i(t)$ and $p_i(t)$ represent a trajectory. Then f becomes a function of time t only: $f(q_i(t), p_i(t), t)$. What is the derivative of this function with respect to time? We have

$$\frac{df}{dt} = \frac{\partial f}{\partial t} + \sum_i \left(\frac{\partial f}{\partial q_i} \dot{q}_i + \frac{\partial f}{\partial p_i} \dot{p}_i \right). \quad (3.30)$$

Substituting Eqs. (3.22) into those equations gives

$$\begin{aligned} \frac{df}{dt} &= \frac{\partial f}{\partial t} + \sum_i \left(\frac{\partial f}{\partial q_i} \frac{\partial H}{\partial p_i} - \frac{\partial f}{\partial p_i} \frac{\partial H}{\partial q_i} \right) \\ &= \frac{\partial f}{\partial t} + \{H, f\}, \end{aligned} \quad (3.31)$$

where we introduced the *Poisson brackets*

$$\{H, f\} = \sum_i \left(\frac{\partial H}{\partial p_i} \frac{\partial f}{\partial q_i} - \frac{\partial H}{\partial q_i} \frac{\partial f}{\partial p_i} \right). \quad (3.32)$$

Poisson brackets have many remarkable properties. We will use the following two in the next lectures. For two functions $f(q_i, p_i, t)$ and $g(q_i, p_i, t)$

$$\{g, f\} = -\{f, g\}, \quad (3.33)$$

and also

$$\{f, f\} = 0. \quad (3.34)$$

If $df/dt = 0$, then it is an *integral of motion*. Note that if $f(q_i, p_i)$ does not depend on time, it is an integral of motion if and only if $\{H, f\} = 0$, as follows from (3.31). A Hamiltonian that does not depend explicitly on time is an integral of motion, as follows from the identity $\{H, H\} = 0$.

It is easy to verify that following identities hold

$$\{q_i, q_k\} = \{p_i, p_k\} = 0, \quad \{p_i, q_k\} = \delta_{ik}. \quad (3.35)$$

Problem 3.9. The angular momentum \mathbf{M} of a particle is defined as $\mathbf{M} = \mathbf{r} \times \mathbf{p}$. Find the Poisson brackets $\{M_i, x_k\}$, $\{M_i, p_k\}$ and $\{M_i, M_k\}$, where the indices i and k take the values x, y and z .

Problem 3.10. Simplify L and H in the nonrelativistic limit $v \ll c$.

Lecture 4

Canonical transformations

We saw that within the Lagrangian approach we can choose the generalized coordinates as we please. We can start with a set of coordinates q_i and then introduce generalized momenta p_i according to Eqs. (3.19) and form a Hamiltonian (3.21). Or, we can choose another set of generalized coordinates $Q_i = Q_i(q_k, t)$, express the Lagrangian as a function of Q_i , go through Eqs. (3.19) and (3.21), and obtain a different set of momenta P_i and a different Hamiltonian $H'(Q_i, P_i, t)$. Although mathematically different, these two representations are physically equivalent—they describe the same dynamics of our physical system. Understanding the freedom that we have in the choice of the conjugate variables for a Hamiltonian is important: a judicious choice of the variables would allow us to simplify the description of the system dynamics.

A more general approach to the problem of using various variables in Hamiltonian formulation of equations of motion is the following. Let us assume that we have canonical variables q_i, p_i and the corresponding Hamiltonian $H(q_i, p_i, t)$ and then make a transformation to new variables

$$Q_i = Q_i(q_k, p_k, t), \quad P_i = P_i(q_k, p_k, t). \quad i = 1 \dots n. \quad (4.1)$$

Can we find a new Hamiltonian $H'(Q_i, P_i, t)$ such that the system motion in new variables is also Hamiltonian? What are the requirements on the transformation (4.1) for such a Hamiltonian to exist?

These questions lead us to the notion of the *canonical transformation*.

4.1 Canonical transformations

We first consider a time independent Hamiltonian H , and later generalize the result for the case when H is a function of time. Let us assume that we have canonical variables q_i, p_i and the Hamiltonian $H(q_i, p_i)$. Instead of q_i, p_i we would like to use a new set of independent variables Q_i, P_i that are related to the old one, see Fig. 4.1,

$$Q_i = Q_i(q_k, p_k), \quad P_i = P_i(q_k, p_k), \quad i = 1 \dots n. \quad (4.2)$$

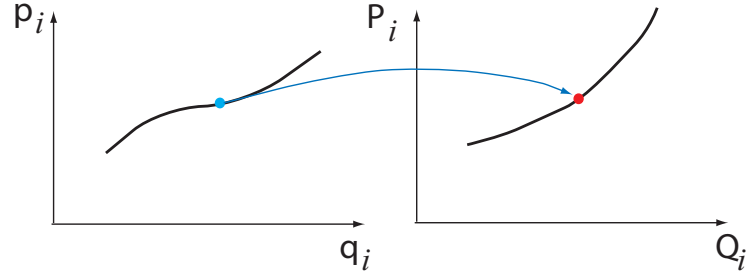


Figure 4.1: Transformation to new variables: a point in the old phase space maps to a point in the new space, and an old orbit is transformed to a new one.

We assume that there exists an inverse transformation from Q_i, P_i to q_i, p_i and write it as follows

$$q_i = q_i(Q_k, P_k), \quad p_i = p_i(Q_k, P_k), \quad i = 1 \dots n. \quad (4.3)$$

It is obtained by considering Eqs. (4.2) as $2n$ equations for the old variables and solving them for q_i, p_i .

Substituting (4.3) in H we can express our Hamiltonian in terms of the new variables:

$$H'(Q_k, P_k) = H(q_i(Q_k, P_k), p_i(Q_k, P_k)), \quad (4.4)$$

where we denote the new function by H' . Let us assume that we solved the Hamiltonian equations (3.22) and found a trajectory $q_i(t), p_i(t)$. This trajectory gives us, through the transformation (4.2), an orbit in new variables as well:

$$Q_i(t) = Q_i(q_i(t), p_i(t)), \quad P_i(t) = P_i(q_i(t), p_i(t)). \quad (4.5)$$

We would like the trajectory defined by the functions $Q_i(t)$ and $P_i(t)$ to be a Hamiltonian orbit, that is to say that we would like it to satisfy the equations

$$\frac{dP_i}{dt} = -\frac{\partial H'(Q_k(t), P_k(t))}{\partial Q_i}, \quad \frac{dQ_i}{dt} = \frac{\partial H'(Q_k(t), P_k(t))}{\partial P_i}. \quad (4.6)$$

If those conditions are satisfied for *every Hamiltonian* H , then the variable transformation (4.2) gives us a *canonical transformation*.

Here are two trivial examples of canonical transformations:

$$Q_i = p_i, \quad P_i = -q_i. \quad (4.7)$$

$$Q_i = -p_i, \quad P_i = q_i. \quad (4.8)$$

Problem 4.1. Later we will also use in one case a transformation that is not canonical. Show that the transformation $P_i = \lambda p_i, Q_i = q_i, H' = \lambda H$, where λ is a constant parameter, preserves the Hamiltonian structure of equations.

4.2 Poisson brackets and canonical transformations

We will now show how to find out if a given transformation (4.2) is canonical. The proof is based on the invariance of the Poisson brackets with respect to canonical transformations.

Let us assume that we have two arbitrary functions of canonical variables, $f(q_i, p_i)$ and $g(q_i, p_i)$, and calculate their Poisson brackets:

$$\{f, g\}_{q,p} = \sum_i \left(\frac{\partial f}{\partial p_i} \frac{\partial g}{\partial q_i} - \frac{\partial f}{\partial q_i} \frac{\partial g}{\partial p_i} \right) \equiv J(q, p), \quad (4.9)$$

where, on the left hand side, we now indicate the variables with respect to which the Poisson brackets are calculated. Using the inverse transformation (4.3) we can express our functions in terms of the new variables Q_i and P_i ; the resulting new functions are denoted as f' and g' : $f'(Q_i, P_i)$ and $g'(Q_i, P_i)$. Let us also calculate the Poisson brackets of the new functions with respect to the new variables:

$$\{f', g'\}_{Q,P} = \sum_i \left(\frac{\partial f'}{\partial P_i} \frac{\partial g'}{\partial Q_i} - \frac{\partial f'}{\partial Q_i} \frac{\partial g'}{\partial P_i} \right) \equiv J_1(Q, P). \quad (4.10)$$

It turns out that if $q_i, p_i \rightarrow Q_i, P_i$ is a canonical transformation, then expressing in $J_1(Q, P)$ the new variables through the old ones gives $J(q, p)$:

$$J_1(Q_i(q_k, p_k), P_i(q_k, p_k)) = J(q_k, p_k). \quad (4.11)$$

To prove this statement let us consider $g(q_i, p_i)$ as a Hamiltonian of a fictitious system. Then according to (3.31)

$$\{f, g\}_{q,p} = -\frac{df}{dt}; \quad (4.12)$$

it is a time derivative taken along the orbit $q_i(t), p_i(t)$, which is computed with the Hamiltonian $g(q_i, p_i)$, see Fig. 4.1. When we formally change to new variables Q_i and P_i in f , the same function $f(t)$ is now given by $f(t) = f'(Q_i(t), P_i(t))$, where $(Q_i(t), P_i(t))$ is the orbit in the new phase space. If the transformation is canonical, the orbit $(Q_i(t), P_i(t))$ satisfies Hamiltonian equation of motions with the new ‘‘Hamiltonian’’ $g'(Q_i, P_i)$. Hence

$$\{f', g'\}_{Q,P} = -\frac{df'}{dt}, \quad (4.13)$$

and using (4.12) we conclude that

$$\{f, g\}_{q,p} = \{f', g'\}_{Q,P}, \quad (4.14)$$

which proves Eq. (4.11) for arbitrary functions f and g .

Let us now choose two arbitrary indices i and k and set $f = Q_i(q_l, p_l)$ and $g = Q_k(q_l, p_l)$. Eq. (4.11) then gives

$$\{Q_i, Q_k\}_{q,p} = \{Q_i, Q_k\}_{Q,P} = 0, \quad (4.15)$$

where we used Eqs. (3.35). Similarly, choosing $f = P_i(q_l, p_l)$ and $g = P_k(q_l, p_l)$ gives

$$\{P_i, P_k\}_{q,p} = \{P_i, P_k\}_{Q,P} = 0, \quad (4.16)$$

and choosing $f = P_k(q_l, p_l)$ and $g = Q_i(q_l, p_l)$ gives

$$\{P_k, Q_i\}_{q,p} = \{P_k, Q_i\}_{Q,P} = \delta_{ik}. \quad (4.17)$$

To summarize, we proved that if Eqs. (4.2) represent a canonical transformation, for any pair of indexes i and k we should have

$$\{Q_i, Q_k\}_{q,p} = \{P_i, P_k\}_{q,p} = 0, \quad \{P_k, Q_i\}_{q,p} = \delta_{ik}, \quad (4.18)$$

that is they are *necessary* conditions for a transformation to be canonical. It turns out (but we do not prove it here), that they also are a *sufficient* condition for a transformation to be canonical. That is if Eqs. (4.18) are satisfied for all pairs i and k , the transformation will be canonical.

Problem 4.2. *Using the Poisson brackets prove that the transformations Eqs. (4.7) and (4.8) are canonical.*

4.3 Generating functions

Poisson brackets helped us to figure out if a given transformation is canonical. They do not, however, provide a method to generate canonical transformations. The technique which allows one to create a transformation that is guaranteed to be canonical is based on the technique of the so called *generating functions*.

We will give a complete formulation of the method of generation functions in the next section. In this section, we consider a special case of a time independent generating function of first type, F_1 . Such a generating function depends on $2n$ variables: n old coordinates q_i and n new coordinates Q_i :

$$F_1(q_i, Q_i). \quad (4.19)$$

Having chosen an arbitrary (smooth) function F_1 , one can generate a transformation of variables (4.1) using the following equations:

$$p_k = \frac{\partial F_1(q_i, Q_i)}{\partial q_k}, \quad P_k = -\frac{\partial F_1(q_i, Q_i)}{\partial Q_k}, \quad k = 1 \dots n. \quad (4.20)$$

Indeed, one can consider n relations $p_k = \partial F_1(q_i, Q_i)/\partial q_k$, $k = 1 \dots n$ as equations for n variables Q_i , and solving them find n functions $Q_i(q_k, p_k)$, $i = 1 \dots n$. Substituting these functions in the right hand side of $P_k = -\partial F_1(q_i, Q_i)/\partial Q_k$

gives n functions $P_k(q_i, p_i)$, $k = 1 \dots n$, in terms of the old variables. It turns out that obtained in such a way transformation of variables is canonical.

We will not give here a full proof of this statement, which can be found in textbooks on classical mechanics. Instead, we will prove here only that Eqs. (4.20) define a canonical transformation in the case of one degree of freedom. In this case, we have two conjugate variables, q and p , and a canonical transformation (4.2) is determined by the two equations

$$Q = Q(q, p), \quad P = P(q, p). \quad (4.21)$$

The generating function $F_1(q, Q)$ is a function of two variables, and from (4.20) we have

$$p = \frac{\partial F_1(q, Q)}{\partial q}, \quad P = -\frac{\partial F_1(q, Q)}{\partial Q}. \quad (4.22)$$

What we need to do is to verify that from (4.22) follow (4.18). Since in one dimension $i = k = 1$ in (4.18), and identically $\{Q, Q\} = \{P, P\} = 0$, we only need to prove that

$$\{P, Q\}_{q,p} = \frac{\partial P}{\partial p} \frac{\partial Q}{\partial q} - \frac{\partial P}{\partial q} \frac{\partial Q}{\partial p} = 1. \quad (4.23)$$

From the second of Eqs. (4.22) we have

$$\frac{\partial P}{\partial q} = -\frac{\partial^2 F_1}{\partial Q \partial q} - \frac{\partial^2 F_1}{\partial Q^2} \frac{\partial Q}{\partial q}, \quad \frac{\partial P}{\partial p} = -\frac{\partial^2 F_1}{\partial Q^2} \frac{\partial Q}{\partial p}. \quad (4.24)$$

Substituting these equation into Eq. (4.23) we obtain

$$\frac{\partial P}{\partial p} \frac{\partial Q}{\partial q} - \frac{\partial P}{\partial q} \frac{\partial Q}{\partial p} = \frac{\partial^2 F_1}{\partial Q \partial q} \frac{\partial Q}{\partial p}. \quad (4.25)$$

The derivative $\partial Q / \partial p$ can be found when we differentiate the first of equations (4.22) with respect to p :

$$1 = \frac{\partial^2 F_1}{\partial q \partial Q} \frac{\partial Q}{\partial p}, \quad (4.26)$$

from which we find

$$\frac{\partial Q}{\partial p} = \left(\frac{\partial^2 F_1}{\partial q \partial Q} \right)^{-1}. \quad (4.27)$$

Substituting this into Eq. (4.25) gives

$$\{P, Q\}_{q,p} = 1. \quad (4.28)$$

The functions (4.19) are not the only type of functions that generate canonical transformations. Below we will list other types that can be used for this purpose. Before that, however, we need to generalize our result for the time dependent transformations and time dependent Hamiltonians.

4.4 Time depending transformations and four types of generating functions

Canonical transformations can be time dependent,

$$Q_i = Q_i(q_k, p_k, t), \quad P_i = P_i(q_k, p_k, t). \quad i = 1 \dots n. \quad (4.29)$$

They can be applied to time dependent Hamiltonians as well. The Poisson brackets are still applicable in this case, and Eqs. (4.18) are necessary and sufficient conditions for a transformation to be canonical (the variable t can be considered as a parameter in calculation of the Poisson brackets). However, a simple rule (4.4) for obtaining a new Hamiltonian is not valid in the general case of time depending transformations—it should be modified as shown below.

In Section (4.3) we introduced the generating function $F_1(q_i, Q_i)$. This is only one of four possible types of the generating functions. All generating functions depend on a set of n old coordinates and a set of n new ones. These sets come in the following combinations: (q_i, Q_i) , (q_i, P_i) , (p_i, Q_i) , and (p_i, P_i) . Correspondingly, we have 4 types of the generating function. The rules how to make a canonical transformation for each type of the generating function, and the associated transformation of the Hamiltonian, are shown below.

The first type of the generating functions is $F_1(q_i, Q_i, t)$:

$$\begin{aligned} p_i &= \frac{\partial F_1}{\partial q_i}, & P_i &= -\frac{\partial F_1}{\partial Q_i}, \\ H' &= H + \frac{\partial F_1}{\partial t}. \end{aligned} \quad (4.30)$$

The second type is $F_2(q_i, P_i, t)$:

$$\begin{aligned} p_i &= \frac{\partial F_2}{\partial q_i}, & Q_i &= \frac{\partial F_2}{\partial P_i}, \\ H' &= H + \frac{\partial F_2}{\partial t}. \end{aligned} \quad (4.31)$$

The third type is $F_3(p_i, Q_i, t)$:

$$\begin{aligned} q_i &= -\frac{\partial F_3}{\partial p_i}, & P_i &= -\frac{\partial F_3}{\partial Q_i}, \\ H' &= H + \frac{\partial F_3}{\partial t}. \end{aligned} \quad (4.32)$$

The fourth type is $F_4(p_i, P_i, t)$:

$$\begin{aligned} q_i &= -\frac{\partial F_4}{\partial p_i}, & Q_i &= \frac{\partial F_4}{\partial P_i}, \\ H' &= H + \frac{\partial F_4}{\partial t}. \end{aligned} \quad (4.33)$$

Problem 4.3. Find generating functions for the transformations (4.7) and (4.8).

Problem 4.4. Find generating functions for the contact transformation

$$Q_i = Q_i(q_1, q_2, \dots, q_n). \quad (4.34)$$

4.5 Examples of canonical transformations

We first consider a simple example of the identity transformation

$$Q_i = q_i, \quad P_i = p_i. \quad (4.35)$$

The generating function of the second type for this transformation is

$$F_2 = \sum_{i=1}^n q_i P_i. \quad (4.36)$$

Problem 4.5. Find the generating function of the third type for the transformation (4.35). This problem illustrates the fact that the choice of the type of the generating function is not unique.

We now show how canonical transformations can be applied to the harmonic oscillator. The Hamiltonian for an oscillator with a unit mass is

$$H = \frac{p^2}{2} + \frac{\omega^2 x^2}{2}. \quad (4.37)$$

It gives the following equations of motion: $\dot{p} = -\partial H/\partial x = -\omega^2 x$, $\dot{x} = \partial H/\partial p = p$ with the solution

$$x = a \cos(\omega t + \phi_0), \quad p = -a \sin(\omega t + \phi_0). \quad (4.38)$$

We would like to introduce a set of new variables, J (new momentum) and ϕ (new coordinate), such that the transformation from new to old coordinates would be

$$x = a(J) \cos \phi, \quad p = -a(J) \omega \sin \phi. \quad (4.39)$$

The advantage of the new variables is clear: the new momentum J is a constant of motion (because $a = \text{const}$), and the new coordinate evolves in a simple way, $\phi = \omega t + \phi_0$.

We will try to construct the canonical transformation (4.39) using a generating function $F_1(x, \phi)$ of the first type. For this we need to express p in terms of the old (x) and new (ϕ) coordinates eliminating $a(J)$ from (4.39),

$$p = -\omega x \tan \phi. \quad (4.40)$$

Now integrating the equation $(\partial F_1/\partial x)_\phi = p = -\omega x \tan \phi$, we find

$$F_1(x, \phi) = \int p dx = -\frac{\omega x^2}{2} \tan \phi. \quad (4.41)$$

We then have

$$\begin{aligned} J &= -\frac{\partial F_1}{\partial \phi} \\ &= \frac{\omega x^2}{2} \frac{1}{\cos^2 \phi} \\ &= \frac{\omega x^2}{2} (1 + \tan^2 \phi) \\ &= \frac{\omega x^2}{2} \left(1 + \frac{p^2}{\omega^2 x^2} \right) \\ &= \frac{1}{2\omega} (\omega^2 x^2 + p^2). \end{aligned} \quad (4.42)$$

This equation expresses the new momentum in terms of the old variables. The new coordinate can be found from Eq. (4.40)

$$\phi = -\arctan \frac{p}{\omega x}. \quad (4.43)$$

Problem 4.6. From Eqs. (4.42) and (4.43) express x and p through J and ϕ . Verify that the result agrees with Eqs. (4.39).

The new Hamiltonian is a function of the new momentum only

$$H = \omega J, \quad (4.44)$$

and gives the following equations of motion in new variables:

$$\dot{J} = -\frac{\partial H}{\partial \phi} = 0, \quad \dot{\phi} = \frac{\partial H}{\partial J} = \omega. \quad (4.45)$$

The oscillator dynamics looks very simple in new coordinates:

$$J = \text{const}, \quad \phi = \omega t + \phi_0. \quad (4.46)$$

The (J, ϕ) pair is called the *action-angle* coordinates for this particular case. They are very useful for building a perturbation theory in a system which in the zeroth approximation reduces to a linear oscillator.

Lecture 5

Liouville's theorem. Action-angle variables.

We take a geometrical look at the Hamilton equations of motion, talk about action-angle variables and the CPT symmetries in classical mechanics.

5.1 Hamiltonian flow in phase space. Symplectic maps

We will now take another look at the Hamiltonian motion focusing on its geometrical aspect. Let us assume that for a Hamiltonian $H(q_i, p_i, t)$, for every set of initial condition p_i^0, q_i^0 from some domain, we can solve the equations of motion starting from an initial time t_0 and find the values p_i, q_i at time t . This gives us a *map*

$$p_i = p_i(p_i^0, q_i^0, t_0, t), \quad q_i = q_i(p_i^0, q_i^0, t_0, t). \quad (5.1)$$

Considering now the time t as a parameter and varying it will move each point (q_i, p_i) along a trajectory in the $2n$ dimensional phase space. A collection of such trajectories starting from some set of initial conditions (q_i^0, p_i^0) constitutes a *Hamiltonian flow*, see Fig. 5.1.

In accelerator context one can associate, for example, each trajectory (5.1) with a different particle in a beam. Assume that one has a beam diagnostic at one location of the ring, which measures coordinates of particles when the beam passes by at time t_0 . On the next turn, at time $t = t_0 + T$, where T is the revolution period in the ring, it measures coordinates again. The relation between the new and the old coordinates will be given by the functions (5.1).

A remarkable feature of the relations (5.1) is that, for a given t_0 and t , they constitute a canonical transformation from p_i^0, q_i^0 to p_i, q_i , which is also called a *symplectic* transfer map. We are not going to prove the canonical properties of this map in the general case of n degrees of freedom, however we

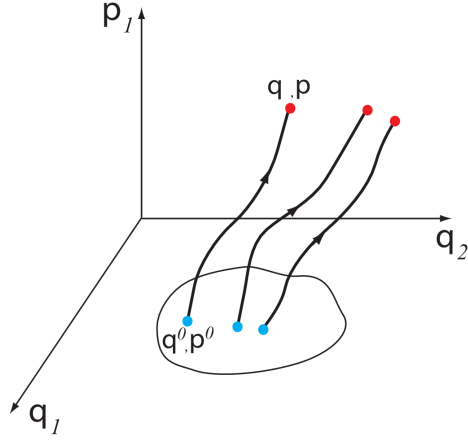


Figure 5.1: Hamiltonian flow in phase space.

will demonstrate it for the case of one degree of freedom dropping the index i , $p_i \rightarrow p$, $q_i \rightarrow q$.

The proof is based on calculation of the time derivatives of the Poisson brackets $\{pq\}_{q^0, p^0}$, $\{pp\}_{q^0, p^0}$ and $\{qq\}_{q^0, p^0}$ and demonstration that they equal to zero. Since at the initial time $t = t_0$ the transformation from p^0, q^0 to p, q is the identity transformation ($p = p^0, q = q^0$), it is clearly canonical. Conservation of the Poisson brackets in time then means that it remains canonical for all values of t .

In what follows, we will focus on calculation of the time derivative of $\{pq\}_{q^0, p^0}$; the others brackets can be analyzed in a similar way. We have

$$\begin{aligned}
 \frac{d}{dt}\{pq\}_{q^0, p^0} &= \frac{d}{dt} \left(\frac{\partial p}{\partial p^0} \frac{\partial q}{\partial q^0} - \frac{\partial p}{\partial q^0} \frac{\partial q}{\partial p^0} \right) \\
 &= \frac{\partial q}{\partial q^0} \frac{\partial}{\partial p^0} \frac{dp}{dt} + \frac{\partial p}{\partial p^0} \frac{\partial}{\partial q^0} \frac{dq}{dt} - \frac{\partial q}{\partial p^0} \frac{\partial}{\partial q^0} \frac{dp}{dt} - \frac{\partial p}{\partial q^0} \frac{\partial}{\partial p^0} \frac{dq}{dt} \\
 &= -\frac{\partial q}{\partial q^0} \frac{\partial}{\partial p^0} \frac{\partial H}{\partial q} + \frac{\partial p}{\partial p^0} \frac{\partial}{\partial q^0} \frac{\partial H}{\partial p} + \frac{\partial q}{\partial p^0} \frac{\partial}{\partial q^0} \frac{\partial H}{\partial q} - \frac{\partial p}{\partial q^0} \frac{\partial}{\partial p^0} \frac{\partial H}{\partial p}.
 \end{aligned} \tag{5.2}$$

Using the chain rules for calculation of the partial derivatives

$$\frac{\partial}{\partial p^0} = \frac{\partial p}{\partial p^0} \frac{\partial}{\partial p} - \frac{\partial q}{\partial p^0} \frac{\partial}{\partial q}, \quad \frac{\partial}{\partial q^0} = \frac{\partial p}{\partial q^0} \frac{\partial}{\partial p} - \frac{\partial q}{\partial q^0} \frac{\partial}{\partial q} \tag{5.3}$$

it is easy to show that all the terms on the right hand side of (5.2) cancel and $d\{pq\}_{q^0, p^0}/dt = 0$.

Somewhat different language of *symplectic maps* is often used in connection with canonical transformation (5.1) or (4.2). A symplectic map is defined with

the help of the matrix J_{2n} :

$$J_{2n} = \begin{pmatrix} J_2 & 0 & 0 & 0 \\ 0 & J_2 & 0 & 0 \\ 0 & 0 & \ddots & 0 \\ 0 & 0 & 0 & J_2 \end{pmatrix}, \quad (5.4)$$

where

$$J_2 = \begin{pmatrix} 0 & -1 \\ 1 & 0 \end{pmatrix}. \quad (5.5)$$

Let us consider the transformation (4.2) and change the notation introducing $w_{2k-1} = q_k$, $w_{2k} = p_k$, $W_{2k-1} = Q_k$, $W_{2k} = P_k$, $k = 1, 2, \dots, n$. For examples, for $n = 2$ we have $w_1 = q_1$, $w_2 = p_1$, $w_3 = q_2$, $w_4 = p_2$, and the same set of relations with small letters replaced by the capital ones. A transformation from old to new variables is then given by $2n$ functions

$$W_i = W_i(w_k), \quad i, k = 1, 2, \dots, 2n. \quad (5.6)$$

It turns out that the requirement that all possible Poisson brackets satisfy Eqs. (4.15), (4.16) and (4.17) (which, as we know is equivalent to the requirement for the transformation to be canonical) can be written as

$$MJ_{2n}M^T = J_{2n}, \quad (5.7)$$

where M is the Jacobian matrix of the transformation (with the elements $M_{i,j} = \partial W_i / \partial w_j$) and the superscript T denotes transposition of a matrix.

Problem 5.1. Derive (5.7) for $n = 2$.

5.2 Action-angle variables in 1D

In this section we introduce the action-angle variables for a system with one degree of freedom.

Let us now consider a one-dimensional system with the Hamiltonian

$$H = \frac{p^2}{2} + U(x), \quad (5.8)$$

where $U(x)$ is a function sketched in Fig. 5.2a, and we assume a unit mass of the particle. The phase trajectories are shown in Fig. 5.2b; each trajectory is characterized by the energy E and the revolution frequency ω which is a function of energy, $\omega(E)$. This frequency dependence can easily be calculated using $p = \sqrt{2(E - U(x))}$ and observing that half a period of the revolution around the orbit with an energy E is given by

$$\frac{1}{2}T = \pi\omega^{-1} = \int_{x_1}^{x_2} \frac{dx'}{p(x')} = \int_{x_1}^{x_2} \frac{dx'}{\sqrt{2(E - U(x'))}}, \quad (5.9)$$

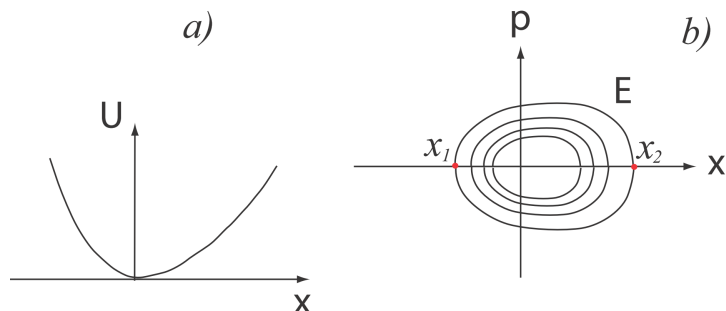


Figure 5.2: The potential energy U (a) and the phase portrait of the system (b).

where x_1 and x_2 are the turning points (see Fig. 5.2b).

Let us transform to new variables, choosing the new momentum to be equal to the energy E ; the corresponding canonical conjugate coordinate is denoted by w . We will use the generating function $F_2(x, E)$. Using $p = \sqrt{2(E - U(x))}$ and integrating the equation $p = \partial F_2 / \partial x$, we obtain

$$F_2(x, E) = \int^x dx' \sqrt{2(E - U(x'))}. \quad (5.10)$$

Since this is a time independent transformation, the new Hamiltonian H' is equal to the old one expressed in terms of the new variables:

$$H'(w, E) = H = E, \quad (5.11)$$

with the equations of motion for the new variables

$$\dot{w} = \frac{\partial H'}{\partial E} = 1, \quad \dot{E} = -\frac{\partial H'}{\partial w} = 0. \quad (5.12)$$

We see that the evolution of the variable w is

$$w = t + t_0, \quad (5.13)$$

which means that the variable conjugate to energy is time.

This choice of our new variables is not very convenient because in one revolution the variable w changes by $2\pi/\omega(E)$ —the quantity that depends on the trajectory. A better choice would be to choose a new coordinate, ϕ , in such a way that in one revolution it changes by 2π —the same quantity for each trajectory. This coordinate is called the *angle*, and the corresponding generalized momentum, I , is called the *action*.

To find I and ϕ for the nonlinear oscillator we assume that the action is a function of energy, or, conversely, $E = E(I)$. This function will be determined below. The generating function $F_2'(x, I)$ which accomplishes the transformation

$(x, p) \rightarrow (\phi, I)$ is the same function F_2 , in which we now assume that E is the function of I

$$F_2'(x, I) = F_2(x, E(I)). \quad (5.14)$$

With this arrangement, the new Hamiltonian is

$$H'(\phi, I) = E(I), \quad (5.15)$$

and the equation for ϕ reads

$$\dot{\phi} = \frac{\partial H'}{\partial I} = \frac{dE}{dI}. \quad (5.16)$$

We require now that $\dot{\phi}$ be equal to ω (which can now be considered as a function of I), so that

$$\phi = \omega(I)t + \phi_0, \quad (5.17)$$

and one revolution corresponds to the change of variable ϕ by 2π . This requirement is satisfied if we chose the dependence $E(I)$ in such a way that

$$\frac{dE}{dI} = \omega(E), \quad (5.18)$$

or, integrating

$$I(E) = \int_{E_{\min}}^E \frac{dE'}{\omega(E')}. \quad (5.19)$$

Problem 5.2. Find the action-angle variables for the system with the following potential

$$U(x) = \begin{cases} \infty, & x < 0 \\ Fx, & x > 0 \end{cases} \quad (5.20)$$

The above transformation to action-angle variables can be implemented in a numerical code, see [6]. One such example is shown in Fig. 5.3 for the potential function $U(x) = x^2 + 0.2x^3$.

5.3 Liouville's theorem

A general Hamiltonian flow in the phase space conserves several integrals of motion. The most important one is the volume occupied by an ensemble of particles. Conservation of the phase space volume is called the *Liouville theorem*.

The phase space volume is expressed as a $2n$ -dimensional integral

$$V_1 = \int_{\mathcal{M}_1} dq_1 dq_2 \dots dq_n dp_1 dp_2 \dots dp_n, \quad (5.21)$$

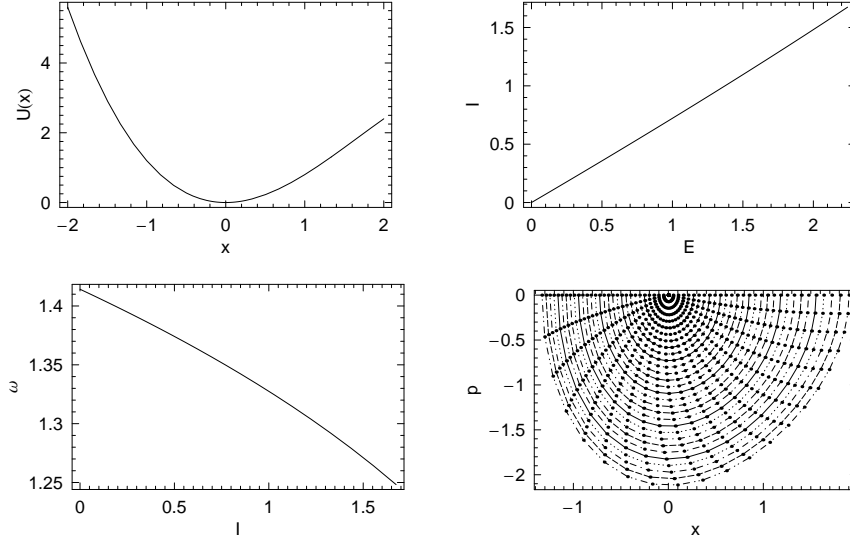


Figure 5.3: Numerical solution of the action-angle variables for $U(x) = x^2 - 0.2x^3$ (top left panel). The top right panel shows the dependence of action I versus energy E ; the bottom left panel shows the $\omega(I)$ function, and the bottom right panel shows the lines of constant action I and the constant angle ϕ .

where the integration goes over a $2n$ -dimensional manifold \mathcal{M}_1 in the phase space. A canonical transformation (4.2) maps the manifold onto a different one \mathcal{M}_2 , and the new volume phase space is

$$V_2 = \int_{\mathcal{M}_2} dQ_1 dQ_2 \dots dQ_n dP_1 dP_2 \dots dP_n. \quad (5.22)$$

The ratio of elementary volumes, as is known from the mathematical analysis is equal to the determinant of the Jacobian of the transformation M

$$\left| \frac{dQ_1 dQ_2 \dots dQ_n dP_1 dP_2 \dots dP_n}{dq_1 dq_2 \dots dq_n dp_1 dp_2 \dots dp_n} \right| = |\det M|. \quad (5.23)$$

Using Eq. (5.7) it is easy to prove that $|\det M| = 1$.

Problem 5.3. Prove that $|\det M| = 1$.

Lecture 6

Coordinate system and Hamiltonian in an accelerator

In this Lecture, we derive the Hamiltonian for a particle moving in an accelerator. The derivation uses several simplifying assumptions.

First, we assume that there is no electrostatic fields, $\phi = 0$, and the magnetic field is static. The magnetic field directs particle's motion in such a way that the particle moves in a closed orbit. This *reference* orbit is established for a particle with the nominal momentum p_0 ($= m\gamma_0 v_0$). Our goal is to describe particles' motion in the vicinity of this reference orbit, with energies (momenta) that can slightly deviate from the nominal one. We will also assume that the reference orbit is a plane curve.

More general consideration of the issues related to the derivation of the Hamiltonian of a charged particle in accelerator can be found in Refs. [7,8].

6.1 Coordinate system

The reference orbit is shown in Fig. 6.1. It is given by the vector $\mathbf{r}_0(s)$, where s is the arclength measured along the orbit *in the direction of motion*. We will define three unit vectors. The first vector $\hat{\mathbf{s}}$ is the tangential vector to the orbit, $\hat{\mathbf{s}} = d\mathbf{r}_0/ds$. The second vector, $\hat{\mathbf{x}}$, is perpendicular to $\hat{\mathbf{s}}$ and lies in the plane of the orbit. The third vector $\hat{\mathbf{y}}$ is perpendicular to the plane of the orbit, $\hat{\mathbf{y}} = \hat{\mathbf{s}} \times \hat{\mathbf{x}}$. The three vectors $\hat{\mathbf{x}}$, $\hat{\mathbf{y}}$, and $\hat{\mathbf{s}}$ constitute a right-hand oriented base for the local coordinate system. The coordinate x is measured along $\hat{\mathbf{x}}$, and the coordinate y is measured along $\hat{\mathbf{y}}$.

Note that simultaneously flipping the directions of both vectors x and y is allowable, because it transforms a right-hand oriented coordinate system to another right-hand oriented one.

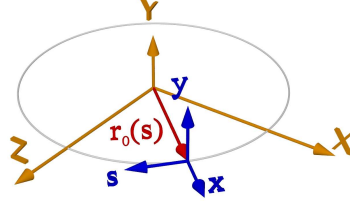


Figure 6.1: A plane reference orbit and a Cartesian coordinate system X , Y and Z . For this orbit, ρ is positive. The orbit is not necessarily a circle.

If the direction of the motion is reversed (e.g., by changing the direction of the magnetic field or the sign of charge of the particles), then vector \hat{s} changes direction. To keep the local coordinate system right-handed, the direction of vector \hat{x} is usually reversed too.

From the differential geometry (the so called Frenet-Serret formulas) we have the following relations between the derivatives of vectors \mathbf{r}_0 , \hat{s} , \hat{x} , and \hat{y} :

$$\begin{aligned} \frac{d\mathbf{r}_0}{ds} &= \hat{s}, \\ \frac{d\hat{s}}{ds} &= -\frac{\hat{x}}{\rho(s)}, \\ \frac{d\hat{x}}{ds} &= \frac{\hat{s}}{\rho(s)}, \\ \frac{d\hat{y}}{ds} &= 0. \end{aligned} \tag{6.1}$$

Problem 6.1. Check that Eqs. (6.1) hold for a circular orbit.

Problem 6.2. Fig 6.2 shows the electron trajectory in a four-dipole chicane (typically used for bunch compressions). Indicate the direction of axis x



Figure 6.2: Electron trajectory in a chicane. Assume that the y axis is directed out of the page.

assuming that the y axis is directed out of the page toward you. Determine the sign of the orbit radius ρ and the magnetic field direction of each of four dipoles along the orbits. What happens with this sign if the particle is moving in the direction opposite to the one shown in the figure?

Since we assumed that the orbit is plane, the magnetic field can only have y (vertical field) and/or s (solenoidal field) components. The bending radius ρ is given by the following equation (see (3.18))

$$\rho(s) = \frac{p_0}{eB_y(s)}. \quad (6.2)$$

Problem 6.3. Verify that from the definition of ρ in Eqs. (6.1) it follows that the sign in Eq. (6.2) is correct for arbitrary sign of the charge e and the direction of motion in the reference orbit.

Most of the particles in the beam deviate from the reference orbit, although they move close to it. This is illustrated by Fig. 6.3. Each point of the orbit

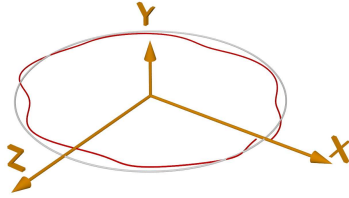


Figure 6.3: A circular reference orbit and a particle's orbit (shown in red).

can be represented in the local coordinate system, as is illustrated by Fig. 6.4. In this system a radius vector \mathbf{r} is represented by coordinates s , x , and y such

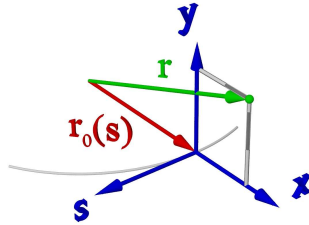


Figure 6.4: A local coordinate system.

that

$$\mathbf{r} = \mathbf{r}_0(s) + x\hat{\mathbf{x}}(s) + y\hat{\mathbf{y}}. \quad (6.3)$$

Below we will need to carry out various differential operations in curvilinear coordinates. Here are useful formulae for the gradient of a scalar function

$\phi(x, y, s)$, and for the curl and divergence of a vector function $\mathbf{A} = (A_x(x, y, s), A_y(x, y, s), A_s(x, y, s))$:

$$\nabla\phi = \hat{\mathbf{x}}\frac{\partial\phi}{\partial x} + \hat{\mathbf{y}}\frac{\partial\phi}{\partial y} + \hat{\mathbf{s}}\frac{1}{1+x/\rho}\frac{\partial\phi}{\partial s}, \quad (6.4)$$

$$(\nabla \times \mathbf{A})_x = -\frac{1}{1+x/\rho}\frac{\partial A_y}{\partial s} + \frac{\partial A_s}{\partial y}, \quad (6.5)$$

$$(\nabla \times \mathbf{A})_s = -\frac{\partial A_x}{\partial y} + \frac{\partial A_y}{\partial x}, \quad (6.6)$$

$$(\nabla \times \mathbf{A})_y = -\frac{1}{1+x/\rho}\frac{\partial A_s(1+x/\rho)}{\partial x} + \frac{1}{1+x/\rho}\frac{\partial A_x}{\partial s}, \quad (6.7)$$

$$\nabla \cdot \mathbf{A} = \frac{1}{1+x/\rho}\frac{\partial A_x(1+x/\rho)}{\partial x} + \frac{\partial A_y}{\partial y} + \frac{1}{1+x/\rho}\frac{\partial A_s}{\partial s}. \quad (6.8)$$

Problem 6.4. Verify that Eqs. (6.1), (6.4)-(6.8) hold for a circular orbit.

6.2 Hamiltonian in curvilinear coordinate system

The Hamiltonian for a charged particle is given by Eq. (3.29)

$$H = \sqrt{(mc^2)^2 + c^2(\boldsymbol{\pi} - e\mathbf{A})^2}. \quad (6.9)$$

This Hamiltonian was derived for a Cartesian coordinate system. We now want to define a Hamiltonian in the coordinate system related to the reference orbit. We will use generating functions to transform the Hamiltonian to the new coordinates.

As a first step, we choose local coordinates s , x , and y as coordinate variables of our new Hamiltonian. To carry out a transformation from the original Cartesian coordinates X , Y and Z (see Fig. 6.1) to the new ones, we will use a generating function of the third type:

$$F_3(\boldsymbol{\pi}, x, y, s) = -\boldsymbol{\pi} \cdot (\mathbf{r}_0(s) + x\hat{\mathbf{x}}(s) + y\hat{\mathbf{y}}). \quad (6.10)$$

In this equation $\boldsymbol{\pi}$ is the *old* momentum and x , y and s are the new coordinates.

We denote by $\mathbf{\Pi}$ the new canonical momentum; it is given by Eqs. (4.32)

$$\begin{aligned}
\Pi_x &= -\frac{\partial F_3}{\partial x} = \boldsymbol{\pi} \cdot \hat{\mathbf{x}} = \pi_x, \\
\Pi_y &= -\frac{\partial F_3}{\partial y} = \boldsymbol{\pi} \cdot \hat{\mathbf{y}} = \pi_y, \\
\Pi_s &= -\frac{\partial F_3}{\partial s} = \boldsymbol{\pi} \cdot \left(\frac{d\mathbf{r}_0}{ds} + x \frac{d\hat{\mathbf{x}}}{ds} \right) \\
&= \boldsymbol{\pi} \cdot \left(\hat{\mathbf{s}} + \frac{x}{\rho} \hat{\mathbf{s}} \right) \\
&= \pi_s \left(1 + \frac{x}{\rho} \right). \tag{6.11}
\end{aligned}$$

Note that

$$\begin{aligned}
(\boldsymbol{\pi} - e\mathbf{A})^2 &= (\pi_x - eA_x)^2 + (\pi_y - eA_y)^2 + (\pi_s - eA_s)^2 \\
&= (\Pi_x - eA_x)^2 + (\Pi_y - eA_y)^2 + \left(\frac{\Pi_s}{1 + x/\rho} - eA_s \right)^2, \tag{6.12}
\end{aligned}$$

and our Hamiltonian becomes

$$H = c \left[m^2 c^2 + (\Pi_x - eA_x)^2 + (\Pi_y - eA_y)^2 + \left(\frac{\Pi_s}{1 + x/\rho} - eA_s \right)^2 \right]^{1/2}. \tag{6.13}$$

We have used the notation $A_x = \mathbf{A} \cdot \hat{\mathbf{x}}$, $A_y = \mathbf{A} \cdot \hat{\mathbf{y}}$, and $A_s = \mathbf{A} \cdot \hat{\mathbf{s}}$. [Some authors use a different notation defining $A_s = (1 + x/\rho)\mathbf{A} \cdot \hat{\mathbf{s}}$.]

Eq. (6.13) is our new Hamiltonian as a function of new coordinates x, y, s and new conjugate momenta Π_x, Π_y and Π_s .

6.3 Using s as a time variable

As was assumed at the beginning of this lecture, our Hamiltonian does not depend on time t and hence is a constant of motion. It describes particle's motion with three degrees of freedom. It turns out that using the constancy of H one can lower the number of degrees of freedom from 3 to 2, which, to some degree, simplifies the description of the motion. To do this, we need to change the independent variable from time t to s .

Let us assume that we solved equations of motion and found all the variables as functions of time, $x(t), y(t), s(t)$, etc. Then the dependence, say, $x(s)$ is obtained in the following way. Solving equation $s = s(t)$ we find the inverse function $t(s)$ and substitute it into the argument of x : $x(t) \rightarrow x(t(s))$. The latter is now a function of s : $x(s) = x(t(s))$. We can do the same trick with coordinate y and components of the momentum vector $\mathbf{\Pi}$, and define $y(s)$ and $\mathbf{\Pi}(s)$.

It turns out that the dependence of x , y , Π_x , and Π_y versus s , can be found directly from a Hamiltonian with 2 degrees of freedoms. We first formulate how to calculate this new Hamiltonian, and then prove that using the formulated approach we indeed obtain the new equations of motion for the two pairs of the canonically conjugate variables.

Let us write down the following equation:

$$h = H(x, \Pi_x, y, \Pi_y, s, \Pi_s), \quad (6.14)$$

(where H is given by (6.13)) and solve it for Π_s

$$\Pi_s = \Pi_s(x, \Pi_x, y, \Pi_y, h, s). \quad (6.15)$$

Here h is the value of the Hamiltonian H . Because our Hamiltonian does not depend on time, the value of H is constant along each orbit—according to Eq. (3.27), for $\phi = 0$, the value of the Hamiltonian is equal to γmc^2 . Let us introduce now a new Hamiltonian K

$$K(x, \Pi_x, y, \Pi_y, h, s) = -\Pi_s(x, \Pi_x, y, \Pi_y, h, s), \quad (6.16)$$

in which x , Π_x , y , Π_y are considered as canonical conjugate variables, s is an independent “time” variable, and h is a (constant) parameter. As we see, the Hamiltonian K has two pairs of conjugate variables, and hence describes motion of a system which has two degrees of freedom. However, this Hamiltonian depends on its time-like variable s and hence is not a conserved quantity any more (in contrast to the original Hamiltonian H).

Let us now show that dependence $x(s)$, $\Pi_x(s)$, $y(s)$, and $\Pi_y(s)$ are governed by the Hamiltonian (6.16). We have to remember that, e.g., $x(s)$ is obtained from $x(t)$ and $s(t)$ by eliminating the variable t , and $x(t)$ with $s(t)$ are governed by the original Hamiltonian H . We have for dx/ds

$$\frac{dx}{ds} = \frac{dx/dt}{ds/dt} = \frac{\partial H/\partial \Pi_x}{\partial H/\partial \Pi_s}. \quad (6.17)$$

On the other hand, the derivative $\partial K/\partial \Pi_x$ can be calculated as a derivative of an implicit function

$$\frac{\partial K}{\partial \Pi_x} = - \left(\frac{\partial \Pi_s}{\partial \Pi_x} \right)_H = \frac{\partial H/\partial \Pi_x}{\partial H/\partial \Pi_s}, \quad (6.18)$$

and we see that

$$\frac{dx}{ds} = \frac{\partial K}{\partial \Pi_x}. \quad (6.19)$$

The same approach works for Π_x ,

$$\frac{d\Pi_x}{ds} = \frac{d\Pi_x/dt}{ds/dt} = \frac{-\partial H/\partial x}{\partial H/\partial \Pi_s} = \left(\frac{\partial \Pi_s}{\partial x} \right)_H = -\frac{\partial K}{\partial x}. \quad (6.20)$$

Similarly one can show that equations for y and Π_y can be obtained with the Hamiltonian K . The price for lowering the number of degrees of freedom is that we now have a “time dependent” Hamiltonian (K is a function of s).

Although time is eliminated from our equations, the time dependence versus s can be easily found, if needed. For this we need to find the function $s(t)$. Since $ds/dt = \partial H/\partial \Pi_s$, the inverse function $t(s)$ satisfies the following equation

$$\frac{dt}{ds} = \frac{\partial \Pi_s}{\partial H} = -\frac{\partial K}{\partial h}. \quad (6.21)$$

Integrating this equation, we can find $t(s)$, invert it, and find $s(t)$.

Problem 6.5. Find the Hamiltonian K for the following model Hamiltonian H :

$$H(x, \Pi_x, s, \Pi_s) = \frac{\Pi_x^2}{2} + \omega(s)^2 \frac{x^2}{2} + v\Pi_s, \quad (6.22)$$

where v is a constant. Prove that both Hamiltonians describe the same dynamics.

6.4 Small amplitude approximation

The Hamiltonian K given by Eq. (6.16) can easily be found from Eq. (6.13):

$$K = -\left(1 + \frac{x}{\rho}\right) \left[\frac{1}{c^2} h^2 - (\Pi_x - eA_x)^2 - (\Pi_y - eA_y)^2 - m^2 c^2 \right]^{1/2} - eA_s \left(1 + \frac{x}{\rho}\right). \quad (6.23)$$

As we will see in the next lectures, in many cases of interest, a single component A_s is sufficient to describe the magnetic field in an accelerator, so we can set $A_x = A_y = 0$ in Eq. (6.23). In this case, Π_x and Π_y are equal to the kinetic momenta, $\Pi_x = p_x = m\gamma v_x$ and $\Pi_y = p_y = m\gamma v_y$ (see Eqs. (6.11) and (3.25)) and we can use p_x and p_y instead of Π_x and Π_y :

$$K = -\left(1 + \frac{x}{\rho}\right) \left(\frac{1}{c^2} h^2 - p_x^2 - p_y^2 - m^2 c^2 \right)^{1/2} - eA_s \left(1 + \frac{x}{\rho}\right). \quad (6.24)$$

We will consider these momenta as small quantities (compared with the total momentum of the particle), because particles usually move at a small angle to the nominal orbit. [Remember that for our choice of coordinates, a particle moving along the nominal orbit have $v_x = v_y = 0$. This is the main advantage of the coordinate system associated with the reference orbit.] Expanding the Hamiltonian in p_x and p_y we get:

$$K \approx -p \left(1 + \frac{x}{\rho}\right) \left(1 - \frac{p_x^2}{2p^2} - \frac{p_y^2}{2p^2}\right) - eA_s \left(1 + \frac{x}{\rho}\right), \quad (6.25)$$

where $p(h) = \sqrt{h^2/c^2 - m^2c^2}$ is the total kinetic momentum of the particle (which together with the energy is a conserved quantity in a constant magnetic field).

Instead of using dimensional momenta p_x and p_y it is convenient to introduce dimensionless variables $P_x = p_x/p_0$ and $P_y = p_y/p_0$, where p_0 is the nominal momentum in the ring. Transformation from x, p_x, y, p_y to x, P_x, y, P_y is not canonical, but a simple consideration shows that it can be achieved by simply dividing the Hamiltonian by p_0 (see the problem on page 34). Denoting the new Hamiltonian by \mathcal{H} we have

$$\begin{aligned} \mathcal{H}(x, P_x, y, P_y) &= \frac{K}{p_0} \\ &= -\frac{p}{p_0} \left(1 + \frac{x}{\rho}\right) \left(1 - \frac{1}{2}P_x^2 \left(\frac{p_0}{p}\right)^2 - \frac{1}{2}P_y^2 \left(\frac{p_0}{p}\right)^2\right) - \frac{e}{p_0}A_s \left(1 + \frac{x}{\rho}\right). \end{aligned} \quad (6.26)$$

As mentioned at the beginning of the Lecture, we are interested here in the case when the energy and the total momentum of the particle can only slightly deviate from the nominal one, that is

$$\frac{p}{p_0} = 1 + \eta, \quad (6.27)$$

with $\eta \ll 1$. With this in mind, we obtain

$$\begin{aligned} \mathcal{H}(x, P_x, y, P_y) & \\ &= -(1 + \eta) \left(1 + \frac{x}{\rho}\right) \left(1 - \frac{1}{2}P_x^2 - \frac{1}{2}P_y^2\right) - \frac{e}{p_0}A_s \left(1 + \frac{x}{\rho}\right), \end{aligned} \quad (6.28)$$

where we replaced $(p_0/p)^2$ by unity in small quadratic terms proportional to P_x^2 and P_y^2 .

Finally, we note that our momenta P_x, P_y are approximately equal to the orbit slopes $x' \equiv dx/ds$ and $y' \equiv dy/ds$, respectively. Indeed

$$x' \equiv \frac{dx}{ds} = \frac{v_x}{v_s} = \frac{p_x}{p_s} \approx P_x, \quad (6.29)$$

with a similar expression for y' . Some authors actually use x' and y' as canonical momenta conjugate to x and y instead of P_x, P_y —in this case one has to be careful to avoid confusion between a canonical variable (say P_x) with the rate of change of its conjugate (that is dx/ds).

6.5 Time dependent Hamiltonian

While we emphasized above that in the case of time independent Hamiltonian the transition from t to s as an independent variable eliminates one degree of freedom, the requirement of being time independent is actually not

needed. Indeed, our derivation in Section 6.3 can be easily modified to include the case of time dependent Hamiltonians. In Eq. (6.14) we will have $H(x, \Pi_x, y, \Pi_y, s, \Pi_s, t)$, and correspondingly the new Hamiltonian K will also be a function of time

$$K(x, \Pi_x, y, \Pi_y, t, h, s) = -\Pi_s(x, \Pi_x, y, \Pi_y, t, h, s), \quad (6.30)$$

where the time t is now understood as a third coordinate (in addition to x and y) and the energy h is the third momentum. The Hamiltonian equation (6.21) should be complemented by

$$\frac{dh}{ds} = \frac{\partial K}{\partial t}. \quad (6.31)$$

Note that Eqs (6.21) and (6.31) have “inverted” signs if t is treated as a coordinate and h as its conjugate momentum. This, however, can be easily fixed, if one accepts $-h$ as the momentum conjugate to t .

Problem 6.6. Make canonical transformation $(t, -h) \rightarrow (z_t, p)$ using the generating function $F_2(p, t) = -ct\sqrt{p^2 + m^2c^2}$. Explain meaning of new variables.

An important effect that is governed by a time-dependent Hamiltonian is particle acceleration by RF electromagnetic field in the ring. In a simple model that assumes a short cavity with voltage V , an additional term that needs to be added to (6.23) to take the acceleration into account is [7]

$$-\frac{eV}{p_0\omega_{\text{RF}}}\delta(s - s_0)\cos(\omega_{\text{RF}}t + \phi), \quad (6.32)$$

where s_0 is the coordinate of the cavity location in the ring (and the cavity is assumed to be infinitely short), ω_{RF} is the RF frequency and ϕ is the RF phase. It is easy to see from (6.31) that a passage through the point s_0 at time t changes the kinetic energy h of the particle by $eV\cos(\omega_{\text{RF}}t + \phi)$.

Lecture 7

Equations of motion in accelerator

A typical accelerator uses a sequence of various types of magnets separated by sections of free space (so called *drifts*). To specify the Hamiltonian (6.28) we need to know vector potential A_s for these magnets.

7.1 Vector potential for different types of magnets

There are several types of magnets that are used in accelerators and each of them is characterized by a specific dependence of A_s versus x and y . In this section we will list a few magnet types and write down expressions for the vector potentials. In those expressions, we will use the fact that we are only interested in fields near the reference orbit, $|x|, |y| \ll |\rho|$. We will be neglecting higher order terms such as $(x/\rho)^2$ and $(y/\rho)^2$.

We first consider *dipole* magnets that are used to bend the orbit. The dipole magnetic field is:

$$\mathbf{B} = \hat{y}B(s). \quad (7.1)$$

The function $B(s)$ is such that it is not zero only inside the magnet and vanishes outside of it. This field can be represented by the following vector potential:

$$A_s = -B(s)x \left(1 - \frac{x}{2\rho}\right). \quad (7.2)$$

Indeed, using Eq. (6.7) we obtain

$$\begin{aligned}
 B_y &= -\frac{1}{1+x/\rho} \frac{\partial A_s(1+x/\rho)}{\partial x} \\
 &\approx B(s) \left(1 - \frac{x}{\rho}\right) \frac{\partial}{\partial x} x \left(1 - \frac{x}{2\rho}\right) \left(1 + \frac{x}{\rho}\right) \\
 &\approx B(s) \left(1 - \frac{x}{\rho}\right) \frac{\partial}{\partial x} \left(x + \frac{x^2}{2\rho}\right) \\
 &\approx B(s) + O\left(\frac{x^2}{\rho^2}\right).
 \end{aligned} \tag{7.3}$$

This is an approximation in which we only keep terms to the first order in $|x/\rho|$. The picture of windings of a dipole magnet is shown in Figs. 7.1 and 7.2.

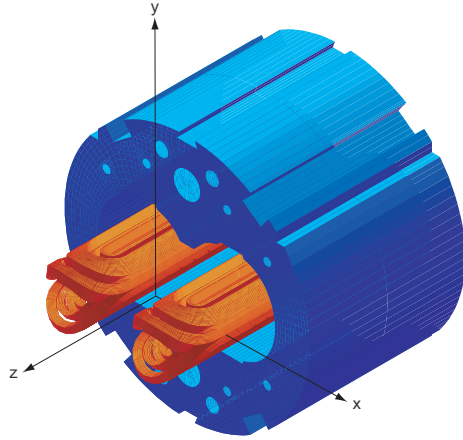


Figure 7.1: Edge of the LHC dipole magnet.

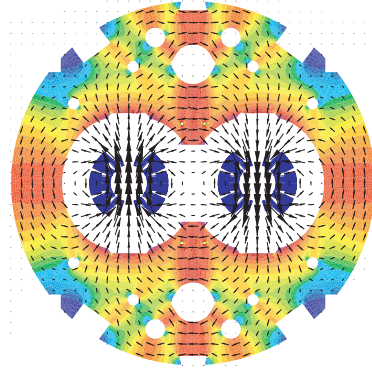


Figure 7.2: Magnetic field in the dipole.

The second type is a *quadrupole* magnet. It is used to focus off-orbit particles close to the reference orbit. It has the following magnetic field:

$$\mathbf{B} = G(s)(\hat{y}x + \hat{x}y). \tag{7.4}$$

The picture of a quadrupole magnet is shown in Fig. 7.3, and the magnetic field lines are shown in Fig. 7.4. As we will see below from the equations of motion, the quadrupole magnetic field focuses particles around the equilibrium orbit. The corresponding vector potential is

$$A_s = \frac{G}{2} (y^2 - x^2). \tag{7.5}$$

A *skew quadrupole* is a normal quadrupole rotated by 45 degrees:

$$\mathbf{B} = G_s(s)(-\hat{y}y + \hat{x}x), \tag{7.6}$$

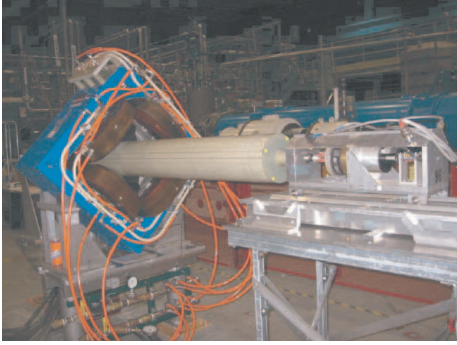


Figure 7.3: A quadrupole magnet.

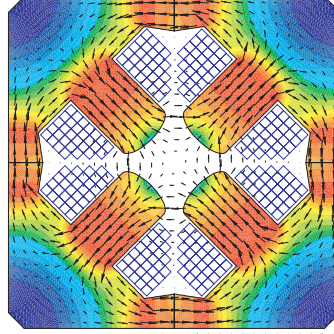


Figure 7.4: Quadrupole magnet field lines.

with

$$A_s = G_s xy. \quad (7.7)$$

Finally, we will also consider a *sextupole magnet*. Sextupoles are used to correct some properties of betatron oscillations of particles around the reference orbit. This element has a nonlinear dependence of the magnetic field with transverse coordinates:

$$\mathbf{B} = S(s) \left[\frac{1}{2} \hat{\mathbf{y}}(x^2 - y^2) + \hat{\mathbf{x}}xy \right], \quad (7.8)$$

with

$$A_s = S \left(\frac{1}{2} xy^2 - \frac{1}{6} x^3 \right). \quad (7.9)$$

The field lines of a sextupole are shown in Fig. 7.5.

Problem 7.1. *The magnetic field $B_s(s)$ of a solenoid cannot be described with a single longitudinal component A_s of the vector potential. Show that this magnetic field can be represented with the vector potential that has two transverse components:*

$$A_x = -B_s y/2, \quad A_y = B_s x/2. \quad (7.10)$$

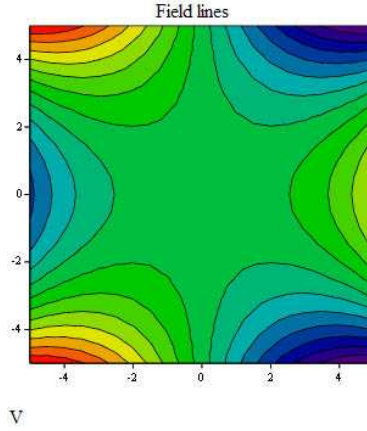


Figure 7.5: Sextupole field lines.

7.2 Taylor expansion of the Hamiltonian

Let us write down the Hamiltonian (6.28) assuming that we have dipoles and quadrupoles in the ring:

$$\begin{aligned}
 \mathcal{H} &\approx -(1 + \eta) \left(1 + \frac{x}{\rho}\right) \left(1 - \frac{1}{2}P_x^2 - \frac{1}{2}P_y^2\right) - \frac{e}{p_0} A_s \left(1 + \frac{x}{\rho}\right) \\
 &= -(1 + \eta) \left(1 + \frac{x}{\rho}\right) \left(1 - \frac{1}{2}P_x^2 - \frac{1}{2}P_y^2\right) \\
 &\quad - \frac{e}{p_0} \left[-B(s)x \left(1 - \frac{x}{2\rho}\right) + \frac{G(s)}{2} (y^2 - x^2)\right] \left(1 + \frac{x}{\rho}\right) \\
 &\approx -1 - \eta - \eta \frac{x}{\rho} + \frac{1}{2}P_x^2 + \frac{1}{2}P_y^2 + \frac{x^2}{2\rho^2} - \frac{e}{p_0} \frac{G(s)}{2} (y^2 - x^2), \quad (7.11)
 \end{aligned}$$

where we made use of $\rho = p_0/eB$ and neglected terms of the third and higher orders (assuming that η , as well as all four canonical variables, x , P_x , y and P_y are of the first order). We can drop the constant first term (unity) on the last line of (7.11). Our main interest in the following lectures will be the case of on-momentum particles, that is $\eta = 0$. In this case the Hamiltonian is the sum of two terms corresponding to the vertical and horizontal degrees of freedom:

$$\mathcal{H} = \mathcal{H}_x + \mathcal{H}_y, \quad (7.12)$$

with

$$\mathcal{H}_x = \frac{1}{2}P_x^2 + \frac{x^2}{2\rho^2} + \frac{e}{p_0} \frac{G(s)}{2} x^2, \quad (7.13)$$

and

$$\mathcal{H}_y = \frac{1}{2}P_y^2 - \frac{e}{p_0} \frac{G(s)}{2}y^2. \quad (7.14)$$

The fact that Hamiltonian (7.12) is split into a sum of two Hamiltonians each of which involves only variables for one degree of freedom means that the horizontal and vertical motions are decoupled. We see that quadrupoles focus or defocus the beam in the transverse direction: focusing in x ($G > 0$) results in defocusing in y , and vice versa. In the next sections we will show that notwithstanding this defocusing effect, a sequence of quadrupoles with alternating polarities confine the beam in the transverse directions near the reference orbit. A particle near the equilibrium orbit executes *betatron* oscillations.

Notice also focusing in the horizontal direction inside dipole magnets (a so called *weak* focusing).

In what follows, to study general properties of the transverse motion in both transverse planes, we will use a generic Hamiltonian

$$\mathcal{H}_0 = \frac{1}{2}P_x^2 + \frac{K(s)}{2}x^2, \quad (7.15)$$

where $K = \rho^{-2} + eG/p_0$ for the horizontal, and $K = -eG/p_0$ for the vertical plane.

Problem 7.2. Using (6.21) and the Hamiltonian (7.11) show that

$$\frac{dt}{ds} = \frac{1}{v} \left(1 + \frac{x}{\rho} \right). \quad (7.16)$$

Explain the meaning of this relation. It follows from it that, for a relativistic particle, ds/dt can be larger than c . Does this constitute violation of the special theory of relativity which forbids motion of bodies faster than the speed of light?

Problem 7.3. Find terms in the Hamiltonian \mathcal{H} responsible for the skew quadrupole (the magnetic field given by Eq. (7.6)).

Problem 7.4. Using the vector potential Eq. (7.10) for the solenoid and starting from the Hamiltonian (6.23) find the contribution to \mathcal{H} of the magnetic field of the solenoid. [Hint: assume that B_s is small and use the Taylor expansion in the Hamiltonian (6.23) keeping linear terms and second order terms in B_s .]

7.3 Hill's equation, betatron function and betatron phase

From the Hamiltonian (7.15) we find the following equation of motion in a transverse plane:

$$x''(s) + K(s)x(s) = 0. \quad (7.17)$$

In an accelerator ring $K(s)$ is a *periodic* function of s with a period that we denote by L (which may be equal to a fraction of the ring circumference), and Eq. (7.17) is called Hill's equation. It describes the so called *betatron* oscillations of a particle in the ring. Note that the same equation (2.16) describes the parametric resonance, with the only difference that we now have s as an independent variable instead of t . We now know that this equation can have both stable and unstable solutions. Of course, for storage and acceleration of beams in an accelerator, one has to design it in a way that avoids unstable solutions of Eq. (7.17).

To understand general properties of the betatron motion in a ring, we seek a solution to Eq. (7.17) in the following form

$$x(s) = Aw(s) \cos \psi(s), \quad (7.18)$$

where A is an arbitrary constant, and ψ is called the *betatron phase*. Note that $w(s)$ is not uniquely defined: we can always multiply it by an arbitrary factor of w_0 and redefine the amplitude $A \rightarrow A/w_0$, so that $x(s)$ is not changed. It turns out that if a particle's motion is stable, we can require that $w(s)$ be a periodic function of s with the period L . In addition, the function ψ is such that $\psi(s + L) = \psi(s) + \psi_0$, where ψ_0 is a constant (or, equivalently, function $d\psi/ds$ is a periodic function of s with the same period L). These two properties of functions w and ψ are guaranteed by the Floquet theory of differential equations with periodic coefficients.

Introducing two unknown functions $w(s)$ and $\psi(s)$ instead of one function $x(s)$ gives us freedom to impose a constraint of our choice on functions w and ψ later in the derivation. We have

$$\begin{aligned} \frac{x'}{A} &= w' \cos \psi - w\psi' \sin \psi, \\ \frac{x''}{A} &= w'' \cos \psi - 2w'\psi' \sin \psi - w\psi'' \sin \psi - w\psi'^2 \cos \psi. \end{aligned} \quad (7.19)$$

Eq. (7.17) now becomes

$$\begin{aligned} w'' \cos \psi - 2w'\psi' \sin \psi - w\psi'' \sin \psi - w\psi'^2 \cos \psi + K(s)w \cos \psi \\ = [w'' \cos - w\psi'^2 + K(s)w] \cos \psi - [2w'\psi' + w\psi''] \sin \psi = 0. \end{aligned} \quad (7.20)$$

We now use the freedom mentioned above and set to zero both the term in front of $\cos \psi$ and the term in front of $\sin \psi$. This gives us two equations:

$$\begin{aligned} w'' - w\psi'^2 + K(s)w &= 0 \\ -2w'\psi' - w\psi'' &= 0. \end{aligned} \quad (7.21)$$

The last equation can be written as

$$\frac{1}{w}(\psi'w^2)' = 0. \quad (7.22)$$

Let us introduce the β function as $\beta(s) = w(s)^2$, then

$$\psi' = \frac{a}{\beta(s)}, \quad (7.23)$$

where a is an arbitrary constant of integration. We can always assume that $a > 0$; if this is not the case, we redefine the angle ψ by $\psi \rightarrow -\psi$, which changes the sign in (7.23) and makes $a > 0$. The first equation in (7.21) now becomes

$$w'' - \frac{a^2}{w^3} + K(s)w = 0. \quad (7.24)$$

As was pointed out at the beginning of this section, the function w can be multiplied by a constant factor. We can now use this freedom and replace $w \rightarrow \sqrt{a}w$ in (7.24) which eliminates a from the equation, $a \rightarrow 1$. This is the usual choice in accelerator physics textbooks. In terms of the β function the resulting equation becomes

$$\frac{1}{2}\beta\beta'' - \frac{1}{4}\beta'^2 + K\beta^2 = 1. \quad (7.25)$$

It is a nonlinear differential equation of the second order. As we pointed out above, in a circular accelerator one has to find a periodic solution to this equation. For a beam line with an entrance and an exit, one solves this equation with initial values for the beta function and its first derivative at the entrance.

Note that, as follows from (7.23), the derivative ψ' is a periodic function of s , with the period equal to that of $\beta(s)$, in agreement with the comment after Eq. (7.18).

Problem 7.5. Derive Eq. (7.25) from Eq. (7.24).

There are several mathematical methods, as well as special computer codes that find $\beta(s)$ (as well as other parameters of interest) for a ring with given magnets (that is given $K(s)$) [9]. In this lecture, we limit our consideration to a simple illustration which solves Eq. (7.24) using an iterative approach. In Fig. 7.6 we show the beta function for the High Energy Ring of PEP-II at SLAC.

Problem 7.6. Find solution of Eq. (7.25) in free space where $K = 0$.

Problem 7.7. Calculate a jump of the derivative of the beta function through a thin quadrupole. Such a quadrupole is defined by $K(s) = f^{-1}\delta(s-s_0)$, where f is called the focal length of a thin quadrupole.

Problem 7.8. A FODO lattice is a sequence of thin quadrupoles with alternating polarities:

$$K_{\text{FODO}}(s) = \sum_{n=-\infty}^{\infty} K_0\delta(s-nl) - K_0\delta\left(s - \left[n + \frac{1}{2}\right]l\right), \quad (7.26)$$

where l is the period of the lattice. Solve Eq. (7.25) for the FODO lattice and find $\beta(s)$. For a given value of l find the maximum value of K_0 for which the motion is stable.

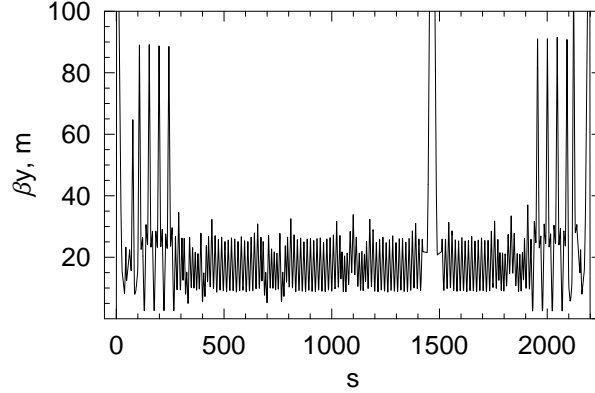


Figure 7.6: The beta function β_y in the HER of PEP-II.

Problem 7.9. Consider two rings with circumferences C_1 and C_2 . Assume that $C_1 = \lambda C_2$ and $K_2(s) = \lambda^2 K_1(\lambda s)$, and prove that $\beta_2 = \lambda^{-1} \beta_1(\lambda s)$.

The betatron phase advance of the ring can be found by integrating Eq. (7.23),

$$\Delta\psi = \int_0^C \frac{ds}{\beta(s)}. \quad (7.27)$$

The quantity $\Delta\psi/2\pi$ is called the *tune* ν (in European literature it is usually denoted by Q)

$$\nu = \frac{1}{2\pi} \int_0^C \frac{ds}{\beta(s)}; \quad (7.28)$$

it is a fundamental characteristic of the beam dynamics in the ring.

Having found the beta function in the system, the general solution of the equation of motion (7.17) can be written as

$$x(s) = A\sqrt{\beta(s)} \cos(\psi(s) + \psi_0), \quad (7.29)$$

where ψ_0 is an initial betatron phase.

Lecture 8

Action-angle variables for circular machines

8.1 Action-angle variables and the Floquet transformation

We start with the Hamiltonian (7.15)

$$\mathcal{H} = \frac{1}{2}P_x^2 + \frac{1}{2}K(s)x^2. \quad (8.1)$$

In Section 7.3 we found a solution to this equation in the form (7.18) which we now write as

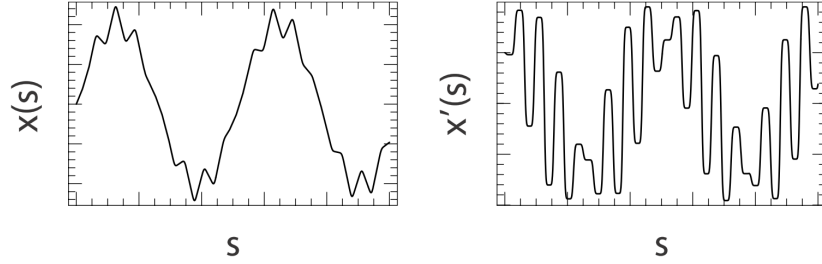
$$x(s) = A\sqrt{\beta(s)} \cos \psi(s). \quad (8.2)$$

Differentiating this equation with respect to s we find

$$\begin{aligned} x'(s) = P_x &= A \frac{\beta'}{2\sqrt{\beta(s)}} \cos \psi(s) - \sqrt{\beta(s)} \psi' \sin \psi(s) \\ &= \frac{A}{\sqrt{\beta}} \cos \psi(s) \left(\frac{\beta'}{2} - \tan \psi(s) \right) \\ &= \frac{x}{\beta} \left(\frac{\beta'}{2} - \tan \psi(s) \right). \end{aligned} \quad (8.3)$$

An example of x and x' as functions of s , for a particular choice of $K(s)$, is shown in Fig. 8.1. One can see that both functions show a complicated pattern when s changes. In many applications one would like to have a simpler representation of particle motion governed by Hamiltonian (8.1). We will now show how this can be achieved using a canonical transformation to new variables.

Let us transform to the action-angle variables ϕ (coordinate) and J (momentum), using a generating function of the first kind, (4.30). In our current

Figure 8.1: Plots of x and x' versus s .

notation x is the old coordinate and P_x is the old momentum. Analogous to the canonical transformation for the linear oscillator we will require that

$$\begin{aligned} x(s) &= A(J)\sqrt{\beta(s)} \cos \phi \\ P_x(s) &= \frac{x}{\beta(s)} \left(\frac{\beta'}{2} - \tan \phi \right). \end{aligned} \quad (8.4)$$

The generating function is

$$F_1(x, \phi, s) = \int P_x dx = \frac{x^2}{2\beta} \left(\frac{\beta'}{2} - \tan \phi \right), \quad (8.5)$$

[compare with Eq. (4.41)] where for P_x we used Eq. (8.4). With this generating function we find the action

$$J = -\frac{\partial F_1}{\partial \phi} = \frac{x^2}{2\beta} \sec^2 \phi, \quad (8.6)$$

Using $\sec^2 \phi = 1 + \tan^2 \phi$, and the expression for $\tan \phi$ from the last equation in (8.4),

$$-\tan \phi = \frac{\beta P_x}{x} + \alpha \quad (8.7)$$

where

$$\alpha = -\frac{\beta'}{2}, \quad (8.8)$$

we obtain J in terms of x and P_x :

$$J = \frac{1}{2\beta} [x^2 + (\beta P_x + \alpha x)^2]. \quad (8.9)$$

Problem 8.1. Using Eqs. (8.7) and (8.9) show by direct calculation of Poisson brackets that the transformation $x, P_x \rightarrow \phi, J$ is canonical.

Equations (8.7) and (8.9) give us the transformation from the old conjugate variables x and P_x to the new ones ϕ and J . The inverse transformation $(\phi, J) \rightarrow (x, P_x)$ can also be found. From the first of Eqs. (8.6) we have

$$x = \sqrt{2\beta J} \cos \phi. \quad (8.10)$$

Substituting this relation to the second of Eqs. (8.4) we obtain the equation for P_x in terms of J and ψ

$$P_x = -\sqrt{\frac{2J}{\beta}} (\sin \phi + \alpha \cos \phi). \quad (8.11)$$

To find the new Hamiltonian which we denote by $\hat{\mathcal{H}}$ we need to take into account that the generating function depends on the time-like variable s :

$$\begin{aligned} \hat{\mathcal{H}} &= \mathcal{H} + \frac{\partial F_1}{\partial s} \\ &= \frac{1}{2} P_x^2 + \frac{1}{2} K(s) x^2 + \frac{\partial}{\partial s} \frac{x^2}{2\beta} \left(\frac{\beta'}{2} - \tan \phi \right) \\ &= \frac{1}{2} P_x^2 + \frac{1}{2} K(s) x^2 + \frac{x^2}{4} \frac{\beta'' \beta - \beta'^2}{\beta^2} + \frac{x^2 \beta'}{2\beta^2} \tan \phi. \end{aligned} \quad (8.12)$$

We now use (7.25) to eliminate β'' from this equation and Eq. (8.7) to eliminate ϕ :

$$\begin{aligned} \hat{\mathcal{H}} &= \\ &= \frac{1}{2} P_x^2 + \frac{1}{2} K(s) x^2 - \frac{x^2}{4} \frac{\frac{1}{2} \beta'^2 + 2K\beta^2 - 2}{\beta^2} - \frac{x^2 \beta'}{2\beta^2} \left(\frac{\beta P_x}{x} + \alpha \right) \\ &= \frac{1}{2} P_x^2 + \frac{1}{2\beta^2} x^2 + \frac{\alpha^2}{2\beta^2} x^2 + \frac{\alpha}{\beta} P_x x \\ &= \frac{1}{2\beta^2} x^2 + \frac{1}{2} \left(P_x + \frac{\alpha}{\beta} x \right)^2 \\ &= \frac{J}{\beta}. \end{aligned} \quad (8.13)$$

Since the new Hamiltonian is independent of ϕ the equation for J is

$$J' = \frac{\partial \hat{\mathcal{H}}}{\partial \phi} = 0, \quad (8.14)$$

which means that J is an integral of motion. The quantity $2J$ is called the Courant-Snyder invariant. The Hamiltonian equation for ϕ gives

$$\phi' = \frac{\partial \hat{\mathcal{H}}}{\partial J} = \frac{1}{\beta(s)}. \quad (8.15)$$

Comparing this equation with Eq. (7.23) we see that the new variable ϕ is actually the old betatron phase, $\phi = \psi + \phi_0$. Particles in the beam will have various initial phases ϕ_0 .

What we have achieved with this transformation is shown in Fig. 8.2—we “straightened out” the behavior of the new momentum variable.

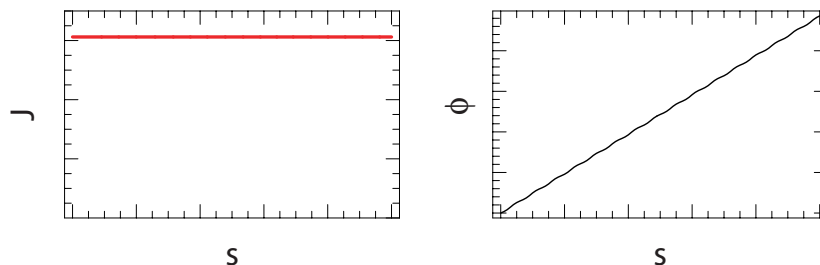


Figure 8.2: Plots of J and ϕ versus s : $J(s)$ is a horizontal straight line, and $\phi(s)$ is slightly wiggling at an angle to the horizontal axis.

We can go further and “straighten out” the ϕ variable as well. This is achieved with one more canonical transformation, from ϕ and J to ϕ_1 and J_1 . The new generating function is of the second type, $F_2(\phi, J_1, s)$,

$$F_2(\phi, J_1, s) = J_1 \left(\frac{2\pi\nu s}{C} - \int_0^s \frac{ds'}{\beta(s')} \right) + \phi J_1, \quad (8.16)$$

where C is the circumference of the ring, and the tune is given by Eq. (7.28). This function gives for the new angle

$$\phi_1 = \frac{\partial F_2}{\partial J_1} = \phi + \frac{2\pi\nu s}{C} - \int_0^s \frac{ds'}{\beta(s')} = \phi + \frac{2\pi\nu s}{C} - \psi(s), \quad (8.17)$$

and the action is not changed

$$J = \frac{\partial F_2}{\partial \phi} = J_1. \quad (8.18)$$

The new Hamiltonian is

$$\hat{\mathcal{H}}_1 = \hat{\mathcal{H}} + \frac{\partial F_2}{\partial s} = \frac{2\pi\nu}{C} J_1 = \text{const}. \quad (8.19)$$

Now the evolution of the new coordinate ϕ_1 is governed by the equation

$$\phi_1' = \frac{\partial \hat{\mathcal{H}}_1}{\partial J_1} = \frac{2\pi\nu}{C}, \quad (8.20)$$

which means that ϕ_1 is a linear function of s . This is illustrated by Fig. 8.3.

In nonlinear theory it is more convenient to work with the angle $\theta = 2\pi s/C$ as an independent variable, instead of s . The Hamiltonian that incorporates this change is $(C/2\pi)\hat{\mathcal{H}}_1(\psi_1, J_1, \theta)$. This Hamiltonian is periodic with period 2π (unless the ring has higher periodicity).

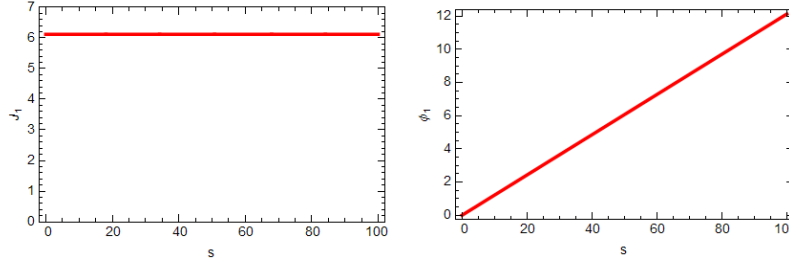


Figure 8.3: Plots of J_1 and ϕ_1 versus s : both $J_1(s)$ and $\phi_1(s)$ are straight lines.

8.2 Phase space motion at a given location

Let us assume that we plot the phase space x, P_x at some location s at the ring and follow particle's motion as it passes through this location. It is convenient to normalize the coordinate x by the beta function at this location $\beta(s)$. A set of consecutive points $x_n/\beta, P_{x,n}$, $n = 1, 2, \dots$, in the phase space will form particle's trajectory, see Fig. 8.4. Because we have an integral of motion J , all these points are located on the curve $J = \text{const}$. From the expression (8.9) for J it follows that this curve is an ellipse whose size and orientation depend on the values J , β , and α . Particles with different values of J have similar ellipses

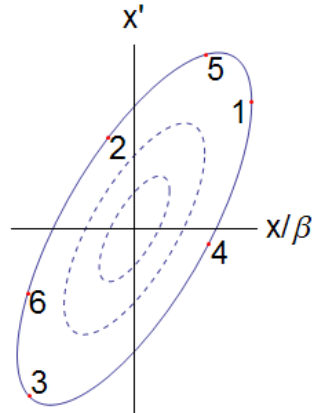


Figure 8.4: Phase space ellipse and a particle's positions at consecutive turns (solid curve). Dashed lines show ellipses for particles with smaller values of J . Instead of P_x we use equal to it x' to mark the vertical axis.

enclosed inside each other, see Fig. 8.4.

Problem 8.2. Find the major and minor half axes, and the tilt of this ellipse.

It is easy to see that the ellipse becomes a circle if $\alpha = 0$. In this case, the trajectory is very simple: each consecutive point of the circle is rotated by the betatron phase advance $\Delta\psi$ in the clockwise direction (7.27).

Set of ellipses at another location in the ring will have a different shapes which are defined by the local values of β and α , see Fig. 8.5. Imagine how

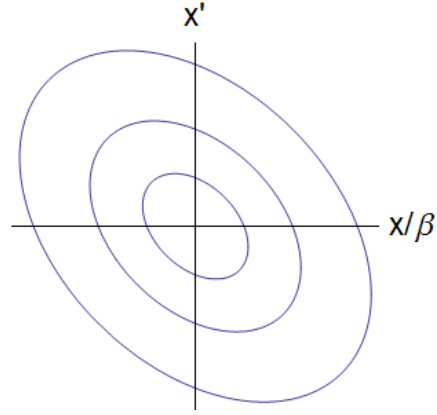


Figure 8.5: Phase space ellipses at a different locations in the ring.

these ellipses are rotating and changing their shape when one travels along the ring circumference.

Problem 8.3. Prove that the transformation $x, P_x \rightarrow \bar{x}, \bar{P}_x$ with

$$\bar{x} = \frac{1}{\sqrt{\beta}}x, \quad \bar{P}_x = \frac{1}{\sqrt{\beta}}(\beta P_x + \alpha x) \quad (8.21)$$

is canonical. Prove that phase space orbits plotted in variables \bar{x}, \bar{P}_x are circles.

Lecture 9

Field errors and nonlinear resonances

The magnetic field in any real machine is different from the ideal design. It is important to understand what is the effect of small magnetic errors on particles' motion in an accelerator. In this lecture we consider the effect of dipole and quadrupole field errors, and then illustrate the effect of sextupoles in the ring.

9.1 Closed orbit distortion

We first consider what happens if a dipole magnetic field is not exactly equal to the design one. We will see that such errors lead to changes in the reference orbit in the accelerator.

Let us assume that the guiding vertical magnetic field in a circular accelerator deviates from the design value by $\Delta B(s)$. The corresponding vector potential, in which we keep only the first order term [see Eq. (7.2)] is $A_s = -\Delta B(s)x$. This vector potential should be added to the Hamiltonian (7.11); it modifies the motion in the horizontal plane only. We can write \mathcal{H}_x as

$$\mathcal{H} = \frac{1}{2}P_x^2 + \frac{1}{2}K(s)x^2 + \frac{e\Delta B(s)}{p_0}x \quad (9.1)$$

(we drop the subscript x in what follows).

The most direct way to deal with this problem is to write the differential equation for x

$$x'' + K(s)x = -\frac{e\Delta B(s)}{p_0}. \quad (9.2)$$

A periodic solution, $x_0(s)$, to this equation gives the *closed orbit distortion*. It satisfies Eq. (9.2),

$$x_0'' + K(s)x_0 = -\frac{e\Delta B(s)}{p_0}, \quad (9.3)$$

with the periodicity condition $x_0(s + C) = x_0(s)$ where C is the circumference of the ring. A general solution to Eq. (9.2) is

$$x(s) = x_0(s) + \xi(s), \quad (9.4)$$

where $\xi(s)$ satisfies

$$\xi'' + K(s)\xi = 0. \quad (9.5)$$

The function $\xi(s)$ describes betatron oscillations around the perturbed orbit. This is illustrated by Fig. 9.1.

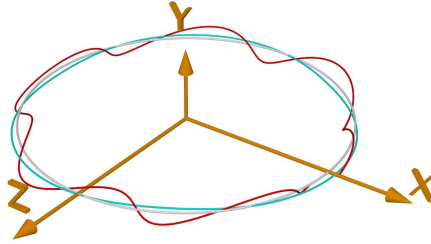


Figure 9.1: An ideal and distorted orbits, and a betatron oscillation.

Let us calculate the orbit distortion $x_0(s)$. We first consider the case of a field perturbation localized at one point: $\Delta B(s) = \Delta B_0(s')\delta(s - s')$. Since the right hand side of Eq. (9.3) is equal to zero everywhere except for the point $s = s'$, we seek solution in the form of Eq. (8.2) with an initial phase ψ_0

$$x_0(s) = A\sqrt{\beta(s)}\cos(\psi(s) - \psi_0). \quad (9.6)$$

Our first requirement is that $x_0(s)$ should be continuous at $s = s'$. This is achieved if we choose $\psi_0 = \psi(s') + \pi\nu$ and assume that $\psi(s)$ varies from $\psi(s')$ to $\psi(s') + 2\pi\nu$ when we go around the orbit. Indeed, when $\psi(s) = \psi(s')$, the argument of the cos function is equal to $-\pi\nu$, and $x_0(s') = A\sqrt{\beta(s')}\cos(-\pi\nu)$. After a turn around the ring, the argument of the cos function becomes equal to $\pi\nu$, and since cos is an even function, $x_0(s' + C) = x_0(s')$. The second requirement is obtained by integrating through the δ -function in Eq. (9.3)—it gives us a jump of the derivative of x_0 at s'

$$x'_0(s') - x'_0(s' + C) = -\frac{e\Delta B(s')}{p_0}. \quad (9.7)$$

From this equation we find

$$A = -\frac{\sqrt{\beta(s')}}{2\sin(\pi\nu)}\frac{e\Delta B(s')}{p_0}. \quad (9.8)$$

For an arbitrary function $B(s)$ we need to add contributions from all locations, which means integration over the circumference of the ring:

$$x_0(s) = \frac{-e}{2p_0 \sin(\pi\nu)} \int_s^{s+C} ds' \Delta B(s') \sqrt{\beta(s)\beta(s')} \cos(\psi(s) - \psi(s') - \pi\nu). \quad (9.9)$$

We see that, as follows from Eq. (9.9), the integer values for the tune ν are not acceptable because they would result in unstable closed orbit.

How can we incorporate the closed orbit distortion into the Hamiltonian formalism? The answer to this question is given in the following problem:

Problem 9.1. *The action-angle variables defined by (8.9)-(8.11) has to be modified in case of field errors. Starting from the Hamiltonian (9.1) transform to the action-angle variables using the following generating function*

$$F_1(x, \phi, s) = \frac{[x - x_0(s)]^2}{2\beta} \left(\frac{\beta'}{2} - \tan \phi \right) + xx'_0(s). \quad (9.10)$$

Show that in this case

$$J(x, P_x, s) = \frac{1}{2\beta} \left[(x - x_0)^2 + (\beta[P_x - x'_0] + \alpha[x - x_0])^2 \right], \quad (9.11)$$

and obtain the Hamiltonian (8.13).

Problem 9.2. *What is the effect on the beam orbit of the error magnetic field $\Delta B_x(s)$ in the horizontal plane?*

A crude estimate of the magnitude of the closed orbit distortion from Eq. (9.9) is

$$x_0 \sim \frac{\Delta B C \beta}{B \rho} \sim \beta \frac{\Delta B}{B}. \quad (9.12)$$

We see from this equation that the effect of magnetic field errors is less in machines with small beta functions, that is with stronger focusing.

9.2 Effect of energy deviation

If particle's energy is not exactly equal to the nominal one, its equilibrium orbit in the horizontal plane changes. Using results of the previous section it is easy to find the new orbit corresponding the the energy deviation η . From the Hamiltonian (7.11) we see that the extra term due to non vanishing η that involves the coordinate x is $-\eta x/\rho$. Hence instead of (9.1) one gets

$$\mathcal{H} = \frac{1}{2}P_x^2 + \frac{1}{2}K(s)x^2 - \frac{\eta}{\rho}x, \quad (9.13)$$

which is formally obtained from (9.1) by replacement

$$\Delta B \rightarrow -\frac{\eta p_0}{e\rho}x. \quad (9.14)$$

Using (9.9) we immediately find that the new orbit is given by

$$x_0(s) = D(s)\eta, \quad (9.15)$$

with the function D is

$$D(s) = \frac{\sqrt{\beta(s)}}{2\sin(\pi\nu)} \int_s^{s+C} ds' \frac{\sqrt{\beta(s')}}{\rho(s')} \cos(\psi(s) - \psi(s') - \pi\nu). \quad (9.16)$$

This function is called the *dispersion function* of the ring.

Using the expression (9.11) and (9.15) one immediately concludes that the action variable for a particle with energy deviation η is

$$J(x, P_x, \eta, s) = \frac{1}{2\beta} \left[(x - \eta D(s))^2 + (\beta[P_x - \eta D'(s)] + \alpha[x - \eta D(s)])^2 \right]. \quad (9.17)$$

9.3 Quadrupole errors

Let us now assume that we have a quadrupole error

$$\mathcal{H} = \frac{1}{2}P_x^2 + \frac{1}{2}K(s)x^2 + \frac{1}{2}\epsilon\Delta K(s)x^2, \quad (9.18)$$

where we introduced a formal smallness parameter ϵ . What kind of effect does this error have on the motion? Since we know that the focusing function $K(s)$ determines the betatron oscillations in the system, clearly, changing the focusing would result in the perturbation of the beta function, and, hence, the tune of the ring.

To find these changes using the Hamiltonian, we first transform to the action-angle variables J and ϕ . This transformation casts the first two terms of the Hamiltonian into J/β :

$$\frac{1}{2}P_x^2 + \frac{1}{2}K(s)x^2 \rightarrow \frac{J}{\beta(s)}. \quad (9.19)$$

In the last term of Eq. (9.18) we express x in terms of J and ϕ using Eq. (8.10)

$$\begin{aligned} \mathcal{H} &= \frac{J}{\beta(s)} + \epsilon\Delta K(s)J\beta(s)\cos^2\phi \\ &= J \left(\frac{1}{\beta(s)} + \frac{1}{2}\epsilon\Delta K(s)\beta(s) \right) + \frac{1}{2}\epsilon\Delta K(s)J\beta(s)\cos 2\phi. \end{aligned} \quad (9.20)$$

We will denote the last term in this equation by $\epsilon V(\phi, J, s)$.

$$V(\phi, J, s) = \frac{1}{2}\Delta K(s)J\beta(s)\cos 2\phi. \quad (9.21)$$

There is a general method that attempts to solve this kind of problems by eliminating the perturbation V in the Hamiltonian in the lowest order. The

method is based on a perturbation theory and uses a canonical transformation to new variables $(\phi, J) \rightarrow (\xi, I)$ with the generating function

$$F_2(\phi, I, s) = \phi I + \epsilon G(\phi, I, s). \quad (9.22)$$

We have

$$\begin{aligned} \xi &= \phi + \epsilon G_I, \\ J &= I + \epsilon G_\phi, \end{aligned} \quad (9.23)$$

where subscripts denote differentiation with respect to the corresponding variable. The new Hamiltonian is

$$\mathcal{H} \approx I \left(\frac{1}{\beta} + \frac{1}{2} \epsilon \Delta K \beta \right) + \epsilon V(\phi, I, s) + \frac{1}{\beta} \epsilon G_\phi + \epsilon G_s + O(\epsilon)^2, \quad (9.24)$$

where we substituted I for J in the argument of V introducing an error of the second order. We will kill the perturbation in the new Hamiltonian in the first order by choosing G in such a way that the following equation is satisfied:

$$V(\phi, I, s) + \frac{1}{\beta} G_\phi + G_s = 0. \quad (9.25)$$

One needs to find a solution to this equation that is periodic over s with the period equal to the ring circumference C .

Problem 9.3. Solve Eq. (9.25) for the function G . Hint: seek solution in the form $G(\phi, I, s) = \text{Re}(\hat{G}(I, s)e^{2i\phi})$.

The solution is given by the following equation

$$G = -\frac{I}{4 \sin 2\pi\nu} \int_s^{s+C} ds' \Delta K(s') \beta(s') \sin 2(\phi - \psi(s) + \psi(s') - \pi\nu), \quad (9.26)$$

and with this choice of the G the new Hamiltonian becomes

$$\mathcal{H} = I \left(\frac{1}{\beta} + \frac{1}{2} \epsilon \Delta K \beta \right), \quad (9.27)$$

where we neglected higher order terms.

Problem 9.4. Verify by direct calculation that G given by Eq. (9.26) satisfies Eq. (9.25).

We see that the new action I is an integral of motion, and the relation between the old action and the new one is

$$J = I - \frac{\epsilon I}{2 \sin 2\pi\nu} \int_s^{s+C} ds' \Delta K(s') \beta(s') \cos 2(\phi - \psi(s) + \psi(s') - \pi\nu). \quad (9.28)$$

A more useful is expression which gives the new action I in terms of the old one. It can easily be obtained from the expression above, if we replace I to J in the second term on the right hand side and move it to the left

$$I = J + \frac{\epsilon J}{2 \sin 2\pi\nu} \int_s^{s+C} ds' \Delta K(s') \beta(s') \cos 2(\phi - \psi(s) + \psi(s') - \pi\nu). \quad (9.29)$$

Again, this introduces an error of the second order, which we neglect.

From Eq. (9.26) we see that at half-integer values of ν the perturbation leads to unstable behavior of the system.

Changing the strength of the focusing in the lattice by $\epsilon\Delta K$ results in a change of the beta function. Let us denote the new beta function by $\beta_1 = \beta + \epsilon\Delta\beta$. The simplest way to compute $\Delta\beta$ is to use the relation (7.23) between the s -derivative of the betatron phase and the beta function. Note that the new phase ξ is related to the unperturbed phase ϕ by Eq. (9.23), hence

$$\frac{1}{\beta + \epsilon\Delta\beta} = \frac{\partial\xi}{\partial s} = \frac{\partial\phi}{\partial s} + \epsilon \frac{\partial G_I}{\partial s} = \frac{1}{\beta} + \epsilon \frac{\partial G_I}{\partial s}. \quad (9.30)$$

Expanding this formula to the first order in ϵ we find

$$\Delta\beta = -\beta^2 \frac{\partial G_I}{\partial s}. \quad (9.31)$$

Using Eq. (9.26) we obtain for the new beta function

$$\beta_1 = \beta - \frac{\beta}{2 \sin 2\pi\nu} \int_s^{s+C} ds' \Delta K(s') \beta(s') \cos 2(-\psi(s) + \psi(s') - \pi\nu). \quad (9.32)$$

The last term in this expression is the correction to the original beta function; it is often called the *beta beating* term.

An important conclusion that follows from the above equation is that one should avoid half-integer values of the tune—they are unstable with respect to errors in the focusing strength of the lattice.

Having found the correction to the beta function, we can find the correction to the tune, using Eq. (7.28).

Problem 9.5. *Show that the tune change is given by the following equation*

$$\Delta\nu = \frac{1}{4\pi} \int_0^C ds \Delta K(s) \beta(s). \quad (9.33)$$

Problem 9.6. *Calculate the beta beat and the tune change for a localized perturbation of the lattice: $\Delta k = \Delta K_0 \delta(s - s_0)$.*

9.4 The third-order resonance

We will now study the effect of sextupoles on betatron oscillations. The sextupole vector potential is given by Eq. (7.9). Our goal is to study 1D effects so we neglect the first term in this equation (assuming $y = 0$) and use $A_s = -S(s)x^3/6$. We need to add the term $-eA_s/p_0$ to the Hamiltonian (7.11)

$$\mathcal{H} = \frac{1}{2}P_x^2 + \frac{1}{2}K(s)x^2 + \frac{1}{6}\mathcal{S}(s)x^3, \quad (9.34)$$

where $\mathcal{S} = eS/p_0$. In what follows we will assume that the last term on the right hand side is small compared with the first two terms and treat it as a perturbation. We then transform to action-angle variables J_1 and ψ_1 from Section 8.1. This transforms the first two terms of the Hamiltonian as follows:

$$\frac{1}{2}P_x^2 + \frac{1}{2}K(s)x^2 \rightarrow \frac{2\pi\nu}{C}J_1. \quad (9.35)$$

In the last term, we first transform to (J, ϕ) using (8.10) and then transform from (J, ϕ) to (J_1, ϕ_1) using Eqs. (8.17) and (8.18):

$$\mathcal{H} = \frac{2\pi\nu}{C}J_1 + \frac{\sqrt{2}}{3}J_1^{3/2}\mathcal{S}(s)\beta(s)^{3/2}\cos^3\left(\phi_1 - \frac{2\pi\nu s}{C} + \psi(s)\right). \quad (9.36)$$

The next step is to transform to the independent variable $\theta = 2\pi s/C$ and drop the subscript 1:

$$\begin{aligned} \mathcal{H} &= \nu J + \frac{\sqrt{2}}{3}\frac{C}{2\pi}J^{3/2}\mathcal{S}(\theta)\beta(\theta)^{3/2}\cos^3(\phi - \nu\theta + \psi(\theta)) \\ &= \nu J + V(\phi, J, \theta), \end{aligned} \quad (9.37)$$

where the perturbation V is

$$\begin{aligned} V(\phi, J, \theta) &= \frac{C}{12\pi\sqrt{2}}J^{3/2}\mathcal{S}(\theta)\beta(\theta)^{3/2} \\ &\quad \times (\cos 3(\phi - \nu\theta + \psi(\theta)) + 3\cos(\phi - \nu\theta + \psi(\theta))). \end{aligned} \quad (9.38)$$

The equations of motion for the action-angle variables are

$$\begin{aligned} \frac{\partial J}{\partial \theta} &= -\frac{\partial \mathcal{H}}{\partial \phi} = -\frac{\partial V}{\partial \phi}, \\ \frac{\partial \phi}{\partial \theta} &= \frac{\partial \mathcal{H}}{\partial J} = \nu + \frac{\partial V}{\partial J}. \end{aligned} \quad (9.39)$$

Let us now analyze the relative role of the two terms on the right hand side of (9.38). Note that if we neglect the perturbation V in the Hamiltonian (9.37) then we have $\phi = \nu\theta + \phi_0$. In this case the combination $\phi - \nu\theta + \psi(\theta)$ changes by $2\pi\nu$ on each turn (because $\nu\theta + \psi(\theta)$ does not change over a complete turn). If the fractional part of ν is close to one-third, $\nu \approx n \pm 1/3$, $\cos 3(\phi - \nu\theta + \psi(\theta))$ will remain approximately constant after each turn, and its effect will be accumulating over many periods leading to large excursions of the orbit. On the contrary, $\cos(\phi - \nu\theta + \psi(\theta))$ will have a phase jumping by $\approx \pm 2\pi/3$ on each turn, and its effect will wash out due to continuous change of sign of the cos function on subsequent turns. This term would be resonant for the tune close to an integer, but as we know, choosing such a value of the tune would be unwise, see Section 9.1. Assuming for the rest of this section that $\nu \approx n \pm 1/3$ we will drop the last term in (9.38),

$$V(\phi, J, \theta) = \frac{C}{12\pi\sqrt{2}}J^{3/2}\mathcal{S}(\theta)\beta(\theta)^{3/2}\cos 3(\phi - \nu\theta + \psi(\theta)). \quad (9.40)$$

To simplify our analysis further let us consider a ring with one short sextupole magnet with length much shorter than the ring circumference C . In this case $\mathcal{S}(\theta)$ can be approximated by a periodic delta function

$$\mathcal{S}(\theta) = \mathcal{S}_0 \tilde{\delta}(\theta), \quad (9.41)$$

where $\tilde{\delta}(\theta) = \sum_{n=-\infty}^{\infty} \delta(\theta + 2\pi n)$ due to the periodicity of motion in the ring. We will assume $\mathcal{S}_0 > 0$. The term V can now be written as

$$\begin{aligned} V(\phi, J, \theta) &= \frac{C}{12\pi\sqrt{2}} J^{3/2} \mathcal{S}_0 \beta(\theta)^{3/2} \tilde{\delta}(\theta) \cos 3(\phi - \nu\theta + \psi(\theta)) \\ &= \frac{1}{3} R J^{3/2} \tilde{\delta}(\theta) \cos 3(\phi - \nu\theta + \psi(\theta)), \end{aligned} \quad (9.42)$$

where $R = C \mathcal{S}_0 \beta_0^{3/2} / (4\pi\sqrt{2})$, with $\beta_0 = \beta(0)$.

Equations of motion (9.39) can now be written as

$$\begin{aligned} \frac{\partial J}{\partial \theta} &= R J^{3/2} \tilde{\delta}(\theta) \sin 3(\phi - \nu\theta + \psi(\theta)), \\ \frac{\partial \phi}{\partial \theta} &= \nu + \frac{1}{2} R J^{1/2} \tilde{\delta}(\theta) \cos 3(\phi - \nu\theta + \psi(\theta)). \end{aligned} \quad (9.43)$$

Let us consider how J and ϕ evolve over one turn in the ring, when θ changes from 0 to 2π , starting from $\theta = -0$, that is right before the delta function kick. Without loss of generality we can assume that $\psi(0) = 0$. We will first integrate these equations through the delta-function kick, that is going from $\theta = -0$ to $\theta = +0$ assuming that initial values are J_1 and ϕ_1 . For this integration the equations are simplified

$$\begin{aligned} \frac{\partial J}{\partial \theta} &= R J^{3/2} \delta(\theta) \sin(3\phi), \\ \frac{\partial \phi}{\partial \theta} &= \frac{1}{2} R J^{1/2} \delta(\theta) \cos(3\phi), \end{aligned} \quad (9.44)$$

where we set $\theta = 0$ everywhere, except in the argument of the delta function, and neglected ν in the second equation (9.43). Let us now introduce a new independent variable ξ instead of θ

$$\xi(\theta) = \int_{-\infty}^{\theta} \delta(\theta') d\theta', \quad (9.45)$$

and transform from J to $\mathcal{J} = R^2 J$. The variable ξ changes from 0 to 1 when θ traverses the delta-function. Eqs. (9.44) can now be written as

$$\begin{aligned} \frac{\partial \mathcal{J}}{\partial \xi} &= \mathcal{J}^{3/2} \sin(3\phi) \\ \frac{\partial \phi}{\partial \xi} &= \frac{1}{2} \mathcal{J}^{1/2} \cos(3\phi), \end{aligned} \quad (9.46)$$

and should be integrated from $\xi = 0$ to $\xi = 1$ with the initial boundary conditions $\mathcal{J}_1 = R^2 J_1$ and ϕ_1 .

The integration is helped by the following observation: Eqs. (9.46) are Hamilton equations of motion with the following Hamiltonian

$$\hat{\mathcal{H}}(\phi, \mathcal{J}) = \frac{1}{3} \mathcal{J}^{3/2} \cos(3\phi). \quad (9.47)$$

Since the Hamiltonian does not depend on the independent variable ξ it is conserved, and its trajectories can be easily found from the equation $\hat{\mathcal{H}}(\phi, \mathcal{J}) = \text{const.}$ They are shown in Fig 9.2.

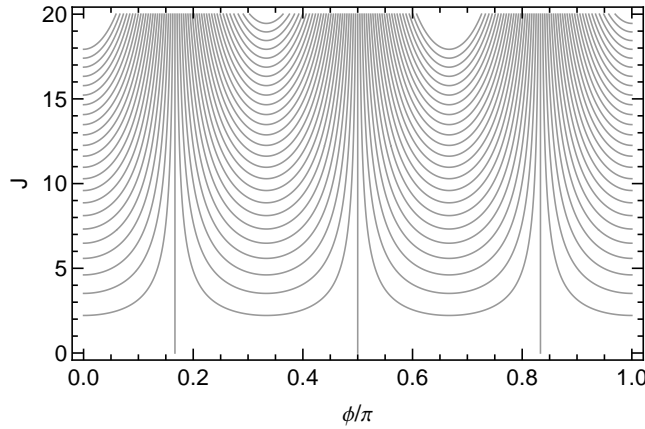


Figure 9.2: The phase space $\phi - \mathcal{J}$ of the Hamiltonian (9.47). Note periodicity along the ϕ axis with the period $\pi/6$.

Let us assume that we solved Eqs. (9.46) and found the map from initial \mathcal{J}_1 and ϕ_1 to final $\tilde{\mathcal{J}}$ and $\tilde{\phi}$: $\tilde{\mathcal{J}} = f(\phi_1, \mathcal{J}_1)$ and $\tilde{\phi} = g(\phi_1, \mathcal{J}_1)$. This map would move our system over the delta-function kick. To get a one-turn map we then need to integrate the equations of motion from $\theta = +0$ to $\theta = 2\pi - 0$ (that is stopping in front of the delta-function). On this interval \mathcal{J} remains constant, and ϕ increases by $2\pi\nu$. If we denote the values of \mathcal{J} and ϕ at $\theta = 2\pi - 0$ as \mathcal{J}_2 and ϕ_2 , we obtain

$$\mathcal{J}_2 = f(\phi_1, \mathcal{J}_1), \quad \phi_2 = g(\phi_1, \mathcal{J}_1) + 2\pi\nu. \quad (9.48)$$

It is now clear that every next revolution over the ring repeats the transformation (9.48), that is the values \mathcal{J}_n, ϕ_n on n -th revolution are expressed through the values from the previous one

$$\mathcal{J}_n = f(\phi_{n-1}, \mathcal{J}_{n-1}), \quad \phi_n = g(\phi_{n-1}, \mathcal{J}_{n-1}) + 2\pi\nu. \quad (9.49)$$

To illustrate the dynamics, we numerically integrated Eqs. (9.46) and implemented the map as a computer program. The results of the simulations are shown in Figs 9.3 for fractional part $[\nu]$ of ν close to $1/3$. The horizontal axis

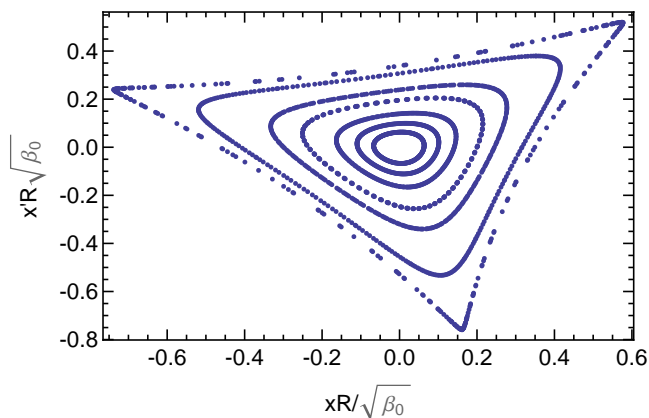


Figure 9.3: Phase orbits for the case $[\nu] - 1/3 = 0.1$. Particle starting from outside of the triangular-shaped area quickly leave the system.

of the phase space portrait in Fig. 9.3 is normalized dimensionless coordinate $xR/\sqrt{\beta_0}$, and the vertical one is normalized angle $P_x R/\sqrt{\beta_0}$. It is assumed that $\alpha = 0$ at the location where the phase plot is drawn. The relations between the normalized physical coordinates and the action-angle variables \mathcal{J} and ϕ follow from (8.10) and (8.11)

$$xR/\sqrt{\beta_0} = \sqrt{2\mathcal{J}} \cos \phi, \quad P_x R/\sqrt{\beta_0} = -\sqrt{2\mathcal{J}} \sin \phi. \quad (9.50)$$

We see that the orbits with large amplitudes of betatron oscillations get a triangular shape. The largest orbit shown in Fig. 9.3 is close to a separatrix—everything outside it quickly leaves the system.

An example of experimentally measured third-order resonance orbits at the IUCF cooler ring is shown in Fig. (9.4).

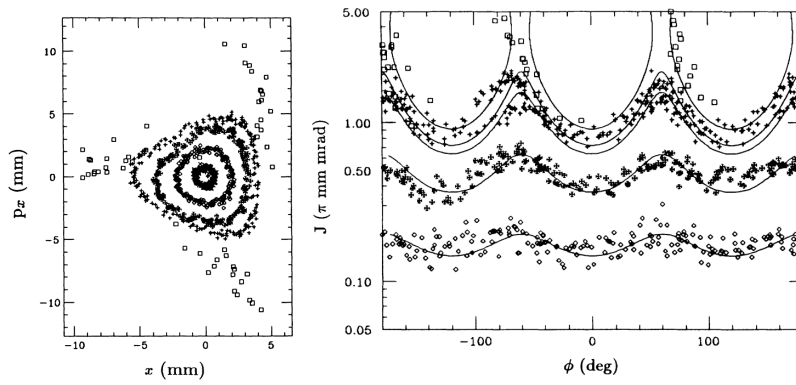


Figure 9.4: Third-order resonance orbits in phase-space coordinates (left) and in action-angle variables (right) (from article [10]).

Lecture 10

Resonance overlapping and dynamic aperture

In the previous lecture we studied the effect on nonlinear terms in the Hamiltonian on particle's motion and, for the case of a sextupole, found a resonant structure in the phase space of third order. In practice it is often happen that a system possesses many resonances of various strengs. Those resonances can interact with each other and lead to stochastic motion. In we consider a simple model, a so called *standard map*, which illustrates qualitative features of what can occur in a system with many resonances.

10.1 Standard model and resonance overlapping

To arrive at the standard map we start from the following Hamiltonian

$$H = \frac{1}{2}I^2 + K\tilde{\delta}(t)\cos\theta, \quad (10.1)$$

where K is a parameter, $\tilde{\delta}(t) = \sum_{n=-\infty}^{\infty} \delta(t+n)$ is the periodic δ function that describes unit kicks repeating with the unit period [note that definition of $\tilde{\delta}(t)$ in this Section differ from the one given in Section 9.4]. Here I can be considered as an action, and θ as an angle variables. Both I and θ are dimensionless. The equations of motion for I and θ are

$$\dot{I} = -\frac{\partial H}{\partial \theta} = K\tilde{\delta}(t)\sin\theta, \quad \dot{\theta} = \frac{\partial H}{\partial I} = I. \quad (10.2)$$

If I_n and θ_n are the values at $t = n - 0$ (before the delta-function kick), then integrating the first of Eqs. (10.2) from $t = n - 0$ to $t = n + 0$ (through the delta-function kick) gives $I_{n+1} = I_n + K\sin\theta_n$, which is conserved over the interval from $t = n + 0$ to $t = (n + 1) - 0$ (where there are no kicks). Integrating the second equation in (10.2) from $t = n + 0$ to $t = (n + 1) - 0$ and remembering

that the action here is already equal to I_{n+1} gives $\theta_{n+1} = \theta_n + I_{n+1}$. Hence we arrive at the following transformation action-angle variables which links their values at time $t = n$ to the values at time $t = n + 1$:

$$\begin{aligned} I_{n+1} &= I_n + K \sin \theta_n \\ \theta_{n+1} &= \theta_n + I_{n+1}. \end{aligned} \quad (10.3)$$

This transformation is called the *standard map*¹.

Problem 10.1. Prove that the standard map defines a canonical transformation $(I_n, \theta_n) \rightarrow (I_{n+1}, \theta_{n+1})$.

Problem 10.2. Prove the following property of the standard map: for two trajectories starting from the same initial value θ_0 but with different values $I_0^{(1)}$ and $I_0^{(2)}$, such that $I_0^{(2)} - I_0^{(1)} = 2\pi m$, where m is an integer, the difference $I_n^{(2)} - I_n^{(1)}$ remains equal to $2\pi m$ for all values of n .

The periodic delta-function in (10.1) can be expanded into the Fourier series

$$\tilde{\delta}(t) = 1 + 2 \sum_{n=1}^{\infty} \cos(2\pi n t). \quad (10.4)$$

Substituting this representation into the Hamiltonian Eq. (10.1) we can rewrite the latter in the following form

$$H = \frac{1}{2} I^2 + K \sum_{n=-\infty}^{\infty} \cos(\theta - 2\pi n t), \quad (10.5)$$

(we used $2 \cos(\theta) \cos(2\pi n t) = \cos(\theta - 2\pi n t) + \cos(\theta + 2\pi n t)$). From this Hamiltonian we see that the system is a pendulum (the term $n = 0$ in the sum) driven by periodic perturbations with frequencies equal to $2\pi n$ (terms with $n \neq 0$).

Selecting only one term in this sum (as we did in the previous lecture) would give us

$$\mathcal{H} = \frac{1}{2} I^2 + K \cos(\theta - 2\pi n t). \quad (10.6)$$

We can make a canonical transformation $I, \theta \rightarrow J, \phi$ with

$$J = I - 2\pi n, \quad \phi = \theta - 2\pi n t. \quad (10.7)$$

The new Hamiltonian for these variables is

$$\mathcal{H}' = \frac{1}{2} J^2 + K \cos \phi + \text{const}. \quad (10.8)$$

Problem 10.3. Prove that Eqs. (10.7) define a canonical transformation, find the corresponding generating function F_2 and obtain the Hamiltonian (10.8).

¹One can also find in the literature a definition of the standard map which differs from Eqs. (10.3) by numerical factors.

One can see that Eq. (10.8) is the pendulum Hamiltonian with the phase space shown in Fig. (2.6). The width of the separatrix is equal $J = \pm 2\sqrt{K}$. In variable I , this phase space is shifted by $2\pi n$ units upward.

Trying to understand what is the overall structure of the phase space of the original Hamiltonian, we can naively superimpose phase portraits for Hamiltonians (10.8) with various values of n . This would give us a picture qualitatively

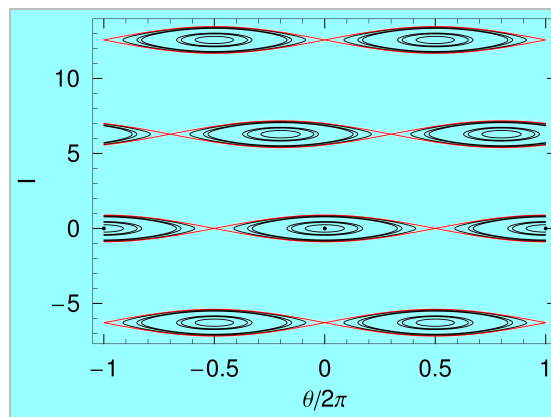


Figure 10.1: Superposition of phase portraits for various resonances of the standard map. The width of each resonance is equal to $4\sqrt{K}$.

shown in Fig. 10.1. Of course, superimposing phase spaces is not a legitimate way of analysis (which is especially clear in the case when the separatrices of neighboring resonances overlap, see below).

Computer simulations show that, indeed, as long as the distance between the islands is much larger than the width of the separatrix, to a good approximation, resonances with different values of n can be considered separately. When the value of K increases the *resonances begin to overlap* and the dynamics becomes complicated. Formally, overlapping occurs for $K > \pi^2/4$, however one should not emphasize this exact value of K . Indeed, as simulations show, when K increases, there is a gradual transition from a regular motion to a fully stochastic regime. The transition from small to large K is illustrated by Fig. 10.2. Qualitatively, the transition occurs at

$$K \sim 1. \quad (10.9)$$

What happens in the regime of developed stochasticity, when $K \gg 1$. All the regular orbits are destroyed and a particle is moving randomly over the phase space. Can we describe this motion? The answer is yes, although the description is statistical. What happens in this limit, is that after each kick the particle loses its memory about the previous phase, and the consecutive kicks can be considered as uncorrelated. The motion along the action axis I becomes diffusive. We can easily estimate the diffusion coefficient corresponding to this

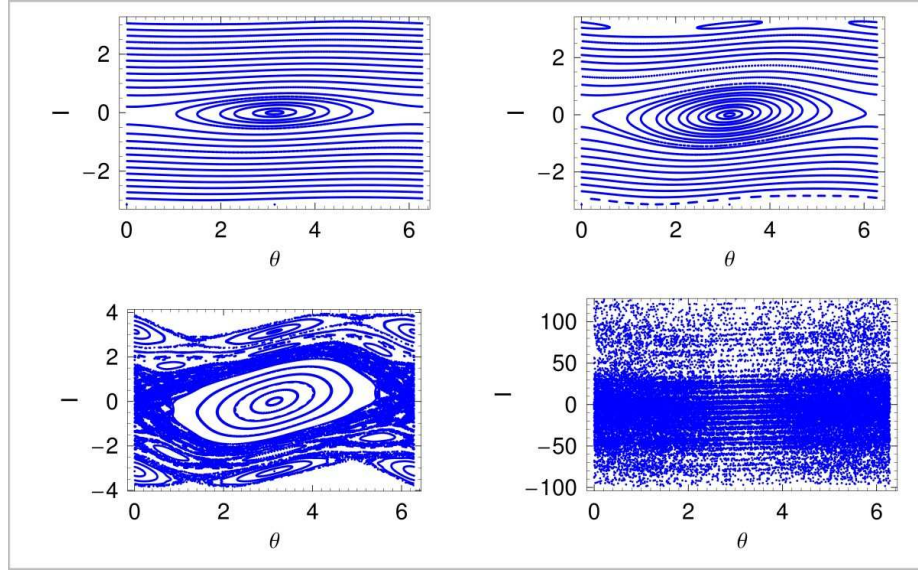


Figure 10.2: The result of computer simulations for the standard map. Shown is the phase space for four different values of the parameter K , $K = 0.1, 0.3, 1, 3$ from left to right and from top to bottom. The last two pictures show an increase and then a complete domination of the stochastic component of the motion.

motion, noting that from Eq. (10.3) the change of the action $\Delta I_n = K \sin \theta_n$. Taking square of ΔI_n and averaging over the random phase θ_n gives

$$\langle \Delta I^2 \rangle = \frac{1}{2} K^2. \quad (10.10)$$

If we plot the dependence I^2 versus the number of iterations N , we expect from Eq. (10.10)

$$I^2 \approx \frac{1}{2} K^2 N. \quad (10.11)$$

A more detailed theory lying beyond the scope of this lecture, shows that Eq. (10.11) gives only the leading term for the diffusion process—there are notable corrections in this equation if K is not very large, [11]. In Fig. 10.3 we confirm Eq. (10.11) by direct numerical simulation².

10.2 Dynamic aperture in accelerators

A modern circular accelerator has many magnets that play various roles in confining the beam in the ring. Nonlinear components of the magnetic field

²The aforementioned corrections vanish for the value $K = 8.41$ chosen for the simulations shown in Fig. 10.3.

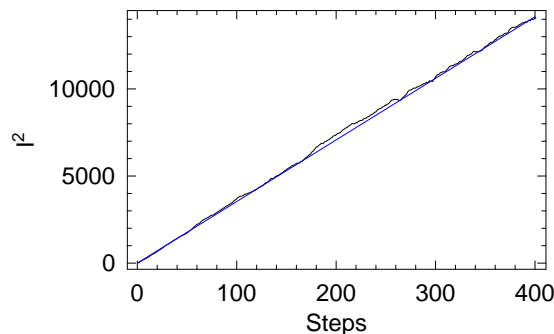


Figure 10.3: The dependence of I^2 versus number of iteration for $K = 8.41$. The straight line is the theoretical expectation given by Eq. (10.11).

of those magnets, as well as errors in manufacturing and installation of the

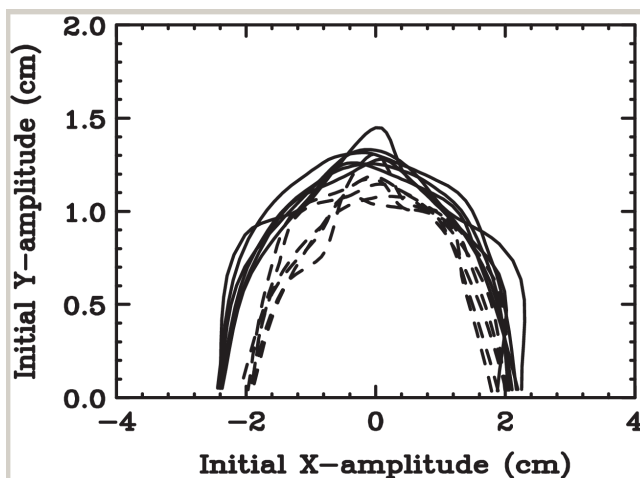


Figure 10.4: Dynamic aperture for the SPEAR3 light source at SLAC (from Ref. [12]). Different curves correspond to 6 seeds of machine errors. The solid lines are for the nominal energy beam and the dashed ones are for the 3% energy deviation.

magnets lead to appearing of resonances in the machine. As we saw in the previous sections, the location of resonances in the phase space depends on the tune. In a typical situation, the nonlinear fields make the phase space at some distance from the reference orbit more prone to stochastic motion, and result

in the situation when only particles in a region near the reference orbit are properly confined. This region is called the *dynamic aperture* of the machine. It is computed with the help of accelerator codes by launching particles at various locations away from the reference orbit and tracking their motion. An example of calculation of the dynamic aperture for the light source SPEAR3 at SLAC is shown in Fig. 10.4.

Lecture 11

The kinetic equation

In the preceding lectures we focused our attention on a single particle motion. In this lecture, we will introduce formalism for treating an ensemble of particles circulating in an accelerator ring.

11.1 The distribution function in phase space and kinetic equation

We start from considering a simple case of one degree of freedom with the canonically conjugate variables q and p . A large ensemble of particles (think about a particle beam) with each particle having various values of q and p constitutes a “cloud” in the phase space, see Fig. 11.1. With time progressing, each particle

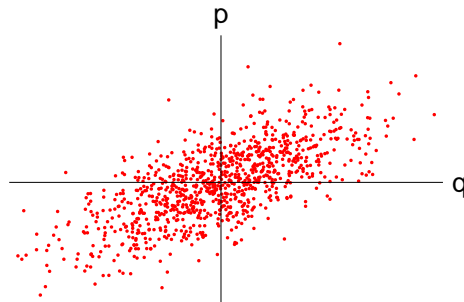


Figure 11.1: Phase space of an ensemble of particles with position of each particle indicated by a red point.

is moving along its own orbit, and the corresponded point is travelling along a trajectory in the phase space. The “cloud” gradually changes shape. The mo-

tion is governed by external fields, as well as interaction between the particles. In this lecture, however, we neglect the interaction effects, and assume that the motion is due to external electromagnetic field only.

Let us consider an infinitesimally small region in the phase space $dq \times dp$ and let the number of particles of the beam at time t in this phase space element be given by dN . Mathematically infinitesimal phase element should be physically large enough to include many particles, $dN \gg 1$. We define the distribution function of the beam $f(q, p, t)$ such that

$$dN(t) = f(q, p, t) dp dq. \quad (11.1)$$

We can say that the distribution function gives the *density* of particles in the phase space.

As was emphasized above, particles travel from one place in the phase space to another, and the distribution function evolves with time. Our goal is to derive a *kinetic equation* that governs this evolution. In this derivation, we will assume that particles' motion is Hamiltonian.

Consider an infinitesimally small region of phase space shown in Fig. 11.2. The number of particles in this region at time t is given by (11.1). At time $t + dt$

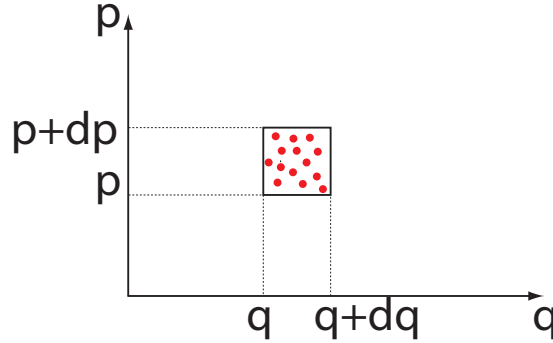


Figure 11.2: To the definition of the distribution function f .

this number will change because of the flow of particles through the boundaries. Due to the flow in the q -direction the number of particles that flow in through the left boundary is

$$f(q, p, t) \times dp \dot{q}(q, p, t) \times dt \quad (11.2)$$

and the number of particles that flow out through the right boundary is

$$f(q + dq, p, t) \times dp \dot{q}(q + dq, p, t) \times dt. \quad (11.3)$$

Similarly, the number of particles which flow in through the lower horizontal boundary is

$$f(q, p, t) \times dq \dot{p}(q, p, t) \times dt \quad (11.4)$$

and the number of particles that flow out through the upper horizontal boundary is

$$f(q, p + dp, t) \times dq \dot{p}(q, p + dp, t) \times dt. \quad (11.5)$$

The number of particles in the volume $dq \times dp$ is now changed

$$\begin{aligned} dN(t + dt) - dN(t) &= [f(q, p, t + dt) - f(q, p, t)]dq dp \\ &= f(q + dq, p, t)dp \dot{q}(q + dq, p, t)dt - f(q, p, t)dp \dot{q}(q, p, t)dt \\ &\quad + f(q, p, t)dq \dot{p}(q, p, t)dt - f(q, p + dp, t)dq \dot{p}(q, p + dp, t)dt. \end{aligned} \quad (11.6)$$

Dividing this equation by $dp dq dt$ and expanding in Taylor's series (keeping only linear terms in dp, dq, dt) gives the following equation

$$\frac{\partial f}{\partial t} + \frac{\partial}{\partial q} \dot{q}(q, p, t)f + \frac{\partial}{\partial p} \dot{p}(q, p, t)f = 0. \quad (11.7)$$

What we derived is the *continuity* equation for the function f .

We will now show that due to the Hamiltonian nature of the flow in the phase space a medium represented by the distribution function f is *incompressible*. This follows from Liouville's theorem (see Section 5.3). Indeed, according to this theorem the volume of a space phase element does not change in Hamiltonian motion. Since the value of f is the number of particles in this volume, and this number is conserved, f within a *moving* elementary volume is also conserved. The density at a given point of the phase space q, p however changes because liquid elements located at this point at a given time leave and replaced by new elements that arrive at a later time.

Mathematically, the fact of incompressibility is reflected in the following transformation of the continuity equation (11.7). Let us take into account the Hamiltonian equations for \dot{q} and \dot{p} :

$$\frac{\partial}{\partial q} \dot{q}(q, p, t) = \frac{\partial}{\partial q} \frac{\partial H}{\partial p} = \frac{\partial}{\partial p} \frac{\partial H}{\partial q} = -\frac{\partial}{\partial p} \dot{p}(q, p, t), \quad (11.8)$$

which allows us to rewrite Eq. (11.7) as follows

$$-\frac{\partial f}{\partial t} + \frac{\partial H}{\partial q} \frac{\partial f}{\partial p} - \frac{\partial H}{\partial p} \frac{\partial f}{\partial q} = 0. \quad (11.9)$$

In accelerator physics this equation is often called the *Vlasov* equation. It is a partial differential equation which is not easy to solve. It is however extremely useful for studying many effects in accelerators because it gives a detailed description of a beam consisting of many particles.

Note, that using the formalism of Poisson brackets, we can also write the Vlasov equation as

$$\frac{\partial f}{\partial t} = \{f, H\}. \quad (11.10)$$

In case of n degrees of freedom, with the canonical variables q_i and p_i , $n = 1, 2, \dots, n$, the distribution function f is defined as a density in $2n$ -dimensional phase space and depends on all these variables, $f(q_1, \dots, p_1, \dots, t)$. The Vlasov equation takes the form

$$\frac{\partial f}{\partial t} = \sum_{i=1}^n \left(\frac{\partial H}{\partial q_i} \frac{\partial f}{\partial p_i} - \frac{\partial H}{\partial p_i} \frac{\partial f}{\partial q_i} \right). \quad (11.11)$$

Sometimes it is more convenient to normalize f by N , then the integral of f over the phase space is equal to one.

11.2 Integration of the Vlasov equation along trajectories

We have stated above that the distribution function is constant within a moving infinitesimal element of the phase space “cloud”. We will now prove mathematically this property of the Hamiltonian motion and derive from it a powerful method of solving the Vlasov equation.

Let us consider a trajectory in the phase space as shown in Fig. 11.3, and calculate the difference of f at two close points on this trajectory. We have

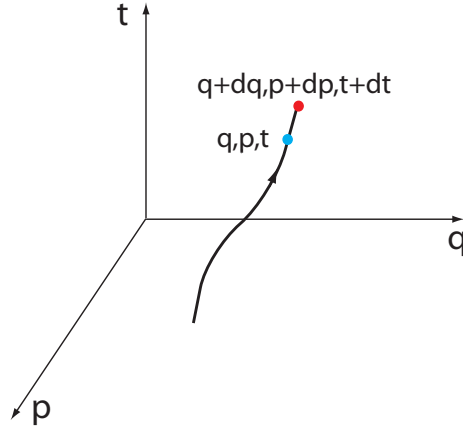


Figure 11.3: A trajectory in phase space.

$$\begin{aligned} df &= f(q + dq, p + dp, t + dt) - f(q, p, t) \\ &= \frac{\partial f}{\partial t} dt + \frac{\partial f}{\partial q} dq + \frac{\partial f}{\partial p} dp. \end{aligned} \quad (11.12)$$

Remember that the two points are on the same trajectory, hence, $dq = \dot{q}dt =$

$\partial H/\partial p dt$ and $dp = \dot{p}dt = -\partial H/\partial q dt$. We find

$$df = \frac{\partial f}{\partial t} dt - \frac{\partial H}{\partial q} \frac{\partial f}{\partial p} dt + \frac{\partial H}{\partial p} \frac{\partial f}{\partial q} dt = 0, \quad (11.13)$$

or

$$\frac{df}{dt} = 0. \quad (11.14)$$

On the last step we invoked Eq. (11.9). We proved that the function f is constant along the trajectories.

The above statement opens up a way to find solutions of the Vlasov equation if the phase space orbits are known. Let $q(q_0, p_0, t)$ and $p(q_0, p_0, t)$ be solutions of the Hamiltonian equations of motion with initial values q_0 and p_0 at $t = 0$, and $F(q_0, p_0)$ be the initial distribution function at $t = 0$. Then the solution of the Vlasov equation is given by the following equations

$$f(q, p, t) = F(q_0(q, p, t), p_0(q, p, t)), \quad (11.15)$$

where the functions $q_0(q, p, t)$ and $p_0(q, p, t)$ are obtained as inverse functions from equations

$$q = q(q_0, p_0, t), \quad p = p(q_0, p_0, t). \quad (11.16)$$

11.3 Steady state solutions of the kinetic equation

One of the powerful methods of solving the Vlasov equation is based on a judicious choice of canonical variables. To demonstrate this method we will find a steady state (time independent) solution of the Vlasov equation for a beam in a linear lattice in a ring. Remember that in a ring the arclength s plays the role of the time.

For a stationary beam the distribution function does not depend on s : $f = f(q, p)$. We can find such a steady state distribution function using the following observation.

Let us use canonical variables J and ϕ introduced in Lecture 8.1 and consider f as a function of these variables, $f(\phi, J)$. Then the Vlasov equation is

$$\frac{\partial f}{\partial s} + \frac{\partial \hat{\mathcal{H}}}{\partial J} \frac{\partial f}{\partial \phi} - \frac{\partial \hat{\mathcal{H}}}{\partial \phi} \frac{\partial f}{\partial J} = \frac{\partial f}{\partial s} + \frac{\partial \hat{\mathcal{H}}}{\partial J} \frac{\partial f}{\partial \phi} = 0, \quad (11.17)$$

where we used that $\hat{\mathcal{H}}$ does not depend on ϕ . In steady state $\partial f/\partial s = 0$, and hence we should have

$$\frac{\partial \hat{\mathcal{H}}}{\partial J} \frac{\partial f}{\partial \phi} = 0, \quad (11.18)$$

which means $\partial f / \partial \phi = 0$, or f depends only on J only. We come to conclusion that any function f that depends only on J is a steady state solution of the Vlasov equation.

The particular dependence $f(J)$ is determined by various other processes in the ring. In many cases, a negative exponential dependence f versus J is a good approximation

$$f = \text{const } e^{-J/\epsilon_0} = \text{const } \exp\left(-\frac{1}{2\beta\epsilon_0} [x^2 + (\beta P_x + \alpha x)^2]\right). \quad (11.19)$$

The quantity ϵ_0 is called the beam *emittance*. It is an important characteristic of the beam quality.

Problem 11.1. Write the Vlasov equation for a beam distribution $f(x, P_x, s)$ in terms of variables x and P_x .

Problem 11.2. Give a direct proof that the function (11.19) satisfies the Vlasov equation.

11.4 Phase mixing and decoherence

Consider an ensemble of linear oscillators with the frequency ω , whose motion is described by the Hamiltonian

$$H(x, p) = \frac{p^2}{2} + \omega^2 \frac{x^2}{2}. \quad (11.20)$$

The distribution function $f(x, p, t)$ for these oscillators satisfy the Vlasov equation

$$\frac{\partial f}{\partial t} - \omega^2 x \frac{\partial f}{\partial p} + p \frac{\partial f}{\partial x} = 0. \quad (11.21)$$

We can easily solve this equation using the method described at the end of Section 11.2. The trajectory of an oscillator with the initial coordinate x_0 and momentum p_0 is

$$\begin{aligned} x &= x_0 \cos \omega t + \frac{p_0}{\omega} \sin \omega t \\ p &= -\omega x_0 \sin \omega t + p_0 \cos \omega t. \end{aligned} \quad (11.22)$$

Inverting these equations, we find

$$\begin{aligned} x_0 &= x \cos \omega t - \frac{p}{\omega} \sin \omega t \\ p_0 &= \omega x \sin \omega t + p \cos \omega t. \end{aligned} \quad (11.23)$$

If $F(x, p)$ is the initial distribution function at $t = 0$, then, according to Eq. (11.15) we have

$$f(x, p, t) = F\left(x \cos \omega t - \frac{p}{\omega} \sin \omega t, \omega x \sin \omega t + p \cos \omega t\right). \quad (11.24)$$

This solution describes rotation of the initial distribution function in the phase space. An initially offset distribution function results in *collective* oscillations of the ensemble.

A more interesting situation occurs if there is a frequency spread in the ensemble. Let us assume that each oscillator is characterized by some parameter δ (that does not change with time), and ω is a function of δ , $\omega(\delta)$. We then have to add δ to the list of the arguments of f and F , and Eq. (11.24) becomes

$$f(x, p, t, \delta) = F \left(x \cos \omega(\delta)t - \frac{p}{\omega(\delta)} \sin \omega(\delta)t, \omega(\delta)x \sin \omega(\delta)t + p \cos \omega(\delta)t, \delta \right). \quad (11.25)$$

To find the distribution of oscillators over x and p only one has to integrate f over δ

$$\hat{f}(x, p, t) = \int_{-\infty}^{\infty} d\delta f(x, p, t, \delta). \quad (11.26)$$

The behavior of the integrated function \hat{f} is different from the case of constant ω at large times, even if the spread in frequencies $\Delta\omega$ is small. For $t \gtrsim 1/\Delta\omega$ the oscillators smear out over the phase. This effect is called the *phase mixing* and it results in *decoherence* of collective oscillations of the ensemble of oscillators.

Problem 11.3. *Action and angle variables are more convenient for the study of the phase mixing. Use these variables and find the limit of the distribution function integrated over δ in the limit $t \rightarrow \infty$.*

Lecture 12

Radiation damping effects

In this lecture we will show how the radiation damping in electron and positron rings can be added to the Hamiltonian and Vlasov formalism.

12.1 Radiation damping in equations of motion

A light relativistic particle (like electron or positron) copiously emits synchrotron radiation when moving in a circular orbit in an accelerator. The energy of the radiation is taken from the kinetic energy of the particle. As we will see in the second part of this course, radiation is emitted almost exclusively in the direction of particle's momentum. The radiation reaction force, hence, acts in the opposite direction, and, similar to a friction force, tends to slow down the motion of the particle. Our goal is to derive equations of motion that take this friction force into account.

We assume relativistic particles, $\gamma \gg 1$. Let \mathcal{P} be the averaged power of radiation (the energy emitted per unit time) at a given location in the ring. Since for a relativistic particle we have approximately $p = h/c$, the quantity \mathcal{P}/c is equal to the decrease of the momentum of a particle per unit time. Since, as mentioned above, the force is acting in the direction opposite to the momentum, we can write the change in the momentum components per infinitesimally small time dt as

$$\begin{aligned} dp_x &= -\frac{p_x}{p} \frac{\mathcal{P}}{c} dt = -\frac{v_x}{v} \frac{\mathcal{P}}{c} dt \approx -\frac{\mathcal{P}}{c^2} v_x dt = -\frac{\mathcal{P}}{c^2} dx = -\frac{\mathcal{P}}{c^2} \frac{dx}{ds} ds, \\ dp_y &= -\frac{p_y}{p} \frac{\mathcal{P}}{c} dt \approx -\frac{\mathcal{P}}{c^2} \frac{dy}{ds} ds, \\ dh &= -\mathcal{P} dt = -\mathcal{P} \frac{dt}{ds} ds. \end{aligned} \tag{12.1}$$

These additional changes of the momenta and energy has to be added to the dynamics governed by the Hamiltonian (6.24). Since Eqs. (12.1) change only

the canonical momenta, the equations for the coordinates remain Hamiltonian

$$\frac{dx}{ds} = \frac{\partial K}{\partial p_x}, \quad \frac{dy}{ds} = \frac{\partial K}{\partial p_y}, \quad \frac{dt}{ds} = -\frac{\partial K}{\partial h}. \quad (12.2)$$

The corrected equations for the momenta are

$$\begin{aligned} \frac{dp_x}{ds} &= -\frac{\partial K}{\partial x} - \frac{\mathcal{P}}{c^2} \frac{\partial K}{\partial p_x}, \\ \frac{dp_y}{ds} &= -\frac{\partial K}{\partial y} - \frac{\mathcal{P}}{c^2} \frac{\partial K}{\partial p_y}, \\ \frac{dh}{ds} &= \frac{\partial K}{\partial t} + \mathcal{P} \frac{\partial K}{\partial h}, \end{aligned} \quad (12.3)$$

where we used (12.1) and eliminated the derivatives dt/ds , dy/ds and dt/ds with the help of (12.2). We emphasize here that Eqs. (12.2) and (12.3) are not Hamiltonian any more, but it is convenient to keep writing them using previously introduced canonical variables and the Hamiltonian function K .

The expression for the radiation power (in SI units) is derived later in the course (20.32)

$$\mathcal{P}(h, x, y, s) = \frac{2}{3} \frac{e^2 r_0 h^2}{m^3 c^3} B(x, y, s)^2, \quad (12.4)$$

where r_0 is the classical radius for the particle, and we indicated explicitly that in general case \mathcal{P} depends on coordinates and particle's energy. Below we will also use the radiation power at the nominal orbit $x = y = 0$ for the particle with the nominal energy h_0

$$\mathcal{P}_0(s) = \frac{2}{3} \frac{e^2 r_0 h_0^2}{m^3 c^3} B(0, 0, s)^2 = \frac{2}{3} \frac{r_0 \gamma^4 m c^3}{\rho(s)^2}. \quad (12.5)$$

Averaging this power over the ring and dividing it by the nominal energy $p_0 c$ defines the characteristic damping time in the ring τ_s ,

$$\frac{1}{\tau_s} = \frac{\langle \mathcal{P}_0(s) \rangle}{p_0 c} = \frac{1}{\gamma m c^2} \frac{1}{cT} \oint ds \mathcal{P}_0(s) = \frac{2}{3} \frac{r_0 \gamma^3}{T} \oint \frac{ds}{\rho(s)^2}, \quad (12.6)$$

where T is the revolution period and the angular brackets denote averaging over the ring circumference.

In a typical accelerator ring the damping time is much longer than the revolution period T and the period of betatron oscillations. This observation will be used, in the next section, when we calculate the effect of the synchrotron radiation on betatron oscillations.

12.2 Synchrotron damping of betatron oscillations

In this section we will consider the effect of synchrotron damping of betatron oscillations using machinery developed in Section 12.1.

At a first step we need to adapt Eqs. (12.2) and (12.3) for the variables of the linearized Hamiltonian (7.11) used in our studies of the betatron oscillations. Recall that \mathcal{H} was obtained from K by division by p_0 with simultaneous transition from p_x, p_y to $P_x = p_x/p_0, P_y = p_y/p_0$ and from h to h/p_0 . As a result two first pairs of Eqs. (12.2) and (12.3) become

$$\begin{aligned} \frac{dx}{ds} &= \frac{\partial \mathcal{H}}{\partial P_x}, & \frac{dP_x}{ds} &= -\frac{\partial \mathcal{H}}{\partial x} - \frac{\mathcal{P}}{p_0 c^2} \frac{\partial \mathcal{H}}{\partial P_x}, \\ \frac{dy}{ds} &= \frac{\partial \mathcal{H}}{\partial P_y}, & \frac{dP_y}{ds} &= -\frac{\partial \mathcal{H}}{\partial y} - \frac{\mathcal{P}}{p_0 c^2} \frac{\partial \mathcal{H}}{\partial P_y}. \end{aligned} \quad (12.7)$$

Because we are now interested in relativistic motion, we can identify h/p_0 with $pc/p_0 = c(1 + \eta)$ (see (6.27)), which means that in the third equation in (12.3) we can use $c\eta$:

$$\frac{dc\eta}{ds} = \frac{\partial \mathcal{H}}{\partial t} + \frac{\mathcal{P}}{cp_0} \frac{\partial \mathcal{H}}{\partial \eta} = -\frac{\mathcal{P}}{cp_0} \left(1 + \frac{x}{\rho}\right), \quad (12.8)$$

where in the last equation we assumed $\partial \mathcal{H}/\partial t = 0$ and used (7.11). One immediately sees from this equation that η monotonously decreases with time due to the continuous energy loss to radiation. Without compensation of the losses all initial energy will be lost within the time of the order of τ_s . In reality the particle energy is replenished by RF cavities in the ring, with the corresponding term in the Hamiltonian given by (6.32). However, to avoid complications associated with treatment of a time-dependent Hamiltonian we will adopt a simpler model of the energy source. We will assume that it is continuously distributed in the ring and is equal, with the opposite sign, to $\mathcal{P}_0(s)$ defined by (12.5):

$$\frac{dc\eta}{ds} = -\frac{\mathcal{P}}{cp_0} \left(1 + \frac{x}{\rho}\right) + \frac{\mathcal{P}_0}{cp_0}. \quad (12.9)$$

Moreover, since we assume that η is small we can expand the difference $\mathcal{P} - \mathcal{P}_0$ keeping only linear terms in η

$$\mathcal{P} - \mathcal{P}_0 \approx cp_0 \eta \frac{\partial \mathcal{P}}{\partial h} \Big|_{h=h_0} = 2\eta \mathcal{P}_0, \quad (12.10)$$

where we took into account the quadratic dependence of \mathcal{P} versus h , see (12.4). As a result, we obtain

$$\frac{d\eta}{ds} = -\frac{\mathcal{P}_0}{p_0 c^2} \left(2\eta + \frac{x}{\rho}\right), \quad (12.11)$$

where we neglected second order terms $\propto x\eta$. The first term on the right hand side describes damping of energy deviations due to the synchrotron radiation, and the second one is a driving term due to the deviation in the x plane from the nominal orbit. In contrast to (12.8) this equation exhibits an equilibrium solution with $x = \eta = 0$.

As it turns out, our results obtained with the model of continuous energy source (12.9) are actually valid for the real machines with localized RF cavities in the ring.

Let us assume that a particle has an initial energy deviation η_0 at some initial position. How does its energy deviation evolve with time? We know that an off-energy particle is moving along the orbit (9.15): $x(s) = \eta D(s)$. Substituting this into (12.11) we obtain

$$\frac{d\eta}{ds} = -\eta \frac{\mathcal{P}_0}{p_0 c^2} \left(2 + \frac{1}{\rho} D(s) \right). \quad (12.12)$$

As was observed at the end of the previous section, synchrotron damping lasts for many revolution periods. It makes sense then to average (12.12) over the circumference of the ring. Recalling that $\mathcal{P}_0 \propto \rho^{-2}$ and using (12.6) it is easy to obtain

$$\left\langle \frac{d\eta}{ds} \right\rangle = -\frac{\eta}{c\tau_s} (2 + \mathcal{D}), \quad (12.13)$$

with

$$\mathcal{D} = \left(\int \frac{ds}{\rho^2} \right)^{-1} \int \frac{ds}{\rho^3} D(s). \quad (12.14)$$

In many practical situations the parameter \mathcal{D} is small and can be neglected. We then have the energy perturbation, on average, exponentially decaying with the time constant equal to half of τ_s .

Consider now damping of vertical betatron oscillations in a ring due to the synchrotron radiation. We know that without damping, when the system is Hamiltonian, the action J_y given by (8.9) is conserved. Due to the synchrotron radiation it will be slowly (over many revolution periods) decreasing with time. To find its damping time, we need to calculate the derivative dJ_y/ds using equations (12.7) and average it over the ring (as we did above for $d\eta/ds$). The calculation is simplified if we note that $dJ_y/ds = 0$ when $\mathcal{P} = 0$, and the damping term in (12.7) involves P_y only. Hence

$$\frac{dJ_y}{ds} = \frac{\partial J_y}{\partial P_y} \times \left(-\frac{\mathcal{P}_0}{p_0 c^2} \frac{\partial \mathcal{H}}{\partial P_y} \right) = -\frac{\mathcal{P}_0}{p_0 c^2} (\beta P_y + \alpha y) P_y \quad (12.15)$$

(to simplify notation we drop the index y in β and α). We then use (8.10) and (8.11) to obtain

$$\begin{aligned} \frac{dJ_y}{ds} &= -\frac{\mathcal{P}_0}{p_0 c^2} \left[2J_y (\sin \phi + \alpha \cos \phi)^2 - 2\alpha J_y \cos \phi (\sin \phi + \alpha \cos \phi) \right] \\ &= -\frac{2\mathcal{P}_0}{p_0 c^2} J_y [(\sin \phi)^2 + \alpha \sin \phi \cos \phi]. \end{aligned} \quad (12.16)$$

Averaging over the ring circumference is equivalent to averaging over the phase ϕ . We find

$$\left\langle \frac{dJ_y}{ds} \right\rangle = -\frac{\langle \mathcal{P}_0 \rangle}{p_0 c^2} J_y = -\frac{1}{c\tau_s} J_y. \quad (12.17)$$

Calculations of damping of betatron oscillations in the horizontal plane are more complicated. This complication comes from the fact that they are coupled to the energy through the term $-\eta x/\rho$ in the Hamiltonian (7.11) and, in addition, the evolution of η is coupled to x through the term x/ρ in (12.8). While the averaged value of η in the course of betatron oscillations is zero, the x/ρ term in (12.8) induces small oscillations of η that has to be taken into account. The easiest way to do that is to calculate the averaged rate of change of the action (9.17) at $\eta = 0$ rather than (8.9). As above, calculation of dJ_x/ds is simplified if one takes into account that it is zero when $\mathcal{P} = 0$, and the damping comes through the variables P_x and η . We then have

$$\begin{aligned} \frac{dJ_x}{ds} &= \frac{\partial J_x}{\partial P_x} \times \left(-\frac{\mathcal{P}_0}{p_0 c^2} \frac{\partial \mathcal{H}}{\partial P_x} \right) + \frac{\partial J_x}{\partial \eta} \frac{d\eta}{ds} \\ &= -\frac{\mathcal{P}_0}{p_0 c^2} [\beta P_x - \beta \eta D' + \alpha x - \alpha \eta D] P_x \\ &\quad - \frac{\mathcal{P}_0}{p_0 c^2} \left(2\eta + \frac{x}{\rho} \right) \frac{1}{\beta} [-D(x - \eta D) - (\beta P_x - \beta \eta D' + \alpha x - \alpha \eta D)(\beta D' + \alpha D)]. \end{aligned} \quad (12.18)$$

As explained above we set $\eta = 0$ on the right hand side which gives

$$\begin{aligned} \frac{dJ_x}{ds} &= -\frac{\mathcal{P}_0}{p_0 c^2} [\beta P_x + \alpha x] P_x \\ &\quad - \frac{\mathcal{P}_0}{p_0 c^2} \frac{x}{\rho} \frac{1}{\beta} [-Dx - (\beta P_x + \alpha x)(\beta D' + \alpha D)], \end{aligned} \quad (12.19)$$

and express x and P_x through J_x and ϕ using (8.10) and (8.11)

$$\begin{aligned} \frac{dJ_x}{ds} &= -\frac{2\mathcal{P}_0}{p_0 c^2} J_x [(\sin \phi)^2 + \alpha \sin \phi \cos \phi] \\ &\quad - \frac{2\mathcal{P}_0}{p_0 c^2} J_x \frac{\cos \phi}{\rho} [-D \cos \phi + (\beta D' + \alpha D) \sin \phi]. \end{aligned} \quad (12.20)$$

Averaging over angle ϕ leaves only two terms on the right hand side

$$\frac{dJ_x}{ds} = -\frac{\mathcal{P}_0}{p_0 c^2} J_x \left(1 - \frac{D}{\rho} \right), \quad (12.21)$$

and then averaging over circumference of the ring gives

$$\left\langle \frac{dJ_x}{ds} \right\rangle = -\frac{1}{c\tau_s} J_x (1 - \mathcal{D}). \quad (12.22)$$

12.3 Vlasov equation and Robinson's theorem

In Lecture 11 we introduced the kinetic equation for description of the ensemble of beam particles. While our initial formulation of the continuity equation (11.7) was general and valid for arbitrary equations of motion, the subsequent assumption of the Hamiltonian motion has lead to the Vlasov equation (11.11) and

even more elegant Eq. (11.14). Our goal now is to include the effect of the synchrotron damping, as described by Eqs. (12.7) and (12.8), into the formalism of the Vlasov equation.

The distribution function f now depends on 7 variables: $f(x, P_x, y, P_y, t, c\tau, s)$. With an evident generalization of equation (11.7) for 3 degrees of freedom, the kinetic equation is

$$\begin{aligned} \frac{\partial f}{\partial s} + \frac{\partial}{\partial x} \left(\frac{dx}{ds} f \right) + \frac{\partial}{\partial P_x} \left(\frac{dP_x}{ds} f \right) + \frac{\partial}{\partial y} \left(\frac{dy}{ds} f \right) + \frac{\partial}{\partial P_y} \left(\frac{dP_y}{ds} f \right) \\ + \frac{\partial}{\partial t} \left(\frac{dt}{ds} f \right) + \frac{\partial}{\partial \eta} \left(\frac{d\eta}{ds} f \right) = 0. \end{aligned} \quad (12.23)$$

Let us calculate df/ds :

$$\frac{df}{ds} = \frac{\partial f}{\partial s} + \frac{dx}{ds} \frac{\partial f}{\partial x} + \frac{dP_x}{ds} \frac{\partial f}{\partial P_x} + \frac{dy}{ds} \frac{\partial f}{\partial y} + \frac{dP_y}{ds} \frac{\partial f}{\partial P_y} + \frac{dt}{ds} \frac{\partial f}{\partial t} + \frac{d\eta}{ds} \frac{\partial f}{\partial \eta} = 0. \quad (12.24)$$

Substituting (12.23) into (12.24) we obtain

$$\frac{df}{ds} = -f \left(\frac{\partial}{\partial x} \frac{dx}{ds} + \frac{\partial}{\partial P_x} \frac{dP_x}{ds} + \frac{\partial}{\partial y} \frac{dy}{ds} + \frac{\partial}{\partial P_y} \frac{dP_y}{ds} + \frac{\partial}{\partial t} \frac{dt}{ds} + \frac{\partial}{\partial \eta} \frac{d\eta}{ds} \right). \quad (12.25)$$

The Hamiltonian part of the equations of motion (12.7) does not contribute to the right hand side of (12.25). Using (12.7) and (12.11) we find

$$\begin{aligned} \frac{df}{ds} &= -f \left(\frac{\partial}{\partial P_x} \frac{dP_x}{ds} + \frac{\partial}{\partial P_y} \frac{dP_y}{ds} + \frac{\partial}{\partial \eta} \frac{d\eta}{ds} \right) \\ &= -4f \frac{\mathcal{P}}{p_0 c^2}. \end{aligned} \quad (12.26)$$

According to this equation the distribution function f in a phase point moving with a particle exponentially grows with time. This happens because, due to the synchrotron radiation, the phase space volume occupied by a given ensemble of particles decreases with time. Since f is the particle density in the phase space, it grows inversely proportionally to the phase volume. This effect is associated with the name of K. Robinson who pointed it out in [13].

There is also a competing mechanism that limits indefinite decrease of the space volume due to the synchrotron radiation—a so called *quantum diffusion*. We will briefly discuss it in Lecture 20.

Lecture 13

Primer in Special Relativity

We will review relativistic transformations for time-space coordinates, frequency, and electromagnetic field.

13.1 Lorentz transformation and matrices

Consider two coordinate systems, K and K' . The system K' is moving with

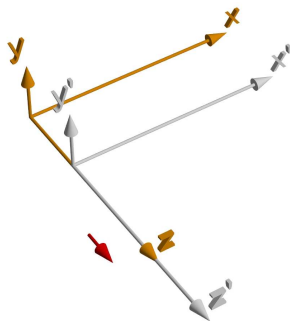


Figure 13.1: Laboratory frame K and a moving frame K' .

velocity v in the z direction relative to the system K (see Fig. 13.1). The coordinates of an event in both systems are related by the Lorentz transformation

$$\begin{aligned}x &= x', \\y &= y', \\z &= \gamma(z' + \beta ct'), \\t &= \gamma(t' + \beta z'/c),\end{aligned}\tag{13.1}$$

where $\beta = v/c$, and $\gamma = 1/\sqrt{1 - \beta^2}$.

The vector $(ct, \mathbf{r}) = (ct, x, y, z)$ is called a *4-vector*, and the above transformation is valid for any 4-vector quantity.

We will often deal with ultrarelativistic particles, which means that $\gamma \gg 1$. In this limit, a useful approximation is

$$\beta = \sqrt{1 - \frac{1}{\gamma^2}} \approx 1 - \frac{1}{2\gamma^2}. \quad (13.2)$$

The Lorentz transformation (13.1) can also be written in the matrix notation

$$\begin{pmatrix} x \\ y \\ z \\ t \end{pmatrix} = \begin{pmatrix} 1 & 0 & 0 & 0 \\ 0 & 1 & 0 & 0 \\ 0 & 0 & \gamma & c\beta\gamma \\ 0 & 0 & \frac{\beta\gamma}{c} & \gamma \end{pmatrix} \begin{pmatrix} x' \\ y' \\ z' \\ t' \end{pmatrix} = L \begin{pmatrix} x' \\ y' \\ z' \\ t' \end{pmatrix}. \quad (13.3)$$

The advantage of using matrices is that they can be easily multiplied by a computer. Here is an example: we want to generate a matrix which corresponds to a moving coordinate system along the x axis, see Fig. 13.2. Let us rotate K'

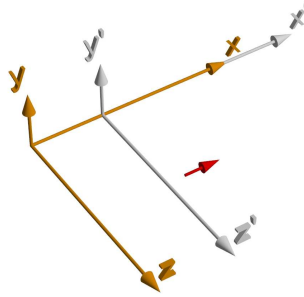


Figure 13.2: The frame K' is moving along x .

system by 90 degrees around the y axis, in such a way the new x axis is directed along the old z . The rotated frame is denoted by K'' (see Fig. 13.3) and the coordinate transformation from K' to K'' is given by $x'' = -z'$, $z'' = x'$, or in matrix notation

$$M_{\text{rot}} = \begin{pmatrix} 0 & 0 & -1 & 0 \\ 0 & 1 & 0 & 0 \\ 1 & 0 & 0 & 0 \\ 0 & 0 & 0 & 1 \end{pmatrix}. \quad (13.4)$$

The new frame K''' is moving along the z'' and has its axes oriented relative to K'' the same way as shown in Fig. 13.1. Hence the Lorentz transformation

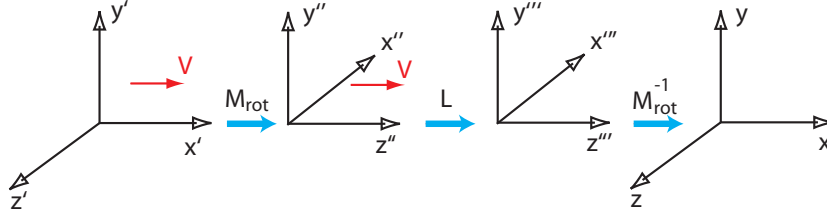


Figure 13.3: Sequence of frames.

is given by L , Eq. (13.3). Finally, we transform from K''' to the lab frame K using the matrix M_{rot}^{-1} . The sequence of these transformations is given by the product

$$(M_{\text{rot}})^{-1} \cdot L \cdot M_{\text{rot}} = \begin{pmatrix} \gamma & 0 & 0 & \gamma\beta c \\ 0 & 1 & 0 & 0 \\ 0 & 0 & 1 & 0 \\ \gamma\beta/c & 0 & 0 & \gamma \end{pmatrix}. \quad (13.5)$$

This result, of course, can be easily obtained directly from the original transformation by exchanging $x \rightleftharpoons z$.

Problem 13.1. Derive the Lorentz transformation when velocity \mathbf{v} is at 45° to the z axis, $\mathbf{v} = v(0, 1/\sqrt{2}, 1/\sqrt{2})$.

Problem 13.2. Using the matrix formalism, show that the inverse Lorentz transformation is given by the following equations:

$$\begin{aligned} x' &= x, \\ y' &= y, \\ z' &= \gamma(z - \beta ct), \\ t' &= \gamma(t - \beta z/c), \end{aligned} \quad (13.6)$$

Explain the meaning of the minus sign in front of β .

13.2 Lorentz contraction and time dilation

Two events occurring in the moving frame at the same point and separated by the time interval $\Delta t'$ will be measured by the lab observers as separated by Δt ,

$$\Delta t = \gamma \Delta t'. \quad (13.7)$$

This is the effect of relativistic *time dilation*.

An object of length l' aligned in the moving frame with the z' axis will have the length l in the lab frame:

$$l = \frac{l'}{\gamma}. \quad (13.8)$$

This is the effect of relativistic *contraction*. The length in the direction transverse to the motion is not changed.

Problem 13.3. *Muon at rest has the mean life time of 2.2 μ s. To what energy one needs to accelerate the muon in order to get the life time (in the lab frame) of 1 ms. The muon mass is equal to 105 MeV.*

Problem 13.4. *A bunch of 10^{10} electrons with energy 15 GeV has a length of 100 micron and a radius of 30 micron (in the lab frame). What is the electron density (in units of particles per cubic centimeter) in the beam frame?*

13.3 Doppler effect

Consider a wave propagating in a moving frame K' . It has the time-space dependence:

$$\propto \cos(\omega' t' - \mathbf{k}' \cdot \mathbf{r}'), \quad (13.9)$$

where ω' is the frequency and \mathbf{k}' is the wavenumber of the wave in the moving frame. What kind of time-space dependence an observer in the frame K would see? We need to make the Lorentz transformation of coordinates and time using Eq. (13.6)

$$\begin{aligned} \cos(\omega' t' - \mathbf{k}' \cdot \mathbf{r}') &= \cos(\omega' \gamma(t - \beta z/c) - k_x' x - k_y' y - k_z' \gamma(z - \beta ct)) \\ &= \cos(\gamma(\omega' + k_z' \beta c)t - k_x' x - k_y' y - \gamma(k_z' + \omega' \beta/c)z). \end{aligned} \quad (13.10)$$

We see that in the K frame this process is also a wave

$$\propto \cos(\omega t - \mathbf{k} \cdot \mathbf{r}), \quad (13.11)$$

with the frequency and wavenumber

$$\begin{aligned} k_x &= k_x', \\ k_y &= k_y', \\ k_z &= \gamma(k_z' + \beta \omega'/c), \\ \omega &= \gamma(\omega' + \beta c k_z'). \end{aligned} \quad (13.12)$$

The object $(\omega, c\mathbf{k})$ is a 4-vector.

The above transformation is valid for any type of waves (electromagnetic, acoustic, plasma waves, etc.) Now let us apply it to electromagnetic waves in vacuum. For those waves we know that

$$\omega = ck. \quad (13.13)$$

Problem 13.5. *Using equations (13.12) prove that from $\omega' = ck'$ follows $\omega = ck$.*

Assume that an electromagnetic wave propagates at angle θ' in the frame K'

$$\cos \theta' = \frac{k'_z}{k'}, \quad (13.14)$$

and has a frequency ω' in that frame. What is the angle θ and the frequency ω of this wave in the lab frame? We can always choose the coordinate system such that $\mathbf{k} = (0, k_y, k_z)$, then

$$\tan \theta = \frac{k_y}{k_z} = \frac{k'_y}{\gamma(k'_z + \beta\omega'/c)} = \frac{\sin \theta'}{\gamma(\cos \theta' + \beta)}. \quad (13.15)$$

In the limit $\gamma \gg 1$ almost all angles θ' (except for those very close to π) are transformed to angles $\theta \sim 1/\gamma$. This explains why radiation of an ultrarelativistic beams goes mostly in the forward direction, within an angle of the order of $1/\gamma$.

Problem 13.6. Prove that

$$\cos \theta' = \frac{\cos \theta - \beta}{1 - \beta \cos \theta}, \quad \sin \theta' = \frac{\sin \theta}{\gamma(1 - \beta \cos \theta)}. \quad (13.16)$$

For the frequency, a convenient formula relates ω with ω' and θ (not θ'). To derive it, we use first the inverse Lorentz transformation

$$\omega' = \gamma(\omega - \beta ck_z) = \gamma(\omega - \beta ck \cos \theta), \quad (13.17)$$

which gives

$$\omega = \frac{\omega'}{\gamma(1 - \beta \cos \theta)}. \quad (13.18)$$

Using $\beta \approx 1 - 1/2\gamma^2$ and $\cos \theta = 1 - \theta^2/2$, we obtain

$$\omega = \frac{2\gamma\omega'}{1 + \gamma^2\theta^2}. \quad (13.19)$$

The radiation in the forward direction ($\theta = 0$) gets a large factor 2γ in the frequency transformation.

Problem 13.7. A laser light of frequency ω copropagates with a relativistic beam with $\gamma \gg 1$. Find the laser frequency in the beam frame.

13.4 Lorentz transformation of fields

The electromagnetic field is transformed from K' to K according to following equations

$$\begin{aligned} E_z &= E'_z, & \mathbf{E}_\perp &= \gamma(\mathbf{E}'_\perp - \mathbf{v} \times \mathbf{B}'), \\ B_z &= B'_z, & \mathbf{B}_\perp &= \gamma\left(\mathbf{B}'_\perp + \frac{1}{c^2}\mathbf{v} \times \mathbf{E}'\right), \end{aligned} \quad (13.20)$$

where \mathbf{E}'_{\perp} and \mathbf{B}'_{\perp} are the components of the electric and magnetic fields perpendicular to the velocity \mathbf{v} : $\mathbf{E}'_{\perp} = (E'_x, E'_y)$, $\mathbf{B}'_{\perp} = (B'_x, B'_y)$.

The electromagnetic potentials $(\phi/c, \mathbf{A})$ are transformed exactly as the 4-vector (ct, \mathbf{r}) :

$$\begin{aligned} A_x &= A'_x, \\ A_y &= A'_y, \\ A_z &= \gamma \left(A'_z + \frac{v}{c^2} \phi' \right), \\ \phi &= \gamma (\phi' + v A'_z), \end{aligned} \tag{13.21}$$

Problem 13.8. Consider Lorentz transformation of fields in a plane electromagnetic wave propagating along axis z . The electric field is directed along x and the magnetic field is directed along y with $E_x = cB_y$. Derive transformation formula for the absolute value of the Poynting vector of the wave.

13.5 Lorentz transformation and photons

It is often convenient, even in classical electrodynamics, consider electromagnetic radiation as a collection of photons. How do we transform photon properties from K' to K ? The answer is simple: the wavevector \mathbf{k} and the frequency of each photon ω is transformed as described above. The number of photons is a relativistic invariant—it is the same in all frames.

Problem 13.9. An electromagnetic wave with the frequency ω and the amplitude electric field E_0 occupies the volume with dimensions $L_x \times L_y \times L_z$. It propagates along the z axis with the fields with $E_x = cB_y$. Using results of the previous problem find the electromagnetic energy W of the wave in the lab frame and the energy W' in a frame K' moving with velocity v relative to the lab frame. Show that $W/\omega = W'/\omega'$, where ω' is the frequency of the wave in K' .

Lecture 14

Selected electrostatic and magnetostatic problems

In this lecture, we present solutions of several electrostatic and magnetostatic problems which can be encountered when a bunch of charged particles propagates in the conducting vacuum chamber of an accelerator.

14.1 Electric field of a 3D Gaussian distribution

A bunch of charged particles in accelerator physics is often represented as having a Gaussian distribution function in all three directions so that the charge density ρ is

$$\rho(x, y, z) = \frac{Q}{(2\pi)^{3/2}\sigma_x\sigma_y\sigma_z} e^{-x^2/2\sigma_x^2 - y^2/2\sigma_y^2 - z^2/2\sigma_z^2}, \quad (14.1)$$

where σ_x , σ_y , and σ_z are the rms bunch lengths in the corresponding directions. What is the electric field of such bunch in the beam frame (that is the frame where the bunch is at rest)? This is a purely electrostatic problem, whose solution we give in this section.

First, we note that due to the Lorentz transformation the bunch length in the beam frame is γ times longer than in the lab frame, $\sigma_{z,\text{beam}} = \gamma\sigma_{z,\text{lab}}$. We assume that this factor is already taken into account and σ_z in (14.1) is the bunch length in the beam frame.

The electrostatic potential ϕ satisfies the Poisson equation

$$\nabla^2\phi = -\frac{\rho}{\epsilon_0}, \quad (14.2)$$

whose solution can be written as

$$\phi(x, y, z) = \frac{1}{4\pi\epsilon_0} \int \frac{\rho(x', y', z') dx' dy' dz'}{[(x-x')^2 + (y-y')^2 + (z-z')^2]^{1/2}}. \quad (14.3)$$

It is not an easy problem to carry out a three-dimensional integration in this equation. A trick that simplifies it and reduces to a one-dimensional integral is to use the following identity

$$\frac{1}{R} = \sqrt{\frac{2}{\pi}} \int_0^\infty e^{-\lambda^2 R^2/2} d\lambda. \quad (14.4)$$

Assuming that $R = [(x - x')^2 + (y - y')^2 + (z - z')^2]^{1/2}$ and replacing $1/R$ in Eq. (14.3) with (14.4) we first arrive at a four-dimensional integral

$$\phi = \frac{1}{4\pi\epsilon_0} \sqrt{\frac{2}{\pi}} \int_0^\infty d\lambda \int e^{-\lambda^2 [(x-x')^2 + (y-y')^2 + (z-z')^2]/2} \rho(x', y', z') dx' dy' dz'. \quad (14.5)$$

With the Gaussian distribution (14.1) the integration over x' , y' and z' can now be easily carried out, e.g.,

$$\int_{-\infty}^\infty e^{-\frac{1}{2}\lambda^2(x-x')^2} e^{-\frac{x'^2}{2\sigma_x^2}} dx' = \frac{\sqrt{2\pi}}{\sqrt{\lambda^2 + \sigma_x^{-2}}} e^{-\frac{x^2\lambda^2}{2(\lambda^2\sigma_x^2+1)}}, \quad (14.6)$$

which gives for the potential

$$\phi(x, y, z) = \frac{1}{4\pi\epsilon_0} \sqrt{\frac{2}{\pi}} \frac{Q}{\pi \sigma_x \sigma_y \sigma_z} \int_0^\infty d\lambda \frac{e^{-\frac{x^2\lambda^2}{2(\lambda^2\sigma_x^2+1)}} e^{-\frac{y^2\lambda^2}{2(\lambda^2\sigma_y^2+1)}} e^{-\frac{z^2\lambda^2}{2(\lambda^2\sigma_z^2+1)}}}{\sqrt{\lambda^2 + \sigma_x^{-2}} \sqrt{\lambda^2 + \sigma_y^{-2}} \sqrt{\lambda^2 + \sigma_z^{-2}}}. \quad (14.7)$$

This integral is much easier to evaluate numerically, and it is often used in numerical simulations of the field of a charged bunch. There are various useful limiting cases of this expression, such as $\sigma_x = \sigma_y$ (axisymmetric beam) or $\sigma_x, \sigma_y \ll \sigma_z$ (a long, thin beam) that can be analyzed.

Problem 14.1. Show that at large distances from the center Eq. (14.7) reduces to

$$\phi = \frac{Q}{4\pi\epsilon_0 \sqrt{x^2 + y^2 + z^2}}. \quad (14.8)$$

Having found the potential in the beam frame, it is now easy to transform it to the laboratory frame using the Lorentz transformation. First we have to recall that σ_z in (14.7) is the bunch length in the beam frame equal to $\gamma\sigma_{z,\text{lab}}$. Second, from (13.21) we see that the potential in the lab frame is γ times larger than in the beam frame (note that $A'_z = 0$ in (14.7)). Third, we need to transform the coordinates x, y, z in (14.7) to the lab frame. According to (13.6) x and y coordinates are not transformed however z should be replaced by $\gamma(z_{\text{lab}} - vt_{\text{lab}})$. The resulting expression is (we drop all “lab” subscripts in what follows)

$$\phi = \frac{1}{4\pi\epsilon_0} \sqrt{\frac{2}{\pi}} \frac{Q}{\pi \sigma_x \sigma_y \sigma_z} \int_0^\infty \frac{d\lambda}{\sqrt{\lambda^2 + \sigma_x^{-2}} \sqrt{\lambda^2 + \sigma_y^{-2}} \sqrt{\lambda^2 + \gamma^{-2}\sigma_z^{-2}}} \times e^{-\frac{x^2\lambda^2}{2(\lambda^2\sigma_x^2+1)}} e^{-\frac{y^2\lambda^2}{2(\lambda^2\sigma_y^2+1)}} e^{-\frac{(z-vt)^2\lambda^2}{2(\lambda^2\sigma_z^2+\gamma^{-2})}}. \quad (14.9)$$

According to (13.21), in addition to the electrostatic potential, in the lab frame there is also a vector potential A_z responsible for the magnetic field of the moving bunch. It is equal to $A_z = \gamma v \phi / c$ with ϕ given by (14.9).

14.2 Electric field of a continuous beam in a pipe

A continuous beam propagating inside a metallic pipe generates electric and magnetic fields. In many applications it is important to know these fields as a function of the beam position inside the pipe. We assume that the beam propagates parallel to the axis of a cylindrical pipe of a given cross section. The electrostatic potential ϕ is a function of the transverse coordinates x and y .

To a good approximation, the transverse beam dimensions, σ_x and σ_y , are often much smaller than the transverse size of the pipe. We can neglect these dimensions and consider the beam as infinitely thin charged wire located at position $x = x_0$ and $y = y_0$. Then the problem of finding the electrostatic potential reduces to the solution of

$$\nabla^2 \phi(x, y) = -\frac{\tilde{Q}}{\epsilon_0} \delta(x - x_0) \delta(y - y_0), \quad (14.10)$$

where \tilde{Q} is the charge per unit length of the beam. This equation is to be solved with the boundary condition $\phi = 0$ at the surface of the pipe.

In the simplest case of a beam located at the center of a round pipe of radius a ($x_0 = y_0 = 0$), the solution is easily found in cylindrical coordinates

$$\phi = -\frac{\tilde{Q}}{2\pi\epsilon_0} \ln\left(\frac{r}{a}\right), \quad (14.11)$$

with the field $E_r = \tilde{Q}/2\pi\epsilon_0 r$.

What if the beam is not at the center of a round pipe? There is also an analytical solution in this case. A compact form of this solution is given as a real part of the complex function

$$\phi = -\frac{\tilde{Q}}{2\pi\epsilon_0} \operatorname{Re} \ln \frac{a(z - z_0)}{a^2 - z z_0}, \quad (14.12)$$

where $z = x + iy$ and $z_0 = x_0 + iy_0$. The equipotential lines computed with this expression are shown in Fig. 14.1.

If the beam is propagating in a pipe with a rectangular cross section $0 \leq x \leq a$, $0 \leq y \leq b$, the potential is given by the following expressions

$$\begin{aligned} \phi_0 &= \frac{2\tilde{Q}}{\pi\epsilon_0} \sum_{k=1}^{\infty} \frac{1}{k \sinh \frac{k\pi b}{a}} \sinh \frac{k\pi(b-y_0)}{a} \sinh \frac{k\pi y}{a} \sin \frac{k\pi x_0}{a} \sin \frac{k\pi x}{a}, \text{ for } y < y_0 \\ \phi_0 &= \frac{2\tilde{Q}}{\pi\epsilon_0} \sum_{k=1}^{\infty} \frac{1}{k \sinh \frac{k\pi b}{a}} \sinh \frac{k\pi(b-y)}{a} \sinh \frac{k\pi y_0}{a} \sin \frac{k\pi x_0}{a} \sin \frac{k\pi x}{a}, \text{ for } y > y_0. \end{aligned} \quad (14.13)$$

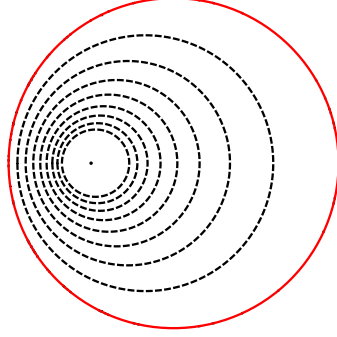


Figure 14.1: Contour plot of the potential of a thin charged wire in a round pipe.

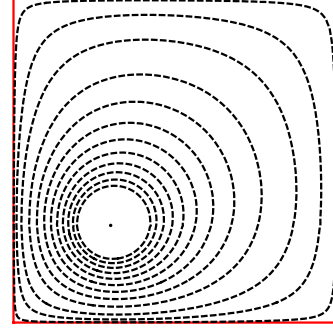


Figure 14.2: Contour plot of the potential of a thin charged wire in a rectangular pipe.

The equipotential lines computed with this expression are shown in Fig. 14.2.

The approximation of an infinitely thin beam is useful for evaluation of the potential outside of the beam. It is however cannot be used directly to calculate the potential between the center of the beam and the wall. Indeed, let us consider the case of an axisymmetric Gaussian beam with the charge density given by

$$\rho(r) = \frac{\tilde{Q}}{2\pi\sigma^2} e^{-r^2/2\sigma^2}, \quad (14.14)$$

with $\sigma \ll a$. We assume that the beam is located at the center of a round pipe. In the infinitely thin beam approximation, the potential is given by Eq. (14.11). This expression is valid for $r \gg \sigma$; for $r = 0$ it gives an infinite value. To find the potential for a Gaussian beam we need to solve

$$\frac{1}{r} \frac{d}{dr} r \frac{d\phi}{dr} = -\frac{\tilde{Q}}{2\pi\sigma^2\epsilon_0} e^{-r^2/2\sigma^2}. \quad (14.15)$$

The solution of this equation that has a finite electric field on the axis and satisfies the boundary condition at the wall is

$$\phi = \frac{\tilde{Q}}{2\pi\epsilon_0} \int_r^a \frac{dr'}{r'} \left(e^{-r'^2/2\sigma^2} - 1 \right). \quad (14.16)$$

In the limit $r \gg \sigma$ we recover Eq. (14.11). The potential difference between the center of the beam and the wall is

$$\phi(r=0) = \frac{\tilde{Q}}{2\pi\epsilon_0} \int_0^a \frac{dr'}{r'} \left(e^{-r'^2/2\sigma^2} - 1 \right). \quad (14.17)$$

14.3 Magnetic field of a beam in a conducting pipe

Expressions (14.13) of the previous Section give us also a solution of another problem—the problem of finding magnetic field of a thin bunch inside a conducting vacuum chamber. Again we neglect the transverse dimensions of the bunch and assume that it is located at position $x = x_0$ and $y = y_0$ inside a vacuum chamber of a given cross section. The beam carries current I which we assume constant in time. The magnetic field vector of this current has only x and y components, $\mathbf{H} = \hat{x}H_x(x, y) + \hat{y}H_y(x, y)$, that depend on x and y , and satisfies the Maxwell equation

$$\nabla \times \mathbf{H} = I\hat{z}\delta(x - x_0)\delta(y - y_0). \quad (14.18)$$

For a good metal and fast processes, the magnetic field does not penetrate inside the metal and the boundary condition on the surface of the metal is that the normal to the surface component of the magnetic field vanishes, $H_n|_{\text{surface}} = 0$, see Section 16.3. With this boundary condition, we will now show how to convert (14.18) to (14.10).

Let us introduce function $\psi(x, y)$ such that

$$\mathbf{H} = \nabla \times (\hat{z}\psi). \quad (14.19)$$

Note that the equation $\nabla \cdot \mathbf{H} = 0$ is automatically satisfied when \mathbf{H} is given by (14.19). Substituting this relation into (14.18) and taking the z component of the resulting equation yields

$$\nabla^2\psi = -I\delta(x - x_0)\delta(y - y_0). \quad (14.20)$$

The normal component of the magnetic field on the surface of the metal is equal to the tangential derivative of ψ (that is along the contour of the surface), and hence vanishing H_n means a constant value of ψ on the surface. Since adding a constant value to ψ does not change the magnetic field, without loss of generality, this constant value can be set to zero. We see that with the correspondence $\psi \rightarrow \phi$ and $I \rightarrow \hat{Q}/\epsilon_0$ our magnetic problem reduces to the electrostatic one of the previous Section. In particular, the solution (14.13) can be used to find the magnetic field of a bunch inside a rectangular vacuum chamber. In the magnetic problem, the lines of constant values of ϕ in Fig. 14.2 represent magnetic field lines inside the vacuum chamber.

14.4 Electric field of a charged metallic ellipsoid

Consider a metallic body that has a shape of an ellipsoid, which is given by the following equation

$$\frac{x^2}{a^2} + \frac{y^2}{b^2} + \frac{z^2}{z^2} = 1, \quad (14.21)$$

where a , b and c are the half axes of the ellipsoid in the corresponding directions. The body is charged with the total charge equal to Q . This charge will be distributed on the surface of the ellipsoid in such a way that the electrostatic potential ϕ is constant on the surface.

It turns out that the electric field outside of the ellipsoid, in free space, can be found relatively easy. We give here the solution of this problem without derivation. Let us assume that $a \geq b \geq c > 0$. We introduce a function $\lambda(x, y, z)$ that is defined as a *positive* solution of the following equation

$$\frac{x^2}{a^2 + \lambda} + \frac{y^2}{b^2 + \lambda} + \frac{z^2}{c^2 + \lambda} = 1. \quad (14.22)$$

Then the potential ϕ outside of the ellipsoid is given by the following integral

$$\phi(x, y, z) = \frac{Q}{8\pi\epsilon_0} \int_{\lambda(x,y,z)}^{\infty} \frac{ds}{R(s)}, \quad (14.23)$$

where $R(s)$ is

$$R(s) = \sqrt{(a^2 + s)(b^2 + s)(c^2 + s)}. \quad (14.24)$$

In case of an elongated axisymmetric ellipsoid ($b = c$) the integration can be done in elementary functions with the result

$$\phi(x, y, z) = \frac{Q}{4\pi\epsilon_0} \frac{1}{\sqrt{a^2 - b^2}} \ln \frac{\sqrt{b^2 + \lambda}}{\sqrt{a^2 + \lambda} - \sqrt{a^2 - b^2}}. \quad (14.25)$$

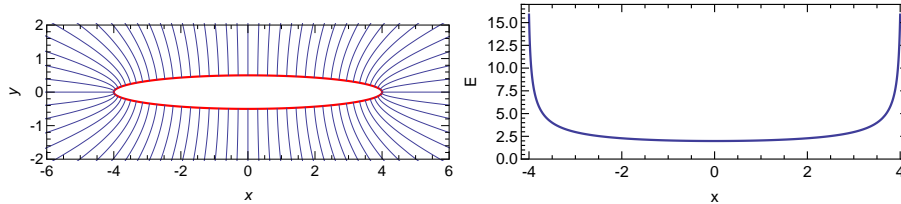


Figure 14.3: Left panel: field lines of an ellipsoid with $a = 4$ and $b = 0.5$ in the plane $z = 0$. Right panel: plot of the strength of the electric field on the surface of the ellipsoid as a function of coordinate x (in arbitrary units). One can see that the field is intensified near the ends of the ellipsoid.

Problem 14.2. Prove by direct calculation that the potential given by (14.19) satisfies the Laplace equation.

14.5 Electric field near metallic edges and protrusions

The electric field has a tendency to concentrate near sharp metallic edges and thin conducting protrusions. This is an important factor that needs to be taken

into account in the design of high-voltage devices. We illustrate this effect in several solvable problems of electrostatic theory.

In the first problem we model a protrusion from a flat metallic surface as a half of an ellipsoid. Specifically, we assume that the half space $z < 0$ is occupied by metal, and the region $z > 0$ is free space except for the interior of the ellipsoid (14.22), which is also metallic, see Fig. 14.4. Far from the protrusion, at $z \rightarrow \infty$, there is a uniform electric field $E_z = E_0$ applied to the system. The problem is to find the electric field in the vicinity of the protrusion. This

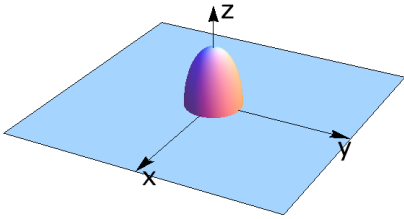


Figure 14.4: Ellipsoidal protrusion.

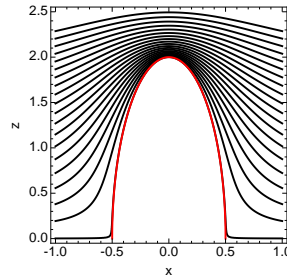


Figure 14.5: Contour plot of the potential around protruding ellipsoidal shape.

problem is closely related the one in the previous Section. It is not surprising then that the solution is given by integrals that involve the same function $R(s)$ (14.24)

$$\phi(x, y, z) = -E_0 z \left[1 - \int_{\lambda(x, y, z)}^{\infty} \frac{ds}{(s + c^2)R(s)} \left(\int_0^{\infty} \frac{ds}{(s + c^2)R(s)} \right)^{-1} \right]. \quad (14.26)$$

Contour plot of the field lines for an elongated protruding ellipsoid with parameters $a = b = 0.5$ and $c = 2$ is shown in Fig. 14.5.

Amplification of the field near sharp angles is most clearly visible in special 2D solutions of the Laplace equation. Consider the following problem: find electrostatic potential near an angle in metallic surface, as shown in Fig. 14.6. The geometry is translationally invariant along the z axis, perpendicular to the plane of the picture. It is convenient to introduce a cylindrical coordinate system with $r = \sqrt{x^2 + y^2}$ and angle θ counted from the x axis. The potential $\phi(r, \theta)$ in cylindrical coordinates satisfies the equation $\nabla^2 \phi = 0$ in the region $0 \leq \theta \leq \alpha$ (see Fig. 14.6) with the boundary condition $\phi = 0$ at $\theta = 0$ and $\theta = \alpha$. We have

$$\frac{1}{r} \frac{\partial}{\partial r} r \frac{\partial \phi}{\partial r} + \frac{1}{r^2} \frac{\partial^2 \phi}{\partial \theta^2} = 0. \quad (14.27)$$

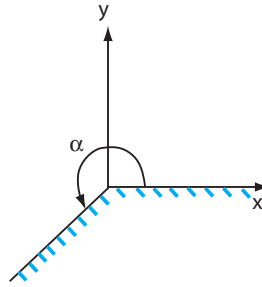
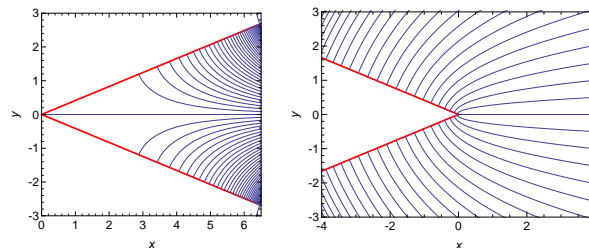


Figure 14.6: Coordinate system near sharp angle.

It is easy to see that this equation is satisfied by the following solution $\phi = r^n \sin(n\theta)$ for arbitrary n . To satisfy the boundary condition, we require $\sin(n\alpha) = 0$ which gives $n = \pi/\alpha$. Hence

$$\phi = Ar^{\pi/\alpha} \sin\left(\frac{\pi\theta}{\alpha}\right), \quad (14.28)$$

where A is a constant. The electric field has a singularity if $n < 1$; it follows from the above expression that the field is singular when $\alpha > \pi$. In the limit $\alpha \rightarrow 2\pi$, which corresponds to the edge of a metallic plane, the potential scales as $\phi \propto \sqrt{r}$, and the field has a singularity $E \propto 1/\sqrt{r}$.

Figure 14.7: Field lines near the edge with $\alpha = \pi/4$ (left figure) and $\alpha = 7\pi/4$ (right figure).

It is interesting to note that the electric field near a sharp tip of a charged thin conical needle increases approximately as $1/r$, where r is the distance to the tip of the needle [14].

Lecture 15

Self field of a relativistic beam

In this lecture, we will study the electromagnetic field of a bunch of charged particles moving in free space with relativistic velocity along a straight line.

15.1 Relativistic field of a particle moving with constant velocity

Consider a point charge q moving with a constant velocity \mathbf{v} along the z axis. We are interested in the case of a relativistic velocity, $v \approx c$, or $\gamma \gg 1$. In the particle's reference frame it has a static Coulomb field,

$$\mathbf{E}' = \frac{1}{4\pi\epsilon_0} \frac{q\mathbf{r}'}{r'^3}, \quad (15.1)$$

where the prime indicates the quantities in the reference frame where the particle is at rest.

To find the electric and magnetic fields in the lab frame we will use the Lorentz transformation (13.1) for coordinates and time, and the transformation for the fields (13.20). We have $E_x = \gamma E'_x$, $E_y = \gamma E'_y$, and $E_z = E'_z$. We also need to transform the vector \mathbf{r}' into the lab frame using Eqs. (13.6). For the length of this vector we have $r' = \sqrt{x^2 + y^2 + \gamma^2(z - vt)^2}$. The Cartesian coordinates of \mathbf{E} are

$$\begin{aligned} E_x &= \frac{1}{4\pi\epsilon_0} \frac{q\gamma x}{(x^2 + y^2 + \gamma^2(z - vt)^2)^{3/2}} \\ E_y &= \frac{1}{4\pi\epsilon_0} \frac{q\gamma y}{(x^2 + y^2 + \gamma^2(z - vt)^2)^{3/2}} \\ E_z &= \frac{1}{4\pi\epsilon_0} \frac{q\gamma(z - vt)}{(x^2 + y^2 + \gamma^2(z - vt)^2)^{3/2}}. \end{aligned} \quad (15.2)$$

These three equations can be combined into a vectorial one

$$\mathbf{E} = \frac{1}{4\pi\epsilon_0} \frac{q\mathbf{r}}{\gamma^2 \mathcal{R}^3}. \quad (15.3)$$

Here vector \mathbf{r} is drawn from the current position of the particle to the observation point, $\mathbf{r} = (x, y, z - vt)$, and \mathcal{R} is given by

$$\mathcal{R} = \sqrt{(z - vt)^2 + (x^2 + y^2)/\gamma^2}. \quad (15.4)$$

Finally, as follows from Eqs. (13.20), a moving charge carries magnetic field

$$\mathbf{B} = \frac{1}{c^2} \mathbf{v} \times \mathbf{E}. \quad (15.5)$$

The above fields can be also obtained by transforming the potentials. Indeed, in the particle's frame we have

$$\phi' = \frac{1}{4\pi\epsilon_0} \frac{q}{r'}, \quad \mathbf{A}' = 0. \quad (15.6)$$

Using the Lorentz transformation (13.21) we find

$$\phi = \gamma\phi', \quad \mathbf{A} = \frac{1}{c} \boldsymbol{\beta}\phi. \quad (15.7)$$

Expressing r' in terms of the coordinates in the lab frame, $r' = \gamma\mathcal{R}$, gives

$$\phi = \frac{1}{4\pi\epsilon_0} \frac{q}{\mathcal{R}}, \quad \mathbf{A} = \frac{Z_0}{4\pi} \boldsymbol{\beta} \frac{q}{\mathcal{R}}. \quad (15.8)$$

Problem 15.1. Verify by direct calculation that Eqs. (1.7) applied to the potentials (15.8) give the fields (15.3) and (15.5).

The field of a relativistic point charge is illustrated by Fig. 15.1. Within a narrow cone with the angular width $\sim 1/\gamma$ the field is large, $E \sim q\gamma/r^2$. On the axis the field is weak, $E \sim 1/r^2\gamma^2$. The absolute value of the magnetic field is almost equal to that of the electric field.

Problem 15.2. Make a plot of the dependence E versus θ , where θ is the angle between \mathbf{r} and the (x, y) plane. Assume $\gamma \gg 1$.

In some problems we can neglect the small angular width of the electromagnetic field of a relativistic particle and consider it as an infinitely thin "pancake", $E \propto \delta(z - ct)$. This approximation formally corresponds to the limit $v \rightarrow c$. Because the field is directed along the vector drawn from the current position of the charge, more precisely, we can write $\mathbf{E} = A\rho\delta(z - ct)$ where $\rho = \hat{x}x + \hat{y}y$ and A is a constant which is determined by the requirements that the areas under the curves $E_x(z)$ and $E_y(z)$ agree with the ones given by Eq. (15.3) in the limit $\gamma \rightarrow \infty$.

Problem 15.3. Using Eq. (15.3) show that in the limit $\gamma \rightarrow \infty$ the following relations hold

$$\int_{-\infty}^{\infty} E_x dz = \frac{1}{4\pi\epsilon_0} \frac{2qx}{\rho^2}, \quad \int_{-\infty}^{\infty} E_y dz = \frac{1}{4\pi\epsilon_0} \frac{2qy}{\rho^2}. \quad (15.9)$$

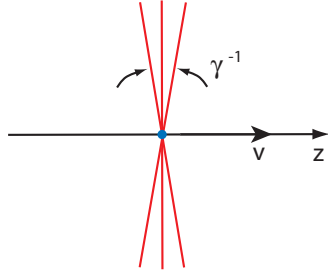


Figure 15.1: Electric and magnetic fields of a relativistic particle is mainly localized around the transverse plane.

Using the result of the problem above we obtain

$$\mathbf{E} = \frac{1}{4\pi\epsilon_0} \frac{2q\rho}{\rho^2} \delta(z - ct), \quad \mathbf{B} = \frac{1}{c} \hat{\mathbf{z}} \times \mathbf{E}. \quad (15.10)$$

15.2 Interaction of Moving Charges in Free Space

Let us now consider a *source* particle of charge q moving with velocity v , and a *test* particle of *unit* charge moving behind the leading one on a parallel path at a distance l with an offset x , as shown in Fig. 15.2. We want to find the force which the source particle exerts on the test one. The longitudinal force is

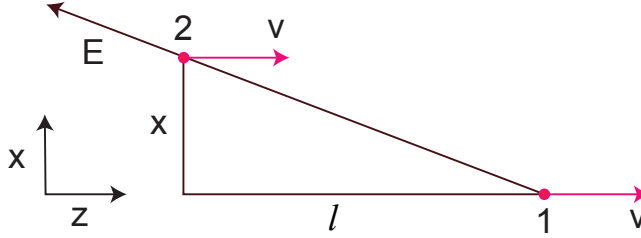


Figure 15.2: A leading particle 1 and a trailing particle 2 traveling in free space with parallel velocities v . Shown also is the coordinate system x, z .

$$F_l = E_z = -\frac{1}{4\pi\epsilon_0} \frac{ql}{\gamma^2(l^2 + x^2/\gamma^2)^{3/2}}, \quad (15.11)$$

and the transverse force is

$$F_t = E_x - vB_y = \frac{1}{4\pi\epsilon_0} \frac{qx}{\gamma^4(l^2 + x^2/\gamma^2)^{3/2}}. \quad (15.12)$$

In accelerator physics, the force \mathbf{F} is often called *the space charge force*.

The longitudinal force decreases with the growth of γ as γ^{-2} (for $l \gtrsim x/\gamma$). For the transverse force, if $l \gg x/\gamma$, $F_t \sim \gamma^{-4}$, and for $l = 0$, $F_t \sim \gamma^{-1}$. Hence, in the limit $\gamma \rightarrow \infty$, the electromagnetic interaction in free space between two particles on parallel paths vanishes.

15.3 Field of a long-thin relativistic bunch of particles

Let us consider a relativistic bunch of length σ_z much larger than the bunch radius $\sigma_z \gg \sigma_\perp$. The bunch is moving in the longitudinal direction along the z axis with a relativistic factor $\gamma \gg 1$. What is the electric field of this bunch?

Let us first calculate the radial electric field outside of the bunch at distance ρ from the z axis. Assuming that $\rho \gg \sigma_\perp$ we can neglect the transverse size of the beam and represent it as a collection of point charges. Each such charge generates the electric field given by Eq. (15.3). From this equation we find that the radial component $d\mathcal{E}_\perp$ created by an infinitesimally small charge dq' located at coordinate z' is

$$d\mathcal{E}_\perp(z, z', \rho) = \frac{1}{4\pi\epsilon_0} \frac{\rho dq'}{\gamma^2((z - z')^2 + \rho^2/\gamma^2)^{3/2}}, \quad (15.13)$$

where z and $\rho = \sqrt{x^2 + y^2}$ refer to the observation point. To find the field of the bunch we assume that the bunch 1D distribution function is given by $\lambda(z)$ ($\int \lambda(z) dz = 1$), so that the charge dq' within dz' is equal to $Q\lambda(z')dz'$, with Q the total charge of the bunch. For the field, we need to add contributions of all elementary charges in the bunch:

$$\begin{aligned} E_\perp(z, \rho) &= \int d\mathcal{E}_\perp(z, z', \rho) \\ &= \frac{Q\rho}{4\pi\epsilon_0\gamma^2} \int_{-\infty}^{\infty} \frac{\lambda(z') dz'}{((z - z')^2 + \rho^2/\gamma^2)^{3/2}}. \end{aligned} \quad (15.14)$$

The function $((z - z')^2 + \rho^2/\gamma^2)^{-3/2}$ in this integral has a sharp peak of width $\Delta z \sim \rho/\gamma$ at $z = z'$. At distances $\rho \ll \sigma_z\gamma$ from the bunch the width of the peak is smaller than the width of the distribution function σ_z , and we can replace it by the delta function:

$$\frac{1}{((z - z')^2 + \rho^2/\gamma^2)^{3/2}} \rightarrow \frac{2\gamma^2}{\rho^2} \delta(z - z'). \quad (15.15)$$

The factor in front of the delta function on the right hand side follows from the requirements that the area under the functions on the left hand side and on the right hand side, considered as functions of z , should be equal, and from the mathematical identity

$$\int_{-\infty}^{\infty} \frac{dz'}{((z - z')^2 + a^2)^{3/2}} = \frac{2}{a^2}.$$

The approximation (15.15) is equivalent to using Eqs. (15.10) instead of (15.3). The result is

$$E_{\perp}(z, \rho) = \frac{1}{4\pi\epsilon_0} \frac{2Q\lambda(z)}{\rho}. \quad (15.16)$$

We see that the factor γ does not enter this formula—this agrees with our expectation because Eqs. (15.10) are valid in the limit $\gamma \rightarrow \infty$.

In the opposite limit, $\rho \gg \sigma_z \gamma$, we can replace $\lambda(z)$ in Eq. (15.14) by the delta function $\delta(z)$, which gives the field of a point charge

$$E_{\perp}(z, \rho) = \frac{1}{4\pi\epsilon_0} \frac{Q\rho\gamma}{(z^2\gamma^2 + \rho^2)^{3/2}}. \quad (15.17)$$

In the intermediate region, $\rho \sim \sigma_z \gamma$, the result is shown in Fig. 15.3 for a Gaussian distribution function $\lambda(z) = (1/\sqrt{2\pi}\sigma_z)e^{-z^2/2\sigma_z^2}$.

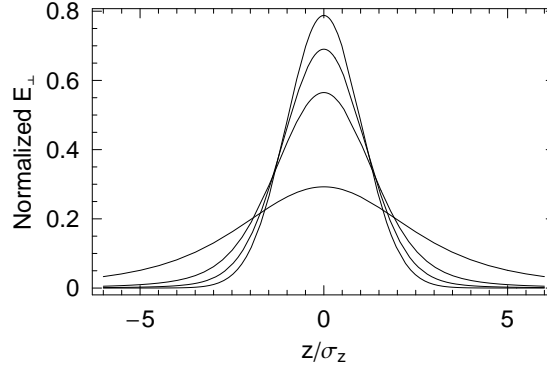


Figure 15.3: Transverse electric field of a relativistic bunch with Gaussian distribution for various values of the parameter $\rho/\sigma_z\gamma$. This parameter takes the values of 0.1, 0.5, 1 and 3 with larger values corresponding to broader curves. The field is normalized by $(4\pi\epsilon_0)^{-1}Q/\rho\sigma_z$.

What is the longitudinal electric field inside the bunch? If we neglect the transverse size of the beam and assume the same infinitely-thin-beam approximation we used above, we can try to integrate the longitudinal field of a unit point charge

$$d\mathcal{E}_{\parallel}(z, z') = \frac{dq'}{4\pi\epsilon_0\gamma^2} \frac{z - z'}{|z - z'|^3}, \quad (15.18)$$

as we did above for the transverse field:

$$E_{\parallel}(z) = \int d\mathcal{E}_{\parallel}(z, z') = \frac{Q}{4\pi\epsilon_0\gamma^2} \int dz' \lambda(z') \frac{z - z'}{|z - z'|^3}, \quad (15.19)$$

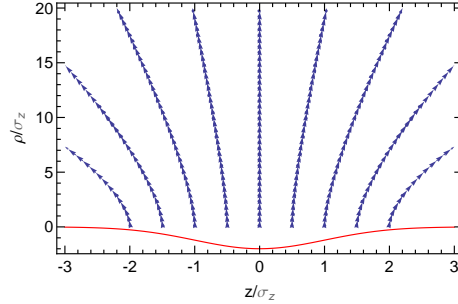


Figure 15.4: Electric field lines of a thin relativistic bunch with $\gamma = 10$. The red line at the bottom shows the longitudinal Gaussian charge distribution in the bunch.

but the integral diverges at $z' \rightarrow z$. This divergence indicates that one has to take into account the finite transverse size of the beam.

Let us calculate the longitudinal electric field in the model where the beam radius is a , and the charge is uniformly distributed over the cross section of the beam up to the radius a . We can slice the beam into infinitesimal disks of

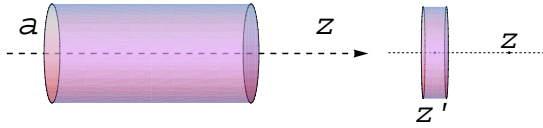


Figure 15.5: Left panel: a beam of cylindrical cross section a ; right panel: a slice of the beam located at z' .

thickness dz' . If the slice has a unit charge and is located at coordinate z' , the longitudinal electric field on the axis z at point z is

$$\mathcal{E}_{\parallel}(z, z') = -\frac{1}{4\pi\epsilon_0} \frac{2}{a^2} (z - z') \left(\frac{1}{\sqrt{a^2/\gamma^2 + (z - z')^2}} - \frac{1}{|z - z'|} \right). \quad (15.20)$$

Problem 15.4. Derive Eq. (15.20) for \mathcal{E}_{\parallel} and analyze it considering limits $|z - z'| \ll a/\gamma$ and $|z - z'| \gg a/\gamma$. Hint: represent a thin charged disk as a collection of infinitesimally small rings.

The longitudinal electric field on the axis of the bunch is obtained by integration

of contributions from the slices

$$\begin{aligned}
 E_{\parallel}(z) &= - \int_{-\infty}^{\infty} dz' Q \lambda(z') \mathcal{E}_{\parallel}(z, z') \\
 &= - \frac{Q}{4\pi\epsilon_0} \frac{2}{a^2} \int_{-\infty}^{\infty} dz' \lambda(z') (z - z') \left(\frac{1}{\sqrt{a^2/\gamma^2 + (z - z')^2}} - \frac{1}{|z - z'|} \right).
 \end{aligned} \tag{15.21}$$

The above integral cannot be calculated analytically. If we assume that the longitudinal distribution of charge is Gaussian, $\lambda(z) = (1/\sqrt{2\pi}\sigma_z)e^{-z^2/2\sigma_z^2}$, then the integral can be computed numerically. The result is shown in Fig. 15.6. One

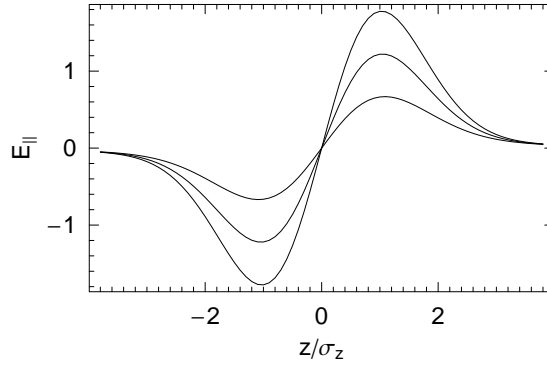


Figure 15.6: Longitudinal electric field of a relativistic bunch with Gaussian distribution function for various values of the parameter $a/\gamma\sigma_z$. This parameter takes the values of 0.1, 0.01, and 0.001 with smaller values corresponding to higher fields. The field is normalized by $(4\pi\epsilon_0)^{-1}2Q/\gamma^2\sigma_z^2$.

can show that in the limit $a/\gamma\sigma_z \ll 1$ a crude estimate for E_{\parallel} is:

$$E_{\parallel} \sim \frac{1}{4\pi\epsilon_0} \frac{Q}{\sigma_z^2\gamma^2} \log \frac{\sigma_z\gamma}{a}. \tag{15.22}$$

Formally, this expression diverges in the limit of infinitely thin beam ($a \rightarrow 0$), but in reality the effect of the longitudinal electric field for relativistic beams is often small because of the factor γ^{-2} (a so called *space charge effect*).

Problem 15.5. Derive an expression for the field $E_{\parallel}(z)$ on the beam axis for a Gaussian bunch using the result of Section 14.1 in Lecture 14. Assume $\sigma_x = \sigma_y$.

Problem 15.6. A bunch of electrons in a future linear collider will have a charge of about 1 nC, bunch length $\sigma_z \approx 200 \mu\text{m}$, and will be accelerated in the linac from 5 GeV to 250 GeV. Estimate the energy spread in the beam induced by the the space charge, assuming the bunch radius of 50 μm .

Lecture 16

Effect of environment on electromagnetic field of a beam

Interaction between particles of a beam moving in a vacuum chamber in the ultrarelativistic limit can occur if 1) the pipe is not uniform along the beam path (which is usually due to presence of RF cavities, flanges, bellows, beam position monitors, slots, etc., in the vacuum chamber), or 2) the wall of the chamber is not perfectly conducting. In this lecture we first consider a relativistic beam moving in a perfectly conducting beam pipe. We then discuss the interaction of the beam with walls of finite conductivity and how a protrusion in a form of an iris affects the beam. We will see that in both cases the interaction with the wall leads to generation of the longitudinal electric field inside the vacuum chamber and results in energy loss. This field is the source of *collective effects* in the beam dynamics.

16.1 Beam Moving in a Perfectly Conducting Pipe

If a relativistic beam is moving parallel to the axis in a perfectly conducting cylindrical pipe of arbitrary cross section, it induces image charges on the surface of the wall that shield the metal from the electromagnetic field of the particles. The image travels with the same velocity¹ v (see Fig. 16.1). Since both the particles and the image charges move on parallel paths, in the limit $v = c$, according to the results of the previous sections, they do not interact with each other, no matter how close to the wall the particles are.

¹Of course, it does not mean that electrons inside the metal move with velocity v . The actual velocity of these electrons is small compared to the speed of light.

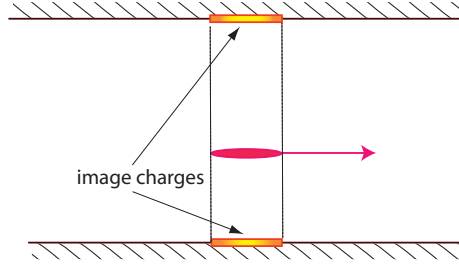


Figure 16.1: A bunch of relativistic particles traveling inside a perfectly conducting pipe of arbitrary cross section. Shown are the image charges on the wall generated by the bunch. In this picture it is assumed that $\sigma_z \gamma$ is much larger than the distance from the beam to the walls, and the divergence of the field lines due to finite value of γ is negligible.

To analyze this problem mathematically, one has to use a boundary condition for the fields on the surface of a perfectly conducting metal. This boundary condition consists in the requirement that the *tangential* component of the electric field on the surface of the metal is equal to zero:

$$\mathbf{E}_t = 0. \quad (16.1)$$

It follows from the fact that a nonzero tangential electric field, penetrating into the metal with infinite conductivity, would drive an infinitely large current in the metal, and hence is not allowed. Below, in Section 16.4, we will show how from this boundary condition it follows that, in the limit $v = c$, the longitudinal electric field vanishes everywhere inside the pipe.

Note that from the boundary condition (16.1) it follows that the *time dependent normal* component of the magnetic field B_n also vanishes. To prove this we consider a small piece of the metal surface which can locally be approximated by a flat piece. We then introduce a Cartesian coordinate system with the origin on the surface of the metal, with the axes x and y located in the plane of the surface and the axis z normal to the surface. According to Eq. (16.1) in the vicinity of the origin $E_x(x, y, z = 0) = E_y(x, y, z = 0)$. It follows then from Maxwell's equation that

$$\left. \frac{\partial B_z}{\partial t} \right|_{z=0} = \frac{\partial E_x}{\partial y} - \frac{\partial E_y}{\partial x} \Big|_{z=0} = 0. \quad (16.2)$$

Hence, if there is no static magnetic field in the system, $B_z = 0$, or using the more general notation B_n for the component perpendicular to the metal surface,

$$B_n = 0. \quad (16.3)$$

16.2 Beam field inside a perfectly conducting cylindrical pipe

Let us assume that a relativistic beam travels inside of a cylindrical pipe with perfectly conducting walls in the direction parallel to the pipe axis z (but not necessarily on the axis). We also assume that the transverse size of the beam is negligibly small. How to find the beam electric and magnetic field in the pipe?

A simple way to solve this problem is to consider it in the beam frame. In this frame the beam is at rest and the pipe flies with the velocity v in the direction opposite to the beam motion. Note that the boundary condition (16.1) is the same in both moving and the lab frames. What is also important is that the bunch length in the beam frame is γ times larger than in the laboratory frame. If the product $\sigma_z \gamma$ (σ_z is the bunch length in the lab frame) is much larger than the transverse size of the pipe, the bunch in the beam frame is much longer than the pipe cross section (which is the same in both the lab and the beam frames). At a given location inside the bunch, we can then neglect variation of the bunch charge with z and consider the beam charge density constant in z -direction. This reduces our problem to the electrostatic one considered in Lecture 14.2. Having solved this problem, one can make the inverse Lorentz transformation of the fields and find them in the lab frame.

16.3 Skin effect and the Leontovich boundary condition

We will now turn to the effect of finite conductivity of the walls. We first need to discuss an approximation that allows a simplified treatment of the electromagnetic properties of a good conductor, and study a so called *skin effect*. A detailed derivation of the skin effect can be found in textbooks, see, e.g., [1], section 5.18. We, reproduce a short version of this derivation here.

The skin effect deals with the penetration of the electromagnetic field inside a conducting medium characterized by conductivity σ and magnetic permeability μ . The equations that describe the electromagnetic field inside the metal are Maxwell's equation in which we neglect the displacement current $\partial \mathbf{D} / \partial t$:

$$\nabla \times \mathbf{H} = \mathbf{j}, \quad \nabla \cdot \mathbf{B} = 0, \quad \nabla \times \mathbf{E} + \frac{\partial \mathbf{B}}{\partial t} = 0, \quad \mathbf{j} = \sigma \mathbf{E}. \quad (16.4)$$

Combining the first, third and last equations we obtain an equation for the

magnetic field \mathbf{B}

$$\begin{aligned}
 \frac{\partial \mathbf{B}}{\partial t} &= -\nabla \times \mathbf{E} \\
 &= -\sigma^{-1} \nabla \times \mathbf{j} \\
 &= -\sigma^{-1} \nabla \times \nabla \times \mathbf{H} \\
 &= \sigma^{-1} (\nabla^2 \mathbf{H} - \nabla (\nabla \cdot \mathbf{H})) \\
 &= \sigma^{-1} \mu^{-1} \nabla^2 \mathbf{B},
 \end{aligned} \tag{16.5}$$

where we used the relation $\nabla \cdot \mathbf{H} = \mu^{-1} \nabla \cdot \mathbf{B} = 0$, (assuming that μ is constant). We found a *diffusion* equation for the magnetic field \mathbf{B} .

Let us now assume that a metal occupies a semi-infinite volume $z > 0$ with the vacuum at $z < 0$, as shown in Fig. 16.2, and assume that at the metal surface the x -component of magnetic field is given by $H_x = H_0 e^{-i\omega t}$. Due to

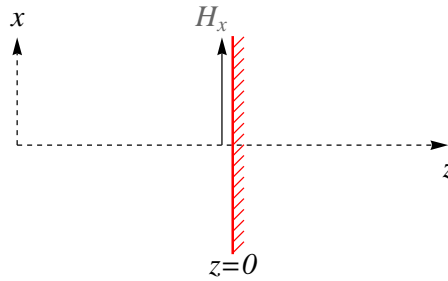


Figure 16.2: To derivation of the boundary condition on the surface of conductor.

the continuity of the tangential components of \mathbf{H} , H_x is the same on both sides of the metal boundary, that is at $z = +0$ and $z = -0$. We seek solution inside the metal in the form $H_x = h(z)e^{-i\omega t}$. Equation (16.5) then reduces to

$$\frac{d^2 h}{dz^2} + i\mu\sigma\omega h = 0, \tag{16.6}$$

with the solution $h = H_0 e^{ikz}$ and

$$k = \sqrt{i\mu\sigma\omega} = (1+i)\sqrt{\frac{\mu\sigma\omega}{2}}. \tag{16.7}$$

Note that we have chosen the root with a positive imaginary part, which gives a solution that vanishes as $z \rightarrow \infty$. The quantity δ ,

$$\delta = \sqrt{\frac{2}{\mu\sigma\omega}}, \tag{16.8}$$

is called the *skin depth*; it characterizes how deeply the electromagnetic field penetrates the metal. In many cases the magnetic properties of the metal can be neglected, then $\mu = \mu_0$, and the above equation can be written as

$$\delta = \sqrt{\frac{2c}{Z_0\sigma\omega}}. \quad (16.9)$$

Problem 16.1. Calculate the skin depth in copper ($\sigma = 5.8 \cdot 10^7$ 1/Ohm·m) and stainless steel ($\sigma = 1.4 \cdot 10^6$ 1/Ohm·m) at the frequency of 5 GHz.

The electric field inside the metal has only y component; it can be found from the first and the last of Eqs. (16.5)

$$E_y = \frac{j_y}{\sigma} = \frac{1}{\sigma} \frac{dH_x}{dz} = \frac{ik}{\sigma} H_x = \frac{i-1}{\sigma\delta} H_x. \quad (16.10)$$

The mechanism that prevents penetration of the magnetic field deep inside the metal is generation of tangential electric field, that drives the current in the skin layer and shields the magnetic field.

The relation (16.10) can be rewritten in vectorial notation:

$$\mathbf{E}_t = \zeta \mathbf{H} \times \mathbf{n}, \quad (16.11)$$

where \mathbf{n} is the unit vector normal to the surface and directed toward the metal, and

$$\zeta(\omega) = \frac{1-i}{\sigma\delta(\omega)}. \quad (16.12)$$

We emphasize that Eq. (16.11) is valid for Fourier transformed components of the field, that is indicated in the frequency dependence of the parameter ζ . In the limit $\sigma \rightarrow \infty$ we have $\zeta \rightarrow 0$ and we recover the boundary condition (16.1) of zero tangential electric field on the surface of a perfect conductor.

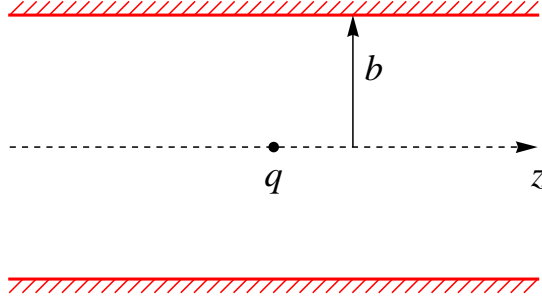
Problem 16.2. Given the tangential component $B_0 e^{-i\omega t}$ of the magnetic field on the surface, find the averaged over time energy absorbed in the metal per unit time per unit area. Hint: compute the averaged over time z -component of the Poynting vector on the surface. Answer: $\omega\delta B_0^2/4\mu_0$.

We derived the boundary condition (16.11) for a flat surface. It however can be used for a curved metal surface as well if the size of the metal body L is much larger than δ (more precisely, the surface curvature should be much larger than the skin depth). Another requirement is that the thickness of the metal wall is much larger than the skin depth. Eq. (16.11) is often called the *Leontovich boundary condition*.

Problem 16.3. Find how the Leontovich boundary conditions transforms into a frame moving with relativistic velocity v parallel to the metal surface in the direction perpendicular to the magnetic field (beam frame).

16.4 Round pipe with resistive walls

Consider now a round pipe of radius b , with finite wall conductivity σ . A point

Figure 16.3: Point charge moving on a round pipe of radius b .

charge moves along the z axis of the pipe with the speed of light, see Fig. 16.3. Because of the symmetry of the problem, the only non-zero component of the electromagnetic field on the axis is E_z . Our goal now is to find the field E_z as a function of z and t .

If the conductivity of the pipe is large enough, we can use a perturbation theory to find the effect of the wall resistivity. In the first approximation, we consider the pipe as a perfectly conducting one. In this case the electromagnetic field of the charge is the same as in free space and is given by Eqs. (15.10). For what follows, we will need only the magnetic field B_θ ,

$$B_\theta = \frac{1}{4\pi\epsilon_0} \frac{2q}{c\rho} \delta(z - ct). \quad (16.13)$$

Using the mathematical identity

$$\delta(z - ct) = \frac{1}{2\pi c} \int_{-\infty}^{\infty} d\omega e^{-i\omega(t-z/c)}, \quad (16.14)$$

we Fourier transform B_θ ,

$$B_\theta(\rho, z, t) = \int_{-\infty}^{\infty} d\omega \hat{B}_\theta(\rho) e^{-i\omega t + i\omega z/c}, \quad (16.15)$$

where

$$\hat{B}_\theta(\rho) = \frac{1}{4\pi\epsilon_0 c^2} \frac{q}{\pi\rho} = \frac{\mu_0}{4\pi} \frac{q}{\pi\rho}. \quad (16.16)$$

In the limit when the skin depth δ corresponding to the frequency ω is much smaller than the pipe radius, $\delta \ll b$ (and also much smaller than the thickness of the pipe walls), we can use the Leontovich boundary condition (16.11). Combining Eqs. (16.11), (16.12) and (16.16), we find

$$\hat{E}_z|_{\rho=b} = -\zeta \frac{\hat{B}_\theta(b)}{\mu_0} = -(1-i) \sqrt{\frac{Z_0\omega}{2c\sigma}} \frac{q}{4\pi^2 b}. \quad (16.17)$$

Equation (16.17) gives us the longitudinal electric field on the wall, but we need the field on the axis of the pipe. To find the radial dependence of $E_{z\omega}$, we use the wave equation (1.5). In the cylindrical coordinate system the wave equation for E_z is

$$\begin{aligned} \frac{1}{c^2} \frac{\partial^2 E_z(\rho, z, t)}{\partial t^2} - \Delta E_z(\rho, z, t) = \\ \frac{1}{c^2} \frac{\partial^2 E_z(\rho, z, t)}{\partial t^2} - \frac{\partial^2 E_z(\rho, z, t)}{\partial z^2} - \frac{1}{\rho} \frac{\partial}{\partial \rho} \rho \frac{\partial E_z(\rho, z, t)}{\partial \rho} = 0. \end{aligned} \quad (16.18)$$

Substituting the Fourier component $\hat{E}_z(\rho)e^{-i\omega(t-z/c)}$ into this equation, we find

$$\frac{1}{\rho} \frac{\partial}{\partial \rho} \rho \frac{\partial \hat{E}_z}{\partial \rho} = 0. \quad (16.19)$$

This equation has a general solution $\hat{E}_z(\rho) = A + B \ln \rho$, where A and B are arbitrary constants. Since we do not expect E_z to have a singularity on the axis, $B = 0$. Hence the electric field does not depend on ρ , $\hat{E}_z(\rho) = \text{const}$, and

$$\hat{E}_z|_{\rho=0} = \hat{E}_z|_{\rho=b}, \quad (16.20)$$

implying that $\hat{E}_z|_{\rho=0}$ is given by the same Eq. (16.17). Note that we have shown here that in the ultrarelativistic case the longitudinal electric field inside the pipe is constant throughout the pipe cross section.

To find $E_z(z, t)$ we make the inverse Fourier transformation,

$$E_z(z, t) = \int_{-\infty}^{\infty} d\omega \hat{E}_z e^{-i\omega(t-z/c)}, \quad (16.21)$$

which gives

$$E_z(z, t) = (i-1) \sqrt{\frac{Z_0}{2c\sigma}} \frac{q}{4\pi^2 b} \int_{-\infty}^{\infty} d\omega \sqrt{\omega} e^{-i\omega(t-z/c)}. \quad (16.22)$$

The last integral can be taken analytically in the complex plane, with the result

$$\int_{-\infty}^{\infty} d\omega \sqrt{\omega} e^{-i\omega\xi} = -\frac{\sqrt{\pi}(i+1)}{\sqrt{2}\xi^{3/2}} \quad (16.23)$$

for $\xi > 0$. This gives

$$E_z(z, t) = -(i-1) \sqrt{\frac{Z_0}{2c\sigma}} \frac{q}{4\pi^2 b} \frac{\sqrt{\pi}(i+1)}{\sqrt{2}(t-z/c)^{3/2}} = \frac{qc}{4\pi^{3/2}b} \sqrt{\frac{Z_0}{\sigma s^3}}, \quad (16.24)$$

with $s = ct - z$ being the distance from the moving charge with positive s corresponding to the points behind the current position of the charge. For the points where $s < 0$, located in front of the charge, $E_z = 0$ in agreement with

the causality principle. The positive sign of E_z indicates that a trailing charge (if it has the same sign as q) will be accelerated in the wake.

In our derivation we assumed that the magnetic field on the wall is the same as in the case of perfect conductivity. However, the magnetic field is generated not only by the beam current, but also by the displacement current

$$j_z^{\text{disp}} = \epsilon_0 \frac{\partial E_z}{\partial t}, \quad (16.25)$$

that vanishes in the limit of the perfect conductivity. To be able to neglect the corrections to H_θ due to j_z^{disp} , we must require the total displacement current to be much less than the beam current. In the Fourier representation, the time derivative $\partial/\partial t$ reduces to multiplication by $-i\omega$, and the requirement is

$$\epsilon_0 \pi b^2 \omega |\hat{E}_z| \ll |\hat{I}|. \quad (16.26)$$

The Fourier component of the current is calculated by making Fourier transform of the equation $I = qc\delta(z - ct)$ and gives $|\hat{I}| = q/2\pi$. Using Eq. (16.17) now gives

$$\frac{\omega}{c} \ll \left(\frac{Z_0 \sigma}{b^2} \right)^{1/3}. \quad (16.27)$$

In the space-time domain, the inverse wavenumber c/ω corresponds to the distance s , hence the condition (16.27) means that our result (16.24) is valid only for distances s larger than a critical value s_0 , $s \gg s_0$. The parameter s_0 can be evaluated as an inverse of the right hand side of (16.27)

$$s_0 = \left(\frac{2b^2}{Z_0 \sigma} \right)^{1/3}. \quad (16.28)$$

Values of s_0 for a pipe of radius $b = 1$ cm made of copper ($\sigma = 5.8 \cdot 10^7$ 1/Ohm·m), aluminum ($\sigma = 3.7 \cdot 10^7$ 1/Ohm·m) and stainless steel ($\sigma = 1.4 \cdot 10^6$ 1/Ohm·m) are shown in table below.

	Copper	Aluminum	Stainless steel
s_0 (μm)	21	24	72

Table 16.1: Parameter s_0 for some materials.

The behavior of E_z for very small values of s , $s < s_0$, can be found in the literature, [15]. In Fig. 16.4 we show how E_z depends on s at distances comparable with s_0 . Note that the singularity in Eq. (16.24) now saturates at small s , the electric field changes sign and becomes negative at $s = 0$. This field decelerates the leading charge, as expected from the energy balance consideration.

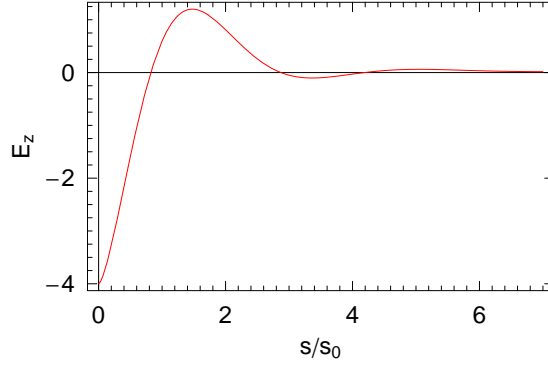


Figure 16.4: Longitudinal electric field as a function of distance s from the particle. The field is normalized by $q/4\pi\epsilon_0 b^2$, and the distance is normalized by s_0 . The value of the normalized field at the origin is equal to 4.

16.5 Point charge and Gaussian bunch passing through an iris

Let us consider a relativistic point charge moving in a pipe that has a diaphragm with a round hole of radius a . We assume that a is much smaller than the pipe radius R and to simplify the problem take the limit $R \rightarrow \infty$. The problem then reduces to passage of the charge through a round hole in a perfectly conducting infinitely thin metal plate, as shown in Fig. 16.5. The iris cuts off a part of the electromagnetic field, $r > a$, that hits the metal. The duration of the field pulse on the edge of the iris is of the order of $\Delta t \sim a/c\gamma$ (see Fig. 16.5b).

First, we calculate the energy U of the electromagnetic field that is “clipped away” by the iris. The field of the ultrarelativistic charge is given by Eq. (15.3) and (15.5),

$$E_\rho = cB_\theta = \frac{1}{4\pi\epsilon_0} \frac{\gamma q \rho}{(\rho^2 + \gamma^2 z^2)^{3/2}}, \quad (16.29)$$

where we use the cylindrical coordinates ρ and z and assume that the charge is located at the origin of the coordinate system. The energy density w of the electromagnetic field is

$$w = \frac{\epsilon_0}{2} (E_\rho^2 + cB_\theta^2). \quad (16.30)$$

Integrating w over the region $\rho > a$ and over z yields

$$U = \int_a^\infty 2\pi \rho d\rho \int_{-\infty}^\infty dz w = \frac{3}{64\epsilon_0} \frac{q^2 \gamma}{a}. \quad (16.31)$$

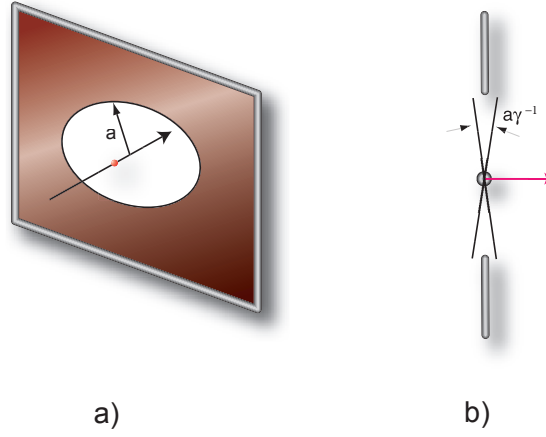


Figure 16.5: An ultrarelativistic particle passes through a hole in a metal screen.

We expect that the radiated energy will be of the order of U , and the spectrum of radiation will involve the frequencies up to $\lambda \sim a/\gamma$ ($\lambda = 1/k$).

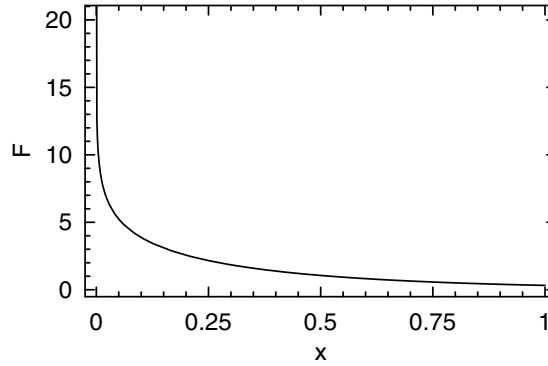


Figure 16.6: Plot of the function $F(x)$.

It turns out that this problem allows for an analytical solution in the limit of high frequency [16], when the wavelength of the radiation is much shorter than the hole radius, $k \gg a^{-1}$. In this limit the radiated energy spectrum is

$$\frac{dW}{d\omega} = \frac{1}{2\pi^2\epsilon_0} \frac{q^2}{c} F\left(\frac{ak}{\gamma}\right), \quad (16.32)$$

where

$$F(x) = x^2 \left[K_0(x) K_2(x) - K_1(x)^2 \right], \quad (16.33)$$

and K_n is the modified Bessel function of the second kind. The function F is plotted in Fig. 16.6; it has a logarithmic singularity at $x = 0$. From this plot we see that, indeed, the typical wavelength in the radiation spectrum is of the order of $\lambda \sim a/\gamma$. The total radiated energy is obtained by integrating $d\mathcal{W}/d\omega$ over the frequency:

$$\int_0^\infty \frac{d\mathcal{W}}{d\omega} d\omega = \frac{3}{32\epsilon_0} \frac{q^2\gamma}{a}. \quad (16.34)$$

Comparing this equation with (16.31), we see that the radiated energy is equal to twice the clipped energy. This can be explained by the following observation. The clipped electromagnetic field is reflected back by the screen. The physical mechanism responsible for this backward radiation is the current induced by the beam in the screen. However, due to the symmetry of the geometry with respect to positive and negative directions of z directions, exactly the same field will also be radiated in the forward direction. Hence the total radiated energy is two times larger than that contained in the clipped field.

Let us now turn our attention to a Gaussian bunch passing through the iris. In this case we will take into account the pipe radius R . We assume that the bunch length satisfies the condition $\sigma_z > R/\gamma$ and use Eq. (15.16) for the beam transverse field. The electromagnetic energy localized between the radii a and R is:

$$U = \frac{\epsilon_0}{2} \int_{-\infty}^{\infty} dz \int_a^R 2\pi\rho d\rho (E^2 + c^2 B^2) = \epsilon_0 \int_{-\infty}^{\infty} dz \int_a^R 2\pi\rho d\rho E_\perp^2. \quad (16.35)$$

Using Eq. (15.16) with the Gaussian distribution, we obtain

$$\begin{aligned} U &= \frac{1}{16\pi^2\epsilon_0} \int_{-\infty}^{\infty} dz \frac{1}{2\pi\sigma_z^2} e^{-z^2/\sigma_z^2} \int_a^R 2\pi d\rho \frac{4Q^2}{\rho} \\ &= \frac{1}{16\pi^2\epsilon_0} \frac{4Q^2\sqrt{\pi}}{\sigma_z} \ln\left(\frac{R}{a}\right). \end{aligned} \quad (16.36)$$

The ratio of this energy to the kinetic energy of the beam $N\gamma mc^2$ (N is the number of particles in the beam) is

$$\begin{aligned} \frac{U}{N\gamma mc^2} &= \frac{1}{16\pi^2\epsilon_0} \frac{4Nq^2\sqrt{\pi}}{\gamma mc^2\sigma_z} \ln\left(\frac{R}{a}\right) \\ &= \frac{1}{\sqrt{\pi}} \frac{Nr_0}{\gamma\sigma_z} \ln\left(\frac{R}{a}\right), \end{aligned} \quad (16.37)$$

where q is the particle's charge ($Q = Nq$) and $r_0 = q^2/4\pi\epsilon_0 mc^2$ is the classical radius. For electrons $r_0 = 2.82 \cdot 10^{-13}$ cm and for protons $r_0 = 1.53 \cdot 10^{-16}$ cm.

In contrast to a diaphragm, a smooth enough transition does not “scrape off” the electromagnetic field. When a beam passes through a smooth transition in a pipe its field is adiabatically adjusted to the shape of the local cross-section.

It does not cause the energy loss but usually results in energy exchange between different parts of the beam (the head and the tail).

Even if the transition is not smooth, the radiation is suppressed for very long bunches, such that the characteristic frequency ω involved in the variation of the beam field, $\omega \sim c/\sigma_z$, is smaller than cut off frequency of the pipe.

Lecture 17

Plane electromagnetic waves and Gaussian beams

In this lecture we will study electromagnetic field propagating in space free of charges and currents.

17.1 Plane electromagnetic waves

A plane electromagnetic wave can propagate in free space (without charges and currents)—it is a field where all components depend only on the variable $\xi = z - ct$,

$$\mathbf{E}(\mathbf{r}, t) = \mathbf{F}(\xi), \quad \mathbf{B}(\mathbf{r}, t) = \mathbf{G}(\xi). \quad (17.1)$$

From the equation $\nabla \cdot \mathbf{E} = 0$ it follows that $\partial F_z / \partial \xi = 0$, and hence $F_z = 0$ (a nonzero F_z would mean a constant longitudinal electric field which has nothing to do with the wave). Similarly, $G_z = 0$ because of $\nabla \cdot \mathbf{B} = 0$. We see that a plane wave is *transverse*.

Let us now apply Maxwell's equation $\partial \mathbf{B} / \partial t = -\nabla \times \mathbf{E}$ to the fields (17.1). We have

$$F'_x = cG'_y, \quad F'_y = -cG'_x, \quad (17.2)$$

from which we conclude that $F_x = cG_y$ and $F_y = -cG_x$ (again, we neglect possible constants of integration). In vector notation, these relations can be written as $\mathbf{F} = -c\mathbf{n} \times \mathbf{G}$ or

$$\mathbf{E} = -c\mathbf{n} \times \mathbf{B}, \quad (17.3)$$

where \mathbf{n} is a unit vector in the direction of propagation (in our case along the z axis). Multiplying vectorially Eq. (17.3) by \mathbf{n} , we also obtain

$$\mathbf{B} = \frac{1}{c}\mathbf{n} \times \mathbf{E}. \quad (17.4)$$

If we use potentials ϕ and \mathbf{A} to describe a plane wave, they would also depend on ξ only: $\phi = \phi(\xi)$, $\mathbf{A} = \mathbf{A}(\xi)$. We will now derive a useful formula that allows us to find the fields in a plane wave using only the vector potential. We have

$$\begin{aligned}\mathbf{B} &= \nabla \times \mathbf{A} \\ &= -\hat{x}A'_y + \hat{y}A'_x \\ &= \mathbf{n} \times \mathbf{A}' \\ &= -\frac{1}{c}\mathbf{n} \times \frac{\partial \mathbf{A}}{\partial t}.\end{aligned}\quad (17.5)$$

After the magnetic field is found, we can find the electric field using Eq. (17.3).

Often a plane wave has a sinusoidal time dependence with some frequency ω . In this case it is convenient to use the complex notation:

$$\mathbf{E} = \text{Re}(\mathbf{E}_0 e^{-i\omega t + i\mathbf{k}\mathbf{r} + i\phi_0}), \quad \mathbf{B} = \text{Re}(\mathbf{B}_0 e^{-i\omega t + i\mathbf{k}\mathbf{r} + i\phi_0}), \quad (17.6)$$

where \mathbf{E}_0 and \mathbf{B}_0 are the amplitudes of the wave, and $\mathbf{k} = \mathbf{n}\omega/c$ is the wave number. The wave propagates in the direction of \mathbf{k} ; the amplitude of the electric and magnetic fields are $E_0 = cB_0$. In general, \mathbf{E}_0 and \mathbf{B}_0 can be complex vectors orthogonal to \mathbf{k} , e.g., $\mathbf{E}_0 = \mathbf{E}_0^{(r)} + i\mathbf{E}_0^{(i)}$ with $\mathbf{E}_0^{(r)}$ and $\mathbf{E}_0^{(i)}$ real. Purely real or purely imaginary \mathbf{E}_0 correspond to a *linear polarization* of the wave; a complex vector \mathbf{E}_0 describes an *elliptical polarization*.

The Poynting vector gives the energy flow in the wave

$$\mathbf{S} = \mathbf{E} \times \mathbf{H} = \sqrt{\frac{\epsilon_0}{\mu_0}} E_0^2 \mathbf{n} \cos^2(\omega t + \mathbf{k}\mathbf{r} + \phi_0), \quad (17.7)$$

(in this formula E_0 is assumed real). The energy flows in the direction of propagation \mathbf{k} . Averaged over time energy flow, $\bar{\mathbf{S}}$, is

$$\bar{\mathbf{S}} = \frac{1}{2} \sqrt{\frac{\epsilon_0}{\mu_0}} E_0^2 \mathbf{n} = \frac{1}{2Z_0} E_0^2 \mathbf{n} = \frac{c^2}{2Z_0} B_0^2 \mathbf{n}. \quad (17.8)$$

In reality we never deal with exact plane waves. Such a wave would occupy the whole space. The usefulness of the notion of the plane wave is that in many cases the electromagnetic field looks like a plane wave *locally* in some limited region. One of the important examples, which we will study in details later, is radiation field at large distances from moving charges, see Fig. 17.1.

In some cases the approximation of the plane wave is enough, in others one wants to understand deviations from the local plane wave approximation.

Another important aspect of sinusoidal plane waves is that an arbitrary solution of Maxwell's equations in free space (without charges) can be represented as a superposition of plane waves with various amplitudes and directions of propagation.

Problem 17.1. At time $t = 0$ the electromagnetic field in free space is given by functions $\mathbf{E}_0(\mathbf{r})$ and $\mathbf{B}_0(\mathbf{r})$ (note that $\nabla \cdot \mathbf{E}_0 = \nabla \cdot \mathbf{B}_0 = 0$). Find the field at time t . [Hint: represent $\mathbf{E}(\mathbf{r}, t)$ and $\mathbf{B}(\mathbf{r}, t)$ as integrals over plane waves.]

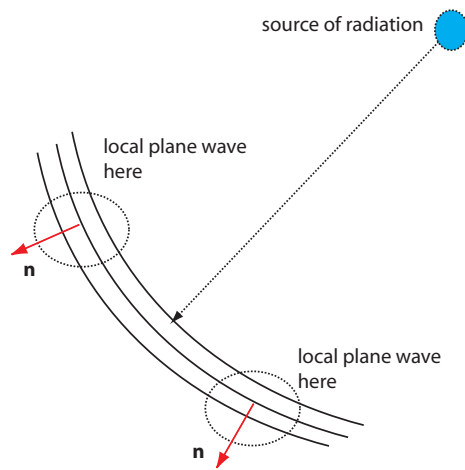


Figure 17.1: Approximation of local plane wave far from a radiated system of charges.

Problem 17.2. A plane electromagnetic wave propagates at some angle in a frame moving with velocity βc along the z axis. The magnitude of the Poynting vector at some location in the wave is equal to S' . Show that in the laboratory frame the magnitude of the Poynting at this location is given by the following equation

$$S = \frac{S'}{\gamma^2(1 - \beta \cos \theta)^2}, \quad (17.9)$$

where θ is the angle between the direction of propagation in the lab frame and the z axis.

Problem 17.3. Prove that the function $u(r, t) = f(r - ct)/r$ where r is the distance to the origin of the coordinate system, satisfies the scalar wave equation $\partial^2 u / \partial x^2 + \partial^2 u / \partial y^2 + \partial^2 u / \partial z^2 - (1/c^2) \partial^2 u / \partial t^2 = 0$, if $r > 0$.

17.2 Gaussian beams

In this section we consider another important example of electromagnetic field in vacuum which is a little more complicated than a plane wave. The importance of this example is that it is typically used for representation of laser beams. It also introduces such an important concept as the Rayleigh length, which we will later use in application to radiation processes.

We consider a *paraxial* approximation for the electromagnetic field. This means that the field is composed of plane waves propagating almost (but not exactly) in the same direction.

We will use the wave equation (1.5) for the x component of the electric field

(a linear polarization of the laser light)

$$\frac{\partial^2 E_x}{\partial x^2} + \frac{\partial^2 E_x}{\partial y^2} + \frac{\partial^2 E_x}{\partial z^2} - \frac{1}{c^2} \frac{\partial^2 E_x}{\partial t^2} = 0, \quad (17.10)$$

and assume

$$E_x(x, y, z, t) = u(x, y, z)e^{-i\omega t + ikz}, \quad (17.11)$$

where u is a slow function of its arguments. More specifically, we require

$$\left| \frac{1}{u} \frac{\partial u}{\partial z} \right| \ll k. \quad (17.12)$$

We will see from the result, that u also slowly varies in the transverse directions. Putting Eq. (17.11) into Eq. (17.10) and neglecting the second derivative $\partial^2 u / \partial z^2$ in comparison with $k \partial u / \partial z$ gives

$$\frac{\partial^2 u}{\partial x^2} + \frac{\partial^2 u}{\partial y^2} + 2ik \frac{\partial u}{\partial z} = 0. \quad (17.13)$$

We will look for an axisymmetric solution to this equation that depends only on $\rho = \sqrt{x^2 + y^2}$, that is $u = u(\rho, z)$. We then have

$$\frac{1}{\rho} \frac{\partial}{\partial \rho} \rho \frac{\partial u}{\partial \rho} + 2ik \frac{\partial u}{\partial z} = 0. \quad (17.14)$$

Moreover, we will assume the following dependence of u on ρ and z :

$$u = A(z)e^{Q(z)\rho^2}, \quad (17.15)$$

where $A(z)$ and $Q(z)$ are yet unknown function. We will see that Q has a negative real part so that we will have an exponentially decaying field in radial direction.

Substituting (17.15) into Eq. (17.14) yields

$$4Q^2 \rho^2 u + 4Qu + 2ik \left(\frac{A'}{A} + Q' \rho^2 \right) = 0, \quad (17.16)$$

where the prime denotes derivative with respect to z . Equating terms that do not contain ρ and terms with ρ^2 , we obtain

$$\begin{aligned} 2Q^2 + ikQ' &= 0, \\ 2Q + ik \frac{A'}{A} &= 0. \end{aligned} \quad (17.17)$$

We solve the first equation with the result

$$Q(z) = -\frac{1/w_0^2}{1 + 2iz/kw_0^2}, \quad (17.18)$$

where w_0 is a constant of integration which has dimension of length. We then integrate the second of Eqs. (17.17) to get

$$A(z) = \frac{E_0}{1 + 2iz/kw_0^2}, \quad (17.19)$$

where E_0 is another constant of integration which gives the amplitude of the field.

We now introduce important geometrical parameters: the *Rayleigh length* Z_R and the angle θ :

$$Z_R = \frac{kw_0^2}{2}, \quad \theta = \frac{w_0}{Z_R} = \frac{2}{kw_0}. \quad (17.20)$$

They can also be written as

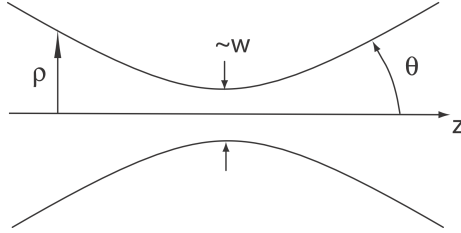


Figure 17.2: Envelope of a Gaussian beam.

$$Z_R = 2\frac{\lambda}{\theta^2}, \quad w_0 = 2\frac{\lambda}{\theta}, \quad (17.21)$$

where $\lambda = k^{-1} = c/\omega$. At $z = 0$ the radial dependence of u is $\propto e^{-\rho^2/w_0^2}$, hence the quantity w_0 gives the transverse size of the focal spot here. And if we rewrite $A = E_0/(1 + iz/Z_R)$, we see that Z_R is the characteristic length of the focal region along the z axis.

We can now obtain a condition for the validity of the paraxial approximation. Evaluating $\partial^2 u/\partial z^2 \sim u/Z_R^2$ and $k\partial u/\partial z \sim ku/Z_R$ we see that in order to neglect the second derivative we need to require $Z_R \gg \lambda$. From this condition it follows that $\lambda \ll w_0 \ll Z_R$ and $\theta \ll 1$. The former implies that the size of the focal spot w_0 is much larger than the reduced wavelength, and the latter means that we use a small angle approximation. Locally, on scale of order of λ , a Gaussian beam can be considered as a plane wave, but on larger scales (w_0 transversely and Z_R longitudinally) we see that the field varies.

The magnetic field in a Gaussian beam can be found, in the lowest order, by using Eq. (17.4), where, in our case, \mathbf{n} is directed along z , and hence, we have the y component of the magnetic field

$$B_y = \frac{1}{c}E_x. \quad (17.22)$$

Problem 17.4. Calculate the longitudinal electric field E_z in the laser beam using equation $\nabla \cdot \mathbf{E} = 0$.

Problem 17.5. Show that the energy flux in the laser beam (the Poynting vector integrated over the cross section of the beam) is equal to

$$\frac{\pi}{4Z_0} E_0^2 w_0^2. \quad (17.23)$$

Problem 17.6. A laser pulse has an energy of 1 J and duration 100 fs. It is focused into a spot of radius 10 μm . Find the magnitude of the electric field in the focus.

Problem 17.7. Expand the laser field over plane waves.

Let us now look at the field at large distance from the focus, $z \gg Z_R$. At this distance we can approximate

$$Q(z) \approx \frac{ik}{2z} - \frac{k^2 w_0^2}{4z^2}, \quad A(z) \approx -\frac{iE_0 k w_0^2}{2z}. \quad (17.24)$$

We see that the amplitude of the field decays in inverse proportionality to the distance z , and there is a radial profile $e^{-k^2 w_0^2 \rho^2 / 4z^2}$ given by the absolute value of the exponential factor. There is also a correction to the phase factor, so that the total phase is

$$\phi = kz + \frac{k\rho^2}{2z}. \quad (17.25)$$

Note, that if we introduce the distance R from the focal point, $R = \sqrt{z^2 + \rho^2}$ (see Fig. 17.3), then, at large z , $R \approx z + \rho^2/2z$, and we see that the phase is approximately equal to kR . This is a characteristic of a *spherical wave*, and we conclude that at large distance a Gaussian beam is seen as a spherical wave propagating from the center of the focus.

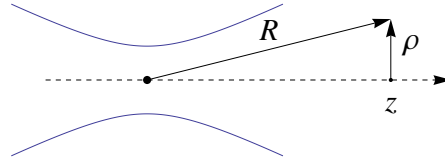


Figure 17.3: To the definition of R and ρ .

Lecture 18

Radiation and retarded potentials

In this lecture, based on simple intuitive arguments we derive the Liénard-Wiechert potentials that solve the problem of the electromagnetic field of a point charge moving in free space.

18.1 Radiation field

Let us assume that a point charge was at rest until $t = 0$, and then it is abruptly accelerated and moves with a constant velocity v at $t > 0$, see Fig. 18.1a. How

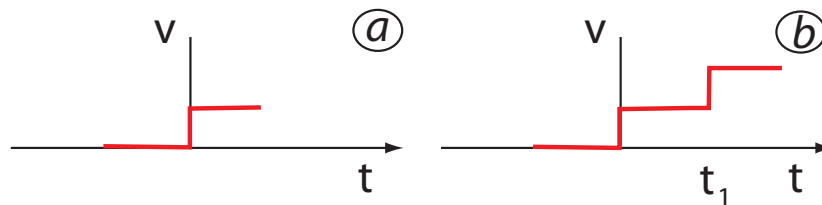


Figure 18.1: The velocity versus time of an abruptly accelerated charge.

do electric field lines look like before and after the acceleration? Those pictures are shown in Fig. 18.2. Before the acceleration we have the electrostatic field of a charge at rest. After the acceleration, at time t , the field outside of the circle of radius ct “does not know” that the charge has been moved. It is still the same static field as it was at $t < 0$. Inside the sphere of radius ct , the field is restructured in such a way that it is now equal to the field of a moving charge described by Eqs. (15.3). In a thin spherical layer around the radius ct there will be a transition region from one field to the other. At large distances from the charge, the field in this layer becomes the *radiation* field.

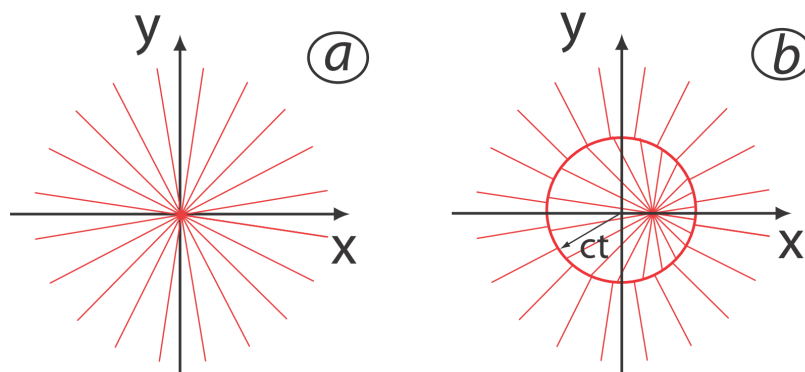


Figure 18.2: Field lines before (a) and after (b) acceleration.

If the charge was moved twice, as shown in Fig. 18.1b, then the field lines at time $t > t_1$ would look like shown in Fig. 18.2—there will be two spheres, with the radiation layers between them.

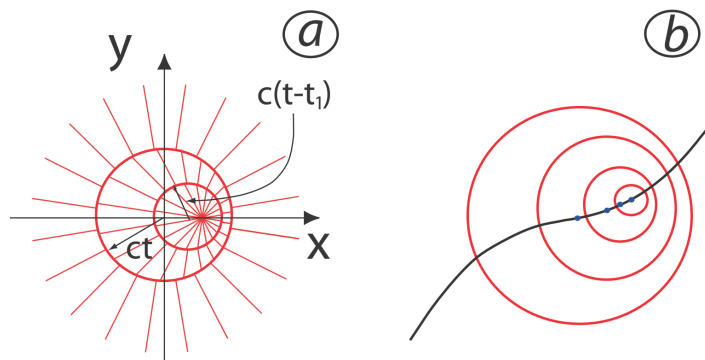


Figure 18.3: Field lines after two short acceleration phases (a) and continuous radiation of spheres (b). The blue dots on figure (b) show the centers of the circles.

One can now easily imagine that a constantly accelerating charge will be radiating the spheres at each moment of time, and those spheres will be expanding increasing their radii with the speed of light.

For a quantitative description of the radiation process, we first need to figure out how to relate a point on such sphere to the time and position of the charge when this particular sphere was radiated. This time is called the *retarded* time and the position of the particle is the *retarded* position. If a particle's orbit is given by the vector-function $\mathbf{r}_0(t)$, and we make an observation at time t at

point \mathbf{r} in space, then the retarded time t_{ret} is determined from the equation

$$c(t - t_{\text{ret}}) = |\mathbf{r} - \mathbf{r}_0(t_{\text{ret}})| \quad (18.1)$$

and the retarded position is $\mathbf{r}_0(t_{\text{ret}})$. Note that both t_{ret} and $\mathbf{r}_0(t_{\text{ret}})$, for a given orbit of the particle (determined by the function $\mathbf{r}_0(t)$), are functions of variables t and \mathbf{r} .

18.2 Retarded time and position for a particle moving with constant velocity

We talked about radiation of spherical electromagnetic shells when a particle is being accelerated. If acceleration becomes smaller and smaller, we approach the limit of a particle moving with a constant velocity or standing still. We should be able to think about such a particle as sending electromagnetic spheres all the time. Let us see how this picture agrees with the calculated in Section 15.1 electromagnetic field of a moving charge.

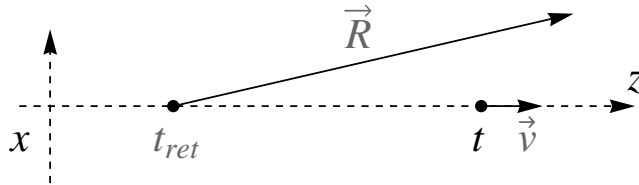


Figure 18.4: Point charge moving with constant velocity along the z -axis.

Assume again that a point charge is moving with a constant velocity v along the z axis, see Fig. 18.4. First we need to find t_{ret} . Using

$$\mathbf{r}_0 = (0, 0, vt) \quad (18.2)$$

we square Eq. (18.1)

$$c^2 t'^2 = (z - v(t - t'))^2 + x^2 + y^2, \quad (18.3)$$

where $t' = t - t_{\text{ret}}$. This is a quadratic equation for t' which can easily be solved. It has two solutions, one of them is an *advanced* solution with $t' < 0$, the other one is our retarded solution with $t' > 0$. The advanced solution is discarded because it does not satisfy the causality.

Problem 18.1. Find solutions of Eq. (18.3) and analyze them.

We will not try to analyze the solution of Eq. (18.3). Instead, we will rewrite the equations for potentials (15.8) for a moving charge in a different form.

Let us first show that the quantity \mathcal{R} in Eq. (15.4) is equal to

$$\mathcal{R} = R(1 - \boldsymbol{\beta} \cdot \mathbf{n}) = R - \boldsymbol{\beta} \cdot \mathbf{R}, \quad (18.4)$$

where $\mathbf{R} = \mathbf{r} - \mathbf{r}_0(t_{\text{ret}})$ and $\mathbf{n} = \mathbf{R}/R$. Taking square of (18.4) we have

$$\mathcal{R}^2 = (R - \boldsymbol{\beta} \cdot \mathbf{R})^2, \quad (18.5)$$

or, using coordinates,

$$(z - vt)^2 + \frac{x^2 + y^2}{\gamma^2} = (ct' - \beta(z - v(t - t')))^2, \quad (18.6)$$

where we used $R = ct'$ and $R_z = z - v(t - t')$. Substituting $x^2 + y^2 = c^2t'^2 - (z - v(t - t'))^2$ from Eq. (18.3) we get

$$(z - vt)^2 + \frac{c^2t'^2 - (z - v(t - t'))^2}{\gamma^2} = (ct' - \beta(z - v(t - t')))^2. \quad (18.7)$$

It is easy to check that the above equation is an identity. Hence, we proved Eq. (18.4).

The potentials (15.8) for a particle moving with a constant velocity can now be written as

$$\phi = \frac{1}{4\pi\epsilon_0} \frac{q}{R(1 - \boldsymbol{\beta} \cdot \mathbf{n})}, \quad \mathbf{A} = \frac{Z_0}{4\pi} \boldsymbol{\beta} \frac{q}{R(1 - \boldsymbol{\beta} \cdot \mathbf{n})}. \quad (18.8)$$

Remember that R involves the retarded position of the particle. We can also formally consider $\boldsymbol{\beta}$ as taken at the retarded time, because it does not depend on time at all.

It turns out that in this new form the equations are valid for arbitrary motion of a point charge, even when the charge is being accelerated.

18.3 Liénard-Wiechert potentials

In the previous Section we “accidentally” derived the *Liénard-Wiechert potentials* which describe electromagnetic field of an arbitrary moving particle. Those equations are:

$$\begin{aligned} \phi(\mathbf{r}, t) &= \frac{1}{4\pi\epsilon_0} \frac{q}{R(1 - \boldsymbol{\beta}_{\text{ret}} \cdot \mathbf{n})}, \\ \mathbf{A}(\mathbf{r}, t) &= \frac{Z_0}{4\pi} \frac{q\boldsymbol{\beta}_{\text{ret}}}{R(1 - \boldsymbol{\beta}_{\text{ret}} \cdot \mathbf{n})}. \end{aligned} \quad (18.9)$$

Here the particle’s velocity $\boldsymbol{\beta}$ should be taken at the retarded time, $\boldsymbol{\beta}_{\text{ret}} = \boldsymbol{\beta}(t_{\text{ret}})$, and we remind that $\mathbf{R} = \mathbf{r} - \mathbf{r}_0(t_{\text{ret}})$ is a vector drawn from the retarded position of the particle to the observation point, and \mathbf{n} is a unit vector in the direction of \mathbf{R} .

Remember that $t_{\text{ret}} = t_{\text{ret}}(\mathbf{r}, t)$. Later we will need the partial derivative $\partial t_{\text{ret}}/\partial t$. This derivative can be calculated if we square both sides of Eq. (18.1) and take the derivative with respect to time:

$$\frac{\partial}{\partial t} c^2(t - t_{\text{ret}})^2 = \frac{\partial}{\partial t} (\mathbf{r} - \mathbf{r}_0(t_{\text{ret}}))^2 \quad (18.10)$$

which gives

$$\begin{aligned}
& -2c^2(t - t_{\text{ret}}) \left(\frac{\partial t_{\text{ret}}}{\partial t} - 1 \right) \\
& = -2(\mathbf{r} - \mathbf{r}_0(t_{\text{ret}})) \frac{\partial \mathbf{r}_0}{\partial t} \\
& = -2(\mathbf{r} - \mathbf{r}_0(t_{\text{ret}})) \frac{\partial \mathbf{r}_0}{\partial t_{\text{ret}}} \frac{\partial t_{\text{ret}}}{\partial t}.
\end{aligned} \tag{18.11}$$

From this equation we find

$$\frac{\partial t_{\text{ret}}}{\partial t} = \frac{1}{1 - \boldsymbol{\beta}_{\text{ret}} \cdot \mathbf{n}}. \tag{18.12}$$

This is exactly the factor that we see in the Liénard-Wiechert potentials.

Problem 18.2. Find $\partial R/\partial t$ and ∇R . Show that

$$\nabla t_{\text{ret}} = -\frac{\mathbf{n}}{c(1 - \mathbf{n} \cdot \boldsymbol{\beta}_{\text{ret}})}. \tag{18.13}$$

The operator ∇ here is understood as $\hat{\mathbf{x}}\partial/\partial x + \hat{\mathbf{y}}\partial/\partial y + \hat{\mathbf{z}}\partial/\partial z$.

Using equations for the fields (1.7) one can obtain formulas that express the electric and magnetic fields of an arbitrary moving point charge (see. Eq. (14.13) and (14.14) in [1]):

$$\begin{aligned}
\mathbf{E} &= \frac{q}{4\pi\epsilon_0} \frac{\mathbf{n} - \boldsymbol{\beta}_{\text{ret}}}{\gamma^2 R^2 (1 - \boldsymbol{\beta}_{\text{ret}} \cdot \mathbf{n})^3} + \frac{q}{4\pi\epsilon_0 c} \frac{\mathbf{n} \times \{(\mathbf{n} - \boldsymbol{\beta}_{\text{ret}}) \times \dot{\boldsymbol{\beta}}_{\text{ret}}\}}{R(1 - \boldsymbol{\beta}_{\text{ret}} \cdot \mathbf{n})^3}, \\
\mathbf{B} &= \mathbf{n} \times \mathbf{E},
\end{aligned} \tag{18.14}$$

where $\dot{\boldsymbol{\beta}}_{\text{ret}}$ is the acceleration (normalized by the speed of light) taken at the retarded time.

Problem 18.3. A point charge is at rest for $t < 0$. It is then uniformly accelerated during time interval Δt with acceleration a , and moves with a constant velocity $v = a\Delta t$ at $t > \Delta t$. Using the retarded potentials find the electromagnetic field in space at $t > \Delta t$. Assume $v \ll c$.

18.4 Retarded potentials for an ensemble of particles

The Liénard-Wiechert potentials given by Eqs. (18.9) are convenient for calculation of fields of a moving point charge. What if we are given a continuous time dependent current and charge distribution $\rho(\mathbf{r}, t)$ and $\mathbf{j}(\mathbf{r}, t)$? Can we integrate the Liénard-Wiechert potentials over the space to obtain the result for such a case?

Naively, one can think that to obtain the potential for a continuous distribution one has to replace the charge q by an infinitesimal charge $\rho(\mathbf{r}', t)d^3r'$ in

the elementary volume d^3r' and integrate over the space,

$$\frac{1}{4\pi\epsilon_0} \int \frac{\rho(\mathbf{r}', t_{\text{ret}}) d^3r'}{|\mathbf{r} - \mathbf{r}'|(1 - \boldsymbol{\beta}_{\text{ret}} \cdot \mathbf{n})}, \quad (18.15)$$

where $\mathbf{n} = (\mathbf{r} - \mathbf{r}')/|\mathbf{r} - \mathbf{r}'|$. This however, would be wrong. Indeed, if we want, using Eq. (18.15), to recover the original Liénard-Wiechert potentials for a point charge we need to do the integral with $\rho(\mathbf{r}, t) = q\delta(\mathbf{r} - \mathbf{r}_0(t))$. Let us for simplicity assume that the particle moves along the z axis with offsets x_0 and y_0 , then

$$\delta(\mathbf{r} - \mathbf{r}_0(t_{\text{ret}})) = \delta(x - x_0)\delta(y - y_0)\delta(z - z_0(t_{\text{ret}})), \quad (18.16)$$

and $\boldsymbol{\beta} = (0, 0, \beta_z)$. Calculating the integral (18.15) we have to remember that t_{ret} is a function of z , so that

$$\begin{aligned} \int \frac{\rho(\mathbf{r}', t_{\text{ret}}) d^3r'}{|\mathbf{r} - \mathbf{r}'|(1 - \boldsymbol{\beta}_{\text{ret}} \cdot \mathbf{n})} &= q \int \frac{\delta(x' - x_0)\delta(y' - y_0)\delta(z' - z_0(t_{\text{ret}}))}{|\mathbf{r} - \mathbf{r}'|(1 - \beta_{\text{ret},z}n_z)} dx' dy' dz' \\ &= q \int \frac{\delta(z' - z_0(t_{\text{ret}}))}{|\mathbf{r} - \mathbf{r}'|(1 - \beta_{\text{ret},z}n_z)} \Big|_{x'=x_0, y'=y_0} dz' \\ &= \frac{q}{|\mathbf{r} - \mathbf{r}_0(t_{\text{ret}})|(1 - \beta_{\text{ret},z}n_z)|1 - v_{\text{ret},z}\partial t_{\text{ret}}/\partial z'|} \\ &= \frac{q}{R(1 - \beta_{\text{ret},z}n_z)^2}, \end{aligned} \quad (18.17)$$

where we used the relation $\partial t_{\text{ret}}/\partial z' = n_z$ which is easy to check by differentiating $c(t - t_{\text{ret}}) = |\mathbf{r} - \mathbf{r}'|$ with respect to z' . We see that we have an extra factor $(1 - \boldsymbol{\beta}_{\text{ret}} \cdot \mathbf{n})$ in comparison to Eq. (18.9). To correct for this factor we have to start from the integrals that do not have this factor in the denominator

$$\begin{aligned} \phi(\mathbf{r}, t) &= \frac{1}{4\pi\epsilon_0} \int \frac{\rho(\mathbf{r}', t_{\text{ret}}) d^3r'}{|\mathbf{r} - \mathbf{r}'|}, \\ \mathbf{A}(\mathbf{r}', t) &= \frac{Z_0}{4\pi c} \int \frac{\mathbf{j}(\mathbf{r}', t_{\text{ret}}) d^3r'}{|\mathbf{r} - \mathbf{r}'|}. \end{aligned} \quad (18.18)$$

These integrals are called the *retarded* potentials. They give the radiation field in free space of a system of charges represented by continuous distribution of charge density ρ and the current density \mathbf{j} .

That these are correct expression, can be verified by using the following problem.

Problem 18.4. Verify that the Liénard-Wiechert potentials can now be derived from the retarded potentials assuming $\rho(\mathbf{r}, t) = q\delta(\mathbf{r} - \mathbf{r}_0(t))$ and $\mathbf{j}(\mathbf{r}, t) = q\mathbf{v}(t)\delta(\mathbf{r} - \mathbf{r}_0(t))$ with $\mathbf{v} = d\mathbf{r}_0/dt$.

Lecture 19

Scattering of electromagnetic waves

In this Lecture we consider scattering of an electromagnetic wave on a free charged particle—so called Thomson scattering. The scattering involves a radiation reaction force, which keeps the energy balance in the process, while the momentum balance is controlled by the light pressure effect. We also briefly discuss the inverse Compton scattering on a point charge moving with a relativistic velocity.

19.1 Thomson scattering

Let us assume that an electron initially at rest is illuminated by a plane electromagnetic wave. This electron will start to oscillate in the wave and to radiate electromagnetic field. We want to calculate this radiation.

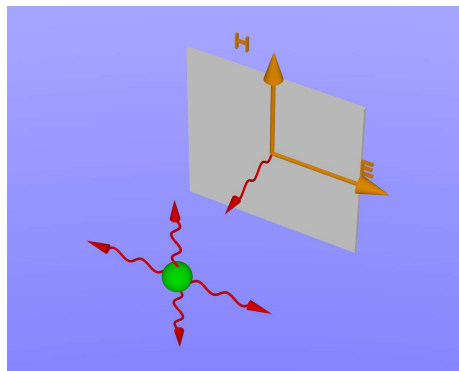


Figure 19.1: Plane electromagnetic wave is incident on a charge at rest. Due to oscillations of the charge in the incident wave, secondary waves will be radiated.

First, we need to calculate the electron motion in the incident wave. We will assume that this wave is weak, so that the electron velocity in the wave is nonrelativistic. The field in the wave is given by Eq. (17.6). The equation of motion for the electron is

$$m \frac{d\mathbf{v}}{dt} = q\mathbf{E}_0 e^{-i\omega t + i\mathbf{k}\mathbf{r}}, \quad (19.1)$$

(we assumed the phase $\phi_0 = 0$). The magnetic force in this equation is dropped because it is much smaller than the electric force when $v \ll c$. We use a complex notation here with the real part having the physical meaning. Assuming that the electron is located near the origin of the coordinate system, $\mathbf{r} \approx 0$, we will drop the term $i\mathbf{k}\mathbf{r}$ on the right-hand side of (19.1) (see explanation below)

$$m \frac{d\mathbf{v}}{dt} = q\mathbf{E}_0 e^{-i\omega t}. \quad (19.2)$$

Integration over time gives

$$\mathbf{v} = \frac{iq}{m\omega} \mathbf{E}_0 e^{-i\omega t}, \quad (19.3)$$

and

$$\mathbf{r} = -\frac{q}{m\omega^2} \mathbf{E}_0 e^{-i\omega t}. \quad (19.4)$$

The condition $v \ll c$ implies that

$$a \equiv \frac{qE_0}{m\omega c} \ll 1, \quad (19.5)$$

where we defined the parameter a which characterizes the strength of the electromagnetic field. This is a very important condition, which we will meet again in a later lecture. Note that this condition also means that the amplitude of the oscillations is much smaller than the reduced wave length, $kr \ll 1$, or

$$r \ll \lambda, \quad (19.6)$$

where $\lambda = c/\omega = \lambda/2\pi$, with λ being the wavelength of the incident wave. It is because of the smallness of the parameter kr we neglected the term $i\mathbf{k}\mathbf{r}$ in (19.1).

Problem 19.1. *Prove that the ratio $qE_0/m\omega c$ is a Lorentz invariant—it does not change under the Lorentz transformation (in other words, it is the same in any coordinate system moving relative to the laboratory reference frame).*

Having calculated the electron motion, we can now find the radiation resulting from this motion. We need to calculate the vector potential Eq. (18.9). We will make several simplifying assumptions. First, we neglect the $\beta_{\text{ret}}\mathbf{n}$ term in the denominator because $\beta \ll 1$. Second, because we are considering radiation at a large distance, much larger than the amplitude of the oscillations, we have approximately $R = r$. Finally, we neglect the term $\mathbf{r}_0(t_{\text{ret}})$ in Eq. (18.1):

$$t_{\text{ret}} = t - \frac{r}{c}. \quad (19.7)$$

The result is

$$\begin{aligned}
 \mathbf{A}(\mathbf{r}, t) &= \frac{Z_0}{4\pi} \frac{q\boldsymbol{\beta}(t_{\text{ret}})}{r} \\
 &= \frac{Z_0}{4\pi} \frac{q\mathbf{v}(t - \frac{r}{c})}{cr} \\
 &= \frac{Z_0}{4\pi} \frac{iq^2}{m\omega cr} \mathbf{E}_0 e^{-i\omega t + ikr}.
 \end{aligned} \tag{19.8}$$

We are dealing here with a spherical electromagnetic wave, whose amplitude decays with distance as $1/r$.

Recall now what we talked about the local plane wave approximation at a large distance from the source in Section 17.1. This is a situation where we can apply this approximation and use Eqs. (17.5) and (17.3) to calculate the radiation fields. Eq. (17.5) gives

$$\begin{aligned}
 \mathbf{B} &= -\frac{1}{c} \mathbf{n} \times \frac{\partial \mathbf{A}}{\partial t} \\
 &= \frac{Z_0}{4\pi} \frac{q^2}{mc^2 r} \mathbf{n} \times \mathbf{E}_0 e^{-i\omega t + ikr}.
 \end{aligned} \tag{19.9}$$

We see that radiation occurs at the frequency of the incident wave. The energy flow in the radiation field is:

$$\begin{aligned}
 \bar{S} &= \frac{1}{2Z_0} |E|^2 = \frac{c^2}{2Z_0} |B|^2 \\
 &= \frac{Z_0}{32\pi^2} \frac{q^4}{m^2 c^2 r^2} |\mathbf{n} \times \mathbf{E}_0|^2 \\
 &= \frac{Z_0}{32\pi^2} \frac{q^4 E_0^2}{m^2 c^2 r^2} \sin^2 \theta,
 \end{aligned} \tag{19.10}$$

with the intensity of radiation

$$\frac{d\mathcal{I}}{d\Omega} = \bar{S} r^2 = \frac{Z_0}{32\pi^2} \frac{q^4 E_0^2}{m^2 c^2} \sin^2 \psi. \tag{19.11}$$

Here the angle ψ is measured relative to the direction of the electric field in the wave. The angular distribution is $\propto \sin^2 \psi$.

Integrating this power over the solid angle gives the total energy radiated per unit time

$$\begin{aligned}
 \mathcal{I} &= \int \frac{d\mathcal{I}}{d\Omega} d\Omega \\
 &= \frac{Z_0}{32\pi^2} \frac{q^4 E_0^2}{m^2 c^2} \int_0^\pi \sin^2 \psi \cdot 2\pi \sin \psi \, d\psi \\
 &= \frac{Z_0}{32\pi^2} \left(\frac{8\pi}{3} \right) \frac{q^4 E_0^2}{m^2 c^2}.
 \end{aligned} \tag{19.12}$$

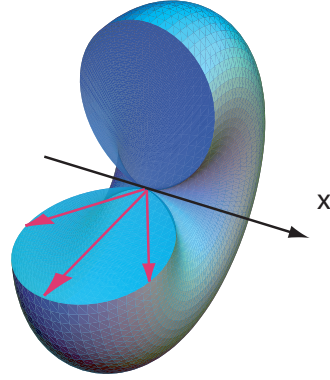


Figure 19.2: The angular distribution of the Thomson scattering. The electric field is directed along the x axis.

What is the number of photons emitted per unit time?

$$\begin{aligned}
 \dot{N}_p &= \frac{\mathcal{I}}{\hbar\omega} \\
 &= \frac{Z_0}{12\pi} \frac{q^4 E_0^2}{m^2 c^2} \frac{1}{\hbar\omega} \\
 &= \frac{1}{12\pi\epsilon_0} \frac{q^2 E_0^2}{m^2 c^2 \omega^2} \omega \frac{q^2}{\hbar c} \\
 &= \frac{1}{3} a^2 \omega \alpha,
 \end{aligned} \tag{19.13}$$

where a is defined by Eq. (19.5) and α is the fine structure constant

$$\alpha = \frac{1}{4\pi\epsilon_0} \frac{q^2}{\hbar c} \approx \frac{1}{137}. \tag{19.14}$$

If we divide the radiated power by the average energy flow in the wave, we obtain a quantity that has dimension of length squared. This quantity can be interpreted as a scattering cross section, and is called the *Thomson cross section*

$$\sigma_T = \frac{\mathcal{I}}{E_0^2/2Z_0} = \left(\frac{1}{4\pi\epsilon_0} \right)^2 \frac{8\pi q^4}{3m^2 c^4} = \frac{8\pi}{3} r_0^2, \tag{19.15}$$

where r_0 is the *classical radius*

$$r_0 = \frac{1}{4\pi\epsilon_0} \frac{q^2}{mc^2}. \tag{19.16}$$

For electrons $r_0 = 2.8 \cdot 10^{-13}$ cm.

In a later lecture we will need the intensity of the radiation written in the spherical coordinate system, in which the wave propagates in the z direction and

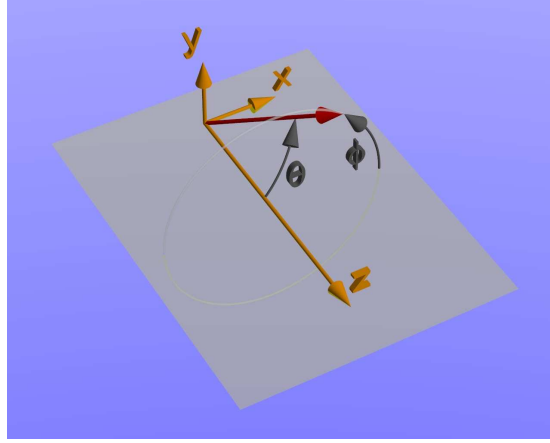


Figure 19.3: A spherical coordinate system. The wave propagates along the z axis, and the electric field in the wave is directed along the x axis.

the electric field is directed along x . We introduce the polar angle θ measured relative to the z axis and the azimuthal angle ϕ measured in the $x - y$ plane, see Fig. 19.3. In this coordinate system

$$\mathbf{n} = (\sin \theta \cos \phi, \sin \theta \sin \phi, \cos \theta), \quad (19.17)$$

and with $\mathbf{E}_0 = (E_0, 0, 0)$ we find

$$|\mathbf{n} \times \mathbf{E}_0|^2 = E_0^2 (1 - \sin^2 \theta \cos^2 \phi). \quad (19.18)$$

Eq. (19.11) takes the form

$$\frac{d\mathcal{I}}{d\Omega} = \frac{Z_0}{32\pi^2} \frac{q^4 E_0^2}{m^2 c^2} (1 - \sin^2 \theta \cos^2 \phi). \quad (19.19)$$

Problem 19.2. Prove Eq. (19.18).

Problem 19.3. Consider scattering of an electromagnetic wave on a charge q that is attached to an immobile point through a spring, and can oscillate with the frequency ω_0 . Find the scattering cross section as a function of frequency of the incident wave ω .

19.2 Radiation reaction force

Because the charge is losing energy on radiation, it should feel a force that, on average, works against the velocity, as a friction force. Indeed, such a force exists, and is called the *radiation reaction* force. Let us calculate this force \mathbf{f}_{rr} using the energy balance equation

$$-\langle \mathbf{f}_{rr} \cdot \mathbf{v} \rangle = \mathcal{I}, \quad (19.20)$$

where the angular brackets indicate averaging over time. We take the expression for the velocity Eq. (19.3) in real form

$$\mathbf{v} = \frac{q}{m\omega} \mathbf{E}_0 \sin \omega t, \quad (19.21)$$

and assume that \mathbf{f}_{rr} is in the direction of the velocity and is in phase with it

$$\mathbf{f}_{rr} = -A\mathbf{v}. \quad (19.22)$$

We then have

$$\langle \mathbf{f}_{rr} \cdot \mathbf{v} \rangle = -\frac{1}{2} A \left(\frac{qE_0}{m\omega} \right)^2. \quad (19.23)$$

Equating this expression to I given by Eq. (19.12), we find

$$A = -\frac{Z_0}{6\pi} \frac{q^2 \omega^2}{c^2}, \quad (19.24)$$

and the force is

$$\mathbf{f}_{rr} = -\frac{Z_0}{6\pi} \frac{q^2 \omega^2}{c^2} \mathbf{v} = \frac{1}{6\pi\epsilon_0} \frac{q^2}{c^3} \ddot{\mathbf{v}} = \frac{2}{3} \frac{r_0 m}{c} \ddot{\mathbf{v}}. \quad (19.25)$$

The last expression, as it turns out, is more general than our derivation assumes—it is valid for arbitrary nonrelativistic motion of a point charge.

As we emphasized above, the radiation reaction force is responsible for the energy balance in the radiation process. There are some subtle issues in the full derivation of this force, which we do not touch here (the details can be found in Refs. [1, 17]). The force is however real, and absolutely vital for understanding the effect of the radiation on particle's dynamics. In Lecture 24 we will consider this force in case of synchrotron radiation of a relativistic particle.

19.3 Light pressure

Let us take a quantum look at the Thomson scattering. The photons of the incident wave within the Thomson cross section are scattered off in different directions. The incident photons carry momentum in the direction of \mathbf{k} , that is the direction of the wave propagation. Because the scattered photons are equally distributed between the forward and backward directions and, on average, their total momentum is zero. Hence the recoil momentum is transferred to the scatterer, which means that there is a force exerted on the charge in the direction of the wave propagation. Let us calculate this force.

The calculation is very easy to do using the quantum language. The power \mathcal{I} given by Eq. (19.12) is the energy of photons scattered per unit time. The ratio of the energy to momentum for each photon is c , and dividing \mathcal{I} by c we

get the momentum scattered per unit time. This momentum is the force f_{lp} in the longitudinal direction

$$f_{lp} = \frac{\mathcal{I}}{c} = \sigma_T \frac{E_0^2}{2cZ_0}. \quad (19.26)$$

Let us now give a classical derivation of this force. First, we need to modify the equation of motion (19.2) by adding on the right-hand side the radiation reaction force

$$m \frac{d\mathbf{v}}{dt} = q\mathbf{E}_0 e^{-i\omega t} + \frac{2}{3} \frac{r_0 m}{c} \frac{d^2\mathbf{v}}{dt^2}. \quad (19.27)$$

With this modification, the solution Eq. (19.3) should also be corrected

$$\mathbf{v} = \frac{iq}{m\omega} \mathbf{E}_0 e^{-i\omega t} + \mathbf{v}_1, \quad (19.28)$$

where the last term on the right-hand side is a correction. We expect that the correction is small and neglect $d^2\mathbf{v}_1/dt^2$ in Eq. (19.27), which gives

$$m \frac{d\mathbf{v}_1}{dt} = -\frac{2}{3} \frac{iqr_0\omega}{c} \mathbf{E}_0 e^{-i\omega t}. \quad (19.29)$$

The solution of this equation is

$$\mathbf{v}_1 = \frac{2}{3} \frac{qr_0}{mc} \mathbf{E}_0 e^{-i\omega t}. \quad (19.30)$$

The final step is to calculate the average over time magnetic force $q\mathbf{v}_1 \times \mathbf{B}$ which arises from the cross product of the velocity \mathbf{v}_1 and the magnetic field in the wave $\mathbf{B} = (\mathbf{k}/ck) \times \mathbf{E}_0 e^{-i\omega t}$. To average the force, we have to take the real parts of \mathbf{v}_1 and \mathbf{B} , with the result

$$q\langle \text{Re}\mathbf{v}_1 \times \text{Re}\mathbf{B} \rangle = \frac{1}{3} \frac{q^2 r_0}{mc^2 k} \mathbf{E}_0 \times \mathbf{k} \times \mathbf{E}_0 = \frac{1}{3} \frac{q^2 r_0 E_0^2}{mc^2} \frac{\mathbf{k}}{k}. \quad (19.31)$$

We see that this force is along the direction of the wave propagation. It is easy to check that it is exactly equal to the expression given by Eq. (19.26).

Problem 19.4. *In the derivation above we neglected the term $q\mathbf{v} \times \mathbf{B}$ where \mathbf{v} is given by the real part of Eq. (19.3). Show that $\langle \mathbf{v} \times \mathbf{B} \rangle = 0$.*

Problem 19.5. *Estimate the pressure of the solar light on the surface of the Earth. The solar radiation power is about 1 kW/m².*

19.4 Inverse Compton scattering

Let us now assume that the scattering electron is moving with a relativistic velocity v ($\gamma \gg 1$) in the z direction and denote the incident wave frequency by ω_0 . We make the Lorentz transformation from the lab frame to the beam frame. First we need to calculate the frequency ω' of the incident wave in the

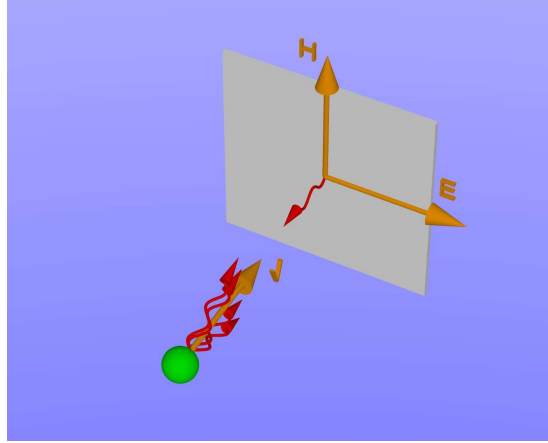


Figure 19.4: Inverse Compton scattering off a moving charge.

beam frame using the Lorentz transformation. We will use Eq. (13.18) in which $\theta = \pi$

$$\omega' = 2\gamma\omega_0. \quad (19.32)$$

This is the frequency of the scattered radiation in the beam frame. To transform it to the lab frame we will assume small angles θ and use Eq. (13.19) again

$$\omega = \frac{4\gamma^2\omega_0}{1 + \gamma^2\theta^2}. \quad (19.33)$$

We see that there is a *spectrum* of frequencies with the maximum frequency equal to $4\gamma^2\omega_0$. Roughly, the frequencies of this order propagate within a small angle

$$\theta \sim \frac{1}{\gamma}. \quad (19.34)$$

We know that in the beam frame the photons are radiated more or less in all directions. The angles in the lab frame θ are related to the angles in the beam frame with Eq. (13.15). This equation tells us that almost all photons propagate within the angle $1/\gamma$ in the direction of the beam motion. The number of photons will be the same as in the beam frame, but their energy in the lab frame is much larger in case $\gamma \gg 1$.

Problem 19.6. *R. Ruth and Z. Huang proposed to use Thomson scattering in a compact electron ring as a source of intense X-ray radiation (PRL, 80, 976, (1998)). The electron energy in the ring is 8 MeV, the number of electron in the bunch is $1.1 \cdot 10^{10}$, the laser energy is 20 mJ, the laser pulse length is 1 mm, and the laser is focused to the spot size 25 micron. Estimate the number of photons from a single collision of the laser pulse with the electron beam.*

Lecture 20

Synchrotron radiation

We will consider a relativistic point charge ($\gamma \gg 1$) moving in a circular orbit of radius ρ . Our goal is to calculate the *synchrotron* radiation of this charge. Using the Liénard-Wiechert potentials we first find the fields at a large distance from the charge in the plane of the orbit. We then discuss properties of the synchrotron radiation using a more general result for the angular dependence of the spectral intensity of the radiation.

20.1 Synchrotron radiation pulses in the plane of the orbit

The layout for our calculation is shown in Fig. 20.1. An observer is located at point O in the plane of the orbit in the far zone. The observer will see a periodic sequence of pulses of electromagnetic radiation with the period equal to the revolution period of the particle around the ring. Each pulse is emitted from the region $x \approx z \approx 0$.

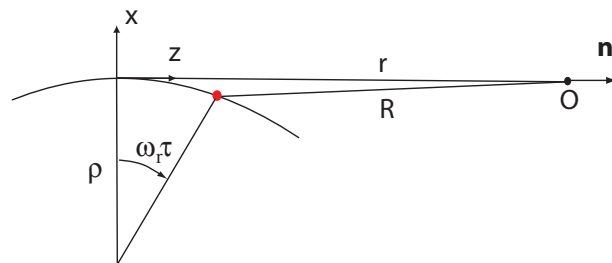


Figure 20.1: A schematic showing the particle's orbit and the observation point. The y axis is directed out of the page.

Radiation is the electromagnetic field at a large distance from the particle, and in Eq. (18.9) we can replace R in the denominator by r —the distance from the observation point to the origin of the coordinate system (where the observation line touches the circle):

$$\mathbf{A}(\mathbf{r}, t) = \frac{Z_0 q}{4\pi r} \frac{\boldsymbol{\beta}(t_{\text{ret}})}{1 - \boldsymbol{\beta}(t_{\text{ret}}) \cdot \mathbf{n}}. \quad (20.1)$$

We will also use the fact that in the far zone the radiation field can locally be represented by a plane wave, and according to Eq. (17.5) the magnetic field can be found from the vector potential:

$$\mathbf{B} = -\frac{1}{c} \hat{\mathbf{z}} \times \frac{\partial \mathbf{A}}{\partial t}, \quad (20.2)$$

where we replaced \mathbf{n} by the unit vector in the z direction.

Let us denote the retarded time by τ , so that $R(\tau) = c(t - \tau)$. We will choose the zero time in such a way that at $t = 0$ the particle is located at the origin of our coordinate system, then the position of the particle at time τ is characterized by the angle $\omega_r \tau$, as shown in Fig. 20.1, with $\omega_r = \beta c / \rho$ the angular revolution frequency of the particle. We approximately have $R \approx r - \rho \sin \omega_r \tau$, or

$$r - \rho \sin \omega_r \tau = c(t - \tau). \quad (20.3)$$

In what follows we will use the dimensionless variable ξ , $\xi = \tau c / \rho \approx \omega_r \tau$. We have

$$ct - r = \rho[\xi - \sin(\beta\xi)]. \quad (20.4)$$

We also have

$$\begin{aligned} \beta_x &= -\beta \sin(\omega_r \tau) = -\beta \sin(\beta\xi), \\ \beta_z &= \beta \cos(\omega_r \tau) = \beta \cos(\beta\xi). \end{aligned} \quad (20.5)$$

As follows from Eq. (20.1) the x component of \mathbf{A} is

$$A_x = \frac{Z_0 q}{4\pi r} \frac{\beta_x}{1 - \beta_z} = -\frac{Z_0 q}{4\pi r} \frac{\beta \sin(\beta\xi)}{1 - \beta \cos(\beta\xi)}. \quad (20.6)$$

Because the vector potential \mathbf{A} has only x and z components, it follows from Eq. (20.2) that \mathbf{B} is directed along y with

$$cB_y = -\frac{\partial A_x}{\partial t} = -\frac{\partial A_x / \partial \xi}{\partial t / \partial \xi}. \quad (20.7)$$

The function $t(\xi)$ is given by Eq. (20.4) and $A_x(\xi)$ is determined by Eqs. (20.6) and (20.5). We now assume that only a small fraction of the particle's trajectory

contributes to the shape of the electromagnetic pulse, $\xi \ll 1$. We then expand the trigonometric functions

$$\begin{aligned}\sin(\beta\xi) &\approx \beta\xi - \frac{1}{6}\xi^3, \\ \xi - \sin(\beta\xi) &\approx \xi(1 - \beta) + \frac{1}{6}\xi^3 \approx \frac{1}{2\gamma^2}\xi + \frac{1}{6}\xi^3 \\ \cos(\beta\xi) &\approx 1 - \frac{1}{2}\xi^2 \\ 1 - \beta \cos(\beta\xi) &\approx 1 - \beta + \frac{1}{2}\xi^2 \approx \frac{1}{2\gamma^2} + \frac{1}{2}\xi^2.\end{aligned}\quad (20.8)$$

Substituting these expressions into Eqs. (20.4) and (20.6) gives

$$A_x = -\frac{Z_0 q}{4\pi r} \frac{2\xi}{\gamma^{-2} + \xi^2}, \quad t = \frac{r}{c} + \frac{\rho}{c} \left(\frac{1}{2\gamma^2}\xi + \frac{1}{6}\xi^3 \right), \quad (20.9)$$

with the magnetic field

$$B_y = \frac{Z_0 q}{\pi r \rho} \frac{\gamma^{-2} - \xi^2}{(\xi^2 + \gamma^{-2})^3}. \quad (20.10)$$

Let us introduce the dimensionless time variable $\hat{t} = (\gamma^3 c/\rho)(t - r/c)$ and the dimensionless magnetic field $\hat{B} = (\pi r \rho / Z_0 q \gamma^4) B_y$. It is easy to see that the dependence $\hat{B}(\hat{t})$ is given by the following implicit relations

$$\hat{B} = \frac{1 - \zeta^2}{(\zeta^2 + 1)^3}, \quad \hat{t} = \frac{1}{2}\zeta + \frac{1}{6}\zeta^3, \quad (20.11)$$

where $\zeta = \xi\gamma$. The plot of the function $\hat{B}(\hat{t})$ is shown in Fig. 20.2. We see from this plot that the characteristic width of the pulse $\Delta\hat{t} \sim 1$, which means that the duration of the pulse in physical units

$$\Delta t \sim \frac{\rho}{c\gamma^3}. \quad (20.12)$$

The spectrum of frequencies presented in the radiation is $\Delta\omega \sim c\gamma^3/\rho$. In the next section we will study this spectrum in more detail.

Problem 20.1. Find asymptotic dependence $B_y(t)$ for $|t - r/c| \gg \rho/c\gamma^3$.

Problem 20.2. Prove that the area under the curve $B_y(t)$ is equal to zero (that is $\int_{t=-\infty}^{t=\infty} B_y(t) dt = 0$).

20.2 Fourier transformation of the radiation field and the radiated power

We will now calculate the energy radiated in unit solid angle $d\Omega$ in the x - z plane. This energy is given by the product of the Poynting vector \mathbf{S} with the

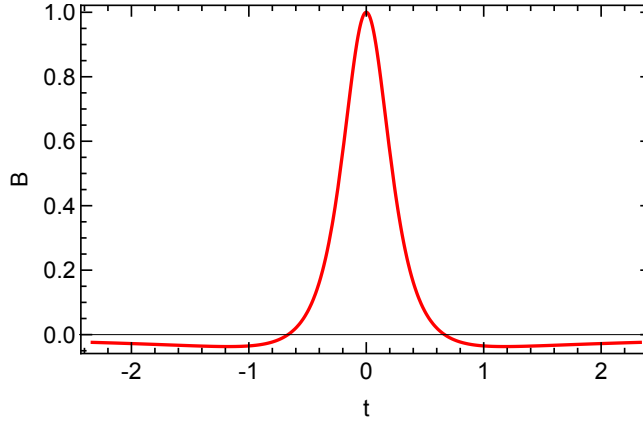


Figure 20.2: The radiation pulse of the electromagnetic field in dimensionless variables.

distance squared integrated over time:

$$r^2 \int_{-\infty}^{\infty} dt S(t) = \frac{c^2 r^2}{Z_0} \int_{-\infty}^{\infty} dt B_y(t)^2. \quad (20.13)$$

In the last equation we used the relation $E = cB$ and the fact that in a plane wave the electric and magnetic fields are perpendicular to each other.

We come to the notion of the *spectrum* of radiation if we take the Fourier transform of the field and represent the radiated energy as an integral over the frequencies ω . From Fourier analysis we know (a so called Parseval's theorem)

$$\begin{aligned} \int_{-\infty}^{\infty} dt B_y(t)^2 &= \frac{1}{2\pi} \int_{-\infty}^{\infty} d\omega |\tilde{B}_y(\omega)|^2 \\ &= \frac{1}{\pi} \int_0^{\infty} d\omega |\tilde{B}_y(\omega)|^2, \end{aligned} \quad (20.14)$$

where

$$\tilde{B}_y(\omega) = \int_{-\infty}^{\infty} dt B_y(t) e^{i\omega t}. \quad (20.15)$$

We introduce the energy radiated per unit frequency interval per unit solid angle as

$$\frac{d^2\mathcal{W}}{d\omega d\Omega} = \frac{r^2 c^2}{\pi Z_0} |\tilde{B}_y(\omega)|^2, \quad (20.16)$$

so that the total energy radiated per unit solid angle can be represented as

$$\frac{d\mathcal{W}}{d\Omega} = \int_0^{\infty} d\omega \frac{d^2\mathcal{W}}{d\omega d\Omega}. \quad (20.17)$$

To calculate $\tilde{B}_y(\omega)$ it is convenient to start from Eq. (20.7) that in Fourier representation becomes

$$c\tilde{B}_y(\omega) = i\omega\tilde{A}_x(\omega). \quad (20.18)$$

We can use Eqs. (20.9) to find the Fourier component of A_x

$$\begin{aligned} \tilde{A}_x(\omega) &= \int_{-\infty}^{\infty} A_x(t)e^{i\omega t} dt \\ &= \int_{-\infty}^{\infty} A_x(\xi)e^{i\omega t(\xi)} \frac{dt}{d\xi} d\xi \\ &= -\frac{Z_0 q}{4\pi r} \frac{\rho}{c} e^{i\omega r/c} \int_{-\infty}^{\infty} \xi e^{i(\omega\rho/2c)(\gamma^{-2}\xi + \xi^3/3)} d\xi. \end{aligned} \quad (20.19)$$

Introducing the new variable $\zeta = \xi\gamma$ and the critical frequency

$$\omega_c = \frac{3c\gamma^3}{2\rho}, \quad (20.20)$$

we find

$$\tilde{A}_x(\omega) = -i \frac{Z_0 q}{4\pi r} \frac{\rho}{c\gamma^2} e^{i\omega r/c} F\left(\frac{3\omega}{4\omega_c}\right), \quad (20.21)$$

where

$$F(x) = \text{Im} \int_{-\infty}^{\infty} \zeta e^{ix(\zeta + \zeta^3/3)} d\zeta = \frac{2}{\sqrt{3}} K_{2/3}\left(\frac{2x}{3}\right), \quad (20.22)$$

with $K_{2/3}$ the MacDonald function. Note that the real part of the integral in Eq. (20.22) is equal to zero because of the symmetry of the integrand.

This gives the spectrum of the radiation

$$\frac{d^2\mathcal{W}}{d\omega d\Omega} = \frac{q^2 Z_0}{12\pi^3} \left(\frac{\rho\omega}{c}\right)^2 \left(\frac{1}{\gamma^2}\right)^2 K_{2/3}^2\left(\frac{\omega}{2\omega_c}\right). \quad (20.23)$$

20.3 Synchrotron radiation for $\psi \neq 0$.

In a more general case of radiation at an angle $\psi \neq 0$ (see Fig. 20.3 for the layout) the calculation is more involved and we will not try to reproduce it here. However, for the reference purposes, we will summarize some of the results of this general case.

A more general formula valid for $\psi \neq 0$ is

$$\frac{d^2\mathcal{W}}{d\omega d\Omega} = \frac{q^2 Z_0}{12\pi^3} \left(\frac{\rho\omega}{c}\right)^2 \left(\frac{1}{\gamma^2} + \psi^2\right)^2 \left[K_{2/3}^2(\zeta) + \frac{\psi^2}{1/\gamma^2 + \psi^2} K_{1/3}^2(\zeta) \right], \quad (20.24)$$

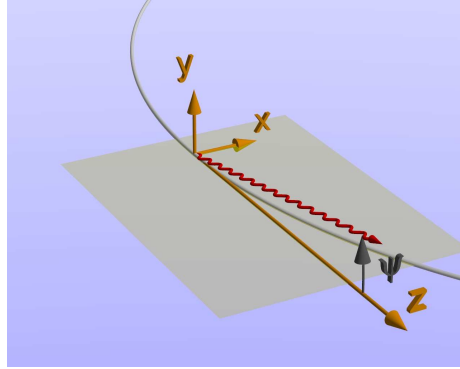


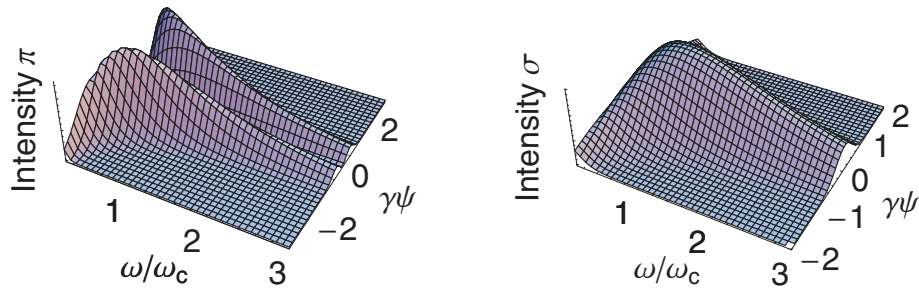
Figure 20.3: The particle's orbit and the coordinate system.

where

$$\zeta = \frac{\omega\rho}{3c} \left(\frac{1}{\gamma^2} + \psi^2 \right)^{3/2}. \quad (20.25)$$

This result was obtained by J. Schwinger in 1949. Setting $\psi = 0$ we recover Eq. (20.23).

The two terms in the square brackets correspond to different polarizations of the radiation. The first one is the so called σ -mode, it has polarization with nonzero E_x and B_y . The second one has the polarization with the electric field E_y and the magnetic field B_x ; it is called the π mode. The angular distribution of intensity for these two modes is shown in Fig. 20.4.

Figure 20.4: Intensity of π and σ modes.

Problem 20.3. Simplify Eq. (20.24) in the limit $\psi \gg 1/\gamma$. Make a plot of the quantity $\omega^{-2/3} d^2\mathcal{W}/(d\omega d\Omega)$ versus the quantity $\omega\rho\psi^3/c$. Infer from these equations that the angular spread of the radiation at frequency $\omega \ll \omega_c$ is of order of $(c/\omega\rho)^{1/3}$.

20.4 Integral characteristic of synchrotron radiation

From Eq. (20.24) we see that the radiation is localized at small angles ψ (unless we go to the frequencies of the order of the revolution frequency c/ρ). To find total radiated spectral energy $d\mathcal{W}/d\omega$ over one revolution, we have to integrate (20.24) over the solid angle Ω . As illustrated in Fig. 20.5 this integration,

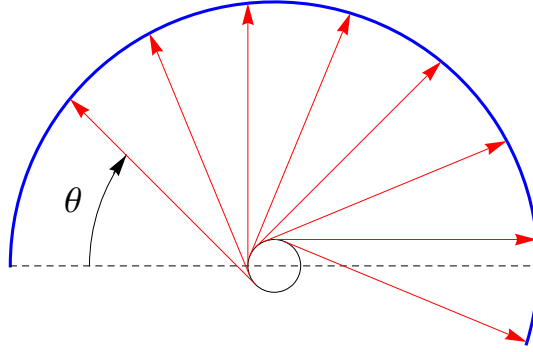


Figure 20.5: Synchrotron radiation “fan” from a circular orbit shown as a small circle at the center. Radiation travels tangentially to the orbit and is detected on a remote surface shown in blue.

in addition to integration over the angle ψ should include integration over the angle θ ,

$$\frac{d\mathcal{W}}{d\omega} = \int d\Omega \frac{d^2\mathcal{W}}{d\omega d\Omega} = \int_0^{2\pi} d\theta \int_{-\infty}^{\infty} d\psi \frac{d^2\mathcal{W}}{d\omega d\Omega} = 2\pi \int_{-\infty}^{\infty} d\psi \frac{d^2\mathcal{W}}{d\omega d\Omega}, \quad (20.26)$$

where the integration over ψ is extended from minus to plus infinity because the function (20.24) is localized in the region of small values of ψ . The result is

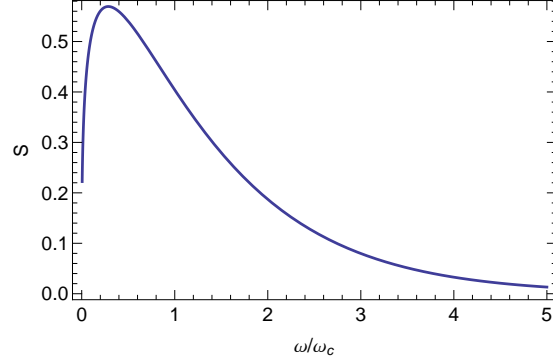
$$\frac{d\mathcal{W}}{d\omega} = \frac{2\pi\rho}{c} \cdot \frac{q^2\gamma Z_0 c}{9\pi\rho} S\left(\frac{\omega}{\omega_c}\right), \quad (20.27)$$

where

$$S(x) = \frac{27x^2}{16\pi^2} \int_{-\infty}^{\infty} d\tau (1 + \tau^2)^2 \times \left[K_{2/3}^2\left(\frac{x}{2}(1 + \tau^2)^{3/2}\right) + \frac{\tau^2}{1 + \tau^2} K_{1/3}^2\left(\frac{x}{2}(1 + \tau^2)^{3/2}\right) \right]. \quad (20.28)$$

This function is shown in Fig. 20.6. The function S is normalized to one: $\int_0^{\infty} dx S(x) = 1$. One can show that the function S can also be written as

$$S(x) = \frac{9\sqrt{3}}{8\pi} x \int_x^{\infty} K_{5/3}(y) dy. \quad (20.29)$$

Figure 20.6: S function.

For small and large values of the argument we have the asymptotic expressions

$$S = \frac{27}{8\pi} \frac{\sqrt{3}}{2^{1/3}} \Gamma\left(\frac{5}{3}\right) x^{1/3}, \quad x \ll 1 \quad (20.30a)$$

$$S = \frac{9}{8} \sqrt{\frac{3}{2\pi}} \sqrt{x} e^{-x}, \quad x \gg 1. \quad (20.30b)$$

Integrating $dW/d\omega$ over all frequencies, we will find the total energy W radiated in one revolution

$$W_r = \int_0^\infty d\omega \frac{dW}{d\omega} = \frac{2\pi\rho}{c} \cdot \frac{q^2\gamma Z_0 c}{9\pi\rho} \omega_c. \quad (20.31)$$

The radiation power (energy radiation per unit time) by a single electron is

$$\mathcal{P} = \frac{W_r}{2\pi\rho/c} = \frac{Z_0 c q^2 \gamma}{9\pi\rho} \omega_c = \frac{Z_0 c^2 q^2 \gamma^4}{6\pi\rho^2} = \frac{2r_0 m c^2 \gamma^4 c}{3\rho^2}. \quad (20.32)$$

If we divide Eq. (20.24) by $\hbar\omega$ we find the number of photons per unit interval of frequencies in the unit solid angle

$$\begin{aligned} \frac{d^2 N_{ph}}{d\omega d\Omega} &= \frac{q^2 Z_0}{12\pi^3 \hbar \omega} \left(\frac{\rho\omega}{c}\right)^2 \left(\frac{1}{\gamma^2} + \psi^2\right)^2 \left[K_{2/3}^2(\xi) + \frac{\psi^2}{1/\gamma^2 + \psi^2} K_{1/3}^2(\xi) \right] \\ &= \frac{3}{4\pi^2} \frac{\alpha\gamma^2}{\omega} \left(\frac{\omega}{\omega_c}\right)^2 F(\xi, \gamma\psi), \end{aligned} \quad (20.33)$$

with

$$F(\xi, x) = (1 + x^2)^2 \left[K_{2/3}^2(\xi) + \frac{x^2}{1 + x^2} K_{1/3}^2(\xi) \right]. \quad (20.34)$$

What we calculated above is the number of photons radiated by a single electron during passage through the point $x = 0$, $y = 0$ on the orbit. If the current in the accelerator is I_c , then the number of photons *per unit time* will be equal to the above quantity multiplied by the number of electron passing per unit time, I_c/q . Hence the photon *flux* is

$$\frac{d^2 \dot{N}_{ph}}{d\omega d\Omega} = \frac{3}{4\pi^2} \frac{I_c}{q} \frac{\alpha \gamma^2}{\omega} \left(\frac{\omega}{\omega_c} \right)^2 F(\xi, \gamma\psi). \quad (20.35)$$

20.5 Quantum fluctuations and energy spread of the beam

Radiation takes away the energy from particles. If this energy is not replenished, the particles would slow down. To keep the particles' energy constant in electron and positron machines, one uses RF cavities that accelerate the beam and compensate for the energy loss due to radiation.

Problem 20.4. Calculate RF power needed to compensate the synchrotron radiation in the High Energy Ring of PEP-II.

The process of energy loss due to synchrotron radiation is perfectly well described by classical electrodynamics. There is, however, one important for accelerator physics effect, which is purely quantum. This effect determines the energy spread in electron and positron beams in circular machines. It is called the *quantum fluctuations* in synchrotron radiation.

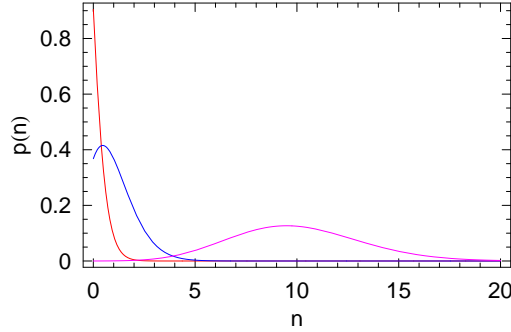
We already discussed that radiation, in quantum language, is emission of photons. Eq. (20.33) gives the spectrum of emitted photons. More precisely, N_{ph} is the averaged number of photons. The actual number of photons would fluctuate from one electron to the other.

Let us now calculate fluctuations of the energy loss ΔE due to synchrotron radiation. There are two sources of fluctuations. One is that even if electron would radiate the same number of photons each time it passes through the magnet, those would be photons of different frequency ω (because there is a spectrum of radiation), and the total energy of all photon would fluctuate. In addition, the number of photons fluctuates as well.

First, we take into account the fluctuation of the number of photons. The only piece of information that we need from the quantum theory is the notion that radiated photons are randomly distributed in time with the Poisson distribution. More precisely, if we know the average number of emitted photons \bar{n} , then the probability that in a particular process there will be radiated n photons is

$$p(n) = \frac{\bar{n}^n e^{-\bar{n}}}{n!}. \quad (20.36)$$

Let's say that an electron passes through a dipole magnet and radiates n photons. For the sake of simplicity we will assume that all photons have the

Figure 20.7: Poisson distributions for $\bar{n} = 0.1, 1, 10$.

same frequency ω . Then the energy loss is

$$\Delta E = n\hbar\omega. \quad (20.37)$$

The number n is a random number here, it will vary somewhat from one electron to another. Fluctuations are characterized by the variance

$$\begin{aligned} \langle \Delta E - \langle \Delta E \rangle \rangle^2 \\ = \langle \Delta E^2 \rangle - \langle \Delta E \rangle^2 = \hbar^2 \omega^2 (\overline{n^2} - \bar{n}^2), \end{aligned} \quad (20.38)$$

where the angular brackets here denote averaging over the number of photons, and $\langle n \rangle = \bar{n}$, $\langle n^2 \rangle = \overline{n^2}$. It is easy to calculate the variance for the Poisson process,

$$\overline{n^2} - \bar{n}^2 = \bar{n}. \quad (20.39)$$

Using this relation, we see that Eq. (20.38) reduces to

$$\langle \Delta E^2 \rangle - \langle \Delta E \rangle^2 = \bar{n} \hbar^2 \omega^2. \quad (20.40)$$

The average number of photons in this formula, \bar{n} can be found from classical calculations.

Now, we take into account that we have a continuous spectrum of radiation. In this case, we can talk about \bar{n}_ω which multiplied by $d\omega$ gives the average number of photons in the frequency interval $d\omega$. The generalization of Eq. (20.40) is

$$\langle \Delta E^2 \rangle - \langle \Delta E \rangle^2 = \int d\omega \bar{n}_\omega \hbar^2 \omega^2. \quad (20.41)$$

Note that the quantity $\bar{n}_\omega \hbar \omega$ is equal to the energy radiated into the spectral interval $d\omega$, and hence is equal to the quantity $d\mathcal{W}/d\omega$.

We can now give a crude estimate of the energy spread induced in the beam in a circular accelerator due to quantum fluctuations. It is determined by the fluctuations of the number of photons emitted by the particle during the time needed to lose all its energy, $n_f = E/\hbar\omega_c$, where $\omega_c \sim \gamma^3 c/\rho$ is the critical frequency. This number fluctuates, so that $\Delta n_f \sim \sqrt{n_f}$. Accordingly the energy spread of particle in the bunch is

$$\Delta E \sim \hbar\omega_c \Delta n_f \sim \sqrt{E\hbar\omega_c} \sim \gamma \sqrt{\frac{\lambda_c}{\rho}}, \quad (20.42)$$

where $\lambda_c = \hbar/mc$ is the Compton length.

Lecture 21

Undulator radiation

Undulator and wigglers are widely used in modern accelerator-based light sources. We derive the properties of the undulator radiation using the solution of the Thomson scattering problem from Lecture 19.

21.1 Undulators and wigglers

An plane undulator is shown in Fig. 21.1. The magnetic field in the undulator

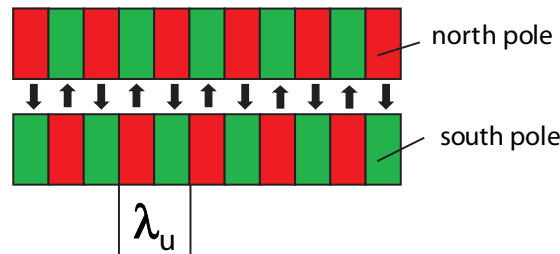


Figure 21.1: Magnetic field in a plane undulator.

is given by

$$B_y(z) = B_0 \cos k_u z, \quad (21.1)$$

with the undulator period $\lambda_u = 2\pi/k_u$. The undulator is characterized by the amplitude magnetic field B_0 , the period λ_u and the number of periods N_u .

First, we need to find the beam orbit inside the undulator. We assume that a relativistic beam propagates along the z axis with velocity v . The equation of motion in the horizontal plane is

$$\begin{aligned} m\gamma \frac{d^2 x}{dt^2} &= -qvB_0 \cos k_u z \\ &\approx -qcB_0 \cos k_u ct, \end{aligned} \quad (21.2)$$

where we used the approximation $z \approx vt \approx ct$. The solution is

$$x = \frac{qB_0}{m\gamma k_u^2 c} \cos k_u ct = \frac{qB_0}{m\gamma k_u^2 c} \cos k_u z. \quad (21.3)$$

This is a sinusoidal orbit with the maximum deflection angle

$$\left. \frac{dx}{dz} \right|_{\max} = \frac{qB_0}{m\gamma k_u c}. \quad (21.4)$$

Comparing this angle with γ^{-1} we introduce an important *undulator parameter* K

$$K = \frac{qB_0}{k_u mc} = 0.934 \lambda_u [\text{cm}] B_0 [\text{Tesla}], \quad (21.5)$$

where we used the value of the electron mass for m . An *undulator* usually means $K \lesssim 1$, and a device with large K is called a *wiggler*.

Since we found above the orbit in an undulator, we could calculate the radiation using the retarded potential formalism, as we did for the synchrotron radiation. We, however, will use a different approach, and calculate the spectrum of the radiation by applying the Lorentz transformation to the solution of the Thomson scattering problem considered in Lecture 19.

21.2 Undulator radiation for $K \ll 1$

Let us consider a long undulator with $K \ll 1$ and a large number of periods, and neglect the effects associated with the entrance to and exit from the undulator. When a particle is moving inside the undulator, we transform to the moving frame of reference and use prime to denote quantities in this frame.

First, we need to find what is the electromagnetic field of the “flying” undulator in the particle frame where the undulator is moving in the negative direction of the z axis with velocity $\mathbf{v} = (0, 0, -v)$. We have

$$z = \gamma(z' - \beta ct') \approx \gamma(z' - ct'). \quad (21.6)$$

Using the Lorentz transformation for the field, and assuming $\gamma \gg 1$, we find

$$\begin{aligned} E'_x &= \gamma v B_0 \cos k_u z \approx \gamma c B_0 \cos k_u \gamma(z' - ct'), \\ B'_y &= \gamma B_0 \cos k_u z \approx \gamma B_0 \cos k_u \gamma(z' - ct'). \end{aligned} \quad (21.7)$$

This is the field of a plane electromagnetic wave moving in the negative z direction with the frequency $\omega' = \gamma k_u c$ and the field γ times larger than the lab field of the undulator. Under the influence of this field the electron starts to radiate, and this is the problem of Thomson scattering that we studied in Lecture 19. Note that the quantity a in Eq. (19.5), where $E_0 = \gamma c B_0$ and $\omega \rightarrow \omega' = \gamma k_u c$ is exactly equal to the undulator parameter (21.5). To be able to use our solution from Lecture 19 that we obtained in the limit $a \ll 1$, we have required $K \ll 1$.

The intensity of the radiation is given by Eq. (19.19), which we rewrite here using the new notation

$$\frac{d\mathcal{P}'}{d\Omega'} = \frac{Z_0}{32\pi^2} \frac{q^4 \gamma^2 B_0^2}{m^2} (1 - \sin^2 \theta' \cos^2 \phi). \quad (21.8)$$

We now need to translate the quantities $d\mathcal{P}'$, $d\Omega'$, ψ' , as well ω' into the lab frame. Eq. (13.16) gives

$$\sin \theta' = \frac{\sin \theta}{\gamma(1 - \beta \cos \theta)} \approx \frac{2\theta\gamma}{1 + \gamma^2\theta^2}, \quad (21.9)$$

where we assumed that $\theta \ll 1$ and expanded $\cos \theta \approx 1 - \theta^2/2$, and used $1 - \beta \approx 1/2\gamma^2$. Eq. (13.19) gives

$$\omega \approx \frac{2\gamma\omega'}{1 + \gamma^2\theta^2} = \frac{2\gamma^2 k_u c}{1 + \gamma^2\theta^2}. \quad (21.10)$$

The maximum frequency goes in the forward direction, $\theta = 0$, and is equal to

$$\omega_0 = 2\gamma\omega' = 2\gamma^2 k_u c. \quad (21.11)$$

The differential of the solid angle is transformed like the following

$$\begin{aligned} d\Omega' &= \sin(\theta') d\theta' d\phi \\ &= |d \cos(\theta')| d\phi. \end{aligned} \quad (21.12)$$

Using Eq. (13.16) we find

$$d\Omega' = \frac{1 - \beta^2}{(1 - \beta \cos \theta)^2} |d \cos(\theta)| d\phi \approx \frac{4\gamma^2}{(1 + \gamma^2\theta^2)^2} d\Omega. \quad (21.13)$$

Finally, we need to transform the differential $d\mathcal{P}'$ which is the radiated energy of the electromagnetic field per unit time $d\mathcal{P}' = dE'/dt'$. We know how to transform time, $dt' = dt/\gamma$. To transform energy we consider radiation as a collection of photons. In quantum language the energy of a photon is $\hbar\omega$, and the number of photons is the same in any reference frame. Hence the energy is transformed as the frequency, $dE' = N_{\text{ph}} \hbar\omega' = dE(\omega'/\omega)$. We now have

$$\begin{aligned} \frac{d\mathcal{P}}{d\Omega} &= \frac{dE}{d\Omega dt} \\ &= \frac{dE'}{d\Omega' dt'} \frac{\omega}{\omega'} \frac{1}{\gamma} \frac{4\gamma^2}{(1 + \gamma^2\theta^2)^2} \\ &= \frac{d\mathcal{P}'}{d\Omega'} \frac{8\gamma^2}{(1 + \gamma^2\theta^2)^3} \\ &= \frac{Z_0}{32\pi^2} \frac{q^4 \gamma^2 B_0^2}{m^2} \left[1 - \frac{4\theta^2 \gamma^2}{(1 + \gamma^2\theta^2)^2} \cos^2 \phi \right] \frac{8\gamma^2}{(1 + \gamma^2\theta^2)^3} \\ &= \frac{Z_0}{4\pi^2} \frac{q^4 \gamma^4 B_0^2}{m^2} \frac{(1 + \gamma^2\theta^2)^2 - 4\theta^2 \gamma^2 \cos^2 \phi}{(1 + \gamma^2\theta^2)^5}. \end{aligned} \quad (21.14)$$

Remember that to each angle θ corresponds a particular energy given by Eq. (21.10). We can take this into account formally introducing the spectral power of radiation $d\mathcal{P}/d\Omega d\omega$

$$\frac{d\mathcal{P}}{d\Omega d\omega} = \frac{d\mathcal{P}}{d\Omega} \delta\left(\omega - \frac{2\gamma^2 k_u c}{1 + \gamma^2 \theta^2}\right), \quad (21.15)$$

where the delta functions indicates an infinitely narrow spectrum at each angle. Integration of $d\mathcal{P}/d\Omega d\omega$ over frequencies gives us the angular distribution of the power $d\mathcal{P}/d\Omega$. Of course, the delta function spectrum here is due to the fact that we neglect the finite time of flight through the undulator (actually, considering the undulator infinitely long). Taking into account the finite length, as we will see in the next section, introduces a non-zero width of the spectrum.

To find the energy radiated per unit time we integrate this equation over Ω (we use $\sin \theta \approx \theta$)

$$\begin{aligned} \mathcal{P}_0 &= \int \frac{d\mathcal{P}}{d\Omega} d\Omega \approx \int_0^\infty \theta d\theta \int_0^{2\pi} d\phi \frac{d\mathcal{P}}{d\Omega} \\ &= \frac{Z_0}{12\pi} \frac{q^4 \gamma^2 B_0^2}{m^2}, \end{aligned} \quad (21.16)$$

where we used $\int_0^\infty (1+x^2)(1+x)^{-5} dx = \frac{1}{3}$. If we replace in this expression the square of the amplitude of the magnetic field B_0^2 by the averaged over length $\langle B^2 \rangle$, $B_0^2 \rightarrow 2\langle B^2 \rangle$ and compare it with the intensity of the synchrotron radiation (20.32) (remembering that $\rho = \gamma mc/qB$), we find that they are equal. Hence the radiated power from the undulator, per unit time, is equal to the radiated power from a bending magnet with the same averaged square of the magnetic field.

Problem 21.1. Integrate Eq. (21.14) over ϕ and find $d\mathcal{I}/d\theta$. Using the relation (21.10) between the frequency and the angle show that the intensity of the radiation per unit frequency is

$$\frac{d\mathcal{P}}{d\omega} = \frac{3\mathcal{P}_0}{\omega_0} \frac{\omega}{\omega_0} \left(2 \left(\frac{\omega}{\omega_0} \right)^2 - 2 \left(\frac{\omega}{\omega_0} \right) + 1 \right), \quad (21.17)$$

for $\omega < \omega_0$ and zero for $\omega > \omega_0$. The plot of this function is shown in Fig. 21.2.

21.3 Effects of finite length of the undulator

Taking now into account the finite length of the undulator, we will assume that the number of periods in the undulator N_u is large, $N_u \gg 1$. As was pointed out in the previous section, the finite number of periods in the undulator results in a non-zero width of the spectrum of the radiation. The shape of the spectrum can be rather easily established if one looks at the time dependence of the electric field in the radiation pulse. An example of such pulse is shown in Fig. 21.3.

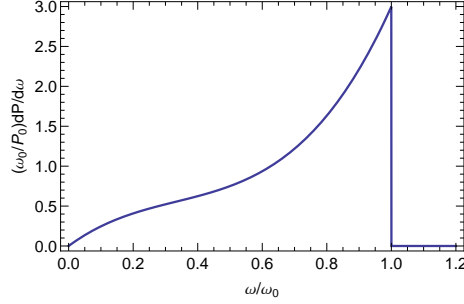


Figure 21.2: The spectrum of the undulator radiation given by Eq. (21.17).

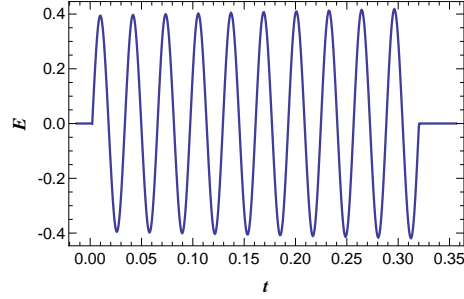


Figure 21.3: Electric field versus time (in arbitrary units) for an undulator radiation with $N_u = 10$, $K = 0.1$ and $\gamma = 10$.

One can see that the pulse in this case is a piece of a sinusoidal function with the number of oscillations equal to the number of periods in the undulator. As is well known, the spectrum of a truncated sinusoidal pulse is given by the sinc function which has a width in relative frequency of the order of $1/N_u$. It is not surprising that the delta function in (21.15) is now replaced the the square (because the power is proportional to the electric field squared) of the sinc function:

$$\frac{d\mathcal{P}}{d\Omega d\omega} = \frac{d\mathcal{P}}{d\Omega} \frac{\sin(\pi N_u \Delta\omega/\omega_1(\theta))^2}{\pi^2 N_u \Delta\omega^2/\omega_1(\theta)}, \quad (21.18)$$

where $\Delta\omega = \omega - \omega_1(\theta)$ and we introduced the notation

$$\omega_1(\theta) = \frac{2\gamma^2 k_u c}{1 + \gamma^2 \theta^2}. \quad (21.19)$$

The total energy radiation from the length of the undulator is obtained by

multiplying the power by the time of flight, equal, for a relativistic particle, to L_u/c where $L_u = 2\pi N_u/k_u$ is the length of the undulator.

21.4 Wiggler radiation for $K \gtrsim 1$

In principle, undulator radiation for large K can be derived using the same approach as for $K \ll 1$ case—the Lorentz transformation from the particle's frame. However, calculations become much more involved in the limit $K \gtrsim 1$. We limit our discussion here by some simple observations of several characteristic feature of the radiation in this case.

First, we need to calculate the averaged velocity \bar{v}_z of the particle along the z -axis when K is not small. This is the velocity of reference frame in which the particle, on average, remains at rest. The x velocity can be found from Eq. (21.3)

$$v_x = \frac{dx}{dt} = -\frac{Kc}{\gamma} \sin(k_u ct), \quad (21.20)$$

which gives

$$v_z = \sqrt{v^2 - v_x^2} \approx v \left(1 - \frac{v_x^2}{2c^2}\right) = v \left(1 - \frac{K^2}{2\gamma^2} \sin^2(k_u ct)\right). \quad (21.21)$$

Averaging over time, we obtain

$$\bar{v}_z = v \left(1 - \frac{K^2}{4\gamma^2}\right). \quad (21.22)$$

When we make the Lorentz transformation we now need to use this velocity. Assuming $K \ll \gamma$, we see that it is still close to the speed of light, but the gamma factor corresponding to this velocity might be very different from the original γ :

$$\begin{aligned} \gamma_z &= \frac{1}{\sqrt{1 - \bar{v}_z^2/c^2}} \approx \left[1 - \frac{v^2}{c^2} \left(1 - \frac{K^2}{2\gamma^2}\right)\right]^{-1/2} \approx \left(1 - \frac{v^2}{c^2} + \frac{K^2}{2\gamma^2}\right)^{-1/2} \\ &= \left(\frac{1}{\gamma^2} + \frac{K^2}{2\gamma^2}\right)^{-1/2} = \frac{\gamma}{\sqrt{1 + K^2/2}}. \end{aligned} \quad (21.23)$$

In the frequency dependence in this case given by (21.10) we need to replace γ by γ_z with the result

$$\omega = \frac{2\gamma_z^2 k_u c}{1 + \gamma_z^2 \theta^2} = \frac{2\gamma^2 k_u c}{1 + K^2/2 + \gamma^2 \theta^2}. \quad (21.24)$$

In particular, for $\theta = 0$, that is on the axis,

$$\omega_0 = \frac{2k_u c \gamma^2}{1 + K^2/2}. \quad (21.25)$$

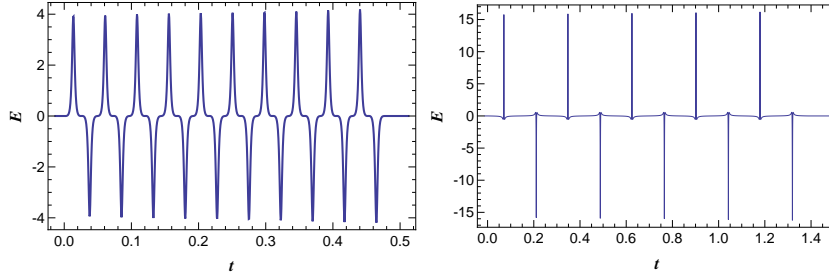


Figure 21.4: Electric field versus time (in arbitrary units) for an undulator radiation with $K = 1$ (left panel) and $K = 4$ (right panel). The undulator has 10 periods, the relativistic factor is $\gamma = 10$.

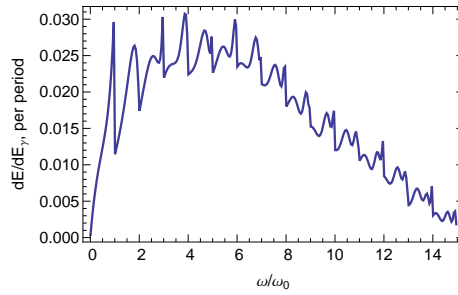


Figure 21.5: Undulator spectrum for $K = 4$ on the axis (in the limit $N_u \gg 1$). The frequency ω_0 is given by Eq. (21.25).

This, however, is not the maximal frequency of the radiation as it used to be in the case $K \ll 1$. The reason for that is illustrated by Fig. 21.4. One can see that increasing the value of K makes each spike of the electric field narrow which leads to rich content of *high harmonics* in the radiation spectrum. Indeed, Fig. 21.5 shows the undulator spectrum on the axis in the case $K = 4$.

More details on the undulator (and synchrotron) radiation can be found in Ref. [18].

Lecture 22

Transition and diffraction radiation

Transition radiation occurs when a moving charged particle crosses a boundary of two media with different electrodynamic properties. In its simplest form, most often used in the experiment, transition radiation is generated by sending a beam through a metallic foil. In this lecture we derive the spectrum and angular distribution of the transition radiation for the normal incidence of the particle. We also discuss radiation generated by the beam when passing through a hole in a metal foil—a so called diffraction radiation.

22.1 Transition radiation

We will calculate the transition radiation for the case when a point charge hits a plane metal surface moving with a constant velocity v in the direction perpendicular to the surface as shown in Fig. 22.1a. We choose the coordinate

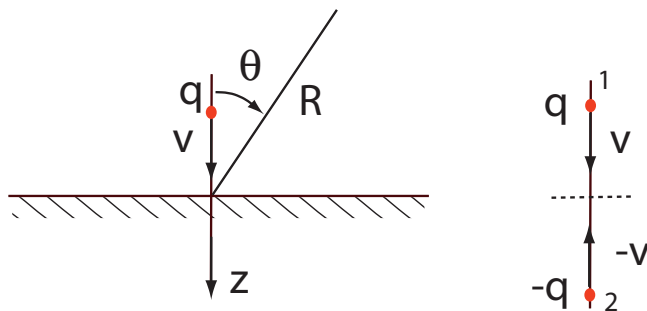


Figure 22.1: A charge moving perpendicular to the metal surface and the image charge.

system with the origin located at the entrance to the metal in such a way that the particle is moving along the z axis in positive direction. The metal occupies the region $z > 0$ and the plane $z = 0$ coincides with the surface of the metal.

Assuming perfect conductivity of the metal, in order to find the electromagnetic field in the system, we need to solve Maxwell's equations with the boundary condition of zero tangential electric field on the surface of the metal. However, for this particular problem, one can avoid solving Maxwell's equation by invoking the method of image charges. The method is based on replacement of the metal with an image charge of an opposite sign, moving with the velocity v in the opposite direction, as shown in Fig. 22.1b. In what follows we will mark the original charge q by index 1, and the image charge $-q$ by index 2. It is easy to verify that in this case the boundary conditions $E_x = E_y = 0$ in the plane $z = 0$ are satisfied automatically. The charges move until they collide at point O at time $t = 0$, where they annihilate. At time $t > 0$ there are no charges in the system.

While we assume that the metal occupies the half-space $z > 0$, we would obtain the same result in the case of a metal slab, $h > z > 0$, where h is the thickness of the slab. This follows from the fact that the boundary condition for the electric field remains the same no matter how thick the slab is (of course, assuming perfect conductivity of the metal).

The trajectories of particles 1 and 2 for $t < 0$ are given by $\mathbf{r}_1(t) = (0, 0, vt)$ and $\mathbf{r}_2(t) = (0, 0, -vt)$ respectively. We also need to define the retarded times for both particles, $t_{\text{ret}}^{(1)}$ and $t_{\text{ret}}^{(2)}$. They satisfy equations $c(t - t_{\text{ret}}^{(1)}) = |\mathbf{R} - \mathbf{r}_1(t_{\text{ret}}^{(1)})|$ and $c(t - t_{\text{ret}}^{(2)}) = |\mathbf{R} - \mathbf{r}_2(t_{\text{ret}}^{(2)})|$ correspondingly (see (18.1)), again for $t_{\text{ret}}^{(1)} < 0$ and $t_{\text{ret}}^{(2)} < 0$. Note that the moment $t_{\text{ret}}^{(1)} = t_{\text{ret}}^{(2)} = 0$ corresponds to $t = R/c$; we will use this observation below.

As always, to calculate the radiation, we need to find the vector potential \mathbf{A} at the observation point. It is easy to do this in our case: for $t_{\text{ret}}^{(1)} < 0$ and $t_{\text{ret}}^{(2)} < 0$ this is the potential corresponding to two charges, and for $t_{\text{ret}}^{(1)} > 0$ and $t_{\text{ret}}^{(2)} > 0$, when there are no charges in the system, $\mathbf{A} = 0$. As noted above $t_{\text{ret}} = 0$ corresponds to $t = R/c$, hence, for $t < R/c$ we can use Eq. (18.8)

$$\mathbf{A} = \frac{Z_0}{4\pi} \left(\boldsymbol{\beta} \frac{q}{R_1(t_{\text{ret}}^{(1)})(1 - \boldsymbol{\beta} \cdot \mathbf{n}_1)} + (-\boldsymbol{\beta}) \frac{(-q)}{R_2(t_{\text{ret}}^{(2)})(1 + \boldsymbol{\beta} \cdot \mathbf{n}_2)} \right) h \left(\frac{R}{c} - t \right), \quad (22.1)$$

where h is the step function, and

$$\begin{aligned} R_1(t) &= \sqrt{(z - vt)^2 + x^2 + y^2}, \\ R_2(t) &= \sqrt{(z + vt)^2 + x^2 + y^2}. \end{aligned} \quad (22.2)$$

Since we observe radiation at large distance from the metal, we can neglect the difference between \mathbf{n}_1 and \mathbf{n}_2 and assume that they both are equal to the unit vector \mathbf{n} directed from the origin of the coordinate system to the observation

point. The magnetic field of the radiation is given by

$$\mathbf{B} = -\frac{1}{c} \mathbf{n} \times \frac{\partial \mathbf{A}}{\partial t}, \quad (22.3)$$

(see Eq. (19.9)). When we differentiate Eq. (22.1) with respect to time, we only need to differentiate the function h —differentiating R_1 and R_2 would give a field that decays faster than $1/R$ (this would actually be the static fields of the moving charges). The result is

$$\mathbf{B} = \frac{Z_0 q}{4\pi c} \delta\left(\frac{R}{c} - t\right) \left(\frac{1}{R_1(0)(1 + \beta \cos \theta)} + \frac{1}{R_2(0)(1 - \beta \cos \theta)} \right) \mathbf{n} \times \boldsymbol{\beta}, \quad (22.4)$$

where the angle θ is defined in Fig. 22.1. Because of the the delta function factor, the values of R_1 and R_2 in this equation are taken at the retarded time $t_{\text{ret}} = 0$:

$$R_1(0) = R_2(0) = \sqrt{z^2 + x^2 + y^2} = R, \quad (22.5)$$

which gives

$$\mathbf{B} = \frac{Z_0 2q}{4\pi Rc} \delta\left(\frac{R}{c} - t\right) \frac{\mathbf{n} \times \boldsymbol{\beta}}{1 - \beta^2 \cos^2 \theta}. \quad (22.6)$$

We see that the radiation field is an infinitely thin spherical shell propagating from the point of entrance to the metal. Since the Fourier transform of the delta function is a constant, we conclude that the spectrum of the radiation does not depend on frequency.

Problem 22.1. Draw a picture of field lines at time $t > 0$.

The spectrum of radiation is given by Eq. (20.16) with

$$\tilde{\mathbf{B}}(\omega) = \int_{-\infty}^{\infty} dt \mathbf{B}(t) e^{i\omega t} = \frac{Z_0 2q e^{i\omega R/c}}{4\pi Rc} \frac{\mathbf{n} \times \boldsymbol{\beta}}{1 - \beta^2 \cos^2 \theta}. \quad (22.7)$$

For the angular distribution of the spectral power we have

$$\frac{d^2 \mathcal{W}}{d\omega d\Omega} = \frac{c^2 R^2}{\pi Z_0} |\tilde{\mathbf{B}}(\omega)|^2 = \frac{Z_0 q^2}{4\pi^3} \frac{\beta^2 \sin^2 \theta}{(1 - \beta^2 \cos^2 \theta)^2}. \quad (22.8)$$

It follows from this equation that for a relativistic particle the dominant part of the radiation goes in the backward direction. Using $\beta^2 = 1 - \gamma^{-2}$ and approximating $\sin \theta \approx \theta$ and $\cos^2 \theta \approx 1 - \theta^2$ we find

$$\frac{d^2 \mathcal{W}}{d\omega d\Omega} \approx \frac{Z_0 q^2}{4\pi^3} \frac{\theta^2}{(\gamma^{-2} + \theta^2)^2}. \quad (22.9)$$

Plot of this function is shown in Fig. 22.2—the maximum intensity of the radiation is emitted at angle $\theta = 1/\gamma$, while the intensity is zero at $\theta = 0$.

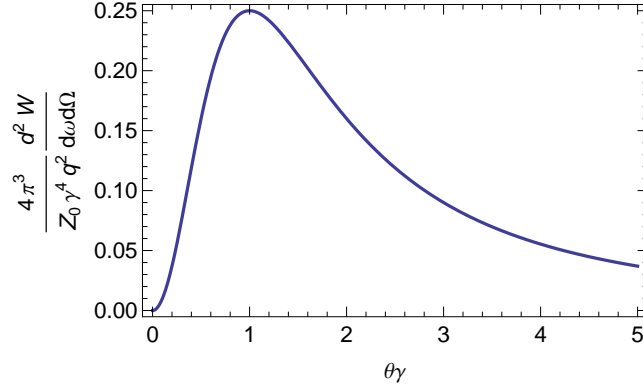


Figure 22.2: Angular distribution of transition radiation for a relativistic particle.

One can integrate Eq. (22.8) over all angles to find the spectrum of the transition radiation

$$\frac{dW}{d\omega} = 2\pi \int_{\pi/2}^{\pi} \sin \theta d\theta \frac{d^2 \mathcal{P}}{d\omega d\Omega} = \frac{Z_0 q^2}{4\pi^2} \left[\left(\frac{1}{\beta} + \beta \right) \operatorname{arctanh}(\beta) - 1 \right]. \quad (22.10)$$

We see that the spectrum of the radiation does not depend on the frequency. Formally, integrating over ω from zero to infinity, we will find that the total radiated energy diverges. In reality, the energy is finite because at very high frequencies metals lose their capability of being perfect conductors, and the transition radiation subsides.

Problem 22.2. *The usual setup in the experiment for the optical transition radiation (OTR) diagnostic is shown in Fig. 22.3: the beam passes through a metal foil tilted at the angle 45 degrees relative to the beam orbit. Show that in this case the radiation propagates predominantly in the direction perpendicular to the orbit. How to solve this problem using the method of image charges?*

As indicated in the problem above transition radiation is often used in accelerators for observation of the transverse size and position of the beam when it is intercepted by a metal foil.

22.2 Diffraction radiation

Interception of the beam with a foil either destroys it or deteriorates the beam properties. Sometimes one would like to generate radiation without strongly perturbing the beam. This can be achieved if the beam passes through a hole

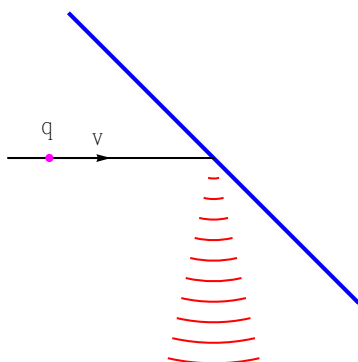


Figure 22.3: Transition radiation with foil tilted at 45 degrees.

in a metal foil as shown in Fig. 16.5—a so called *diffraction radiation*. The radiation properties depend on the size and the shape of the hole. The complete electromagnetic solution of the radiation problem in this case requires methods which are beyond the scope of this course. Below we will present some results of such a solution and show connection of the diffraction radiation with the transition one.

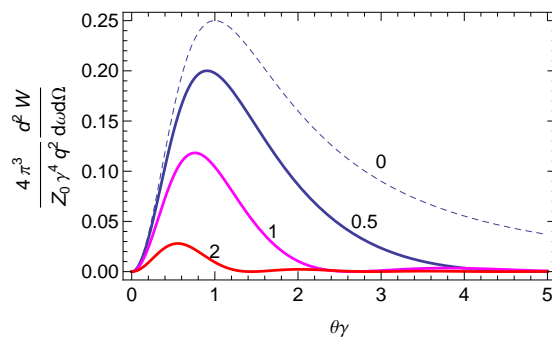


Figure 22.4: Angular distribution of the diffraction radiation for various values of the parameter $a\omega/c\gamma$ (indicated by numbers near the curves). The dashed line shows the limit $a \rightarrow 0$, corresponding to the case of the transition radiation.

It can be shown (see, e.g., [19]) that in the limit $\gamma \gg 1$ and $\theta \ll 1$ the angular

spectral distribution of the diffraction radiation is given by the following formula

$$\frac{d^2\mathcal{W}}{d\omega d\Omega} \approx \frac{Z_0 q^2}{4\pi^3} \frac{\theta^2}{(\gamma^{-2} + \theta^2)^2} F\left(\frac{\omega a \theta}{c}, \frac{\omega a}{c\gamma}\right), \quad (22.11)$$

where

$$F(x, y) = \left(y J_2(x) K_1(y) - \frac{y^2}{x} J_1(x) K_2(y) \right)^2, \quad (22.12)$$

with $J_{1,2}$ the Bessel functions and $K_{1,2}$ the modified Bessel functions.

Note first that in the limit $a \rightarrow 0$ the function $F \rightarrow 1$ and we recover the result of the transition radiation (22.9). The hole has a small effect on the transition radiation at a given frequency ω if it is small, $a \ll c\gamma/\omega$. In Fig. 22.4 we plot the spectral intensity of the radiation as a function of the angle θ for several values of the parameter $a\omega/c\gamma$.

Lecture 23

Formation length of radiation and coherent effects

It takes some volume of free space for a particle to generate radiation. In this lecture we estimate the longitudinal and transverse size of this volume for the synchrotron radiation. We then analyze the radiation of a bunch of particles.

23.1 Longitudinal formation length

It takes some time and space for a moving charge to generate radiation. Let's take a closer look at the derivation in Section 20.1 and try to figure out what fraction of the length of the orbit is involved into the formation of the synchrotron pulse.

In Eq. (20.10) the variable $\xi = c\tau/\rho$ is related to the retarded time τ . We saw that the characteristic width of the electromagnetic pulse in ξ variable is $\Delta\xi \sim \gamma^{-1}$, which corresponds to the time duration $\tau \sim \rho/c\gamma$. Hence the length of the orbit necessary for formation of the radiation pulse, which we call the *formation length*, l_f is

$$l_f \sim c\tau \sim \frac{\rho}{\gamma}. \quad (23.1)$$

How does this formation length agree with the duration of the radiation pulse of the order of $\rho/c\gamma^3$? Since the charge is moving with the velocity $v \approx c(1 - 1/2\gamma^2)$, the relative velocity between the charge and the electromagnetic field is $\Delta v \sim c/\gamma^2$, and during the formation time τ the field propagates away from the charge at the distance $\Delta v\tau \sim \rho/c\gamma^3$, which is the duration of the pulse.

The practical importance of the formation length is that one has to have the length of the bending magnet several times longer than l_f in order to generate the full spectrum of the synchrotron radiation. Radiation from a magnet

that is shorter than l_f has very different properties than what we calculated in Lecture 20.

Some of the properties of radiation from a short magnet can be easily explained using the time profile of the radiation pulse. Let us assume that the angular extension of the circular part of the orbit is limited by $\varphi_{\min} < \varphi < \varphi_{\max}$, and outside of the arc the particle is moving along straight lines (tangential to the end points of the arc) with constant velocity. Since there is no acceleration on the straight parts of the orbit, the radiation pulse shown in Fig. 20.2 will be truncated: the value of the radiation field \hat{B} becomes zero for $\omega\tau < \varphi_{\min}$ and $\varphi_{\max} < \omega\tau$, while it remains the same for the points on the arc where $\varphi_{\min} < \omega\tau < \varphi_{\max}$. Remembering the relation $\zeta = \gamma\omega\tau$, we conclude that the radiation pulse for a short magnet is given by the same Eqs. (20.11), where ζ now is constrained by $\varphi_{\min}/\gamma < \zeta < \varphi_{\max}/\gamma$. An example of the pulse shape for $\varphi_{\min}/\gamma = -0.5$ and $\varphi_{\max}/\gamma = 0.7$ is shown in Fig. 23.1. The discontinuities of

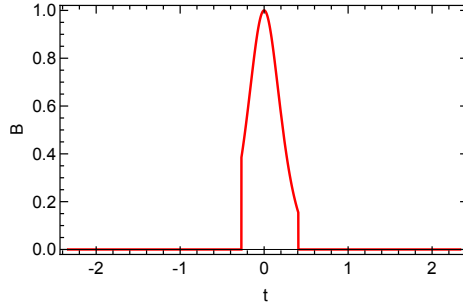


Figure 23.1: The radiation pulse of the electromagnetic field for a short magnet with $\varphi_{\min}/\gamma = -0.5$ and $\varphi_{\max}/\gamma = 0.7$.

the field at the front and the tail of the pulse generate so called edge radiation¹ and lead to increased intensity at small frequencies.

More subtle, but practically important, question is what formation length is needed for radiation of the frequency $\omega \ll \omega_c$? In order to answer it we need to analyze Eq. (20.19) and to find out what is the integration length $\Delta\xi$ that contributes to the integral for given ω . We first note that for $\omega \ll \omega_c$ one can neglect the term with γ^{-2} in the exponent, and the integral becomes

$$\int_{-\infty}^{\infty} \xi e^{i(\omega\rho/2c)(\xi^3/3)} d\xi, \quad (23.2)$$

from which it follows that $\Delta\xi \sim (c/\omega\rho)^{1/3}$. When ξ is much larger than this quantity, the function $e^{i\omega\rho\xi^3/6c}$ begins to rapidly oscillate, and the contribution to the integral from this region is small. The corresponding formation length is

$$l_f(\omega) \sim \rho\Delta\xi \sim \rho^{2/3}\lambda^{1/3}, \quad (23.3)$$

¹In reality, the abrupt changes of the field will be somewhat smeared out due to finite extension of the edge magnetic field at the entrance to and the exit from the magnet.

where $\lambda = c/\omega$. For the critical frequency $\omega = \omega_c$ this formula gives us the previous expression (23.1).

If we use the result of the Problem on page 162 that the angular spread of the synchrotron oscillations at frequency $\omega \ll \omega_c$ is of order $\Delta\psi \sim (\lambda/\rho)^{1/3}$, we then can write the formation length as

$$l_f \sim \frac{\lambda}{\Delta\psi^2}. \quad (23.4)$$

Problem 23.1. Find the vector potential for the radiation from a magnet of length $L \ll \rho/\gamma$. Hint: introduce the bending angle θ and consider the passage through the magnet as an instantaneous change in the direction of motion of the particle (see the transition radiation derivation).

In quantum language, the formation length gives time for a virtual photon carried by the electromagnetic field of a particle to free from the charge and become a real photon.

23.2 Transverse coherence length

In addition to the requirement of having a necessary length of the path, the charge also needs some space in the direction perpendicular to the orbit to form radiation. We can estimate the extension of this space if we note that the angular spread $\Delta\psi$ of radiation involves a transverse wave vector component $k_\perp \sim k\Delta\psi$. The field with k_\perp cannot be squeezed into space smaller than k_\perp^{-1} , hence the minimal transverse size needed for formation of the radiation is

$$l_\perp \sim \frac{\lambda}{\Delta\psi} \sim \rho^{1/3} \lambda^{2/3}. \quad (23.5)$$

We will call this transverse size the *transverse coherence length*.

An interesting connection of l_\perp to properties of Gaussian beams can be made if we recall the results of Section 17.2. Note that far from the focus the electromagnetic field of a Gaussian beam falls off inversely with the distance and can locally be considered as a plane wave. If a Gaussian beam has the angular spread θ , then the minimal transverse size of the beam w_0 (at the focal point) is of the order of λ/θ . We now make an analogy between the radiation in the far zone and a Gaussian laser beam with the focal point of the laser beam being an analog of the point on the charge's trajectory where the radiation comes from. From this analogy, using Eq. (17.21) for the transverse size of the laser beam at the focal point, we conclude that l_\perp is equivalent to the waist size w_0 .

Note also that in our analogy the formation region l_f corresponds to the Rayleigh length Z_R .

The practical importance of the transverse coherence is that the radiation can be suppressed by metal walls, if they are put close to the beam. More specifically, if the beam propagates through a dipole magnet in a metal pipe of radius a , then the radiation with wavelength $\lambda \gtrsim \sqrt{a^3/\rho}$ is suppressed. This

is called a *shielding* effect and it is important for suppression of undesirable coherent radiation of short bunches.

To give a quantitative illustration of the shielding effect, in Fig. 23.2 we plot the suppression factor for synchrotron radiation when a particle is moving (on a circular orbit) between two parallel perfectly conducting plates in the plane equally removed from each plate. The distance between the plates is $2h$. Detailed calculations of the shielded synchrotron radiation can be found in

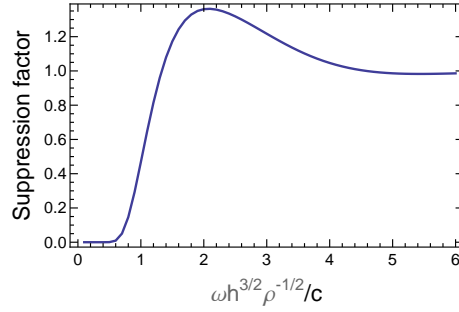


Figure 23.2: Suppression factor for the intensity of the synchrotron radiation for the case of parallel conducting plates as a function of frequency.

Ref. [20].

The result shown in Fig. 23.2 is valid in the limit of small frequencies, when the free space radiation is given by Eq. ((20.30a)). Note that the horizontal axis in the plot is $\omega h^{3/2} \rho^{-1/2} / c \sim (h/l_{\perp})^{3/2}$, and one can see that the suppression factor approaches zero when h becomes much smaller than l_{\perp} .

23.3 Coherent radiation

We now consider radiation of a bunch of particles. First, we neglect the transverse size of the bunch and take into account the longitudinal distribution. So we assume a filament bunch with the longitudinal distribution given by the function $\lambda(s)$. This function gives the probability for a particle to be located at s ; it is normalized so that $\int \lambda(s) ds = 1$.

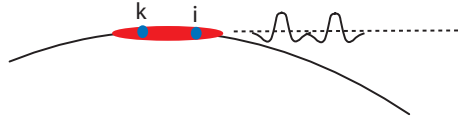


Figure 23.3: Two particles in a bunch emit separate pulses of electromagnetic radiation.

Let each particle in a bunch radiate an electromagnetic pulse as shown in Fig. (23.3). The magnetic field of the pulse at the observation point is $B(t)$ (for synchrotron radiation the function $B(t)$ is calculated in Section 20.1). The Fourier transform of this field is

$$\tilde{B}(\omega) = \int_{-\infty}^{\infty} dt B(t) e^{i\omega t}. \quad (23.6)$$

The field radiated by the bunch is sum of pulses

$$\mathcal{B}(t) = \sum_{i=1}^N B(t - t_i), \quad (23.7)$$

where $t_i = s_i/c$ with s_i the position of the particle i in the bunch, and N is the total number of particles in the bunch. The Fourier image of this field is

$$\tilde{\mathcal{B}}(\omega) = \int dt \mathcal{B} e^{i\omega t} = \sum_{i=1}^N \int dt B(t - t_i) e^{i\omega t} = \sum_{i=1}^N \tilde{B}(\omega) e^{i\omega t_i}. \quad (23.8)$$

The spectral intensity of the radiation is proportional to $|\tilde{\mathcal{B}}(\omega)|^2$ (see Eq. (20.16))

$$\begin{aligned} |\tilde{\mathcal{B}}(\omega)|^2 &= \left| \sum_{i=1}^N \tilde{B}(\omega) e^{i\omega t_i} \right|^2 = |\tilde{B}(\omega)|^2 \left(N + \sum_{i \neq k} e^{i\omega(t_i - t_k)} \right) \\ &= N |\tilde{B}(\omega)|^2 + 2 |\tilde{B}(\omega)|^2 \sum_{i < k} \cos \left(\omega \frac{s_i - s_k}{c} \right). \end{aligned} \quad (23.9)$$

The first term in the last equation is the *incoherent* radiation—it is proportional to the number of particles in the beam. The second one is the *coherent* radiation term. The number of terms in the last sum is $N(N-1)/2 \approx N^2/2$. Instead of doing summation we can average $\cos(\omega(s_i - s_k)/c)$ assuming that s_i and s_k are distributed with the probability given by $\lambda(s)$:

$$\begin{aligned} 2 \sum_{i < k} \cos \left(\omega \frac{s_i - s_k}{c} \right) &\approx N^2 \int ds' ds'' \lambda(s') \lambda(s'') \cos \left(\omega \frac{s' - s''}{c} \right) \\ &= N^2 F(\omega), \end{aligned} \quad (23.10)$$

where the *form factor* $F(\omega)$ is

$$F(\omega) = \int ds' ds'' \lambda(s') \lambda(s'') \cos \left(\omega \frac{s' - s''}{c} \right), \quad (23.11)$$

and

$$\left. \frac{d\mathcal{W}}{d\omega} \right|_{\text{bunch}} = \frac{d\mathcal{W}}{d\omega} (N + N^2 F(\omega)). \quad (23.12)$$

Eq. (23.11) can also be written as

$$F(\omega) = \left| \int_{-\infty}^{\infty} ds \lambda(s) e^{i\omega s/c} \right|^2, \quad (23.13)$$

which is easily established by writing the square of the absolute value as a product of the integral $\int_{-\infty}^{\infty} ds \lambda(s) e^{i\omega s/c}$ with its complex conjugate. Eq. (23.13) shows that the form factor is equal to the square of the absolute value of the Fourier transform of the longitudinal distribution function of the beam.

For the Gaussian distribution function

$$\lambda(s) = \frac{1}{\sqrt{2\pi}\sigma_z} e^{-s^2/2\sigma_z^2}, \quad (23.14)$$

we have

$$F(\omega) = e^{-(\omega\sigma_z/c)^2}. \quad (23.15)$$

We see that for the reduced wavelengths longer than the bunch length, $\lambda \gtrsim \sigma_z$, the power scales as the number of particles squared. This radiation by a factor of N is larger than the *incoherent* radiation. For a bunch with $N \sim 10^{10}$ this makes a huge difference! However, this radiation can only occur at long wavelengths, and those are in many cases shielded by the walls.

23.4 Effect of the transverse size of the beam

We considered the above radiation in the longitudinal direction. We now take into account the radiation at an angle and consider a 3D distribution of the beam. The 3D distribution function is $\lambda(\mathbf{r})$ normalized so that $\int d^3r \lambda(\mathbf{r}) = 1$. From Fig. 23.4 it is seen that the delay between pulses radiated by the central

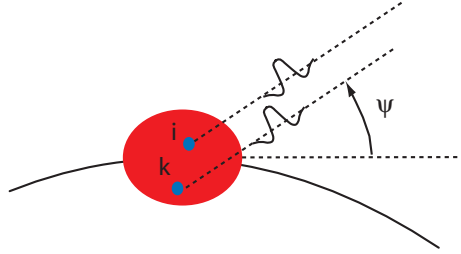


Figure 23.4: Radiation of particles in a bunch.

particle and a particle located at position \mathbf{r} in the bunch is equal to $\Delta t = (\mathbf{r}_i - \mathbf{r}_k) \cdot \mathbf{n}/c$. The field (23.9) can now be written as

$$|\tilde{\mathcal{B}}(\omega, \mathbf{n})|^2 = N|\tilde{B}(\omega, \mathbf{n})|^2 + 2|\tilde{B}(\omega, \mathbf{n})|^2 \sum_{i < k} \cos\left(\omega \frac{\mathbf{n} \cdot (\mathbf{r}_i - \mathbf{r}_k)}{c}\right), \quad (23.16)$$

which gives for the form factor

$$F(\omega, \mathbf{n}) = \int d^3r' d^3r'' \lambda(\mathbf{r}') \lambda(\mathbf{r}'') \cos\left(\omega \frac{\mathbf{n} \cdot (\mathbf{r}' - \mathbf{r}'')}{c}\right). \quad (23.17)$$

Similar to transition from (23.11) to (23.13) one can show that (23.17) can be written as

$$F(\omega, \mathbf{n}) = \left| \int d^3r \lambda(\mathbf{r}) e^{i\omega \mathbf{n} \cdot \mathbf{r}/c} \right|^2, \quad (23.18)$$

that is the square of the absolute value of the three dimensional Fourier transform of the distribution function.

We can now calculate the form factor due to the transverse size of the beam. We will find that the coherent radiation is suppressed if

$$\sigma_r > \lambda/\psi, \quad (23.19)$$

that is if the transverse size of the beam is larger than the transverse coherence size.

Problem 23.2. Calculate the integral Eq. (23.17) for a “pancake” distribution

$$\lambda(\mathbf{r}) = \delta(z) \frac{1}{2\pi\sigma_r^2} e^{-(x^2+y^2)/2\sigma_r^2}. \quad (23.20)$$

The vector \mathbf{n} is directed at angle ψ to the z axis.

Lecture 24

Synchrotron radiation reaction force

We compute the synchrotron radiation reaction force of a relativistic particle and show, by explicit calculations for a Gaussian bunch, that the work of this force is equal to the energy radiated per unit time.

24.1 Radiation reaction force for a relativistic charge

When a bunch of charged particle emits radiation, the energy of the electromagnetic field is taken from its kinetic energy. The energy balance in the process is maintained through a force that acts in the direction opposite to the velocity of the bunch. This force is called the *radiation reaction force*. We talked about this force in Lecture 19 for a nonrelativistic motion. In this lecture we address this issue for the synchrotron radiation of a relativistic charge.

To simplify calculations, we will systematically neglect terms of the order of $1/\gamma$ in our derivation. This means that we consider the limit $\gamma \rightarrow \infty$ and $\beta = 1$. An additional advantage of this approach is that we automatically neglect the longitudinal Coulomb field of the bunch, that is proportional to γ^{-2} (see Section 15.1).

Consider a thin bunch with the distribution function $\lambda(s)$ moving in a circular orbit, where s is the arclength. We first calculate the force with which a radiated point charge acts on a test one located distance s away. We assume $s \ll \rho$ and use the Liénard-Wiechert potentials (18.9)

$$\phi = \frac{1}{4\pi\epsilon_0} \frac{q}{R(1 - \boldsymbol{\beta}_{\text{ret}} \cdot \mathbf{n})}, \quad \mathbf{A} = \frac{Z_0}{4\pi} \frac{q\boldsymbol{\beta}_{\text{ret}}}{R(1 - \boldsymbol{\beta}_{\text{ret}} \cdot \mathbf{n})}, \quad (24.1)$$

and the expression for the fields (1.7)

$$\mathbf{E} = -\nabla\phi - \frac{\partial\mathbf{A}}{\partial t}. \quad (24.2)$$

We introduce the angle $\psi = s/\rho$ as shown in Fig. 24.1 where the arc length s

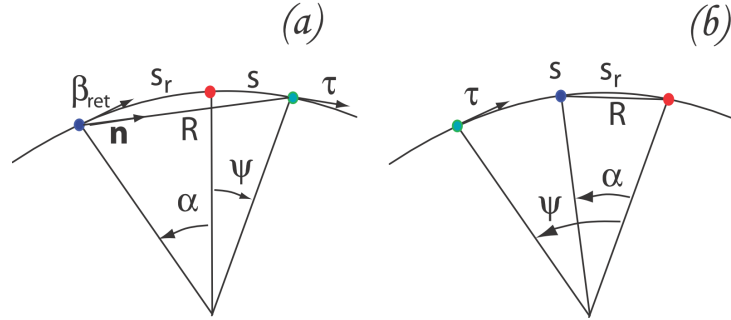


Figure 24.1: CSR wake geometry for positive (a) and negative (b) values of ψ . The red dots show particle's position at the observation time t ; the green dots show the observation points; the blue dots show the position of the particle at the retarded time. For both cases shown in the figure, α is positive, and ψ is positive on the left figure, and negative on the right.

is measured from the *current position* of the charge in the forward. We also introduce the distance s_r from the *current position* of the charge to its retarded position, and the angle $\alpha = s_r/\rho$ as shown in Fig. 24.1. The arc length s_r is measured from the current position of the charge in the backward directions.

With this convention, the positive and negative values of ψ correspond to positions in front of and behind the source particle, respectively; for the angle α , however, the positive values mark positions behind, and the negative values ahead of the charge. We will also use the variable S as an arc length measured from some fixed position on the circle; assuming that the charge moves according to $S = ct$, we have $s = S - ct$.

We are interested in the longitudinal field $E_s = -\partial\phi/\partial S - \partial A_s/\partial t$ where $A_s = \mathbf{A} \cdot \boldsymbol{\tau}$. Note that due to the rotational symmetry of the problem the functions ϕ and A_s depend on the difference $S - ct$ only (remember that we assume $v = c$), and hence

$$E_s = -\frac{\partial(\phi - cA_s)}{\partial s}. \quad (24.3)$$

First we need to solve the equation for the retarded time. The time needed for a particle to move from the radiation point to its current position is equal to $s_r/c = \rho\alpha/c$. It is also equal to the time R/c that the electromagnetic field

takes to propagate along the chord connecting these two points, with

$$R = 2\rho \left| \sin \left(\frac{\alpha + \psi}{2} \right) \right|. \quad (24.4)$$

We have

$$\rho\alpha = R = 2\rho \left| \sin \left(\frac{\alpha + \psi}{2} \right) \right|. \quad (24.5)$$

It turns out that $\alpha + \psi > 0$ for $\psi > 0$ (that is in the case when the observation point is in front of the charge) and, in this case, we can drop the absolute value sign in the above equations. We then expand the right hand side into the Taylor series using the smallness of ψ and α and keeping terms up to the third order,

$$\alpha = \alpha + \psi - \frac{1}{24} (\alpha + \psi)^3. \quad (24.6)$$

We will see in a moment that $\alpha \gg \psi$, so we can approximate $\alpha + \psi \approx \alpha$ in the second term on the left which gives

$$\alpha = (24\psi)^{1/3}. \quad (24.7)$$

Indeed, we now see that for $\psi \ll 1$ we have $\alpha \gg \psi$ and $\alpha + \psi > 0$, as we assumed.

In the case $\psi < 0$ (the observation point is behind the charge), as we will see from the result, $\alpha + \psi < 0$. Eq. (24.5) takes the form

$$\alpha = -2 \sin \left(\frac{\alpha + \psi}{2} \right), \quad (24.8)$$

and using the Taylor expansion we need only to keep the first order terms

$$\alpha \approx -(\alpha + \psi), \quad (24.9)$$

which gives

$$\alpha = -\frac{\psi}{2}. \quad (24.10)$$

We now proceed to the calculation of the field E_s for $\psi > 0$ and calculate the quantity $1 - \boldsymbol{\beta}_{\text{ret}} \cdot \mathbf{n}$. As is seen from Fig. 24.1, the angle between $\boldsymbol{\beta}_{\text{ret}}$ and \mathbf{n} is equal to $(\alpha + \psi)/2$, which gives

$$1 - \boldsymbol{\beta}_{\text{ret}} \cdot \mathbf{n} = 1 - \cos \left(\frac{\alpha + \psi}{2} \right) \approx \frac{\alpha^2}{8}. \quad (24.11)$$

We also have

$$1 - \boldsymbol{\beta}_{\text{ret}} \cdot \boldsymbol{\tau} = 1 - \cos(\alpha + \psi) \approx \frac{\alpha^2}{2}. \quad (24.12)$$

Finally, for the difference of the potentials we have

$$\begin{aligned}\phi - cA_s &= \frac{q}{4\pi\epsilon_0} \frac{1 - \boldsymbol{\beta}_{\text{ret}} \cdot \boldsymbol{\tau}}{R(1 - \boldsymbol{\beta}_{\text{ret}} \cdot \mathbf{n})} \approx \frac{q}{4\pi\epsilon_0} \frac{4}{R} \approx \frac{q}{4\pi\epsilon_0} \frac{4}{\rho\alpha} \\ &\approx \frac{q}{4\pi\epsilon_0} \frac{4}{\rho(24\psi)^{1/3}} = \frac{q}{4\pi\epsilon_0} \frac{2}{\rho^{2/3}(3s)^{1/3}},\end{aligned}\quad (24.13)$$

with the electric field given by the derivative of this expression.

Problem 24.1. Find the difference $\phi - cA_s$ behind the particle ($\psi < 0$) and show that $E_s \approx 0$ in that region. [A more accurate calculation shows that actually $4\pi\epsilon_0 E_s \approx q/8\rho^2$ in that region.]

Using Eq. (24.3) we now find the electric in front of the moving charge

$$E_s = \frac{q}{4\pi\epsilon_0} \frac{2}{3^{4/3}} \frac{1}{\rho^{2/3}s^{4/3}}. \quad (24.14)$$

The longitudinal electric field behind the charge in our approximation is equal to zero.

One often uses a so called *CSR wake field*:

$$w_{\text{CSR}} = -\frac{1}{q} E_s = -\frac{1}{4\pi\epsilon_0} \frac{2}{3^{4/3}} \frac{1}{\rho^{2/3}s^{4/3}}. \quad (24.15)$$

It follows from our result that the electric field has a strong singularity, $\propto s^{-4/3}$, in front of the particle. This is the consequence of our assumption $\beta = 1$. Taking into account the effect of finite γ would show us that our approximation breaks down at the distance $s \sim \rho/\gamma^3$, and the growth of E_s saturates at small distances (see a detailed analysis in [20]). Fig. 24.2 shows the plot of $E_s(0)$ in the vicinity (in front of) the particle. Notice, that the

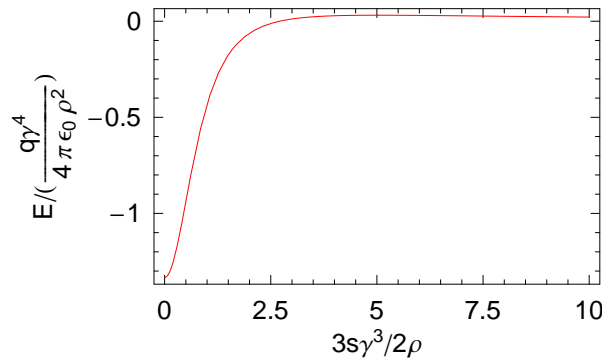


Figure 24.2: The radiation reaction field near the charge; the distance is measured in units of $3\gamma^3/2\rho$, and the field is measured in units of $q\gamma^4/4\pi\epsilon_0\rho^2$.

field changes sign, reaching a negative value at the location of the charge. This negative value is responsible for taking kinetic energy from the particle and translating it into the energy of the radiation.

Problem 24.2. Find the value of $E_s(s)$ using the known intensity of the radiation given by Eq. (20.32). Does it agree with the value shown in Fig. 24.2? If not, explain the discrepancy.

24.2 Radiation reaction field in a bunch of particles

It is important, however, that even using the singular expression (24.13) we can calculate the electric field inside a bunch with a given distribution of particles $\lambda(s)$. The longitudinal electric field of the bunch $\mathcal{E}_s(s)$ is given by the following integral

$$\begin{aligned}
 \mathcal{E}_s(s) &= N \int_{-\infty}^{\infty} E_s(s-s')\lambda(s') ds' \\
 &= -N \int_{-\infty}^s \frac{\partial(\phi - cA_s)}{\partial s} \Big|_{s-s'} \lambda(s') ds' = N \int_{-\infty}^s \frac{\partial(\phi - cA_s)}{\partial s'} \Big|_{s-s'} \lambda(s') ds' \\
 &= -N \int_{-\infty}^s (\phi - cA_s) \Big|_{s-s'} \frac{\partial\lambda(s')}{\partial s'} ds' \\
 &= -\frac{Nq}{4\pi\epsilon_0} \frac{2}{\rho^{2/3}3^{1/3}} \int_{-\infty}^s \frac{1}{(s-s')^{1/3}} \frac{\partial\lambda(s')}{\partial s'} ds', \tag{24.16}
 \end{aligned}$$

where N is the number of particles in the bunch. Let us assume a Gaussian distribution, $\lambda(s) = (2\pi)^{-1/2}\sigma^{-1}e^{-s^2/2\sigma^2}$. The last integral can be computed numerically with the result shown in Fig. 24.3.

As we pointed out at the beginning of the lecture, the longitudinal field keeps the energy balance between the kinetic energy of the particle and the radiation. Let us demonstrate by direct calculation for a Gaussian bunch that this is indeed the case. First we calculate the energy that the beam loses in one turn around the ring

$$\begin{aligned}
 &-Nqc \frac{2\pi\rho}{c} \int_{-\infty}^{\infty} ds \mathcal{E}_s(s)\lambda(s) \\
 &= \frac{N^2q^2\rho^{1/3}}{3^{1/3}\epsilon_0} \int_{-\infty}^{\infty} \lambda(s) ds \int_{-\infty}^s \frac{1}{(s-s')^{1/3}} \frac{\partial\lambda(s')}{\partial s'} ds'. \tag{24.17}
 \end{aligned}$$

We then have to compare this expression with the power of coherent synchrotron radiation. The latter is calculated using the second term in (23.12) in which the

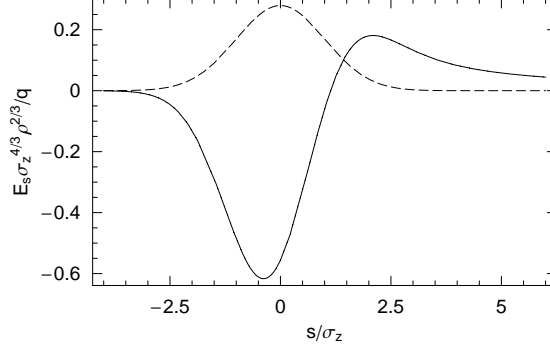


Figure 24.3: CSR field of a Gaussian bunch. The distance is measured in units of σ_z , and the field is measured in units of $Q/\sigma_z^{4/3}\rho^{2/3}$, where Q is the total charge of the bunch.

intensity $d\mathcal{W}/d\omega$ is taken at low frequencies given by Eqs. (20.27) and (20.30a)

$$\begin{aligned} N^2 \int_{-\infty}^{\infty} d\omega F(\omega) \frac{d\mathcal{W}}{d\omega} &= \frac{2}{9} q^2 \gamma Z_0 N^2 \int_{-\infty}^{\infty} d\omega F(\omega) S\left(\frac{\omega}{\omega_c}\right) \\ &= N^2 q^2 \gamma Z_0 \frac{3}{4\pi\omega_c^{1/3}} \frac{\sqrt{3}}{2^{1/3}} \Gamma\left(\frac{5}{3}\right) \int_{-\infty}^{\infty} d\omega e^{-\omega^2 \sigma_z^2 / c^2} \omega^{1/3}. \end{aligned} \quad (24.18)$$

In order to prove that Eq. (24.17) is equal to (24.18) we need to show that

$$3\sqrt{3}\Gamma\left(\frac{5}{3}\right) \int_{-\infty}^{\infty} d\omega e^{-\omega^2} \omega^{1/3} = -2 \int_{-\infty}^{\infty} e^{-s^2/2} ds \int_{-\infty}^s \frac{s' e^{-s'^2/2}}{(s-s')^{1/3}} ds'. \quad (24.19)$$

The easiest way to do this is to compare their numerical values. And, indeed, calculations give that they are both equal to 3.17594966.

Lecture 25

Waveguides and RF cavities

A good conductor has a propensity to guide and trap electromagnetic field in a confined region. In this lecture we will consider an example of a radio frequency (RF) waveguides and cavities, and discuss some of their properties from the point of view of acceleration of charged particles.

25.1 TM modes in cylindrical waveguides

Let us consider a cylindrical waveguide of radius a made from a perfect conductor. Such a waveguide has a number of electromagnetic modes that can propagate in it. We will focus first our attention here on so called *TM modes* that have a nonzero longitudinal component of the electric field E_z , with $B_z = 0$. To find the distribution of the electric field in the waveguide for a mode that has frequency ω , we will assume that in cylindrical coordinates r, ϕ, z ,

$$E_z(r, \phi, z, t) = \mathcal{E}(r)e^{-i\omega t - im\phi + i\kappa z}, \quad (25.1)$$

use Eq. (1.5) for E_z

$$\frac{1}{r} \frac{d}{dr} r \frac{d\mathcal{E}}{dr} - \frac{m^2}{r^2} \mathcal{E} + \left(\frac{\omega^2}{c^2} - \kappa^2 \right) \mathcal{E} = 0. \quad (25.2)$$

The solution of this equation is given by

$$\mathcal{E} = E_0 J_m(k_\perp r), \quad (25.3)$$

where J_m is the Bessel function of m -th order and $k_\perp = c^{-1} \sqrt{\omega^2 - c^2 \kappa^2}$. The boundary condition $E_z = 0$ at $r = a$ requires that $k_\perp r$ be equal to a zero of J_m . For each function J_m there is an infinite sequence of such zeros, which we denote by $j_{m,n}$ with $n = 1, 2, \dots$. Hence $k_\perp = j_{m,n}/a$ and recalling the definition of k_\perp we find that

$$\kappa_{m,n} = \pm \left(\frac{\omega^2}{c^2} - \frac{j_{m,n}^2}{a^2} \right)^{1/2}. \quad (25.4)$$

We see from this equation that in order for a mode with indices m and n to have a real value of \varkappa , its frequency should be larger than the *cut-off frequency* $cj_{m,n}/a$. Then the plus sign defines the modes propagating in the positive direction, and the minus sign corresponds to the modes in the opposite direction. If $\omega < cj_{m,n}/a$, then we deal with *evanescent* modes that exponentially decay along the z -axis (and, correspondingly exponentially grow in the opposite direction). Such modes play important role in formation of localized fields around an obstacle inside a waveguides.

Given $E_z(r, \phi, z, t)$ as defined by (25.1) we can find all other components of the electric and magnetic fields using Maxwell's equations. They will all have the same dependence $e^{-i\omega t - im\phi + i\varkappa z}$ versus time, angle and z . The radial distribution of the four unknown components E_ϕ , E_r , B_ϕ and B_r (remember that $B_z = 0$) are found from the four algebraic equations, which are r and ϕ components of the two vectorial equations $\nabla \times \mathbf{E} = i\omega \mathbf{B}$ and $c^2 \nabla \times \mathbf{B} = -i\omega \mathbf{E}$. Here is the result

$$E_r = E_0 \frac{i\varkappa_{m,n} a}{j_{m,n}} J'_m \left(j_{m,n} \frac{r}{a} \right) e^{-i\omega t - im\phi + i\varkappa_{m,n} z} \quad (25.5)$$

$$E_\phi = -E_0 \frac{m\varkappa_{m,n} a^2}{r j_{m,n}^2} J_m \left(j_{m,n} \frac{r}{a} \right) e^{-i\omega t - im\phi + i\varkappa_{m,n} z} \quad (25.6)$$

$$B_r = E_0 \frac{m\omega a^2}{c^2 r j_{m,n}^2} J_m \left(j_{m,n} \frac{r}{a} \right) e^{-i\omega t - im\phi + i\varkappa_{m,n} z} \quad (25.7)$$

$$B_\phi = E_0 \frac{i\omega a}{c^2 j_{m,n}} J'_m \left(j_{m,n} \frac{r}{a} \right) e^{-i\omega t - im\phi + i\varkappa_{m,n} z}, \quad (25.8)$$

where J'_m is the derivative of the Bessel function of order m and we dropped the indices m, n on the left sides. These modes are designated TM_{mn} or E_{mn} . Note that in addition to vanishing E_z on the wall, which we have satisfied by choosing $k_\perp = j_{m,n}/a$, we should also require $E_\phi = 0$ on the surface of the wall (because it is tangential there). This however is automatically satisfied because the radial dependence of E_ϕ in (25.6) is the same as E_z in (25.3).

Of course the physical meaning has the real parts of Eqs. (25.5). Since the longitudinal wavenumbers (25.4) do not depend on m , the modes with positive and negative values of m (assuming $m > 0$) are degenerate—they have the same values of $\varkappa_{m,n}$. A sum and difference of m and $-m$ modes, which convert $e^{im\phi}$ and $e^{-im\phi}$ into $\cos m\phi$ and $\sin m\phi$, are often used as another choice for the set of fundamental eigenmodes in circular waveguide.

Problem 25.1. Calculate TM modes in a rectangular waveguide with cross section $a \times b$.

25.2 TE modes in cylindrical waveguides

TE modes have nonzero longitudinal magnetic field B_z with $E_z = 0$. There derivation follows closely that of TM modes. However, a simple observation of

special symmetry of Maxwell's equations allows one to obtain the fields in TE modes without any calculation.

Indeed, assuming the time dependence $\propto e^{-i\omega t}$ for all fields, Maxwell's equations in free space are

$$\nabla \times \mathbf{E} = i\omega \mathbf{B}, \quad c^2 \nabla \times \mathbf{B} = -i\omega \mathbf{E}, \quad \nabla \cdot \mathbf{E} = 0, \quad \nabla \cdot \mathbf{B} = 0. \quad (25.9)$$

Note that a transformation

$$(\mathbf{E}, \mathbf{B}) \rightarrow (c\mathbf{B}, -\mathbf{E}/c) \quad (25.10)$$

converts (25.9) into itself. This means that having found a solution of Maxwell's equation one can obtain another solution by means of a simple transformation (25.10). The only problem with this approach is that one has to make sure that the boundary conditions are also satisfied. Remember that in the derivation of TM modes we satisfied the boundary condition by choosing $k_{\perp} = j_{m,n}/a$. Since we now need to satisfy a different boundary condition, we will change the notation and replace $j_{m,n}$ in (25.5)-(25.8) by yet unknown $j'_{m,n}$. Applying the transformation (25.10) to (25.3) and (25.5)-(25.8) we obtain (we also replace E_0 with cB_0)

$$\begin{aligned} B_z &= B_0 J_m \left(j'_{m,n} \frac{r}{a} \right) e^{-i\omega t - im\phi + i\mathcal{K}_{m,n} z} \\ B_r &= B_0 \frac{i\mathcal{K}_{m,n} a}{j_{m,n}} J'_m \left(j'_{m,n} \frac{r}{a} \right) e^{-i\omega t - im\phi + i\mathcal{K}_{m,n} z} \\ B_{\phi} &= -B_0 \frac{m\mathcal{K}_{m,n} a^2}{r j_{m,n}^2} J_m \left(j'_{m,n} \frac{r}{a} \right) e^{-i\omega t - im\phi + i\mathcal{K}_{m,n} z} \\ E_r &= -B_0 \frac{m\omega a^2}{r j_{m,n}^2} J_m \left(j'_{m,n} \frac{r}{a} \right) e^{-i\omega t - im\phi + i\mathcal{K}_{m,n} z} \\ E_{\phi} &= -B_0 \frac{i\omega a}{j_{m,n}} J'_m \left(j'_{m,n} \frac{r}{a} \right) e^{-i\omega t - im\phi + i\mathcal{K}_{m,n} z}. \end{aligned} \quad (25.11)$$

These modes are designated TE_{mn} or H_{mn} . The only tangential component of the electric field on the wall is E_{ϕ} and in order for it to be equal to zero at $r = a$ we require

$$J'_m(j'_{m,n}) = 0, \quad (25.12)$$

which means that $j'_{m,n}$ are the roots of the derivative J'_m of the Bessel function.

Problem 25.2. Follow up on the problem 25.1 and derive TE modes in a rectangular waveguide by applying transformation (25.10) to TM modes and satisfying the boundary conditions on the wall.

25.3 RF modes in cylindrical resonator

Cylindrical resonator is a cylindrical pipe with the ends closed by metallic walls. Various modes of electromagnetic field that can exist in such a resonator are

characterized by their frequency. The resonator modes can be easily obtained from the waveguide modes derived above.

In comparison with waveguides, a resonator requires one more boundary condition—vanishing tangential electric field on the end walls. Let's assume that the resonator left wall is located at $z = 0$, and the right wall is located at $z = L$. Start with TM modes. To satisfy the boundary condition $E_r = E_\phi = 0$ at $z = 0$ we choose two TM modes with the same frequency and the same m and n indices but opposite values of $\varkappa_{m,n}$ (that is two identical waves propagating in the opposite directions) add them and divide the result by 2. Using

$$\begin{aligned}\frac{1}{2}(e^{i\varkappa_{m,n}z} + e^{-i\varkappa_{m,n}z}) &= \cos(\varkappa_{m,n}z), \\ \frac{1}{2}(\varkappa_{m,n}e^{i\varkappa_{m,n}z} - \varkappa_{m,n}e^{-i\varkappa_{m,n}z}) &= i\varkappa_{m,n} \sin(\varkappa_{m,n}z),\end{aligned}\quad (25.13)$$

it is easy to see that both E_r and $E_\phi = 0$ acquire the factor $\sin(\varkappa_{m,n}z)$ and hence satisfy the boundary condition at $z = 0$. In order to satisfy the boundary condition at the opposite wall, at $z = L$, we require $\varkappa_{m,n}L = l\pi$, where $l = 1, 2, \dots$ is an integer number. The result is

$$\begin{aligned}E_z &= E_0 J_m \left(j_{m,n} \frac{r}{a} \right) \cos \left(\frac{l\pi z}{L} \right) e^{-i\omega t - im\phi} \\ E_r &= -E_0 \frac{l\pi a}{L j_{m,n}} J'_m \left(j_{m,n} \frac{r}{a} \right) \sin \left(\frac{l\pi z}{L} \right) e^{-i\omega t - im\phi} \\ E_\phi &= -E_0 \frac{iml\pi a^2}{L r j_{m,n}^2} J_m \left(j_{m,n} \frac{r}{a} \right) \sin \left(\frac{l\pi z}{L} \right) e^{-i\omega t - im\phi} \\ B_r &= E_0 \frac{m\omega a^2}{c^2 r j_{m,n}^2} J_m \left(j_{m,n} \frac{r}{a} \right) \cos \left(\frac{l\pi z}{L} \right) e^{-i\omega t - im\phi} \\ B_\phi &= E_0 \frac{i\omega a}{c^2 j_{m,n}} J'_m \left(j_{m,n} \frac{r}{a} \right) \cos \left(\frac{l\pi z}{L} \right) e^{-i\omega t - im\phi}.\end{aligned}\quad (25.14)$$

Eq. (25.4) should now be interpreted differently: we replace $\varkappa_{m,n}$ by $l\pi/L$, square it, and find the frequency ω of the mode

$$\frac{\omega^2}{c^2} = \pm \left[\left(\frac{l\pi}{L} \right)^2 + \frac{j_{m,n}^2}{a^2} \right]^{1/2}.\quad (25.15)$$

The modes given by (25.14) and (25.15) are called TM_{mnl} modes.

A similar procedure can be done with the TE modes, but instead of adding, we need to subtract the mode with negative $\varkappa_{m,n}$ from the mode with the

positive $\kappa_{m,n}$ and divide the result by $2i$. The result is

$$\begin{aligned}
 B_z &= B_0 J_m \left(j'_{m,n} \frac{r}{a} \right) \sin \left(\frac{l\pi z}{L} \right) e^{-i\omega t - im\phi} \\
 B_r &= B_0 \frac{l\pi a}{L j'_{m,n}} J'_m \left(j'_{m,n} \frac{r}{a} \right) \cos \left(\frac{l\pi z}{L} \right) e^{-i\omega t - im\phi} \\
 B_\phi &= B_0 \frac{iml\pi a^2}{L r j_{m,n}^2} J_m \left(j'_{m,n} \frac{r}{a} \right) \cos \left(\frac{l\pi z}{L} \right) e^{-i\omega t - im\phi} \\
 E_r &= -B_0 \frac{m\omega a^2}{r j_{m,n}^2} J_m \left(j'_{m,n} \frac{r}{a} \right) \sin \left(\frac{l\pi z}{L} \right) e^{-i\omega t - im\phi} \\
 E_\phi &= -B_0 \frac{i\omega a}{j_{m,n}} J'_m \left(j'_{m,n} \frac{r}{a} \right) \sin \left(\frac{l\pi z}{L} \right) e^{-i\omega t - im\phi}.
 \end{aligned} \tag{25.16}$$

The frequency is defined by

$$\frac{\omega^2}{c^2} = \pm \left[\left(\frac{l\pi}{L} \right)^2 + \left(\frac{j'_{m,n}}{a} \right)^2 \right]^{1/2}. \tag{25.17}$$

The modes given by (25.16) and (25.17) are called TE_{mnl} modes.

An important quantity associated with the mode is the energy W of the electromagnetic field. This energy is given by the integral over the volume of the cavity of $(\epsilon_0/2)(E_z^2 + c^2 B_\theta^2)$, where one has to take the real parts of the fields before squaring them.

For illustration, let us calculate the energy of TM_{010} mode. The calculation can be simplified if one notices that although E_z and B_θ depend on time, the energy W does not. Because there is a phase shift of $\pi/2$ between these fields, one can find a moment when $B_\theta = 0$, and then

$$\begin{aligned}
 W &= \frac{\epsilon_0}{2} \int dV |E_z|^2 = \frac{\epsilon_0}{2} \int dV \mathcal{E}^2 \\
 &= \frac{\epsilon_0}{2} \pi E_0^2 a^2 L J_1^2(j_1),
 \end{aligned} \tag{25.18}$$

where we used the property $\int_0^1 J_0^2(bx) x dx = \frac{1}{2} J_1^2(b)$.

Problem 25.3. Consider a point charge passing through a cylindrical cavity where the fundamental mode is excited with amplitude E_0 . Calculate the maximum energy gain for the charge.

Taking into account the finite conductivity of the wall, one finds that an initially excited mode decays with time because its energy is absorbed in the walls. This damping is manifested in appearing of the imaginary part γ in the mode frequency, $\omega = \omega' - i\gamma$, where ω' and γ are real and positive. The imaginary part of the frequency can be calculated with the help of the Leontovich boundary condition.

A related quantity is the *quality factor* Q of the cavity equal to

$$Q = \frac{\omega'}{2\gamma}. \tag{25.19}$$

We will give here without derivation the quality factor for the fundamental mode of the cylindrical cavity

$$Q = \frac{aL}{\delta(a+L)}, \quad (25.20)$$

where δ is the skin depth at the frequency of the cavity. More generally, a crude estimation of the quality factor is $Q \sim l/\delta$, where l is a characteristic size of the cavity (assuming that all dimensions of the cavity are of the same order).

Typical copper cavities used in accelerators have $Q \sim 10^4$; superconducting cavities may have $Q \sim 10^9$.

25.4 Electromagnetic field pressure

It turns out that the electromagnetic field in a cavity exerts a force on the metallic surface of the walls. In the most general formulation this force can be derived from the so called *Maxwell stress tensor*, see [1], Chapter 6.7. In this lecture we will give a simplified treatment of this force.

If electric field lines are terminated on a metal plate as shown in Fig. 25.1, there are image charges on the surface of the metal with the surface density

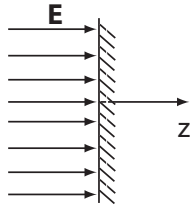


Figure 25.1: Electric field lines are terminated on the metallic surface.

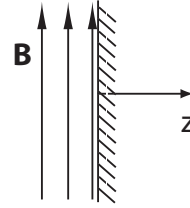


Figure 25.2: Magnetic field lines near the metallic surface.

equal to $\epsilon_0 E_n$, where the subscript n indicates that the field is normal to the surface of the metal. To calculate the force, we need to consider in more detail the distribution of the electric field inside the metal. Let us assume that $z = 0$ corresponds to the surface of the metal, and the metal occupies the region $z > 0$. The charge density inside the metal is given by the function $\rho(z)$, and the electric field is $E_z(z)$. The equation for E_z is

$$\frac{dE_z}{dz} = \frac{\rho(z)}{\epsilon_0}. \quad (25.21)$$

The force per unit area is given by the integral

$$f_z^{(E)} = \int_0^\infty dz \rho E_z. \quad (25.22)$$

If we multiply Eq. (25.21) by E_z and integrate it over z , we find

$$f_z^{(E)} = \epsilon_0 \int_0^\infty dz E_z \frac{dE_z}{dz} = -\frac{\epsilon_0}{2} E_n^2, \quad (25.23)$$

where we took into account that deeply inside the metal $E_z(\infty) = 0$, and on the surface $E_z(0) = E_n$. The minus sign in this equation means that the electric field has a “negative pressure”—it pulls the surface toward the free space.

In a similar fashion, a tangential magnetic field also exerts a force on the surface. To compute it, we assume that the magnetic field $B_y(z)$ is directed along y , and varies along z due to the current $j_x(z)$ flowing in the x direction, see Fig. 25.2. The Maxwell equation

$$\frac{dH_y}{dz} = -j_x \quad (25.24)$$

with the expression for the force per unit area

$$f_z^{(M)} = \int_0^\infty dz j_x B_y \quad (25.25)$$

gives

$$f_z^{(M)} = - \int_0^\infty dz B_y \frac{dH_y}{dz} = \frac{1}{2\mu_0} B_t^2, \quad (25.26)$$

where we took into account that $B_y(\infty) = 0$, and on the surface $B_y(0) = B_n$. We see that $f_z^{(M)}$ is positive—it acts as a real pressure applied to the surface.

Problem 25.1. Estimate the electromagnetic pressure in a cavity with $E = 20$ MV/m.

The effect of the electromagnetic pressure is usually small, however it causes a so called *Lorentz detuning* in modern superconducting cavities which should be compensated by a special control system (see [21], p.580).

25.5 Slater’s formula

The electromagnetic forces derived in the previous section allow us to solve the following problem: what happens to the frequency of a cavity, if its shape is slightly distorted as shown in Fig. 25.3?

To calculate the frequency shift for such a cavity, we first compute the work against the electromagnetic field needed to change the cavity shape. We assume that the distortion of the cavity occurs slowly in comparison with the frequency of the mode. This work, with a proper sign, is equal to the energy change δW of the mode. Since the distortion is small, we can take the unperturbed distribution of the electric and magnetic fields on the surface, compute the sum of the electric and magnetic pressures $f_z^{(E)} + f_z^{(M)}$ and average over the period

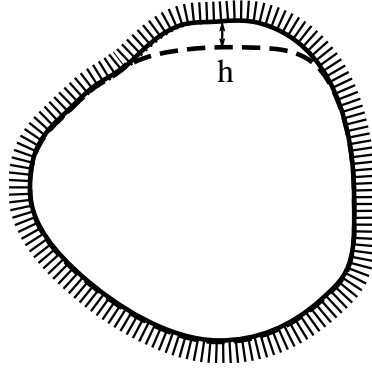


Figure 25.3: An initial (solid curve) and distorted (dashed curve) cavity shapes.

of oscillations. This averaging introduces a factor of $\frac{1}{2}$. We then multiply it by the offset h , and integrate over the area of the dent

$$\delta W = \frac{1}{2} \int \left(\frac{1}{2\mu_0} |B_t|^2 - \frac{\epsilon_0}{2} |E_n|^2 \right) dSh, \quad (25.27)$$

where we assume that h is positive in the case when the volume of the cavity decreases, and it is negative in the opposite case. The quantities B_t and E_n are understood as the amplitude values of the field on the surface. The positive (negative) value of this expression means that the electromagnetic energy in the mode increases (decreases).

To relate the mode frequency change to the energy change, we invoke a quantum argument. The number of quanta of the electromagnetic field in the cavity does not change if the process of cavity reshaping occurs adiabatically slow. This number is proportional to the ratio of the electromagnetic energy to the frequency, hence we have $W/\omega = \text{const}$, from which it follows that

$$\frac{\delta\omega}{\omega} = \frac{\delta W}{W}. \quad (25.28)$$

This gives us

$$\frac{\delta\omega}{\omega} = \frac{\epsilon_0}{4W} \int_{\Delta V} dV (c^2 |B_t|^2 - |E_n|^2), \quad (25.29)$$

where the integration in the numerator goes over the volume of the dent, and the integration in the denominator goes over the volume of the cavity. This is often called *Slater's formula*.

Note that the applicability condition of this formula requires that the perturbation of the cavity shape be not only small but also smooth enough—otherwise the field variation near possible edges of the dent is large, and one cannot use the unperturbed fields in Eq. (25.27).

Problem 25.2. *The radius of a cylindrical cavity is changed by a small quantity δa , and the length is changed by δL . Consider this as a deformation of the cavity shape and find the frequency change of the fundamental mode in the cavity using Slater's formula. Verify that the result agrees with Eq. (25.15).*

25.6 Excitation of a cavity mode by a beam

In accelerators, cavity resonators are excited by an external RF source. In addition to this, a beam of particles passing through the resonator also contributes to the excitation of the mode. In this section we will calculate the amplitude of the mode that is excited by a relativistic charge passing through a cavity resonator using a method proposed by P. Wilson in Ref. [22]. We assume that the charge moves with the speed close to the speed of light and use approximation $v = c$.

The derivation is based on principles of superposition and conservation of energy. Assume that a point charge q enters an empty cavity which does not have field in it at time $\tau = 0$, and is moving along the z axis. We represent the *real* longitudinal component of the electric field of the mode under consideration as

$$\mathcal{E}_z(z) = E_0 e(z), \quad (25.30)$$

where E_0 is the amplitude and $e(z)$ gives the distribution along the z axis at a given time. Note that the function $e(z)$, being a solution of an eigenfunction problem, is defined within an arbitrary numerical normalization factor. Correspondingly, E_0 is also defined with the same uncertainty. As we will see, however, at the end our result does not depend on the particular choice of the normalization factor.

The total electromagnetic energy W of the mode is proportional to E_0^2 and we write it as

$$W = AE_0^2, \quad (25.31)$$

where A is a factor that depends on the geometry of the cavity and the distribution of the field in the mode.

The particle arrives at location $z = c\tau$ at time τ , and at this time the amplitude of the mode is E_0 . When the particle moves from z to $z + dz$ due to the interaction with the field of the mode it changes its amplitude by an infinitesimal value dE_0 . We can find dE_0 using the energy conservation. The energy change of the mode is equal to the work of the electric field of the mode on the charge taken with the minus sign:

$$dW = -q\mathcal{E}_z dz = -qE_0 e(z) dz. \quad (25.32)$$

On the other hand we have $dW = 2AE_0 dE_0$. This gives

$$dE_0 = -\frac{q}{2A} e(z) dz. \quad (25.33)$$

The added (at time τ) component to the field dE_0 will oscillate with the frequency of the mode ω , and at time t will evolve to $dE_0 \exp[-i\omega(t - \tau)] = dE_0 \exp[-i\omega(t - z/c)]$. In this formula we implicitly assumed that the excited field starts oscillations with a zero phase. To obtain the complete amplitude at the end of the process we need to sum all the infinitesimal contributions with proper phases:

$$E_0 = -\frac{q}{2A} e^{-i\omega t} \int_0^L e^{i\omega z/c} e(z) dz = -\frac{qV}{2A} e^{-i\omega t}, \quad (25.34)$$

where

$$V = \int_0^L e^{i\omega z/c} e(z) dz, \quad (25.35)$$

and L is the cavity length.

As was mentioned above, the definition of E_0 depends on the normalization of the function $e(z)$, which is reflected in Eq. (25.34). The energy deposited by the beam to the cavity, however, is uniquely defined. This energy, per unit charge, is called the *loss factor*. Since our final amplitude is complex, we need to use the relation $W = A|E_0|^2$, which gives for the loss factor k

$$k_{\text{loss}} = \frac{1}{q^2} A|E_0|^2 = \frac{|V|^2}{4A} = \frac{|V|^2}{4W_0}, \quad (25.36)$$

where in the last formula $W_0 = A$ has a meaning of the energy in the mode with unit amplitude, $E_0 = 1$. Changing normalization of the function $e(z)$ by a factor of N would add a factor N^2 to both V^2 and W , and, as it follows from Eq. (25.36), does not change the value of k_{loss} .

Problem 25.3. Find the loss factor for the fundamental mode of the cylindrical cavity.

Lecture 26

Laser acceleration in vacuum. Inverse FEL acceleration

A focused laser beam can easily produce an extremely high electric field at the focal point. For example, for 1 J, 100 fs laser beam focused into a spot size of 10 micron, has a maximum electric field about 40 GV/cm. We would like to use this field for particle acceleration.

26.1 The Lawson-Woodward theorem

The first obstacle that we encounter on this way is that the field is mostly transverse to the direction of propagation. There is, however, a smaller longitudinal component of the field $E_z \sim \theta E_x$, see Section 17.2. Second, we may send a particle through a focal point at an angle as shown in Fig. 26.1. It turns out however, that no matter how we organize the interaction of the laser beam with the particles, in *linear* approximation, there is no net acceleration in free space. This is often called the *Lawson-Woodward theorem*.

We will now explain what the linear approximation is. This is an approximation in which we calculate the energy gain W of a particle passing through an external field $\mathbf{E}(\mathbf{r}, t)$ assuming that it moves with a constant velocity \mathbf{v} ,

$$W = q \int_{-\infty}^{\infty} \mathbf{v} \cdot \mathbf{E}(\mathbf{r}_0 + \mathbf{v}t, t) dt. \quad (26.1)$$

In this approximation we neglect the influence of the accelerating field on the velocity and the orbit of the particle. This approximation is motivated by the desire to accelerate relativistic particles, and such particles move in free space with almost constant velocity (close to the velocity of light). Due to the

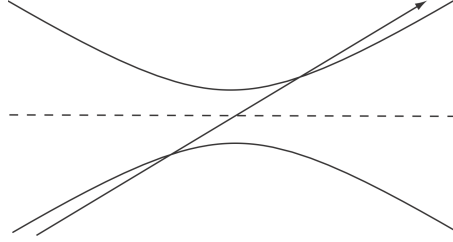


Figure 26.1: Particle's trajectory is tilted relative to the direction of the laser beam.

relativistically increased inertia of such particles, it is difficult to change their velocity and deflect them from a straight trajectory.

Let us now prove that in free space, without material boundaries, and in the absence of static fields, the above integral is equal to zero. The proof is based on the fact that any electromagnetic field in vacuum can be represented as a superposition of plane electromagnetic waves that propagate with the speed of light:

$$\mathbf{E}(\mathbf{r}, t) = \int d^3k \tilde{\mathbf{E}}(\mathbf{k}) e^{i\mathbf{k} \cdot \mathbf{r} - i\omega t}, \quad (26.2)$$

with $\omega = ck$. We have

$$\begin{aligned} W &= q\mathbf{v} \cdot \int_{-\infty}^{\infty} dt \int d^3k \tilde{\mathbf{E}}(\mathbf{k}) e^{i\mathbf{k} \cdot (\mathbf{r}_0 + \mathbf{v}t) - i\omega t} \\ &= 2\pi \int d^3k q\mathbf{v} \cdot \tilde{\mathbf{E}}(\mathbf{k}) e^{i\mathbf{k} \cdot \mathbf{r}_0} \delta(\omega - \mathbf{k} \cdot \mathbf{v}). \end{aligned} \quad (26.3)$$

The argument in the delta function in the last integral is never equal to zero, because

$$\omega - \mathbf{k} \cdot \mathbf{v} = ck - vk \cos \alpha = ck(1 - \beta \cos \alpha) > 0, \quad (26.4)$$

and hence the integral vanishes (α is the angle between \mathbf{k} and \mathbf{v}).

Problem 26.1. Prove that $W = 0$ even if $v = c$.

The physical reason for vanishing W is that the waves propagate with the speed of light, and the particle always moves slower. As a result, it will be slipping with respect to the phase of the wave, and the acceleration phase will be alternating with the deceleration, with the average total effect equal to zero.

There are several ways to try to resolve this problem. First, one can limit interaction between the particle and the waves in space putting material boundaries. We consider a model of such acceleration in the next section. The problem here is that the laser beam would hit material surfaces and the damage threshold would limit the attainable laser field. Second, one can work in the regime where the effect of the electric field on the particle orbit is relatively large and changes

its velocity and trajectory. This means that one has to drop the assumption of constant velocity and the straight orbit in Eq. (26.3). This method is limited to relatively small energies. Finally, one can have an external magnetic field that bends the orbit. An example of such acceleration is a so called the *inverse FEL* acceleration which we consider in the last section of this Lecture.

26.2 Laser acceleration in space with material boundaries

We will now calculate the energy gain of a charged particle passing through a focussed laser field reflected back by a flat mirror as shown in Fig. 26.2. The

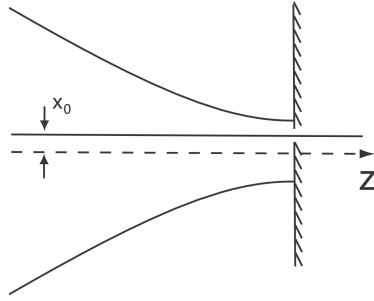


Figure 26.2: The laser beam is reflected by a metal surface; the particle passes through a hole in the metal.

mirror is located at $z = 0$ and has a small hole for the passage of the particle. We assume that the hole does not perturb much the laser field except for a small vicinity near the hole. In the calculations, we neglect interaction with the reflected part of the field, which turns out to be small (see the problem at the end of this section).

We assume that the particle moves along a straight line parallel to the z axis with velocity v and an offset x_0 . The z coordinate of the particle at time t is equal to $z_0 + vt$. The energy gain is given by the following equation

$$\Delta W = q \int_{-\infty}^0 dt v E_z(x_0, 0, z_0 + vt, t) = q \int_{-\infty}^0 dz E_z(x_0, 0, z, (z - z_0)/v). \quad (26.5)$$

The longitudinal component of the electric field in the laser focus was calculated in a problem of Section 17.2, and is given by

$$E_z(x, y, z, t) = -\frac{1}{ik} \frac{\partial E_x}{\partial x} = -\frac{2x}{ik} A(z) Q(z) e^{Q(z)\rho^2} e^{-i\omega t + ikz}, \quad (26.6)$$

where A and Q are given by Eqs. (17.18) and (17.19). Of course we need to

take the real part of the field to calculate ΔW . We then have

$$\begin{aligned}\Delta W &= -\text{Re} \left(\frac{2x_0 q}{ik} e^{ikz_0 \beta^{-1}} \int_{-\infty}^0 dz A(z) Q(z) e^{Q(z)x_0^2} e^{-ikz(\beta^{-1}-1)} \right) \\ &= \text{Re} \left(\frac{2E_0 x_0 q}{ikw_0^2} e^{ikz_0 \beta^{-1}} \int_{-\infty}^0 \frac{dz}{(1+2iz/kw_0^2)^2} e^{-x_0^2/w_0^2(1+2iz/kw_0^2)} e^{-ikz(\beta^{-1}-1)} \right).\end{aligned}\tag{26.7}$$

Let us use an integration variable $\xi = 2z/kw_0^2 = z/Z_R$:

$$\Delta W = -\text{Re} \left(iE_0 x_0 q e^{ikz_0 \beta^{-1}} \int_{-\infty}^0 \frac{d\xi}{(1+i\xi)^2} e^{-x_0^2/w_0^2(1+i\xi)} e^{-i\xi k^2 w_0^2 (\beta^{-1}-1)/2} \right).\tag{26.8}$$

We first note that if the upper limit in this integral is set to infinity, then the integral is equal to zero. This can be proved analytically for $\beta \leq 1$. Of course, this result also follows from the Lawson-Woodward theorem.

Problem 26.2. *Prove the statement in the previous paragraph for $\beta = 1$.*

To simplify calculations, let us now consider an ultrarelativistic particle and set $\beta = 1$. Then the integration in (26.8) is easy to do, and the result is

$$\begin{aligned}\Delta W &= -\text{Re} \left(iE_0 x_0 q e^{ikz_0} \int_{-\infty}^0 \frac{d\xi}{(1+i\xi)^2} e^{-x_0^2/w_0^2(1+i\xi)} \right) \\ &= \frac{E_0 q w_0^2}{x_0} (1 - e^{-x_0^2/w_0^2}) \cos(kz_0).\end{aligned}\tag{26.9}$$

The factor $\cos(kz_0)$ in this equation indicates that the sign of the energy gain depends on the position of the charge relative to the phase of the laser field; for bunches of particles longer than the wavelength of the laser radiation such an interaction modulates the energy of the beam with the period equal to the laser wavelength.

Problem 26.3. *Calculate the contribution to ΔW of the reflected part of the laser field.*

Problem 26.4. *Assume that you are given a laser with a given energy E_L , frequency ω and duration τ of the laser pulse. Optimize parameters of a laser acceleration experiment to achieve the maximum energy gain for relativistic particles. Express the energy gain in terms of E_L , ω and τ .*

Many more details of laser acceleration can be found in Ref. [23].

26.3 Inverse FEL acceleration

One can accelerate the beam if its orbit is not a straight line. In this section we consider acceleration when a point charge is moving in an undulator with $K \ll 1$ and is irradiated by a laser beam copropagating with the beam. This kind of acceleration is called the *inverse FEL* acceleration.

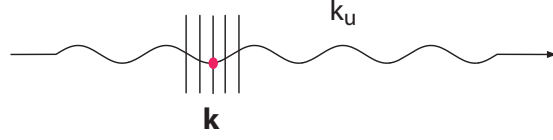


Figure 26.3: Particle's trajectory in an undulator and a the laser pulse copropagating with the particle.

We will represent the laser field by a plane electromagnetic wave with electric field E_x propagating in the z direction,

$$E_x(z, t) = E_0 \cos(\omega t - \omega z/c), \quad (26.10)$$

and calculate the energy gain as

$$W = q \int dt \mathbf{E} \cdot \mathbf{v} = q \int dt E_x v_x. \quad (26.11)$$

We know the velocity in a small- K undulator (see Eq. (21.3))

$$v_x = \frac{cK}{\gamma} \sin(k_u z). \quad (26.12)$$

Using the approximation $z \approx z_0 + c(1 - 1/2\gamma^2)t$ gives

$$\begin{aligned} W &= q \int dt \mathbf{E} \cdot \mathbf{v} \\ &= q \int dt \frac{cK}{\gamma} \sin(k_u(z_0 + ct)) E_0 \cos\left(\omega t - kct \left(1 - \frac{1}{2\gamma^2}\right) - kz_0\right) \\ &\approx \frac{cqKE_0}{2\gamma} \int dt \sin\left(k_u ct - \omega t + \omega t \left(1 - \frac{1}{2\gamma^2}\right) + (k + k_u)z_0\right) \\ &\approx \frac{cqKE_0}{2\gamma} \int dt \sin\left(\left(k_u c - \omega \frac{1}{2\gamma^2}\right)t + (k + k_u)z_0\right). \end{aligned} \quad (26.13)$$

In this equation we discarded the term with the sum of the arguments in the sine function because it adds only an oscillating small contribution to the result. The most effective acceleration occurs if

$$\omega = 2\gamma^2 k_u c, \quad (26.14)$$

which means that the laser frequency is equal to the frequency of the undulator radiation. In this case

$$W = \frac{qKE_0L_u}{2\gamma} \sin((k + k_u)z_0). \quad (26.15)$$

Depending on the position of the particle z_0 relative to the phase of the laser the energy gain can have both positive and negative signs. This will result in the energy modulation of the beam.

As a final note, we mention that the plane wave approximation is valid if the Raleigh length for the laser beam is much larger than the undulator length. This is not the most efficient way to interact the laser beam with electrons. A better approach to the problem is based on exploring a link between the interference of the undulator radiation with the field of the laser beam [24].

Problem 26.5. *Take the the following parameters of the IFEL experiment from Ref. [25]: beam energy 30 MeV, laser pulse length 2 ps, laser energy 0.5 mJ, laser focused spot size 110 μm , undulator period 1.8 cm, number of periods 3, $K = 0.6$, and estimate the amplitude of the energy modulation of the beam.*

Bibliography

- [1] J. D. Jackson. *Classical Electrodynamics*. Wiley, New York, third edition, 1999.
- [2] Jorge V. Josè and Eugene J. Saletan. *Classical dynamics: a contemporary approach*. Cambridge University Press, 1998.
- [3] Herbert Goldstein, Charles Poole, and John Safko. *Classical mechanics*. Edison-Wesley, 3d edition, 2000.
- [4] Gerald Jay Sussman and Jack Wisdom. *Structure and Interpretation of Classical Mechanics*. MIT Press, 2001.
- [5] L. D. Landau and E. M. Lifshitz. *Mechanics*, volume 1 of *Course of Theoretical Physics*. Pergamon, London, 1976. (Translated from the Russian).
- [6] Scott Berg and Robert Warnock. A code to compute the action-angle transformation for a particle in an arbitrary potential well. Report SLAC-PUB-95-6839, SLAC, 1995.
- [7] John M. Jowett. Introductory statistical mechanics for electron storage rings. *AIP Conf.Proc.*, 153:864–970, 1987.
- [8] Keith R. Symon. Derivation of Hamiltonians for accelerators. Report ANL/APS/TB-28, Argonne National Laboratory, 1997.
- [9] S. Y. Lee. *Accelerator Physics*. World Scientific, 1999.
- [10] D. D. Caussyn, M. Ball, B. Brabson, J. Collins, S. A. Curtis, V. Derenchuck, D. DuPlantis, G. East, M. Ellison, T. Ellison, D. Friesel, B. Hamilton, W. P. Jones, W. Lamble, S. Y. Lee, D. Li, M. G. Minty, T. Sloan, G. Xu, A. W. Chao, K. Y. Ng, and S. Tepikian. Experimental studies of nonlinear beam dynamics. *Phys. Rev. A*, 46(12):7942–7952, Dec 1992.
- [11] A. B. Rechester and R. B. White. Calculation of turbulent diffusion for the Chirikov-Taylor model. *Physical Review Letters*, 44:1586, 1980.
- [12] J. Corbett, Y. Nosochkovy, J. Safranek, and A. Garren. Dynamic aperture studies for SPEAR 3. In *Proceedings of the 1999 Particle Accelerator Conference*, page 2364, 1999.

- [13] Kenneth W. Robinson. Radiation effects in circular electron accelerators. *Phys. Rev.*, 111(2):373–380, Jul 1958.
- [14] L. D. Landau and E. M. Lifshitz. *Electrodynamics of Continuous Media*, volume 8 of *Course of Theoretical Physics*. Pergamon, London, second edition, 1960. (Translated from the Russian).
- [15] K. L. F. Bane and M. Sands. The short-range resistive wall wakefields. Technical Report SLAC-PUB-95-7074, SLAC, December 1995.
- [16] G. Dome, E. Gianfelice, L. Palumbo, V. G. Vaccaro, and L. Verolino. Longitudinal coupling impedance of a circular iris. *Nuovo Cimento A*, 104:1241, 1991.
- [17] W. Panofsky and M. Phillips. *Classical Electricity and Magnetism*. Addison-Wesley, 2nd edition, 1962.
- [18] Albert Hofmann. *The Physics of Synchrotron Radiation*. Cambridge Univ. Press, 2004.
- [19] Z. Huang, G. Stupakov, and M. Zolotarev. Calculation and optimization of laser acceleration in vacuum. *Phys. Rev. ST Accel. Beams*, 7:011302, 2004.
- [20] J. B. Murphy, S. Krinsky, and R. L. Gluckstern. Longitudinal wakefield for an electron moving on a circular orbit. *Part. Accel.*, 57:9–64, 1997.
- [21] Alexander Wu Chao and Maury Tigner. *Handbook of Accelerator Physics and Engineering*. World Scientific, Singapore, 3d edition, 2006.
- [22] P. Wilson. High energy electron linacs: Applications to storage ring rf systems and linear colliders. Technical Report SLAC-AP-2884 (Rev.), SLAC, November 1991.
- [23] Eric Esarey, Phillip Sprangle, and Jonathan Krall. Laser acceleration of electrons in vacuum. *Physical Review E*, 52:5443, 1995.
- [24] A. A. Zholents and M. S. Zolotarev. Femtosecond X-Ray pulses of synchrotron radiation. *Phys. Rev. Lett.*, 76:912, 1996.
- [25] Christopher M. S. Sears, Eric R. Colby, Benjamin M. Cowan, Robert H. Siemann, James E. Spencer, Robert L. Byer, and Tomas Plettner. High-harmonic inverse-free-electron-laser interaction at 800 nm. *Physical Review Letters*, 92:194801, 2005.